Characterisation and quantification of the polymorphic forms of stavudine

Schalk Strydom
B.Pharm

Dissertation submitted in partial fulfillment of the requirements for the degree Magister Scientiae in the Department of Pharmaceutics at the North-West University, Potchefstroom Campus.

Supervisor: Prof. W. Liebenberg
Co-supervisor: Mr. M. Brits
Potchefstroom
2007

TABLE OF CONTENT

ABSTRACT

Characterisation and quantification of the polymorphic forms of stavudine

Objective: Stavudine is a nucleoside reverse transcriptase inhibitor (NRTI) that is used in the treatment of human immunodeficiency virus (HIV) infections. Stavudine exhibits polymorphism and various polymorphic forms of stavudine are described in the literature, however the available information on these solid states, at the start and during this study, was limited. This study was conducted in order to (1) generate supplementary and/or possibly new information on the physicochemical properties of the various polymorphs of stavudine, (2) to possibly prepare and characterise a new polymorphic form of stavudine, (3) to determine and compare the dissolution behaviour of the stavudine polymorphs and (4) to investigate the possibility of applying analytical techniques to quantify the stavudine polymorphs in solid state mixtures.

Methods: Various characterisation methods were used to determine the physicochemical properties of the polymorphic forms of stavudine, including X-ray powder diffraction (XRPD); variable temperature X-ray powder diffraction (VT-XRPD); diffuse reflectance infrared Fourier transform spectroscopy (DRIFTS); differential scanning calorimetry (DSC); thermogravimetric analysis (TGA); polarising optical microscopy; hot-stage microscopy (HSM); scanning electron microscopy (SEM); as well as Karl Fischer (KF) analysis. The dissolution behaviour of the various polymorphic forms of stavudine, that were prepared during this study, was also determined, whilst quantitative XRPD and DRIFTS methods were developed for the quantitative study.

Results: Polymorphic form I and form II of stavudine were prepared by recrystallisation of stavudine raw material from various solvents, whereas form III (hydrate) and the *N*-methyl-2-pyrrolidone (NMP) solvate of stavudine were recrystallised from water and NMP respectively. The results generated from the VT-XRPD analyses of form I and form II demonstrated that these solid states are monotropically related (supportive of the findings of Mirmehrabi *et al.* (2006:141)), and that form I and II do not interconvert to one another. The hydrate of stavudine was not observed to convert to polymorphic form I upon heating, as was determined by Gandhi *et al.* (2000:228). However, VT-XRPD analysis of form III and the NMP solvate showed that upon heating, both these pseudopolymorphs interconvert to form a polymorphic mixture consisting of form I and II. A glassy (amorphous) form of stavudine that was previously not described in the available literature was also prepared and characterised during this study.

Dissolution testing of polymorphic form I, form II, the glassy (amorphous) stavudine and the form I/II mixture of stavudine revealed that a greater amount of the glassy stavudine dissolved within one minute compared to the other polymorphic forms. A comparison of the dissolution profiles, based on the requirements of the Medicines Control Council of South Africa, indicated that the profiles of form I and form II, form I and the glassy stavudine, and form I and the form I/II mixture are similar.

Two different methods (based on the analytical techniques of XRPD and DRIFTS) were developed to quantify the amount of form I and form II of stavudine in solid state mixtures. Each method was validated, and the results indicated that the quantitative DRIFTS method showed the greatest agreement between the experimental and theoretical polymorphic content. Preferred orientation was assumed to be the reason for the deviation of the quantitative XRPD results, and it was suggested that this might be corrected by background subtraction, $K_{\alpha 2}$ stripping and smoothing of the X-ray diffraction peaks. A test sample with an unknown concentration was analysed using both methods, and the comparison between the XRPD and DRIFTS results revealed that the DRIFTS method might be more accurate when compared with the XRPD method.

Conclusion: Stavudine exhibits polymorphism and this study confirmed that the physicochemical properties of the various polymorphs differ. A glassy (amorphous) form of stavudine was, according to available literature, prepared and characterised for the first time during this study. Two methods for quantifying the amount of form I and form II of stavudine in mixtures comprising these two polymorphs were successfully developed and tested. The DRIFTS method may have generated the more accurate results, since it shows the best correlation between the experimental and theoretical results.

UITTREKSEL

Karakterisering en kwantifisering van die polimorfiese vorms van stavudien

Doelstelling: Stavudien is 'n nukleosied omgekeerde transkriptase inhibeerder wat gebruik word vir die behandeling van menslike immuungebreksvirus (MIV) infeksies. Stavudien openbaar polimorfisme en verskeie polimorfiese vorms van stavudien word beskryf in die literatuur, maar die beskikbare inligting rakende dié vaste toestande, met aanvang en tydens hierdie studie, was beperk. Hierdie studie is onderneem ten einde (1) stawende en/of moontlike nuwe inligting oor die fisies-chemiese eienskappe van die verskillende polimorfe vorme van stavudien te genereer, (2) om 'n moontlik nuwe polimorfe vorm van stavudine te berei en te karakteriseer, (3) om die dissolusie eienskappe van die polimorfe vorme van stavudien te bepaal en te vergelyk en (4) om die moontlikheid van die toepassing van analitiese metodes vir kwantifisering van mengsels van polimorfe vorme van stavudien te ondersoek.

Metodes: Verskeie karakteriserings metodes is gebruik om die fisies-chemiese eienskappe van die polimorfe vorme van stavudien te bepaal, insluitend X-straal poeier diffraktometrie (XRPD); variërende temperatuur X-straal poeier diffraktometrie (VT-XRPD); diffuse refleksie infrarooi Fourier transformspektrometrie (DRIFTS); differensiële skanderingskalorimetrie (DSC); termogravimetriese analise (TGA); polariserende optiese mikroskopie; termiese mikroskopie (HSM); skanderings elektronmikroskopie (SEM); sowel as Karl Fischer (KF) - analise. Die dissolusie gedrag van die polimorfe vorme van stavudien, wat tydens hierdie ondersoek berei is, is ook bepaal, en kwantitatiewe XRPD- en DRIFTS-metodes is ontwikkel vir die kwantitatiewe studie.

Resultate: Polimorfe vorm I en vorm II van stavudien is berei deur middel van rekristallisasie van stavudien grondstof vanuit verskeie oplosmiddels, terwyl vorm III (hidraat) en die *N*-metiel-2-pirrolidoon (NMP) solvaat van stavudien gerekristalliseer is vanuit water en NMP respektiewelik. Die resultate wat verkry is van die VT-XRPD analises van vorm I en vorm II het aangetoon dat hierdie vaste toestande monotropies verwant is (bevestigend van die resultate van Mirmehrabi *et al.* (2006:141)), en dat vorm I en vorm II nie na mekaar toe omskakel nie. Die hidraat van stavudien skakel ook nie om na vorm I tydens verhitting nie, soos bevind deur Gandhi *et al.* (2000:228). VT-XRPD analise van vorm III en die NMP solvaat van stavudien het aangetoon dat beide dié pseudopolimorfiese vorme omskakel na 'n polimorfiese mengsel bestaande uit vorm I en vorm II tydens verhitting van dié solvate. 'n

Glasagtige (amorfe) vorm van stavudien wat voorheen nie beskryf is in die beskikbare literatuur nie, is ook tydens hierdie studie berei en gekarakteriseer.

Dissolusie-toetsing van polimorfe vorm I, vorm II, die glasagtige (amorfe) stavudien en die vorm I/II mengsel van stavudien het aangedui dat 'n groter hoeveelheid van die glasagtige stavudien opgelos het in een minuut in vergelyking met die ander polimorfe vorme van stavudien. 'n Vergelyking van die dissolusie profiele, deur gebruik te maak van die aanbevelings van die Medisyne Beheerraad van Suid-Afrika, het aangedui dat die profiele van vorm I en vorm II, vorm I en die glasagtige stavudien, en vorm I en die vorm I/II mengsel soortgelyk is.

Twee verskillende metodes (wat gebaseer is op die analitiese tegnieke van XRPD en DRIFTS) is ontwikkel om die hoeveelheid van vorm I en vorm II van stavudien in vaste toestand mengsels te kwantifiseer. Elke metode is gevalideer, en die resultate het aangedui dat die kwantitatiewe DRIFTS-metode die beste ooreenkoms toon tussen die eksperimentele en teoretiese resultate. Voorkeur-oriëntasie is moontlik die rede vir die afwyking van die kwantitatiewe XRPD resultate, en dit kan moontlik reggestel word deur agtergrond-aftrekking, $K_{\alpha 2}$-stroping en gelykmaking van die X-straal diffraksie pieke. 'n Toets monster met 'n onbekende konsentrasie is geanaliseer deur gebruik te maak van albei metodes, en 'n vergelyking van die XRPD en die DRIFTS resultate het aangedui dat die DRIFTS-metode moontlik meer akkuraat is in vergelyking met die XRPD-metode.

Gevolgtrekking: Stavudien openbaar polimorfisme en hierdie ondersoek het bevestig dat die fisies-chemiese eienskappe van die verskillende polimorfe vorme verskil. 'n Glasagtige (amorfe) vorm van stavudien is, volgens beskikbare literatuur, die eerste maal tydens hierdie studie berei en gekarakteriseer. Twee metodes is suksesvol ontwikkel om die hoeveelheid van vorm I en vorm II van stavudien in mengsels bestaande uit dié twee vaste toestande te kwantifiseer. Die DRIFTS-metode het waarskynlik die meer akkurate resultate gelewer, aangesien dit die beste ooreenkoms tussen die eksperimentele en teoretiese resultate getoon het.

AIMS AND OBJECTIVES

Characterisation and quantification of the polymorphic forms of stavudine

The occurrence of polymorphism in respect of stavudine is reported in the literature. However, key information relating to such polymorphic and pseudopolymorphic forms was unavailable in those sources used. Questions were raised as to the transformations and/or interconversions that occur between the different polymorphic and pseudopolymorphic forms of stavudine, affecting the stability of the solid states. The preparation of mixtures of polymorphic form I and form II of stavudine were possible from recrystallisation processes, as reported in the literature. Furthermore, the only method found for the quantification of form I and form II in such polymorphic mixtures was developed and described by Mirmehrabi *et al.* (2006:143) using infrared spectroscopy, which to date, however, had not yet been verified.

The above issues formed the basis of the aims and objectives of this study, which were:

- To confirm the existence of and to characterise the various polymorphic forms of stavudine that are described in the literature, and to possibly prepare a new polymorphic form that had not yet been reported.

- To generate supplementary and/or new physicochemical information regarding the polymorphic and pseudopolymorphic forms of stavudine that had not yet been described in the literature.

- To determine and to compare the dissolution behaviour of the polymorphic forms of stavudine prepared during this study.

- To develop methods to quantify the amount of polymorphic form I and form II of stavudine in mixtures of these two polymorphs, using analytical techniques based on infrared spectroscopy and X-ray powder diffractometry, and to determine and compare the validity and relevance of these quantitative methods. This was considered necessary since the stavudine raw material purchased for use in the pharmaceutical industry in South Africa is often found to be such a mixture, and these methods may thus be used to establish the composition of such stavudine raw material for quality control purposes.

CHAPTER 1

Polymorphism in pharmaceutical solids

Introduction

In 1818 Eilhardt Mitscherlich noticed that the crystals of certain phosphates and arsenates were very similar and he called this phenomenon isomorphism. Although this discovery was serendipitous, he pursued it further, concentrating on what he called "the dimorphism of sulphur". He subsequently published his findings and although he is considered to be the first person to use the term "polymorphism", he was not the first person to notice this phenomenon. In 1798 Klaproth recognised that calcite and aragonite have the same chemical composition, and in the same year Davey discovered that diamond is a form of carbon (Bernstein, 2002:19-20). During this section a brief overview of polymorphism will be given and the most important principles relating to this subject matter will be explained.

1.1 The crystalline state

1.1.1 Theory and description of crystals and unit cells

The definition of a crystal is a solid in which the constituent molecules (or ions) are arranged in a highly ordered fashion, and this is in contrast to amorphous solids which have no long range ordered arrangement of the component molecules (see section 1.3.6). The molecules or ions in the crystal are arranged into unit cells, which are defined as the smallest three dimensional volume that the crystal can be broken down into which would still retain the properties of the original crystal. This arrangement of the unit cells leads to the creation of the crystal lattice in three dimensions. Crystals are thus built up of a repetition of the unit cells in three dimensions, and it can be viewed as though the unit cells are the different coloured blocks that make up a Rubik's Cube, whilst the crystal is the Rubik's Cube itself (Byrn *et al.*, 1999:5,48).

A unit cell is defined in space by three axes denoted as a, b and c, and by three angles between these axes signified by α (the angle between b and c), β (the angle between a and c) and γ (the angle between a and b). All crystals are built up out of one of the seven fundamental unit cells which are displayed in table 1.1, and drug crystals are commonly found to be built up out of either triclinic, monoclinic or orthorhombic unit cells (Byrn *et al.*, 1999:48; Brittain & Byrn, 1999:77).

Table 1.1 The seven fundamental unit cells and their dimensional properties (Brittain & Byrn, 1999:77, Microsoft Encarta Premium Suite, 2005)

Unit cell	Relationship between the unit cell axes	Relationship between the unit cell angles
Cubic	a = b = c	$\alpha = \beta = \gamma = 90°$
Tetragonal	a = b ≠ c	$\alpha = \beta = \gamma = 90°$
Orthorhombic	a ≠ b ≠ c	$\alpha = \beta = \gamma = 90°$
Monoclinic	a ≠ b ≠ c	$\alpha = \gamma = 90°$; $\beta \neq 90°$
Triclinic	a ≠ b ≠ c	$\alpha \neq \beta \neq \gamma \neq 90°$
Hexagonal	a = b ≠ c	$\alpha = \beta = 90°$; $\gamma = 120°$
Trigonal	a = b = c	$\alpha = \beta = 90°$; $\gamma \neq 120°$
	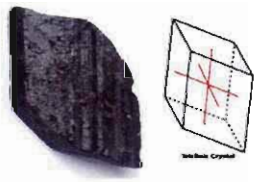	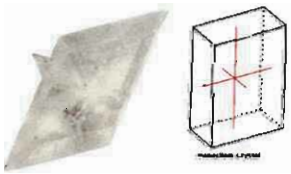
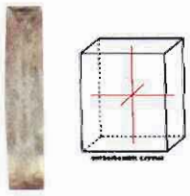	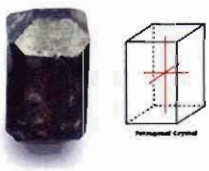	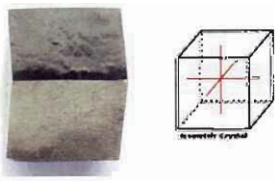

Crystal lattices have five possible symmetry operations which are defined as operations that change the configuration of the crystal but that leaves the appearance of the crystal lattice unchanged. These five symmetry operations (or symmetry elements) are: (1) identity (which leaves the system unchanged), (2) reflection of the crystal through a plane, (3) inversion of the crystal through a point, (4) proper rotation (which is a simple rotation about an axis that passes through a lattice point), (5) and improper rotation (which is proper rotation followed by reflection of the crystal). When the different unit cells and the symmetry elements are combined, they yield fourteen possible space lattices which is known as the Bravias Lattices (see table 1.2), and when these are combined with the 32 possible crystallographic point groups (i.e. the arrangement of the molecules in the lattice), it yields 230 possible space groups which describes the spatial symmetry of the crystal (Byrn *et al.*, 1999:6; Brittain & Byrn, 1999:76-84).

Table 1.2 The fourteen Bravias lattices (Brittain & Byrn, 1999:81)

Unit cell	Lattices			
Orthorhombic	Simple a ≠ b ≠ c 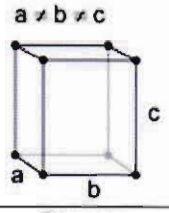	Base-centered a ≠ b ≠ c 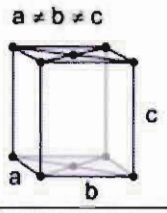	Body-centered a ≠ b ≠ c 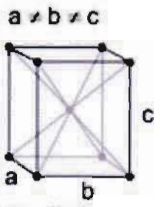	Face-centered a ≠ b ≠ c 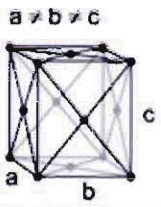
Cubic	Simple 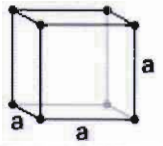	Body-centered 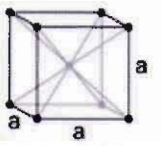	Face-centered 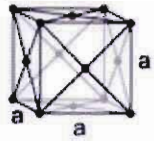	
Tetragonal	Simple a ≠ c 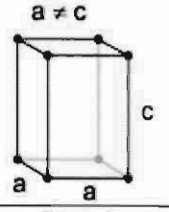	Body-centered a ≠ c 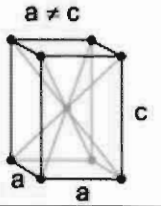		
Monoclinic	Simple α ≠ 90° β,γ = 90° 	Base-centered α ≠ 90° β,γ = 90° 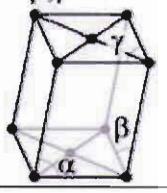		
Triclinic	α,β,γ ≠ 90° 			
Hexagonal	a=b≠c 			
Trigonal	α,β,γ ≠ 90° 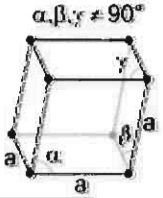			

1.1.2 The formation of crystals

Crystals usually form out of supersaturated solutions, i.e. solutions that are at a higher concentration than the saturation value, and the first step in the formation of a crystal is the assembly of nuclei consisting of the unit cells that will eventually comprise the crystal. Nucleation is subdivided into primary nucleation and secondary nucleation. Primary nucleation is the generation of nuclei in a system that does not already contain crystals and is classified as either spontaneous (homogeneous), or as a result of the introduction of foreign particles into the system to induce nucleation (heterogeneous). Secondary nucleation is the formation of nuclei due to the presence of pre-existing crystals in the system, and figure 1.1 illustrates this subdivision of the nucleation process (Bernstein, 2002:68).

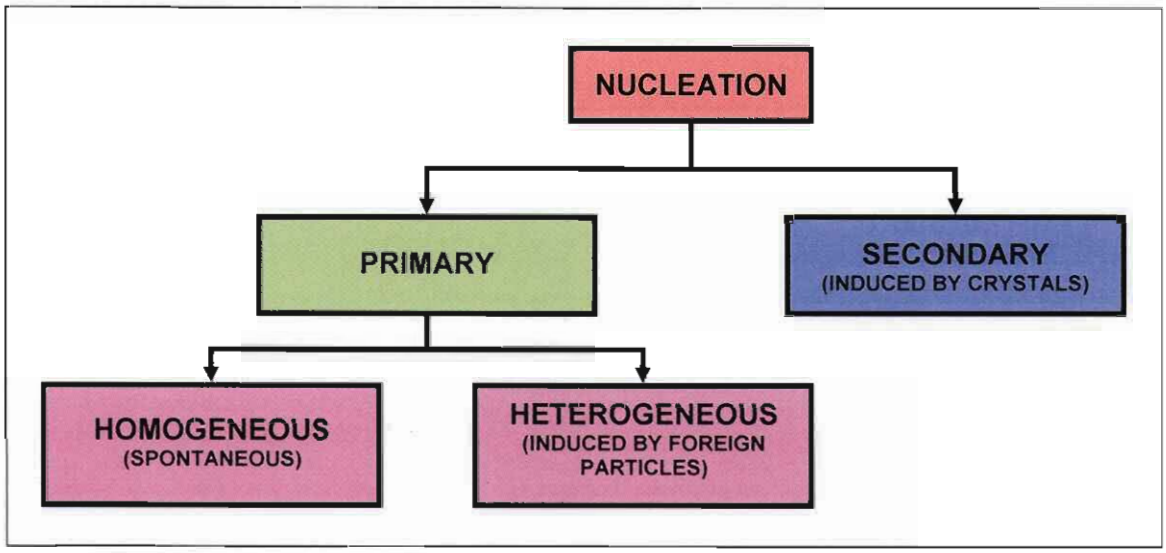

Figure 1.1 The subdivision of the nucleation process of crystallisation (Bernstein, 2002:68).

Various factors may influence and initiate nucleation including the presence of foreign particles, temperature irregularities, ultrasonic waves and deliberate seeding (which is the process of adding nuclei of the desired crystal to the system in order to control the outcome of the crystallisation process). After the nuclei have formed, they grow and form crystals and each nucleus results in the formation of only one crystal, i.e. the more nuclei that initially form the more crystals will eventually form (Byrn *et al.*, 1999:18).

The forces that are responsible for the arrangement of molecules in unit cells in crystals are ionic interactions for ionic substances (which include salts such as sodium chloride), and non-covalent interactions for organic molecules (which include hydrogen bonding and van der Waals forces) (Byrn *et al.*, 1999:18).

1.2 The theory of polymorphism

1.2.1 Description of the term polymorphism

The term polymorphism (derived from the Greek words "poly" meaning many and "morph" meaning form), when used in relation to the solid state studies of chemicals, describes two or more crystals that have the same chemical composition but different internal crystal structures, i.e. the molecular packing or unit cells in the crystals differ. The most well known example of polymorphism is the three polymorphs of carbon namely diamond, graphite and fullerenes. Polymorphism of crystals should not be confused with the term crystal habits (see section 1.2.2), which is defined as crystals that have the same chemical composition and crystal structure (i.e. they are thus one polymorphic crystal form), but these crystals display different shapes which are termed crystal habits (Bernstein, 2002:2; Byrn *et al.*, 1999:13).

1.2.2 Crystal shapes (habits)

Molecules of a certain substance may be arranged into various unit cells to form different polymorphic forms, however a single polymorph may have different crystal shapes (or crystal habits), and there are six different basic crystal shapes (habits) which a crystal may attain. These six basic crystal shapes are described and illustrated in table 1.3 (Nichols, 2006:191).

Table 1.3 A description and illustration of the six basic crystal shapes (Nichols, 2006:191)

Crystal shape	Description
Equant	Equi-dimensional crystals (such as cubes or spheres)
Plate	Flat, tubular crystals with similar breadth and width (thicker than flakes)
Flake	Thin, flat crystals with similar breadth and width (thinner than plates)
Lath	Elongated, thin and blade-like crystals (may be ribbon-like if flexible)
Needle	Acicular, thin and highly elongated crystals with similar breadth and width
Column	Elongated, prismatic crystals with greater width and thickness than needles

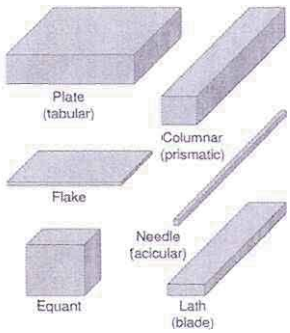

1.2.3 Physical properties of different polymorphs

A phase is defined as any homogeneous and physically distinct part of a system which is separated from other parts of the system by definite bounding surfaces, and from this definition it can be stated that each substance can have only one gaseous and liquid phase. The different crystalline forms of a compound is each considered to be a distinct phase because the different polymorphs can be separated from one another, and since each phase of a substance has its own unique properties, the different polymorphs of a substance also has different properties. Some of the properties that differ among various polymorphs are crystal packing properties (crystal volume and density), thermodynamic properties (melting temperatures and solubility), spectroscopic properties (infrared spectra), kinetic properties (dissolution rate and solubility), surface properties (habits) and mechanical properties. The two properties that are of greatest importance for drug substances are the stability and the solubility of the different polymorphic forms (Bernstein, 2002:30; Grant, 1999:5-8).

1.2.3.1 The influence of polymorphism on stability

Different polymorphic forms of a substance consist of different unit cells and the molecules that form these unit cells have to be arranged differently in space. This means that the ionic forces (in the case of ionic substances), and the hydrogen bonding forces and van der Waals forces (in the case of organic substances) that are responsible for retaining these molecules in their arrangements have to be different for each different unit cell. Simply put, the strength and amount of the intermolecular forces responsible for forming the various unit cells differ, and thus the internal energy of each crystal structure (the lattice energy) also differs. It can also be explained that the greater the strength and amount of the intermolecular forces that form the crystal, the greater the amount of energy required to break these bonds, thus the more stable the crystal lattice (i.e. it has the lowest free energy). Under a set of defined experimental conditions one polymorphic form has the lowest free energy and is said to be the stable polymorph. Polymorphic forms can be divided into two groups based on the stability of the polymorphs in each system, i.e. enantiotropic and monotropic polymorphic systems (Lund, 1994:179; Grant, 1999:18; Bernstein, 2002:31).

In an enantiotropic system a reversible transition can be observed between the polymorphs at a specific transition temperature that is below the melting point of the polymorphs (i.e. a different polymorph is stable under a different set of experimental conditions). In a monotropic system however, only one polymorph is stable, irrespective of the temperature and pressure, while all the other polymorphic forms are metastable and will tend to transform to the stable polymorph over time (this is detrimental to the pharmaceutical industry as it may

result in the formation of a polymorph with lower solubility and thus reduced bioavailability – see section 1.2.3.2). Figure 1.2 illustrates the relationship between two polymorphic forms in a monotropic and enantiotropic system (Grant, 1999:18-19; Lund, 1994:179).

There are six known rules that can be used to determine whether a polymorphic system is either enantiotropic or monotropic, i.e. (1) the heat of transition rule, (2) the heat of fusion rule, (3) the entropy of fusion rule, (4) the heat capacity rule, (5) the density rule and (6) the infrared rule. The heat of transition rule and the heat of fusion rule are the most accurate and universally applicable rules and are most often used to determine the relationship between polymorphs. The heat of transition rule states that if an endothermic polymorphic transition occurs, the system is enantiotropic, whereas if an exothermic polymorphic transition occurs, the polymorphic system is monotropic. The heat of fusion rule states that if the higher melting polymorph has the lower heat of fusion, the polymorphs are enantiotropes, otherwise they are monotropes. The entropy of fusion rule states that if the polymorph with the higher melting point has a lower entropy of fusion, the two polymorphs are enantiotropically related, whereas if the polymorph with the higher melting point has a higher entropy of fusion, the two polymorphs are monotropically related. The heat capacity rule states that for a pair of polymorphs, the relationship is enantiotropic if the polymorph with the higher melting point also has the higher heat capacity at a given temperature, whereas if the higher melting polymorph has a lower heat capacity, the polymorphs are monotropes. The density rule states that for a non-hydrogen-bonded system at absolute zero the most stable polymorph will have the highest density because of stronger van de Waals interactions. The infrared rule states that for hydrogen-bonded polymorphs the polymorph with the higher bond stretching frequency may be assumed to have the greater entropy (Bernstein, 2002:38-41; Lohani & Grant, 2006:21).

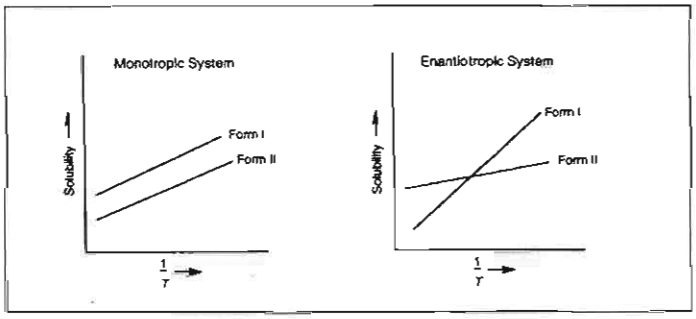

Figure 1.2 Schematic representation of monotropic and enantiotropic systems (as can be seen the monotropic graphs never intersect, thus one polymorph is stable irrespective of the temperature, whilst the enantiotropic graphs intersect, indicating that at higher temperatures one polymorph is the most stable and at lower temperatures another polymorph is) (Byrn *et al.*, 1999:20).

The instability of polymorphic forms can either be attributed to the physical instability (also known as physical transformation) of the polymorphs, or the chemical instability (also known as chemical transformation) of the polymorphs. The physical and chemical stability of different polymorphic forms of drug molecules has an impact on the manufacturing process of pharmaceutical products and the final dosage form, and some examples will be given to illustrate this (Haleblian *et al.*, 1969:913).

1.2.3.1.1 Polymorphism and physical instability

The physical instability of drug polymorphs results in the transformation (conversion) of the desired polymorphic form in the dosage form to an undesired polymorphic form. This is demonstrated by sulfamethoxazole, which, when microencapsulated, transforms from polymorphic form I to polymorphic form II as a result of the environmental stress it is subjected to during the manufacturing process. Another example of physical instability of polymorphs is the metastable polymorph of cortisone acetate, which, when formulated in a suspension, transforms to the stable polymorph resulting in caking of the suspension. The same polymorphic conversion in creams containing cortisone acetate results in the cream becoming coarse (gritty) and cosmetically unacceptable. A few more drugs whose polymorphs show mechanical instability (either during the manufacturing process or during storage) are metoprolol tartrate, paracetamol, sufamerazine, phenobarbitone, carbamazepine and phenylbutazone (Takenaka *et al.*, 1981:1256; Carless *et al.*, 1966:190S; Singhal & Curatolo, 2004:338).

1.2.3.1.2 Polymorphism and chemical instability

The chemical instability of drug polymorphs results in the degradation of drugs at a faster rate than expected, leading to a decrease in the effectiveness of the drug product. This is demonstrated by the polymorphic forms of carbamazepine for example, of which polymorphic form II is 5 and 1.5 times as susceptible to photodecay as forms I and III respectively. The polymorphic forms of paroxetine maleate, indomethacin, methylprednisolone, furosemide and enalapril maleate also demonstrate different rates of degradation (oxidation and hydrolysis) and thus demonstrate differences in chemical stability (Byrn *et al.*, 1999:222-223; Singhal & Curatolo, 2004:337).

1.2.3.2 The influence of polymorphism on solubility

The process of dissolving a solid phase in a liquid phase involves removing the molecules from the solid and dispersing them in the liquid to create a solution. This requires that the intermolecular forces in the solid phase be broken before the molecules are dispersed in the liquid. Hence, the stronger these forces in the solid phase, the more energy would be required to break these bonds and this results in a decreased solubility rate and a decreased amount of the substance dissolving (Brittain & Grant, 1999:296).

The stable polymorph of a substance consists of unit cells made up of molecules with either a greater strength, or a greater amount of intermolecular forces, compared to the metastable polymorphs, and the stable polymorph will thus demonstrate a slower dissolution rate and may also demonstrate a decreased amount of the drug in solution. Since a drug has to be in solution for it to be absorbed into the systemic circulation and exert a therapeutic effect, the difference in solubility between the various polymorphs of a drug substance will influence the bioavailability of the drug molecule (Lund, 1994:179; Bernstein, 2002:243-244).

A classic example of the dependence of the bioavailability of a drug on its polymorphic form, is chloramphenicol palmitate. Chloramphenicol has a very bitter taste and this led to the formulation of a tasteless chloramphenicol 3-palmitate oral suspension. Chloramphenicol 3-palmitate has three polymorphic forms (A, B and C), and an amorphous form, of which form A is the most stable (and thus the least soluble), whilst only form B and the amorphous form are soluble enough to be absorbed in sufficient quantities to be biologically active. Suspensions of chloramphenicol 3-palmitate were made to contain the tasteless metastable form B, which, as a result of high temperatures during storage of the suspension, converted to the more stable and least soluble form A, resulting in the suspensions being biologically ineffective. Figure 1.3 demonstrates the peak serum blood concentrations of chloramphenicol following a dose of pure polymorph A and B and various mixtures of these polymorphs, and it clearly shows the reduced bioavailability of polymorph A of chloramphenicol (Aguiar *et al.*, 1967:849-852; De Villiers *et al.*, 1991:1295).

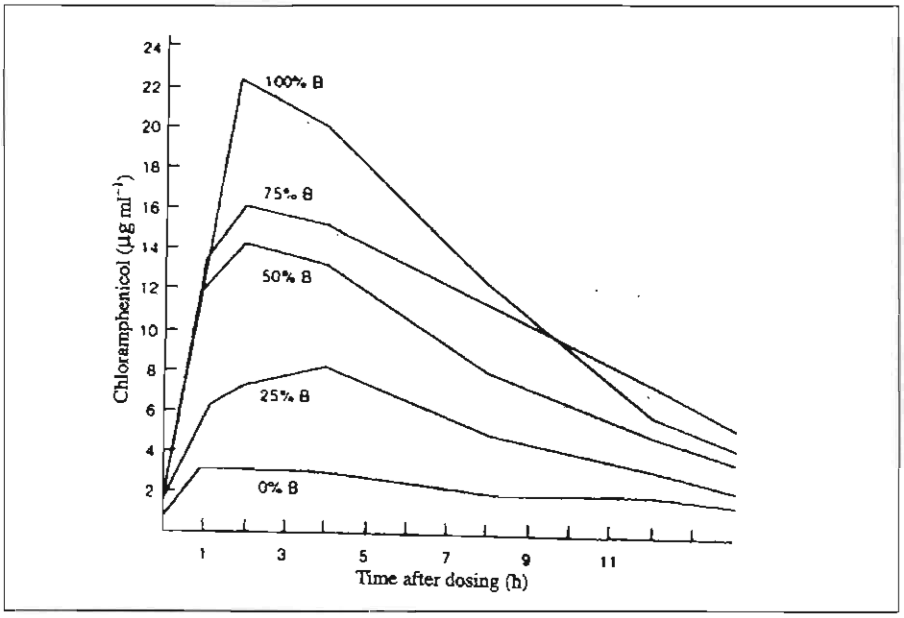

Figure 1.3 The peak blood serum levels of chloramphenicol polymorphs A and B and various mixtures thereof (Aguiar *et al.*, 1967:851).

The most recent example of the influence of polymorphism on the solubility of a drug product, is the protease inhibitor ritonavir, which after having been on the market for two years, began to precipitate from the semisolid formulation to form a more stable and less soluble polymorph (form II) with a lower bioavailability than the original polymorph (form I). The manufacturer (Abbott Laboratories) withdrew this product from the market and a year later released a new liquid filled capsule containing a solution of ritonavir. Figure 1.4 shows the video micrographs of the two polymorphs of ritonavir mentioned above (Chemburkar *et al.*, 2000:413).

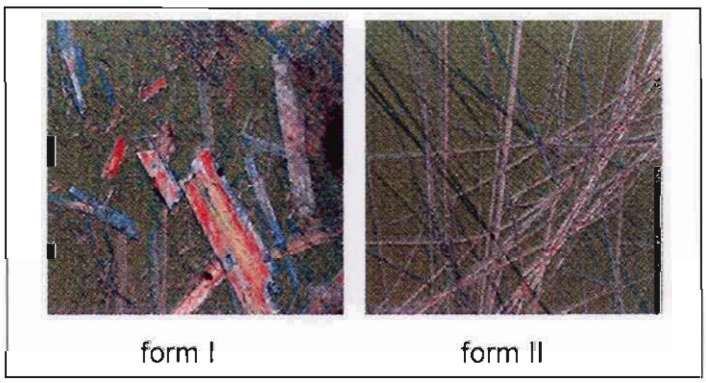

Figure 1.4 The two polymorphic forms of ritonavir (Chemburkar *et al.*, 2000:415).

1.2.3.3 The influence of the manufacturing process on polymorph stability

As stated in section 1.2.3.1, polymorphic forms of drug molecules show differences in physical stability, and one polymorphic form may transform to a different polymorphic form over time as a result of stress conditions during the manufacturing process. These transformations are undesirable, since it may lead to the formation of a more stable and less soluble solid state, hence reducing the bioavailability of the drug. A polymorphic form of a drug may undergo such a transformation during various stages in the manufacturing process, and as an example figure 1.5 illustrates the possible polymorphic transformations that may take place during the wet granulation step in the manufacturing process (Newman & Byrn, 2003:903).

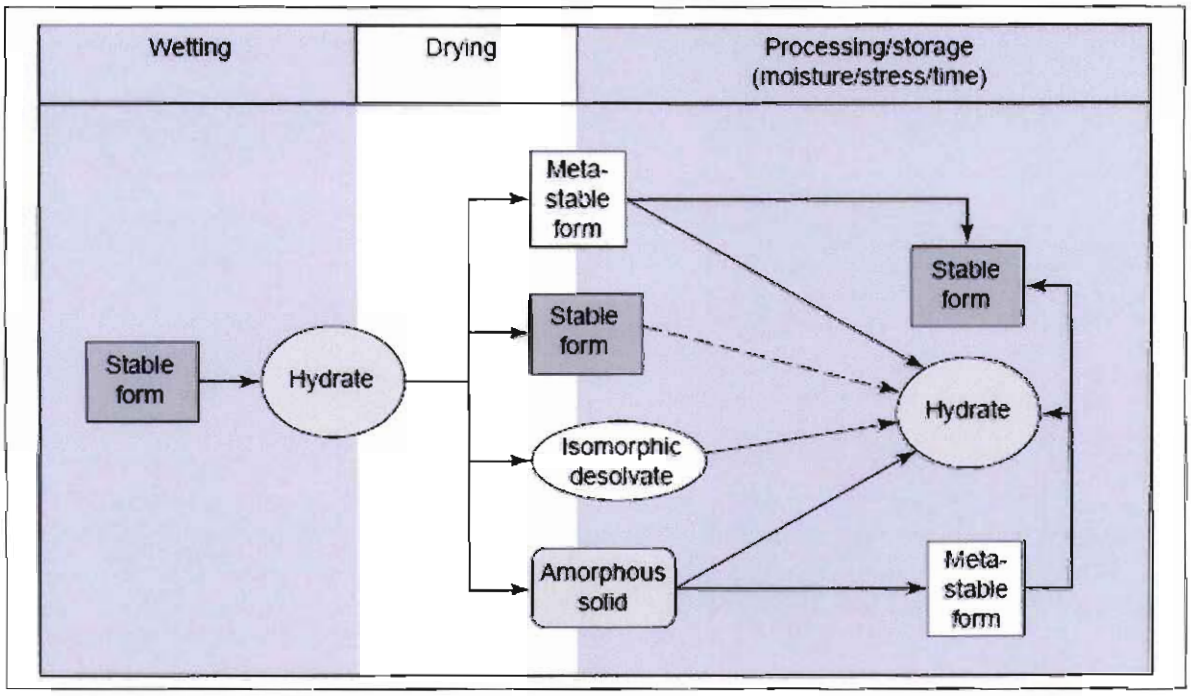

Figure 1.5 The possible polymorphic transformations that may occur during wet granulation (Morris *et al.*, 2001:107).

An example of a drug which demonstrates polymorphic transformation during wet granulation is theophylline. It converts from the anhydrous forms (form I and form II) to the undesirable monohydrate (the hydrate phase is undesirable since it shows a decreased dissolution rate compared to the anhydrous forms). When the theophylline monohydrate is dried during the manufacturing process in an attempt to eliminate the water, a different polymorphic form, having a different dissolution profile than the original anhydrous theophylline, is obtained. Polymorphic transformations may also occur during other types of induced stresses, as demonstrated by the amorphous form of cimetidine which crystallises upon compression, and the polymorphic form I (monoclinic) of paracetamol which transforms to form II

(orthorhombic) upon direct compression of paracetamol tablets. Polymorphic transformations may occur during a variety of other manufacturing processes including milling, freezing and drying, and this should be born in mind before commencing the large scale manufacturing of a new drug substance (Newman & Byrn, 2003:903; Airaksinen *et al.*, 2003:516; Phadnis & Suryanarayanan, 1997:1256; Bauer-Brandl, 1996:195).

1.3 Types of polymorphs

Figure 1.6 summarises the types of polymorphs that are discussed during this section.

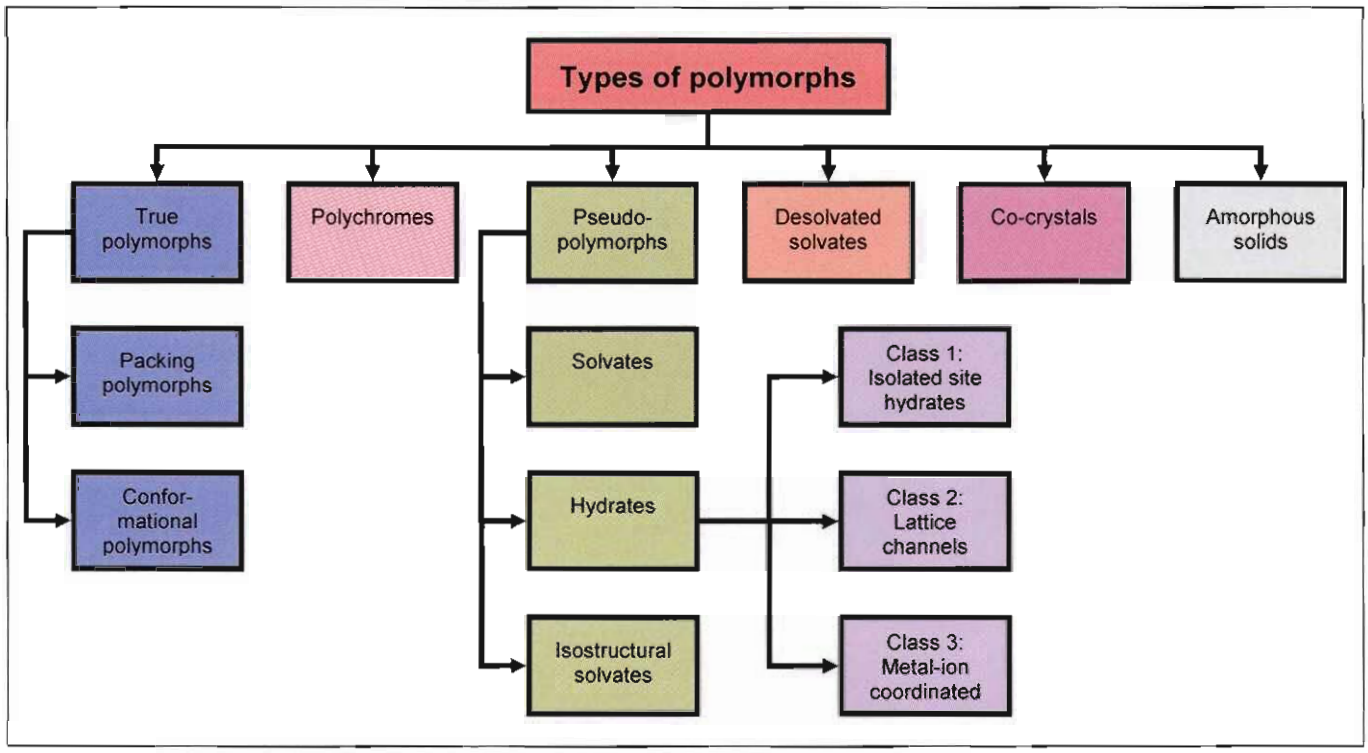

Figure 1.6 A summary of the subdivision of the different types of polymorphism.

1.3.1 True polymorphs

There are a variety of methods that can be used to obtain different polymorphic forms of substances, and these methods are briefly summarised in table 1.4. There are two main types of true polymorphism which include packing polymorphism and conformational polymorphism.

Table 1.4 The different method used to obtain unique polymorphic forms (Guillory, 1999:183-202)

Methods employed to obtain unique polymorphic forms
Sublimation
Crystallisation from a single solvent
Evaporation from a binary mixture of solvents
Vapour diffusion
Thermal treatment
Crystallisation from the melt
Rapidly changing the solution pH to precipitate acidic or basic substances
Thermal desolvation of crystalline solvates
Growing crystals in the presence of additives
Grinding

1.3.1.1 Packing polymorphism

Packing polymorphism is considered to be a classic type of polymorphism, since it occurs when conformationally rigid molecules are packed differently in the unit cells as a result of different intermolecular forces. Examples of packing polymorphism are shown in figure 1.7 (a) for the two polymorphic forms of nabumetone, and figure 1.7 (b) for the four polymorphic forms of carbamazepine, which clearly illustrate how molecules with the same conformation are packed differently in these different polymorphic forms. As seen in figure 1.7 (a), the packing of nabumetone in the two polymorphic forms differ, with the molecules packed head-to-tail in form I and tail-to-tail head-to-head in form II. The polymorphic forms of carbamazepine also demonstrate different packing arrangements of the carbamazepine dimmers (Vippagunta, 2001:7; Byrn *et al.*, 1999:145-146; Rodrígues-Spong *et al.*, 2004:254-255).

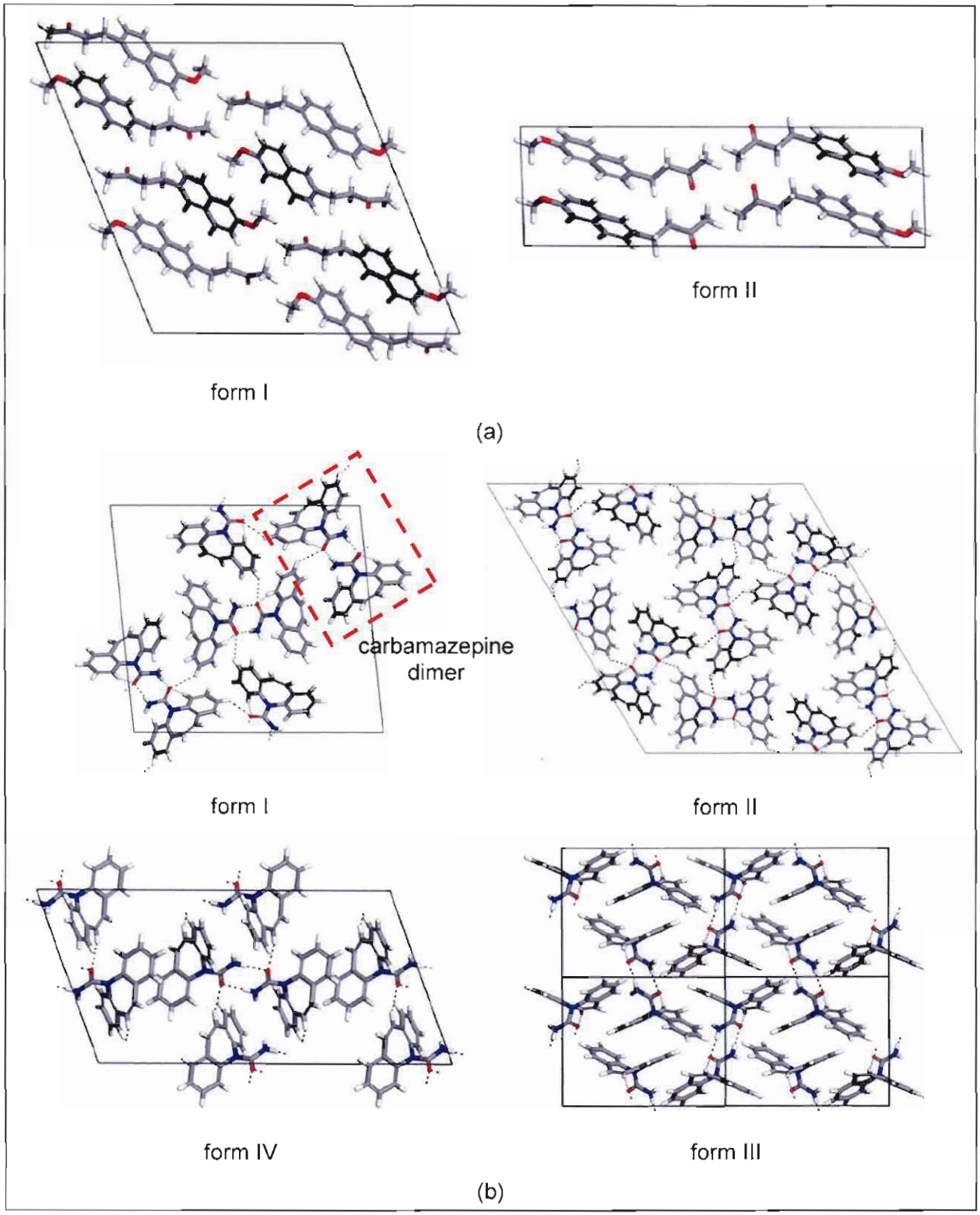

Figure 1.7 The crystal packing diagrams of (a) nabumetone form I and II, and (b) carbamazepine forms I, II, III and IV (Rodrígues-Spong *et al.*, 2004:254-255).

1.3.1.2 Conformational polymorphism

Conformational polymorphism occurs when conformationally non-rigid molecules of the same compound crystallise into different polymorphic forms as a result of the folding of the molecules into different arrangements in three dimensions (i.e. different conformations of the molecules). The term configurational polymorphism is used to describe crystals in which the constituent molecules exist as different isomers of the same molecule (i.e. geometric isomerism such as *cis*, *trans* isomers or tautomers, or different *E* and *Z* isomers). However, the term polymorphism is not applicable in this case, since such crystals are in fact comprised of different molecules. Crystal structures that differ only as a result of different tautomers of the constituent molecules, are also referred to as desmotropes, and this is exemplified by the polymorphs of the drug irbesartan. Figure 1.8 illustrates an example of conformational polymorphism for the drug sulfapyridine. Forms II, III and IV of sulfapyridine are in fact packing polymorphs, since the sulfapyridine molecule has similar conformations in these three polymorphs, but form V is unique in that it contains two different conformers of sulfapyridine in the same unit cell (Vippagunta, 2001:7; Byrn *et al.*, 1999:151-152; Lohani & Grant, 2006:22; Ochsenbein & Schenk, 2006:144-147; Rodrígues-Spong *et al.*, 2004:256).

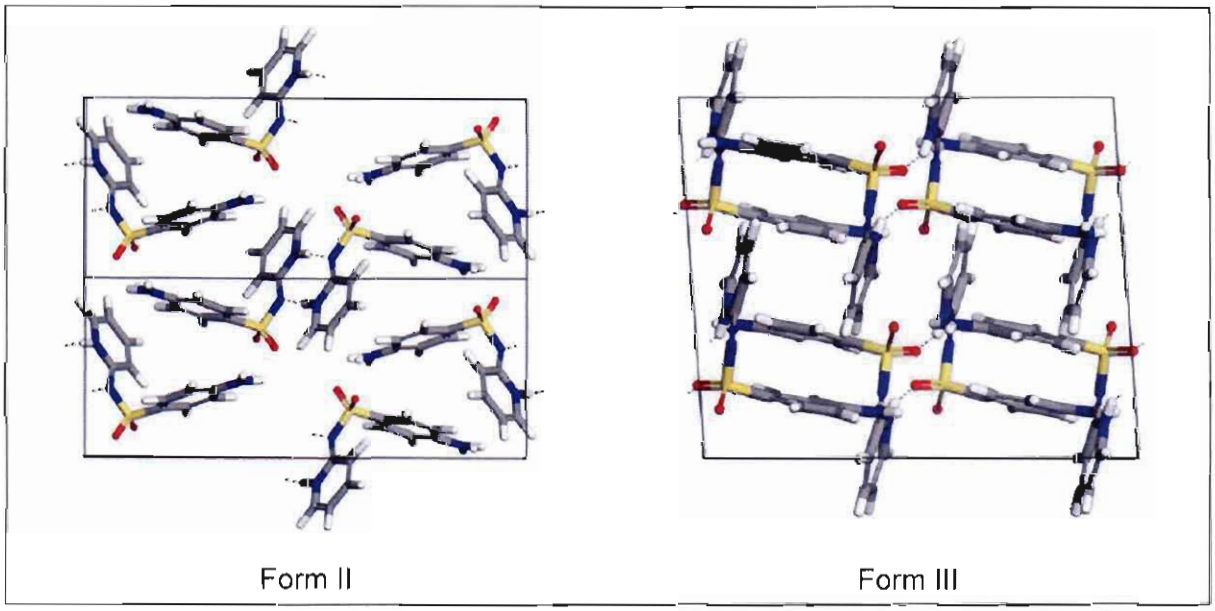

Figure 1.8 The crystal packing diagram of the conformational polymorphs of sulfapyridine (Rodrígues-Spong *et al.*, 2004:256).

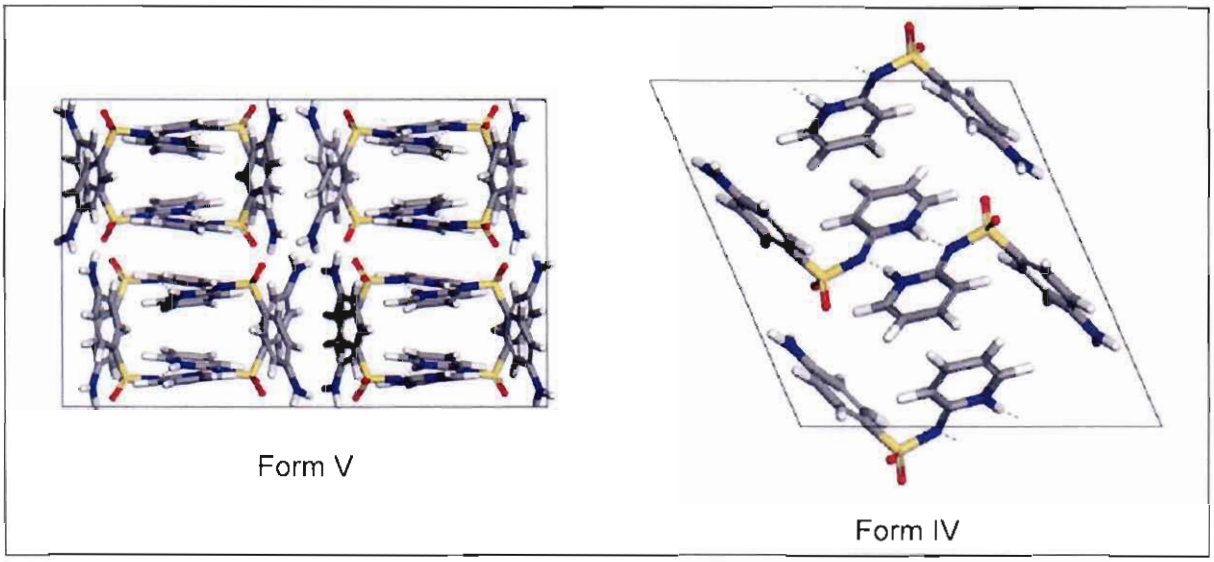

Figure 1.8 (continued)

1.3.2 Polychromism

Polychromism (pleochromism) is the term that is used when the different polymorphic forms of a substance display different colours. The most striking example of polychromism occurs in the polymorphic forms of 5-methyl-2-[(2-nitrophenyl)amino]-3-thiophenecarbonitrile (also known as ROY). ROY crystallises as a variety of red, orange and yellow crystals, with the yellow crystals being most stable. The different colours of the crystals are caused by the different conformations adopted by the ROY molecules in each crystal structure. The different conformations of ROY are the result of a variation in the intramolecular hydrogen bonding between the amine and the nitro substituents, resulting in an out-of-plane rotation of the phenyl and thiophene rings (see figure 1.9), decreasing the electron delocalisation of the system, which is presumed to be the source of the different colours (Yu *et al.*, 2000:585; Byrn *et al.*, 1999:156-157, Smith *et al.*, 1998:11711).

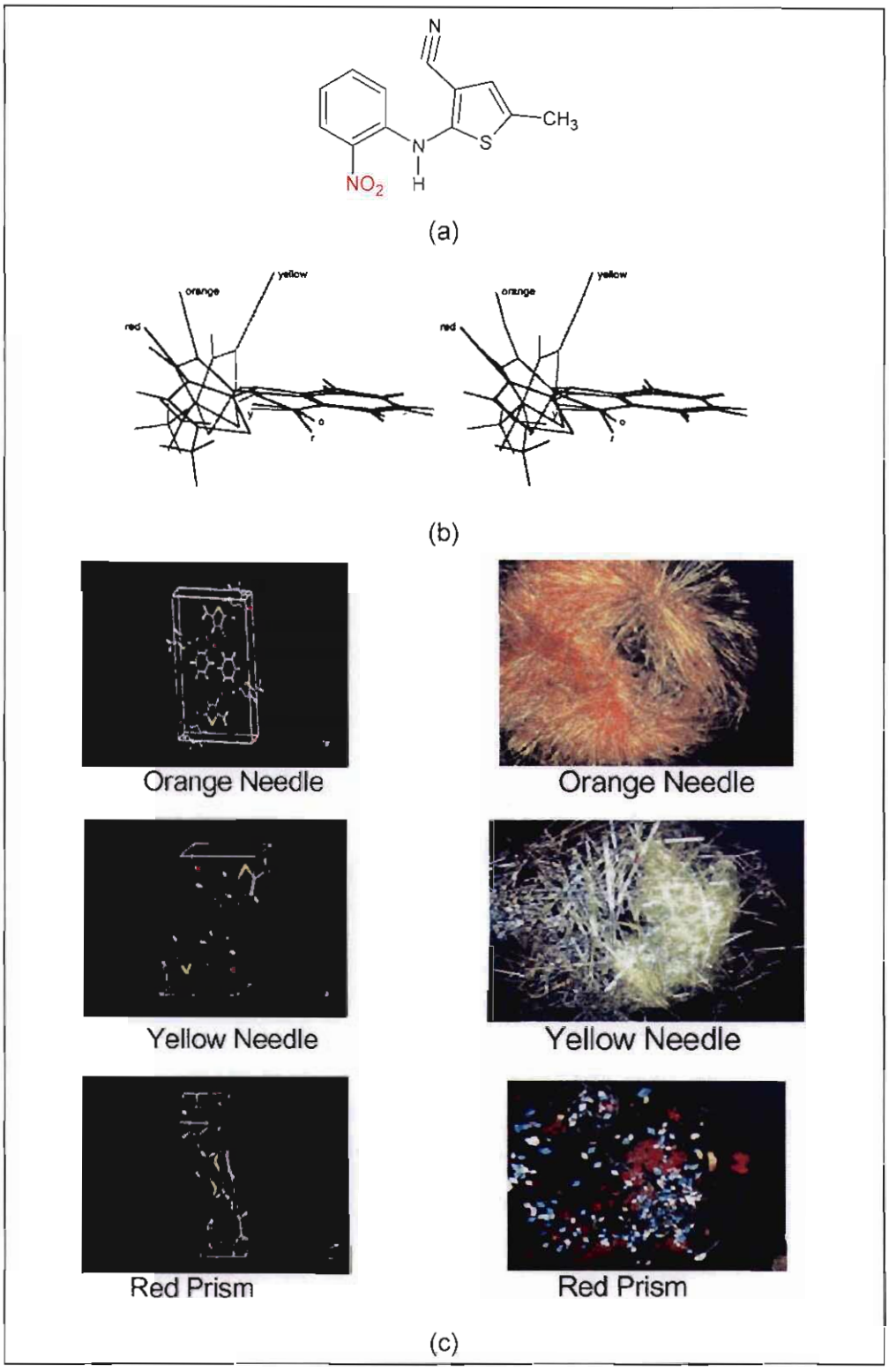

Figure 1.9 (a) The chemical structure of ROY indicating the nitro and the amine substituents responsible for the intramolecular hydrogen bonding. (b) An illustration of the different conformations of the thiophene ring responsible for the different colours of each polymorphic form. (c) The packing diagrams of the various colour crystals of ROY with photomicrographs of the crystals (Yu *et al.*, 2000:585; Byrn *et al.*, 1999:156-157; Stephenson, 2005:6).

Another example of polychromism is the dye, copper phthalocyanine (CuPc), which has four different colour polymorphic forms (α, β, γ and ε), which also forms the basis of its wide application in the dye industry. Figure 1.10 illustrates the packing diagrams for the four different polychromes of CuPc (Erk *et al.*, 2004:479-480).

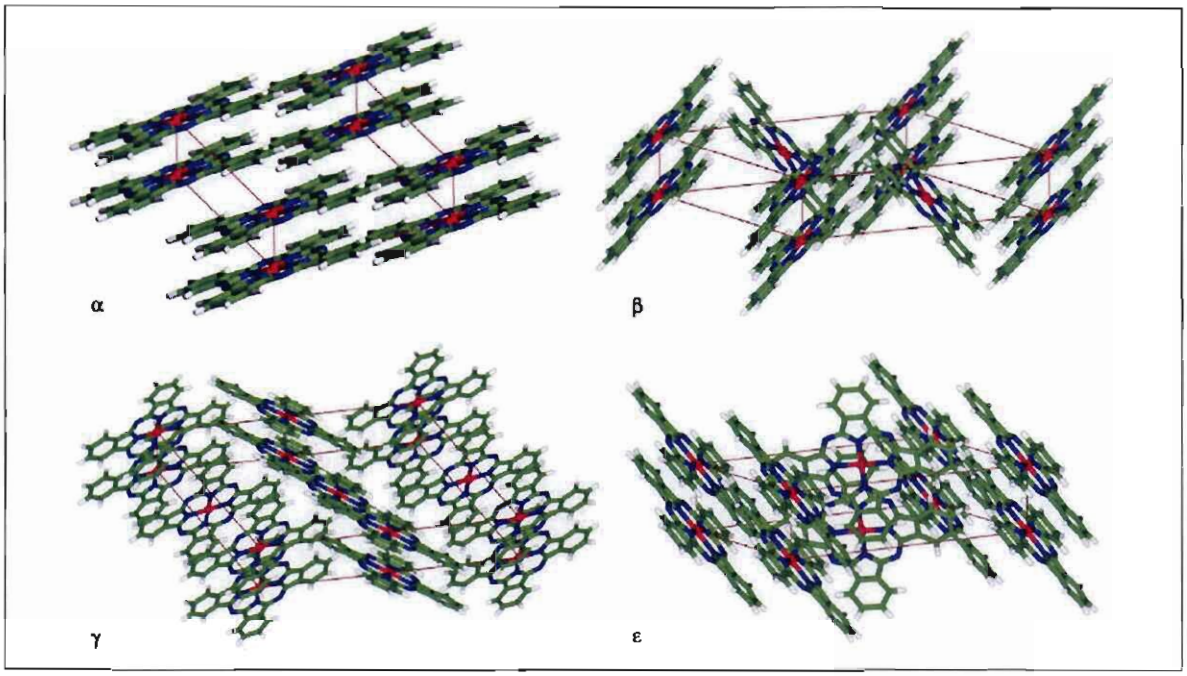

Figure 1.10 The packing diagrams of the polychromes of CuPc (Erk *et al.*, 2004:479-480).

1.3.3 Pseudopolymorphism (solvatomorphism)

Pseudopolymorphs are different crystal forms, which in addition to containing the same chemical substance than the true polymorphic forms, also have solvent molecules incorporated into the unit cells of the crystal. The solvent molecules can either be an organic solvent (in which case the pseudopolymorph is known as a solvate), or it can be water (in which case the pseudopolymorph is known as a hydrate). The solvates and hydrates of a substance have different properties compared to the true polymorphs of the same substance, hence the name pseudopolymorphs. The solubility and dissolution rate of the solvate is lower in the corresponding solvent which is included into the unit cells, when compared to that of the anhydrous polymorphs. This difference in the solubility of the different solvates of a drug was demonstrated for the various solvates of the anthelmintic drug niclosamide (Byrn *et al.*, 1999:13; Lund, 1994:179; Van Tonder *et al.*, 2004:1; Lohani & Grant, 2006:37).

It is possible for the pseudopolymorph to contain both an organic solvent and water in the same unit cell, and the most well known example of such a mixed solvate is doxycycline hydrochloride hyclate ([doxycycline · $HCl]_2C_2H_6O$ · H_2O), which is a hemi-ethanolate

hemihydrate, i.e. for every two doxycycline hydrochloride in the unit cell there is one ethanol and one water molecule. Another characteristic feature of pseudopolymorphs is that the stoichiometric ratio between the solvent molecules in the unit cell and the host molecules may vary between different pseudopolymorphic forms, and the most common encountered ratio being 1:1, whilst non-stoichiometric ratios are also possible (Guillory, 1999:203-208; Stezowski, 1977:1122).

1.3.3.1 Solvates

The techniques that are used to prepare solvates are similar to the methods used to prepare polymorphs, i.e. crystallisation from a single solvent, crystallisation from mixed solvents or vapour diffusion. There are a great variety of drugs that form solvates, including the anti-epileptic drug carbamazepine which has three solvates including a hydrate, an acetone solvate and an acetic acid solvate. The packing diagrams of these three solvates are illustrated in figure 1.11 (Guillory, 1999:205-206; Rodrígues-Spong *et al.*, 2004:256).

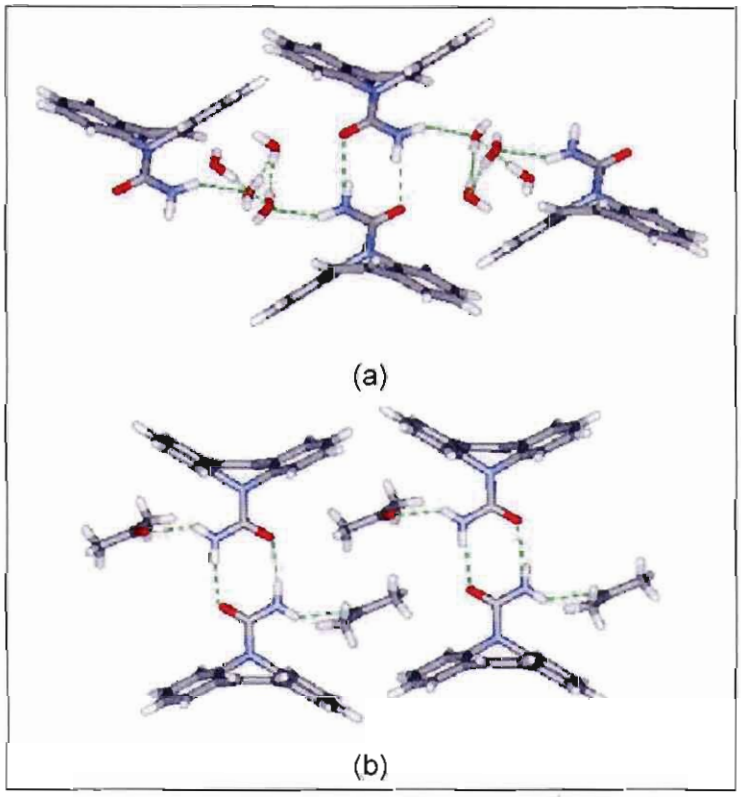

Figure 1.11 The packing diagrams of the three solvates of carbamazepine: (a) hydrate, (b) acetone solvate and (c) acetic acid solvate (Rodrígues-Spong *et al.*, 2004:256).

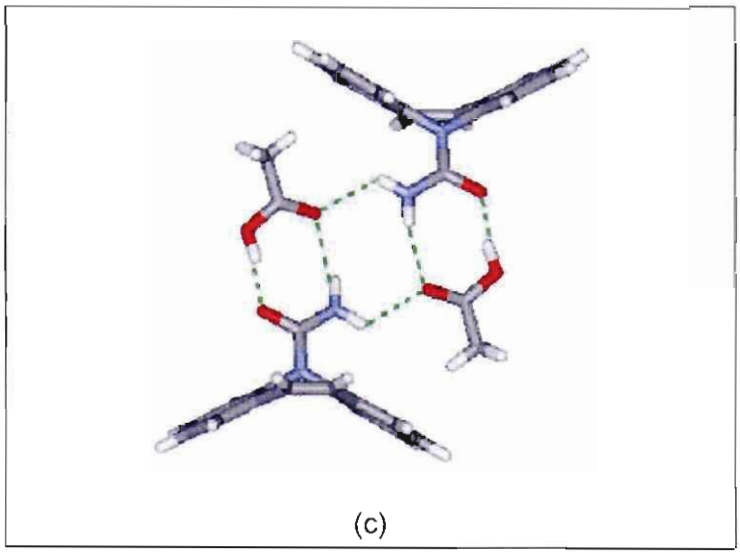

(c)

Figure 1.11 (continued)

1.3.3.2 Hydrates

Hydrates of drug molecules are prepared by simply recrystallising the anhydrate of the drug from water, or from binary mixtures of solvents containing water, or by exposing the anhydrous powder of the drug to high relative humidity which may result in the formation of a hydrate. Hydrates are classified according to the structure of the crystalline lattice that is formed by the inclusion of water molecules. Table 1.5 summarises the structural classification of hydrates (Guillory, 1999:202-205; Perold, 2006:242).

Table 1.5 The classification of crystalline hydrates (Morris, 1999:141)

Class	Description	
1	Isolated lattice sites	
2	Lattice channels	2a Expanded channels (non-stoichiometric)
		2b Lattice planes
		2c Dehydrated hydrates
3	Metal-ion coordinated water	

1.3.3.2.1 Class 1: Isolated site hydrates

In this class of hydrates, the water molecules in the crystal lattice are isolated from other water molecules as a result of the intervening drug molecules (i.e. the water molecules in the hydrate are packed in the unit cells of the crystal and are not in contact with the water molecules from adjacent unit cells). Cephradine dihydrate is an example of such a hydrate. The unit cell of this crystal contains two molecules of cephradine and four molecules of

water, which are isolated pairs of water forming hydrogen bonds with each other and with the cephradine molecules. Nitrofurantoin monohydrate is another example of this class of hydrate, and its unit cell is illustrated in figure 1.12 (Morris, 1999:142-143; Florey, 1976:37-43; Pienaar, 1994:129; The Danish University of Pharmaceutical Sciences, 2006).

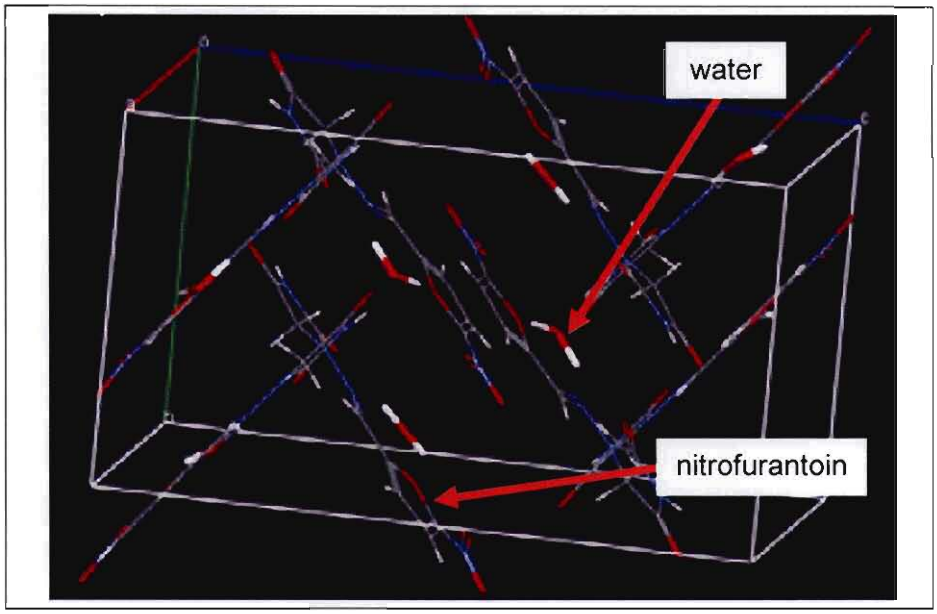

Figure 1.12 A packing diagram of the nitrofurantoin monohydrate unit cell showing the isolated water molecules in the unit cell (The Danish University of Pharmaceutical Sciences, 2006).

1.3.3.2.2 Class 2: Lattice channels

In the second class of hydrates, the water molecules of adjacent unit cells lie along an axis in the crystal lattice resulting in the formation of "channels" of water molecules through the crystal. An example of a drug that forms water channels in its crystal lattice is ampicillin trihydrate. Its crystal lattice contains channels in which the water molecules are hydrogen bonded to four other water molecules, as well as to two ampicillin molecules. The crystal lattice of niclosamide monohydrate also forms a water channel, as well as theophylline monohydrate and the hydrate of 1,8-dipyridylnaphthalene (see figure 1.13) (Morris, 1999:142-143; Ivashkiv, 1973:17-19; Rodrigues-Spong *et al.*, 2004:256; The Danish University of Pharmaceutical Sciences, 2006; Mei & Wolf, 2006:378).

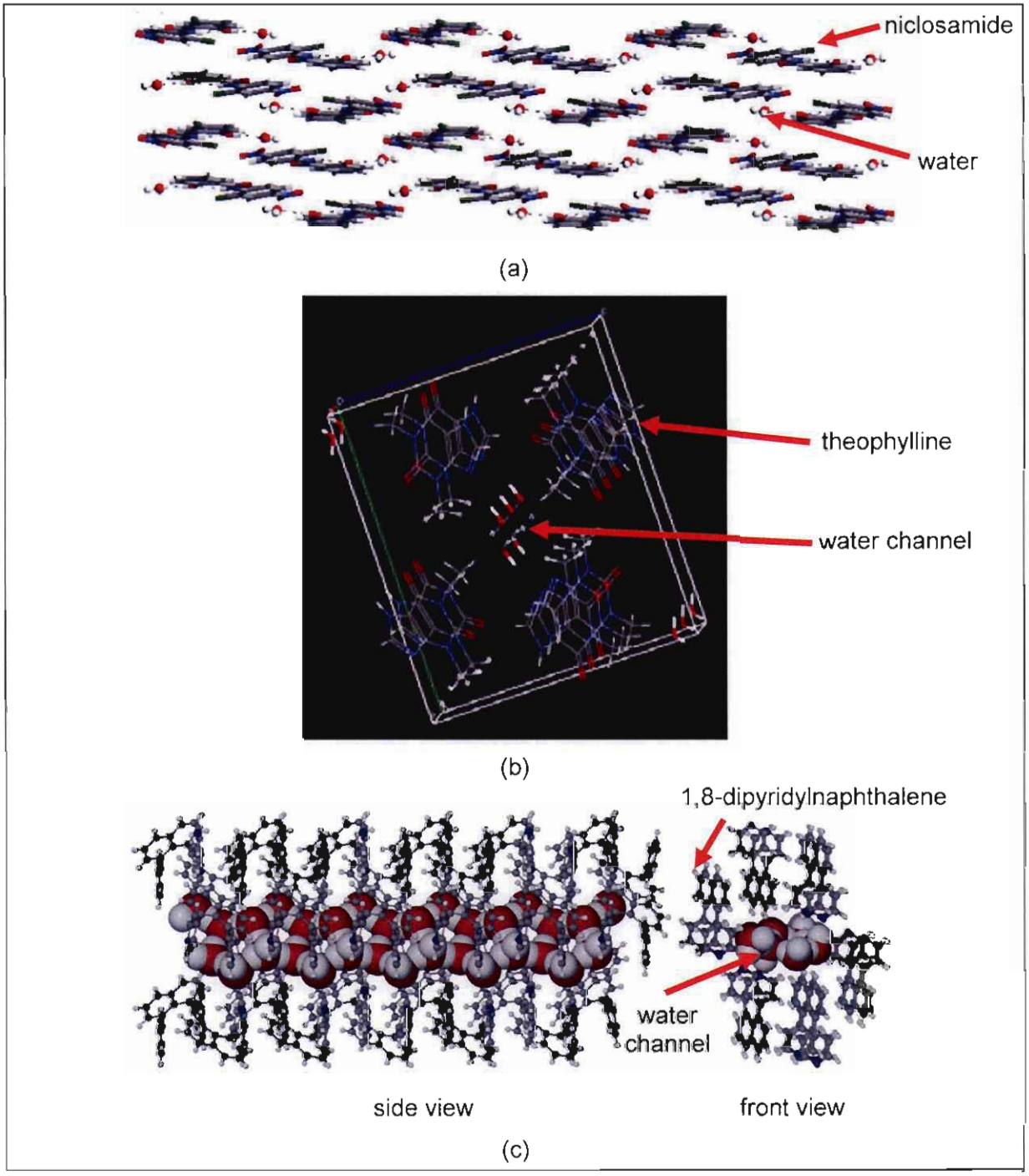

Figure 1.13 The packing diagrams of (a) niclosamide monohydrate, (b) theophylline monohydrate, and (c) the hydrate of 1,8-dipyridylnaphthalene illustrating the water channels in the crystal structures (Rodrígues-Spong *et al.*, 2004:256; The Danish University of Pharmaceutical Sciences, 2006; Mei & Wolf, 2006:378).

Expanded channel hydrates are a form of channel hydrates in which the water channels incorporate additional moisture at high humidity, and this is demonstrated by the hydrate of chromylin sodium in which water channels expand to accommodate more water molecules

(i.e. a non-stoiciometric ratio of organic molecules to water molecules). The crystal expands until the channels are too large to maintain the same crystal structure, resulting in the formation of another crystal structure, or the formation of an amorphous form (Cox *et al.*, 1971:1458).

Lattice planes (or planar hydrates) are crystalline hydrates that have their water localised in two dimensional order, and this type of crystal lattice is demonstrated by the hydrate of sodium ibuprofen, in which the water of hydration is ion associated (Morris, 1999:153-154).

1.3.3.2.3 Class 3: Metal-ion coordinated water

In this class of hydrates the water molecules are coordinated with a metal ion, and examples of molecules that demonstrates this type of hydrate structure is calteridol calcium and disodium uridine diphosphoglucose dihydrate (as illustrated in figure 1.14) (Morris, 1999:155-158; The Danish University of Pharmaceutical Sciences, 2006).

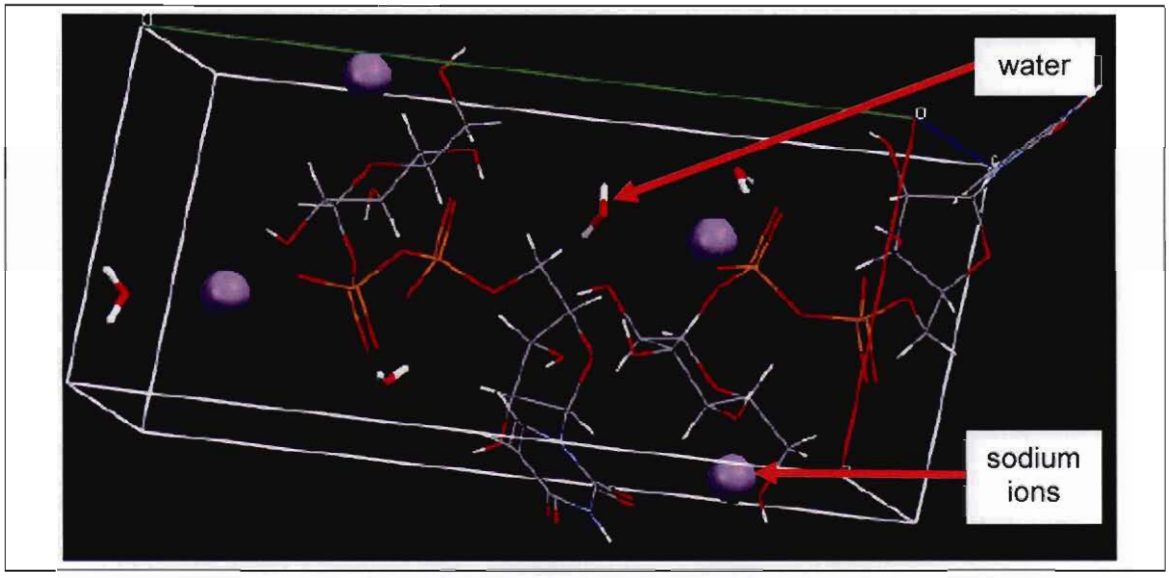

Figure 1.14 The packing diagram of the unit cell of disodium uridine diphosphoglucose dihydrate (The Danish University of Pharmaceutical Sciences, 2006).

1.3.3.3 Isostructural solvates

When the different solvates of a substance crystallise to form identical crystal structures, but with different solvents, it is termed isostructural solvates or isomorphic solvates. Isostructural solvates show only small distortions in the unit cell dimensions and the host molecules in these different solvates are in the same conformation and packing in the different unit cells. This phenomenon was clearly demonstrated by the macrolide antibiotic, dirithromycin, which crystallised into two anhydrous polymorphic forms, one amorphous form and nine

stoichiometric solvate forms, of which six of these are isomorphic (they have identical X-ray powder diffraction patterns although they are different solvates composed of different solvents) (Griesser, 2006:218; Stephenson *et al.*, 1994:5767).

1.3.4 Desolvated solvates (pseudomorphs)

Desolvated solvates are sometimes classified as a separate class of polymorphism and involves the desolvation of the solvate with the original crystal structure remaining intact afterwards. Since no solvent molecules remain in the unit cells after the desolvation, this is a new polymorph (called an isomorph) that forms and is not classified as a solvate or a hydrate anymore. The desolvation process thus leaves the crystal lattice intact, resulting in the formation of an isomorph (i.e. a solid that has a similar X-ray diffraction pattern compared to the original solvated form). The loss of the solvent molecules from the crystal lattice may also result in the collapse of the crystal structure, since the intermolecular forces between the residual molecules are insufficient to compensate for the lost solvent, and an amorphous solid is thus formed. An example of a drug which solvate demonstrates this phenomenon is carbamazepine dihydrate, which becomes amorphous after dehydration at 45°C, and it illustrates that desolvation of this hydrate reduces the physicochemical stability of this solid and leads to a loss of crystallinity of carbamazepine dihydrate. A pseudomorph (desolvated solvate) may also be formed during the recrystallisation process by the spontaneous loss of the solvent, and this process is called paramorphosis (Morris, 1999:154; Yu, 2001:29; Yu *et al.*, 1998:124; Nichols, 2006:205).

1.3.5 Co-crystals

The term co-crystal is mistakenly used to refer to solvates, however co-crystals are very similar to solvates, the only difference being that the substance that is incorporated into the crystal unit cell is a solid at room temperature, and not liquid as in the case of solvates. An example of this phenomenon is clearly demonstrated in figure 1.15 for the co-crystals of carbamazepine containing (a) saccharin, (b) nicotinamide and (c) 5-nitroisophthalic acid (Griesser, 2006:214; Rodrígues-Spong *et al.*, 2004:261).

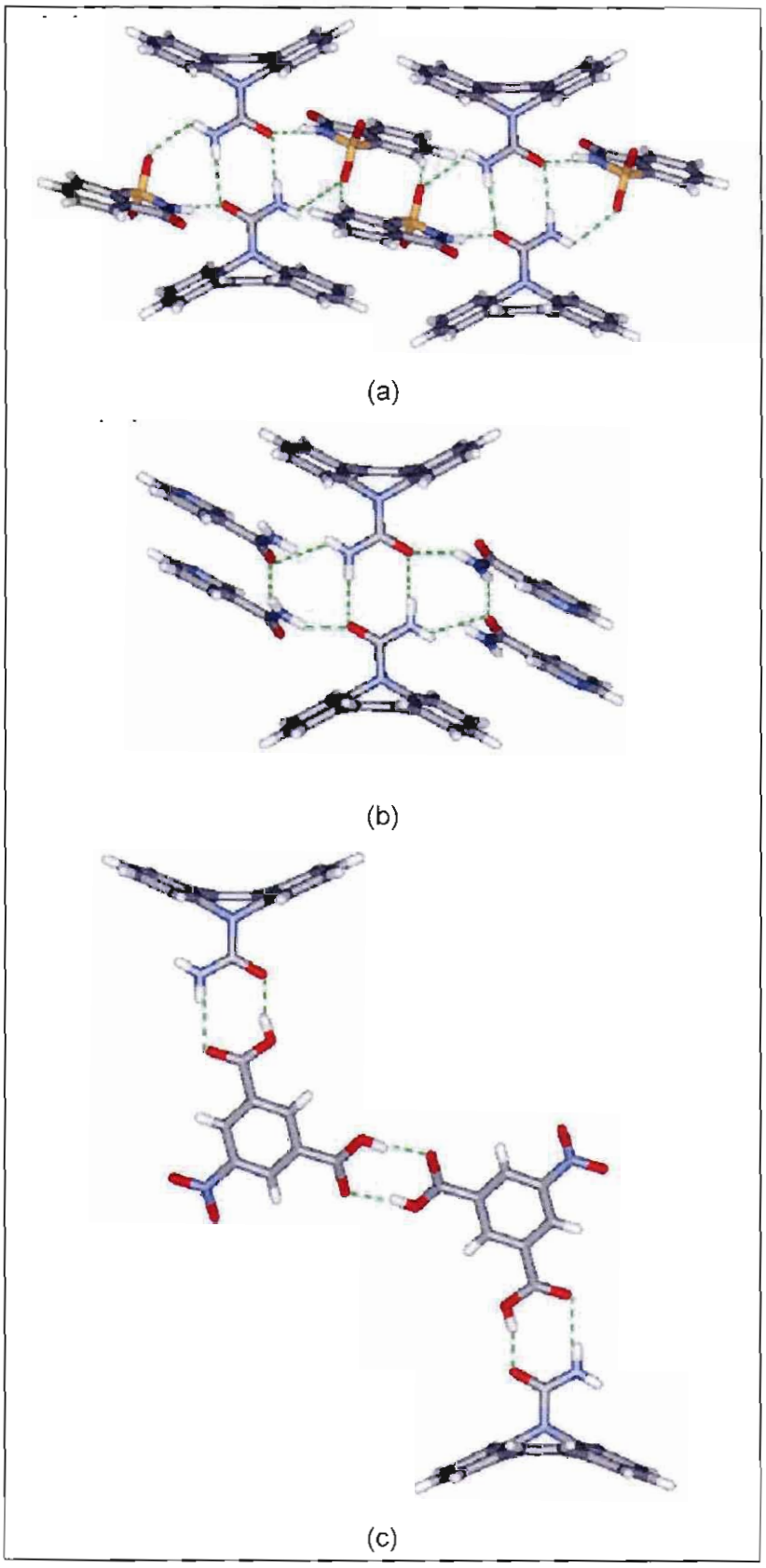

Figure 1.15 The packing diagrams of the co-crystals of carbamazepine: (a) carbamazepine-saccharin, (b) carbamazepine-nicotinamide and (c) carbamazepine-5-nitroisophthalic acid (Rodrígues-Spong *et al.*, 2004:261).

1.3.6 Amorphous solids

Amorphous solids are defined as solids having no long range order like crystalline solids, they are not crystalline and give no unique X-ray diffraction pattern, they have no crystal faces and they do not demonstrate birefringence of polarised light (i.e. light of a single wavelength travels through amorphous solids at equal velocity in all directions and are not split into different colours of light). Simply put, the molecules or atoms that constitute amorphous solids are not arranged into unit cells like crystalline solids, but are non-uniformly arranged throughout the solid (amorphous solids can be viewed as an extension of the liquid state of the specific substance). Amorphous solids do have some short range order which include the same hydrogen bonds between molecules for the length of a few Angstroms (Byrn *et al.*, 1999:22,249-250).

There are three circumstances that result in the possible formation, or existence, of the amorphous state. Firstly, the deliberate production of amorphous solids by freeze drying or glass formation in order to enhance dissolution behaviour of the drug; secondly, the substance existing in the amorphous state at ambient conditions (example polyvinylpyrrolidone); and thirdly, the accidental generation of the amorphous state during the manufacturing process of the dosage form of the drug (Craig *et al.*, 1999:180).

Amorphous materials can be prepared through a variety of methods, including solidification of the melt of a drug, reduction in the particle size, spray-drying, lyophilisation, removal of a solvent from a solvate or a hydrate, or by precipitation of acids or bases by a change in the pH. A recently developed method used for the preparation of amorphous solids involves using super critical fluid technology (two techniques called (1) Solution Enhanced Dispersion by Supercritical fluids (SEDS) and (2) Rapid Expansion of Supercritical Solution (RESS)) to obtain an amorphous form of a substance. SEDS was applied to obtain an amorphous form of sodium chromoglycate from a methanol solution, and it is also applied to control the polymorphic form of a drug and for the micronisation of drugs. The most common methods used to obtain an amorphous form of a drug are illustrated in figure 1.16 (Guillory, 1999:184; Bernstein, 2002:254; Hancock & Zografi, 1997:1; Yu, 1999:436).

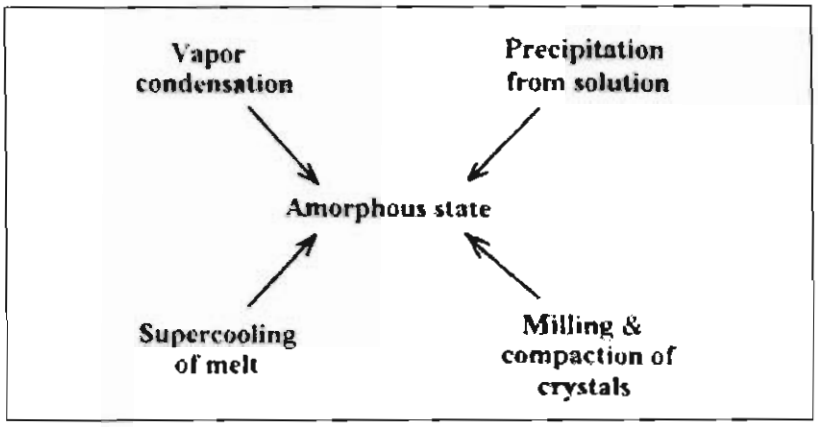

Figure 1.16 A schematic diagram of the most common methods used to obtain an amorphous form of pharmaceuticals (Hancock & Zografi, 1997:1).

Figure 1.17 illustrates the difference in the formation of amorphous and crystalline solids, and it is clear that a decrease in the temperature from the liquid state to the melting point (T_m) results in the transition to the crystalline state, whilst for a glass forming material the cooling process is too fast for crystallisation to take place resulting in the formation of a glass (Craig *et al.*, 1999:181).

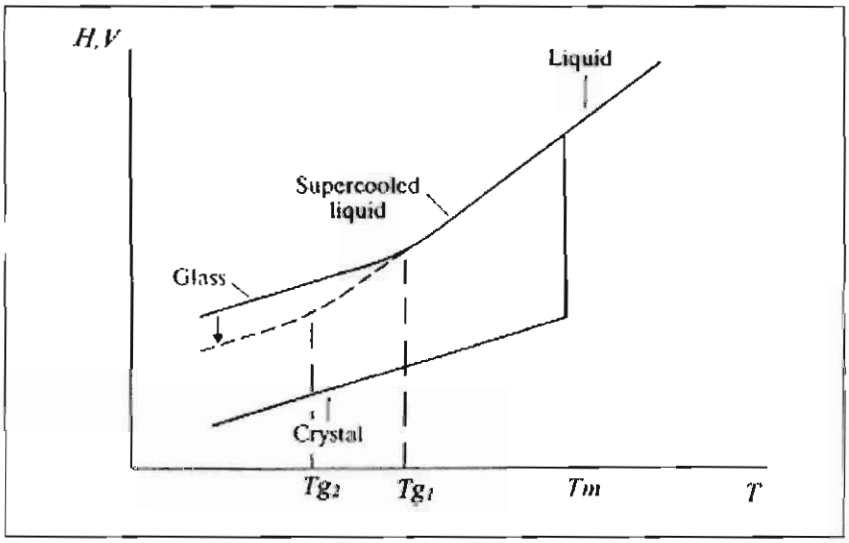

Figure 1.17 A diagram illustrating the difference in the formation of a glass and a crystalline solid (Craig *et al.*, 1999:181).

Another characteristic feature of amorphous solids is the glass transition temperature (T_g) (see figure 1.17) which is defined as the temperature below which the molecules in the amorphous solid are frozen in a glassy state, and thus lack the motion of molecules in the liquid state. Above the glass transition temperature the molecules are said to be in a rubbery state and will flow, thus the molecules have substantially more configurational motion than in the glassy state. There is, however, not an exact definition of the glass transition, but it has

been described as (1) a second order thermodynamic phase change, as (2) an equilibrium process involving excess entropy, or as (3) a kinetic relaxation process. For the majority of amorphous solids the ratio between the glass transition temperature and the melting temperature is between 0.7 and 0.85, indicating that the glass transition temperature of the amorphous form may be estimated if the melting temperature is known. Glasses are also classified as fragile glasses when the ratio T_m/T_g is less than 1.5, and strong glasses when this ratio is greater than 1.5 (low molecular weight pharmaceuticals tend to form fragile glasses). The glass transition temperature is, however, not a constant value and fluctuates depending on the rate of cooling of the melt, with a slower cooling rate resulting in a lower T_g (see figure 1.17, the difference between T_{g1} and T_{g2}). The glass transition temperature of a batch of amorphous material (prepared using exactly the same method), however, stays constant, and a plot of $1/T_g$ versus the logarithm of the heating rate should yield a linear relationship (Byrn *et al.*, 1999:22,249-250; Craig *et al.*, 1999:183-184; Fukuoka *et al.*, 1986:4316).

Amorphous solids are of great interest because of their superior solubility and dissolution rate, compared to the crystalline solids of the same substance. Figure 1.18 illustrates that the amorphous/glassy form of indomethacin has a greater dissolution rate and solubility compared to the crystalline gamma-form. The amorphous form of a poorly soluble drug thus offers an alternative that could be used in a dosage form to increase the bioavailability of such a drug (Byrn *et al.*, 1999:250; Fukuoka *et al.*, 1986:4318).

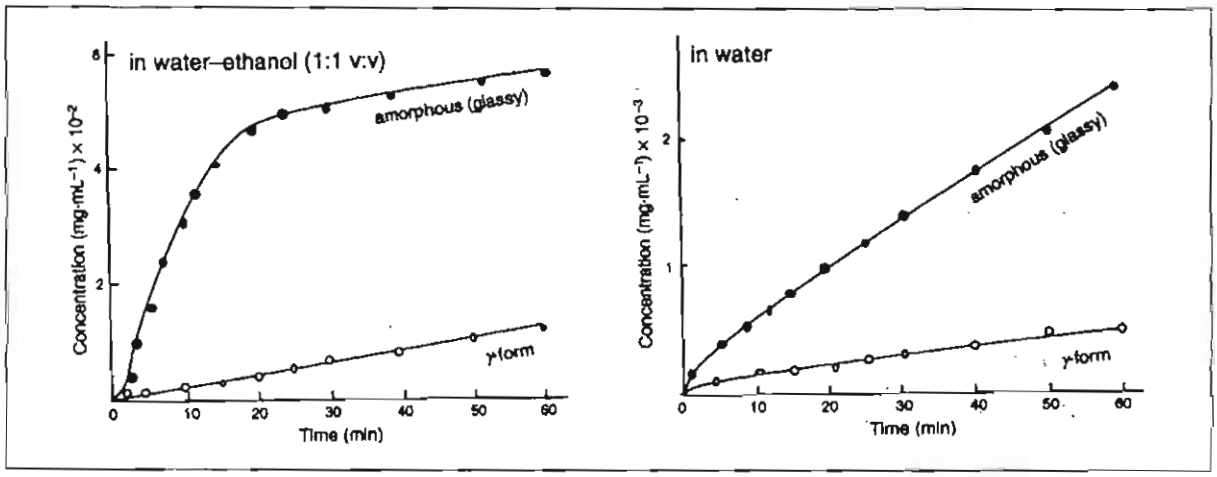

Figure 1.18 The dissolution profile of the amorphous and the γ-form of indomethacin (Fukuoka *et al.*, 1986:4318).

Amorphous solids have no long range order, i.e. there are only weak intermolecular forces between the molecules, and this result in amorphous solids being highly soluble but also highly unstable (chemically and physically), when compared to crystalline solids. Amorphous

solids also show a greater vapour sorption behaviour compared to the crystalline state. Amorphous materials are thermodynamically metastable with respect to the crystalline form, thus the amorphous form will eventually transform to the crystalline form (a process known as devitrification). This was demonstrated for the glassy form of phenobarbital which completely devitrified within a week after preparation. Figure 1.19 demonstrates the temperature dependence of crystallisation from the glassy state, and it is clear that in order to limit vitrification of the glass, it has to be kept below its glass transition temperature (T_g). However this may not prevent vitrification since the nucleation rate is at a maximum below the glass transition temperature and some crystallisation may still occur at this point (Byrn *et al.*, 1999:256; Fukuoka *et al.*, 1989:1047; Hancock & Zografi, 1997:9).

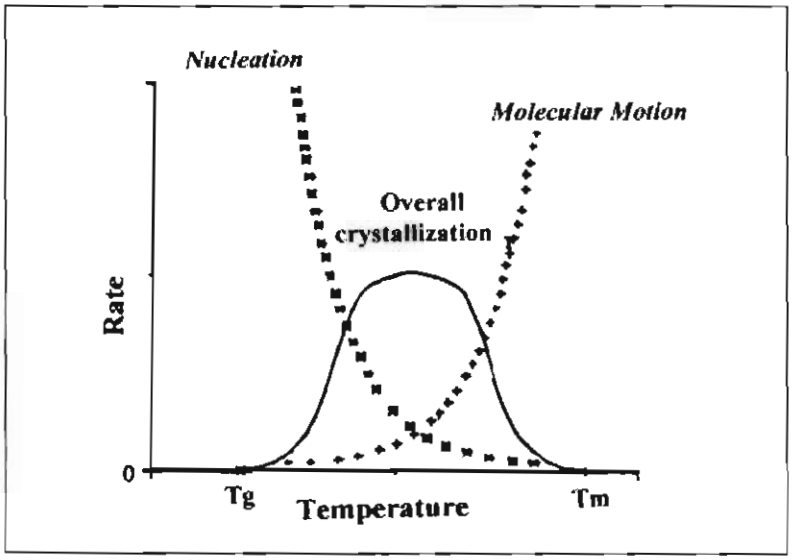

Figure 1.19 A schematic representation of the temperature dependence of the crystallisation process of amorphous solids (Hancock & Zografi, 1997:9).

One of the first examples demonstrating the chemical instability of amorphous solids is the amorphous forms of potassium penicillin G and sodium penicillin G, which are significantly less stable than the crystalline forms. The crystalline forms can withstand dry heat for several hours, but when the amorphous forms are exposed to the same temperatures, it results in a loss of activity of the dosage forms. A similar phenomenon exists between amorphous and crystalline cephalosporins, specifically cephalotin sodium, which was proven to be highly unstable compared to the crystalline solids of this antibiotic. The amorphous form of cephalotin sodium had an accelerated rate of degradation (oxidation and hydration), resulting in a loss of the antibacterial effect compared to the crystalline form. This accelerated degradation is as a result of the increase in the sorption of water by the amorphous cephalotin sodium which results in the drug degrading more rapidly (Byrn *et al.*, 1999:256; Pfeiffer, 1976:848; Pikal *et al.*, 1977:1312).

The term polyamorphism is used to describe the existence of two or more distinct amorphous forms of a single substance (for example a fragile and a strong glass of the same substance), and triphenyl phosphite (TPP) is an example of a compound that displays polyamorphism. TPP has three known different amorphous phases, which include a supercooled liquid, glacial TPP and glass TPP (Yu, 2001:31; Kivelson & Tarjus, 2002:633-634).

Amorphous solids are not usually favoured for use in commercial pharmaceutical products as a result of their instability and tendency to recrystallise. However, amorphous solids can be stabilised by dispersing the amorphous form in polyvinylpyrrolidone or by using nano-coating with polymeric substances to inhibit nucleation and crystal growth in the amorphous solid. These two methods were successfully used to inhibit the surface vitrification of amorphous indomethacin. Novobiocin is an example of a drug of which the amorphous form is used commercially, since the crystalline form is poorly soluble and thus poorly absorbed, and does not yield therapeutic blood levels after administration. However, the solubility of the amorphous form of novobiocin is 70 times greater than the crystalline form, and thus the amorphous form is used exclusively in pharmaceutical formulations in order to ensure that therapeutic blood levels are attained (Byrn *et al.*, 1999:22; Bernstein, 2002:254; Wu *et al.*, 2006:1; Mullins & Macek, 1960:245).

1.4 Patents and polymorphism

The year 2005 was a record year for the pharmaceutical industry worldwide, and for the first time ever global spending on prescription drugs topped the 600 billion US dollar mark, with sales of prescription medication rising seven percent from 2004 to 602 billion US dollars (at the time of printing of this dissertation, no sales figures for 2006 were available in the literature). The United States still accounted for the greatest share of this spending with 252 billion US dollars worth of prescription medication being sold in the United States alone. The ten best selling drugs worldwide for the year 2005 is illustrated in table 1.6, with the corresponding annual growth rate, the annual sales for 2005 for each drug and the company that manufactures each drug product indicated. It is clear form table 1.6 that the top ten selling drugs had combined annual global sales of nearly 100 billion US dollars and accounted for 16% of global prescription sales, and that the best selling drug Lipitor®, had sales of more than double its nearest competitor (this is the fifth year that Lipitor® is the top selling drug worldwide) (Herper & Kang, 2006).

Table 1.6 The ten best selling drugs worldwide and corresponding information (Herper & Kang, 2006)

Rank	Drug	Global annual sales (US dollars)	Annual growth	Manufacturer
1	Lipitor®	$12.9 billion	6.4%	Pfizer
2	Plavix®	$5.9 billion	16.0%	Bristol-Myers Squibb & Sanofi-Aventis
3	Nexium®	$5.7 billion	16.7%	AstraZeneca
4	Advair®/ Seretide®	$5.6 billion	19.0%	GlaxoSmithKline
5	Zocor®	$5.3 billion	-10.7%	Merck
6	Norvasc®	$5.0 billion	2.5%	Pfizer
7	Zyprexa®	$4.7 billion	-6.8%	Eli Lilly
8	Risperdal®	$4.0 billion	12.6%	Johnson & Johnson
9	Prevacid®	$4.0 billion	0.9%	Abbot Laboratories & Takeda Pharmaceuticals
10	Effexor®	$3.8 billion	1.2%	Wyeth
Total sales		**$97.3 billion**		

The reason that these drugs (and others not mentioned) generated such huge global sales in 2005, and will possibly continue to do so in the near future, is because they are still protected by patents taken out by the respective companies that originally manufactured and marketed these drugs. These patents prevent other companies, i.e. generic drug companies, from also manufacturing and selling the same products for the duration of the patent. This provides the innovator companies the opportunity to generate revenue from the sale of these drugs to recover the cost of research and development, and to generate maximum profits from the sale of these drugs. Once the patents expire, the innovator companies lose billions of dollars in sales, since generic drug companies now have the opportunity to manufacture and sell the same drug product at a fraction of the original cost. This was the case in 2006 when the patents on two of the biggest selling drugs from two of the biggest drug manufacturers worldwide expired. Zocor® (simvastatin, manufactured by Merck) and Zoloft® (sertraline, manufactured by Pfizer) both lost patent protection in June 2006 (Bernstein, 2002:297-298; Smith, 2006).

Innovator drug companies have developed strategies to protect their long term investments in, and current sales of, blockbuster drugs, and these strategies are known as pharmaceutical life-cycle management, and are intended to extend the commercial life of an innovator product. Before the product reaches the market, or after a product has been on the market for several years (i.e. before or after approval of the drug by a drug registration agency like the Food and Drug Administration (FDA)), new therapeutic uses for the drug often arise, requiring new formulations, new routes of administration and/or new dosage forms, which in turn often requires new solid states of the drug. These new dosage forms and solid states of the drug form the basis of acquiring an extension of the original patent on the drug, resulting in an increase in the period over which this drug is protected from generic competitors, and extending the period during which the innovator company can generate the maximum profits from this drug. An example of the exploitation of a different solid state of a drug in pharmaceutical life cycle management is the sodium salt of diclofenac, which was marketed as Voltaren® by Ciba-Geigy. Before the patent on Voltaren® expired, other salts of diclofenac with enhanced transdermal penetration were discovered and patented, thus enabling Ciba-Geigy to retain an exclusive position in this market segment (Blomsma, 2006; Voet, 2005:85-101; Gardner *et al.*, 2004:934; Hilfiker *et al.*, 2006:15).

Each polymorphic form of a new drug molecule may be protected by a separate patent, since each polymorphic form of the same drug substance has different physicochemical properties, and is thus considered to be a new invention that adheres to the four requirements for patentability, i.e. (1) being novel (new), (2) useful, (3) non-obvious, and (4) invented by the patent applicant. However, the scope of protection provided by polymorph patents is restricted, as was demonstrated by the patent battle between GlaxoSmithKline and Apotex, pertaining to the antidepressant drug Paxil® which contains paroxetine hydrochloride hemihydrate. Apotex manufactured a generic version of Paxil® containing paroxetine hydrochloride anhydrate and sought FDA approval of this product. Subsequently GlaxoSmithKline claimed that Apotex had infringed on its polymorph patent of paroxetine hydrochloride hemihydrate, since the anhydrous paroxetine hydrochloride is hygroscopic and transforms to the hemihydrate form over time. Apotex argued that the amount of paroxetine hydrochloride hemihydrate that forms in their dosage form is negligible and they ultimately won the legal battle, but not without this patent dispute delaying the appearance of the generic versions of Paxil® on the market. According to the FDA, whenever a patent infringement claim is made in the United States, it automatically results in the approval of that generic drug being postponed for a minimum of 30 months, and each successive patent dispute results in the approval being delayed by an additional 30 months. Polymorph patents are thus now mostly used by big pharma, not to ensure exclusivity of the polymorph of a

blockbuster drug, but to hinder the generic drug companies by delaying the appearance of their generic versions on the market. The same scenario occurred during the legal battle between the Glaxo Group (now known as GlaxoSmithKline) and Novopharm regarding the polmorph patents of the blockbuster drug ranitidine hydrochloride (marketed as Zantac®). Novopharm also won the legal battle but this process delayed the appearance of its generic ranitidine product on the market (Voet, 2005:85-101; Bernstein, 2006:366-378).

Conclusion

It is clear that polymorphism of active pharmaceutical ingredients impacts on the stability (physical and chemical), on the solubility (i.e. the bioavailability) and on the selection of a particular manufacturing process of the final dosage form of the drug. There are a variety of different types of polymorphism of chemicals, including true polymorphism, polychromism, pseudopolymorphism, desolvated solvates, co-crystals and amorphous solids. Polymorphic studies thus form an essential part of the development of a novel drug substance, and sufficient resources should be expended during the research and development of a new drug to determine the existence of all the possible polymorphic forms of the drug, before registration and large scale production commences. This should help ensure that the innovator companies can delay the marketing of generic versions of their innovator drugs in order to ensure maximum profitability and return on investments. Solid state studies should thus be part of a drug company's research and development budget for each new project and should not be regarded as a trivial process.

CHAPTER 2

Physicochemical and pharmacological properties of stavudine

Introduction

Stavudine belongs to the nucleoside reverse transcriptase inhibitor (NRTI) class of antiretroviral drugs and is a synthetic thymidine analogue and a potent inhibitor of the reverse transcriptase enzyme of the human immunodeficiency virus (HIV). It is active against both HIV-1 and HIV-2 subtypes, and it is used in combination with other antiretroviral drugs as part of the highly active antiretroviral therapy (HAART) treatment strategy in the treatment of HIV infected patients (Raffanti & Haas, 2001:1357; Riddler *et al.*, 1995:189-190).

2.1 Physicochemical properties

2.1.1 Structural formula and chemical name

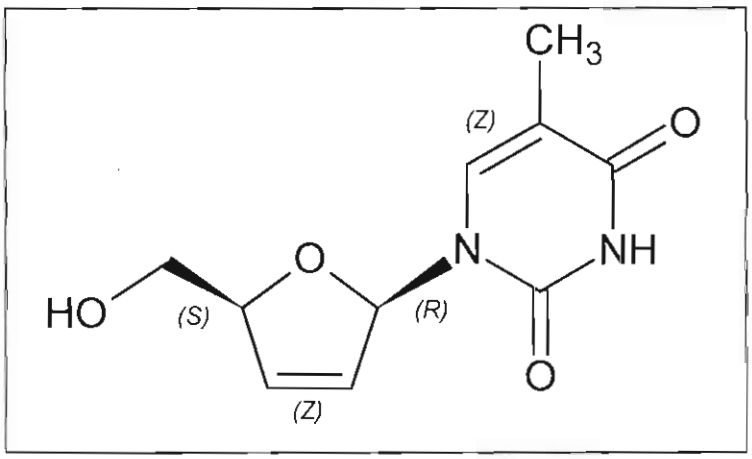

Figure 2.1 The structural formula of stavudine (Mirmehrabi *et al.*, 2006:141).

The chemical name of stavudine is 1-(2,3-Dideoxy-β-D-*glycero*-pent-2-enofuranosyl)thymine and stavudine is also known as d4T (United States Pharmacopeial Convention, 2007).

2.1.2 Molecular formula

Stavudine has the following molecular formula: $C_{10}H_{12}N_2O_4$ (Pharmaceutical Press, 2006).

2.1.3 Molecular weight

The molecular weight of stavudine is 224.21 g/mol (Pharmaceutical Press, 2006).

2.1.4 Appearance and colour

Stavudine is a white to off-white crystalline powder (Pharmaceutical Press, 2006).

2.1.5 Stability and storage instructions

Stavudine is highly labile to hydrolysis in acidic solutions, however it remains fairly stable when exposed to light and thermal stress. Stavudine should be stored in an airtight container, protected from moisture at a temperature of 25°C, and it should also be protected from light (Dunge *et al.*, 2005:1118; Pharmaceutical Press, 2006).

2.1.6 Melting point and solubility

The melting point of stavudine ranges from 164 – 174°C, depending on the solvent from which it has been recrystallised. The solubility of stavudine at 23°C is 83 mg/ml in water and 30 mg/ml in propylene glycol, and the n-octanol/water partition coefficient of stavudine at 23°C is 0.144 (Merck & Co., Inc., 2001:1567; Bristol-Myers Squibb, 2000). A more detailed description of the physicochemical properties of stavudine will be given in the next chapter.

2.1.7 Method of preparation

Stavudine was first synthesised on a small scale by Horwitz *et al.* (1966:210) at the Detroit Institute of Cancer Research in Detroit, Michigan, and since then Joshi *et al.* (1992:2537-2538) has developed another small scale synthetic pathway (see figure 2.2).

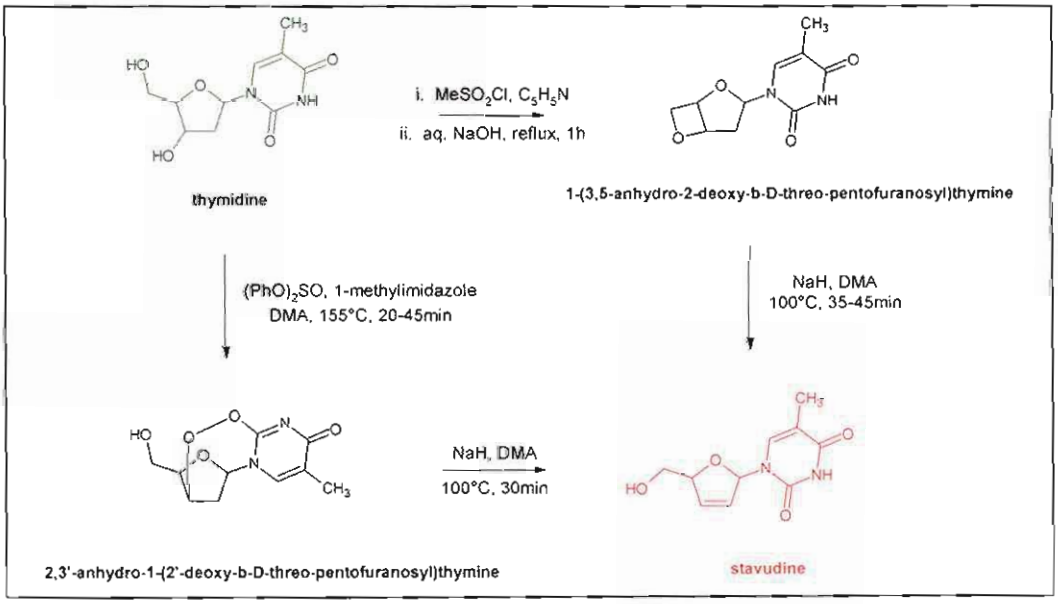

Figure 2.2 A pathway for the synthesis of stavudine developed by Joshi *et al.* (1992:2537-2538).

The large scale manufacturing process of stavudine is described by Gandhi *et al.* (1996:6), Starrett *et al.* (1990) and Lin and Prusoff (1990), whilst the biological activity of stavudine is described by Lin and Prusoff (1990).

2.2 Pharmacology

2.2.1 Indications

Stavudine is approved for the treatment of patients infected with HIV (HIV-1 and HIV-2 subtypes) in combination with other antiretroviral medication as part of the highly active antiretroviral therapy (HAART) treatment strategy (Raffanti & Haas, 2001:1357).

2.2.2 Mechanism of action

Stavudine rapidly enters cells by way of passive diffusion after which it is phosphorylated intracellularly by kinase enzymes to the active form of the drug, stavudine triphosphate (see figure 2.3). Nucleoside reverse transcriptase inhibitors (NRTIs) like stavudine are thus considered to be prodrugs because they have to be phosphorylated (activated) intracellularly to exert an antiretroviral (pharmacological) effect. Stavudine is a thymidine analogue and relies on the same enzymes which convert thymidine to deoxythymidine triphosphate, in order to be activated intracellularly (deoxythymidine triphosphate is used for the synthesis of DNA in cells). Zidovudine is dependant on this same thymidine kinase enzyme in order to be converted to its active molecule zidovudine triphosphate, but this enzyme has a 600-fold higher affinity for zidovudine than for stavudine, and it has been postulated that a combination of these two antiretroviral drugs may be antagonistic, since zidovudine would prevent the activation of stavudine to its active form (Bristol-Myers Squibb, 2000; Ho & Hitchcock, 1989:844).

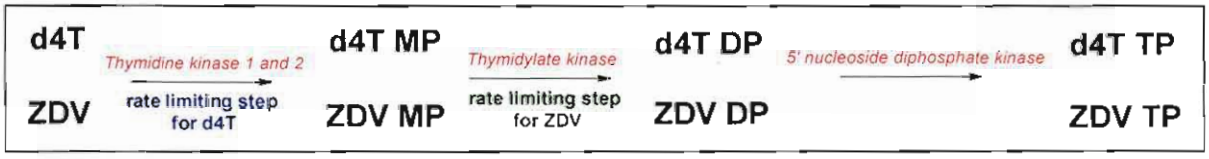

Figure 2.3 Schematic representation of the process of intracellular activation of stavudine to the active molecule stavudine triphosphate. d4T, stavudine; d4T MP, stavudine monophosphate; d4T DP, stavudine diphosphate; d4T TP, stavudine triphosphate; ZDV, zidovudine; ZDV MP, zidovudine monophosphate; ZDV DP, zidovudine diphosphate; ZDV TP, zidovudine triphosphate (Anderson *et al.*, 2004; Ho & Hitchcock, 1989:844).

In order to understand the pharmacological mechanism of action of stavudine, a brief description of the life cycle of the human immunodeficiency virus (HIV) is given (see figure 2.4):

- HIV infects a susceptible host cell by binding (adsorbing) to the CD4 receptor, found on lymphocytes (including the T4-lymphocytes which form part of the body's immune system). Binding with a chemokine co-receptor (CCR5) is also required for the HIV envelope to fuse with the host cell membrane.

- The virus' nucleocapsid (a protein shell encompassing its genetic material and reverse transcriptase enzymes) penetrates into the cell's cytoplasm where it is uncoated to release the genetic material (a single strand of RNA), the reverse transcriptase enzyme, and other necessary enzymes such as integrase.

- The reverse transcriptase enzyme transcribes the single strand of viral RNA into a single strand of viral DNA while at the same time degrading this strand of viral RNA. It then synthesizes a complementary strand of viral DNA to form a double-stranded viral DNA intermediate. The reverse transcriptase enzyme is the target of the nucleoside reverse transcriptase inhibitors, like stavudine, and the non-nucleoside reverse transcriptase inhibitors (NNRTIs) **(Stavudine triphosphate inhibits the activity of the HIV reverse transcriptase enzyme by competing with the natural substrate, deoxythymidine triphosphate, during the synthesis of the viral DNA. It also lacks the essential 3'-hydroxy group found in thymidine that enables further 3'-5'-phosphodiester linkages to be formed, and thus results in the termination of the viral DNA chain elongation process when incorporated into the viral DNA molecule)**.

- This double-stranded viral DNA intermediate then enters the host cell's nucleus and is inserted into one of the host cell's chromosomes to form a provirus. This is accomplished by the viral enzyme integrase, which could become a new target for the development of anti-HIV medications. The provirus then generates different products necessary for the formation of new virions.

- Activation of the host cell's nucleus results in the transcription of the viral DNA into viral messenger RNA (mRNA) by the enzyme RNA polymerase II. This viral mRNA is translated by the host cell's ribosomes into structural proteins, enzymes, glycoproteins and regulatory proteins, and it also serves as the viral RNA for the next generation of human immunodeficiency (HI) viruses.

- The viral RNA and viral proteins are assembled at the cell's membrane into a new HI virus. This new virus has to mature before, or directly after its release from the cell, in order to be able to infect other cells. This maturation process is facilitated by HIV proteases which transform the newly formed viral proteins into functional units, and these protease enzymes are the targets of another class of anti-HIV medications called protease inhibitors.

- The mature virion is released from the cell and acquires a piece of the cell's lipid membrane during this process, and this is believed to result in eventual cell death. The virion is now able to infect another host cell (Bristol-Myers Squibb, 2000; Gandhi *et al.*, 1999; Kaiser, 2005).

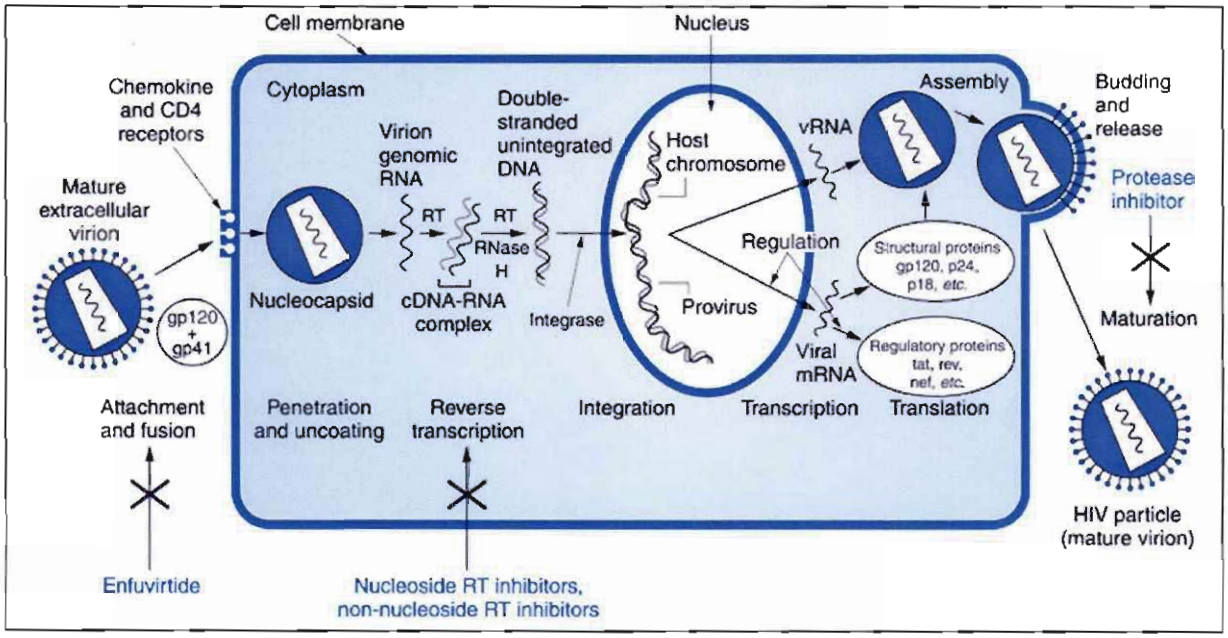

Figure 2.4 An illustration of the HIV life cycle with the different steps in this cycle, and the areas where antiretroviral drugs exert an effect (Raffanti & Haas, 2001:1350).

2.2.3 Resistance

Some strains of HIV-1 are resistant to the effects of stavudine and there are mainly two mutations in the HIV-1 reverse transcriptase gene that enables the development of resistance to stavudine. The first mutation is at codon 75 and results in a 7-fold resistance to the effects of stavudine. This mutation also confers cross-resistance to the effects of zalcitabine, lamivudine and didanosine. The second mutation is at codon 50 and results in a 30-fold resistance to the effects of stavudine but shows no cross-resistance to the effects of zidovudine or zalcitabine (Riddler *et al.*, 1995:192; Lacey & Larder, 1994:1428; Gu *et al.*, 1994).

2.3 Pharmacokinetics

2.3.1 Absorption and distribution

Stavudine is rapidly absorbed systemically after an oral dose, with the peak plasma concentration (C_{max}) occurring within 1 hour after administration, and the C_{max} and the area under the plasma concentration-time curve (AUC) increasing proportionally with an increase in the dose within the dosage range of 0.03 – 4 mg/kg. The administration of stavudine with food delays its absorption, but the bioavailability (AUC) remains the same compared to when it is administered during the fasted state. Multiple doses at 6, 8 and 12 hours show no significant accumulation in the body, whilst the systemic absorption of the capsule and the solution are identical. The binding of stavudine to serum proteins is negligible in the concentration range of 0.01 – 11.4 µg/ml, and it distributes equally between the red blood cells and the plasma, and easily crosses the blood-brain barrier (Bristol-Myers Squibb, 2000; Riddler *et al.*, 1995:194).

2.3.2 Metabolism and excretion

The metabolism of stavudine in humans has not been clearly characterised, but it is known that stavudine is metabolised intracellularly to the mono-, di- and triphosphate molecules, of which the latter is responsible for its pharmacological effect. Cretton *et al.* (1993) determined that stavudine is metabolised in the liver to thymine (which degrades to beta-aminoisobutyric acid – BAIBA), water and a novel metabolite which they designated "X". These metabolites are converted to biological macromolecules, which may explain why no metabolites of stavudine are detectable in the urine. Renal elimination accounts for 40% of the total clearance of stavudine and this means that the dosage of stavudine has to be reduced in patients with decreased creatinine clearance and in patients undergoing haemodialysis. The value of the mean renal clearance of stavudine is twice the value of the endogenous creatinine clearance, indicating that stavudine undergoes active tubular secretion and glomerular filtration in the kidneys. The intracellular half-life of stavudine triphosphate, the active metabolite of stavudine, is 3.5 hours. The pharmacokinetic data of stavudine is summarised in table 2.1 (Bristol-Myers Squibb, 2000; Pharmaceutical Press, 2006).

Table 2.1 Pharmacokinetic parameters of stavudine in adult and paediatric HIV-infected patients (Bristol-Myers Squibb, 2000)

Parameter	Adult patient	Paediatric patient
Oral bioavailability (F)	86.4 ± 18.2%	76.9 ± 31.7%
Volume of distribution (Vd)	58 ± 21 L	18.5 ± 9.2 l/m^2
Apparent oral volume of distribution (Vd/F)	66 ± 22 L	not determined
Ratio of CSF:plasma concentrations (as %)	not determined	59 ± 35%
Total body clearance (Cl)	8.3 ± 2.3 ml/min/kg	247 ± 94 ml/min/kg
Apparent oral clearance (Cl/F)	8.0 ± 2.6 ml/min/kg	333 ± 87 ml/min/kg
Elimination half-life ($t_{1/2}$), I.V. dose	1.15 ± 0.35 h	1.11 ± 0.28 h
Elimination half-life ($t_{1/2}$), oral dose	1.44 ± 0.30 h	0.96 ± 0.26 h
Urinary recovery of stavudine (% of dose)	39 ± 23%	34 ± 16%

2.3.3 Dosage and administration

The recommended dosage regime for stavudine for each specific patient population according to bodyweight is given in table 2.2.

Table 2.2 A summary of the recommended dosages of stavudine in different patient groups (Bristol-Myers Squibb, 2000)

Recommended dosage by weight of stavudine in adult and paediatric patients		
Adult patients	≥ 60 kg	< 60 kg
	40 mg every 12 hours	30 mg every 12 hours
Paediatric patients (older than 6 months)	≥ 30 kg	< 30 kg
	the same as for adults	1 mg/kg every 12 hours
Patients with renal impairment (creatinine clearance (ml/min))	≥ 60 kg	< 60 kg
>50	40 mg every 12 hours	30 mg every 12 hours
26-50	20 mg every 12 hours	15 mg every 12 hours
10-25	20 mg every 24 hours	15 mg every 24 hours
Patient experiencing peripheral neuropathy	≥ 60 kg	< 60 kg
	20 mg every 12 hours	15 mg every 12 hours
Haemodialysis patients	≥ 60 kg	< 60 kg
	20 mg every 24 hours after completion of dialysis, and on non-dialysis days	15 mg every 24 hours after completion of dialysis, and on non-dialysis days

2.4 Side-effects, precautions, interactions and contra-indications

2.4.1 Side-effects and precautions

The most prominent side-effect experienced by patients taking stavudine is peripheral neuropathy. This is a dose related side-effect and it occurs more frequently in patients taking other neurotoxic drugs like didanosine. Stavudine related neuropathy is usually resolved by the discontinuation of the treatment, and patients may tolerate the resumption of the stavudine treatment at half the previous dosage. Other common side-effects include headache, diarrhoea, nausea and vomiting, fat redistribution (resembling Cushing's syndrome), anaemia, myalgia and insomnia (Bristol-Myers Squibb, 2000).

The most serious side-effects that may occur during treatment with stavudine include lactic acidosis, hepatomegaly with steatosis, and pancreatitis. These conditions may be fatal, and although they are not very common, the incidence of these side-effects are higher in patients treated with a combination of stavudine and didanosine (Bristol-Myers Squibb, 2000).

Patients with a history of neuropathy or patients using other neurotoxic drugs (especially didanosine), should be cautioned about the risk of developing peripheral neuropathy when treated with stavudine. Patients with a history of lactic acidosis, liver disease, pancreatitis and/or patients using stavudine and didanosine in combination should be cautioned about the possibility of developing these serious side-effects (Bristol-Myers Squibb, 2000).

2.4.2 Interactions and contra-indications

Zidovudine inhibits the intracellular phosphorylation of stavudine and should not be used in combination with stavudine. Drugs which cause neuropathy, like ethambutol, isoniazid, phenytoin and vincristine should not be used with stavudine, since it may lead to an increase in the incidence of peripheral neuropathy. There has been one report of lactic acidosis in a patient using metformin and stavudine concurrently, and the combination of these two drugs may lead to the development of this serious side-effect (Bristol-Myers Squibb, 2000; Raffanti & Haas, 2001:1357; Pharmaceutical Press, 2006).

Stavudine is contra-indicated in patients demonstrating hypersensitivity to this drug, and patients with a history of lactic acidosis, liver disease and/or pancreatitis should use this drug with caution. No adequate studies on the use of stavudine during pregnancy have been performed as yet, and it is advisable to not breast-feed whilst using stavudine. The use of stavudine and didanosine in pregnant woman may be dangerous due to the increased potential for the development of fatal lactic acidosis (Bristol-Myers Squibb, 2000).

2.5 Registered pharmaceutical preparations containing stavudine

The first mono-drug preparation containing stavudine to be registered and approved by the Food and Drug Administration in the United States for the treatment of HIV infected patients was Zerit®. It was also the first mono-drug preparation containing stavudine to be registered and approved by the Medicines Control Council (MCC) of South Africa (see figure 2.5). Zerit® is available as 15, 20, 30 and 40 mg capsules, and as a 1 mg/ml powder for oral solution for use in paediatric patients, and since it is registered as a schedule 4 substance in South Africa, it requires a prescription from a licensed/registered prescriber before it can be sold to a patient (Bristol-Myers Squibb, 2000).

Figure 2.5 A photograph showing a container of Zerit® 40 mg and 20 mg capsules.

Other generic stavudine-only and stavudine-combination products are also registered and approved by the MCC of South Africa, including Aspen Stavudine® capsules and Stavir® capsules, which are stavudine only products, and Triomune-40® tablets, which is a stavudine combination product containing stavudine, lamivudine and nevirapine (Johnnic Communications, 2006:471).

Conclusion

Stavudine was one of the first antiretroviral drugs approved for the treatment of HIV infections in humans, and is still widely used in combination with other antiretroviral drugs for the treatment of this devastating disease. Its favourable side-effect profile enables it to be used safely in patients of all age groups, and its efficacy in the treatment of HIV infections result in it still remaining one of the first choices in combination treatment of HIV. The following chapters will focus more extensively on the physicochemical properties of stavudine.

CHAPTER 3

Preparation and characterisation of the polymorphic forms of stavudine

Introduction

There are a variety of methods that are used to prepare polymorphic forms of active pharmaceutical ingredients (API's), and when one of these methods is applied to a single API, it may yield more than one distinct polymorphic form of that drug substance. This may be due to differences in environmental conditions such as temperature and/or humidity (Bernstein, 2002:75). Since the different solid states of an API may have different physicochemical properties, it is important to be able to clearly distinguish between these polymorphic forms. During the course of this chapter the methods used to prepare and characterise the various polymorphic forms of stavudine will be described, and the results of the analysis on these solid states will also be presented.

3.1 Preparation of stavudine polymorphs

3.1.1 Recrystallisation method

The various polymorphic forms of stavudine that were obtained during this study were prepared by evaporation of saturated solutions of stavudine in different organic solvents at ambient conditions (this method is also known as single solvent recrystallisation – Guillory, 1999:183-202). Approximately 500 mg of stavudine raw material was added to a glass beaker after which an organic solvent was added (preliminary studies indicated that 500 mg of stavudine would yield enough polymorphic product necessary to perform all the required analyses). The solution was heated to the boiling point of the specific solvent in a fume hood and stirred magnetically using a Velp® Scientifica (Italy) heating magnetic stirrer. Additional solvent was slowly added using a Pasteur pipette until all the stavudine had dissolved, ensuring that the final solution was saturated. The saturated solution was removed from the heat source, the stirring magnet was removed, the beaker was covered using Parafilm® (Pechiney Plastic Packing, Chicago IL, USA) and holes were made in the Parafilm® (Pechiney Plastic Packing, Chicago IL, USA) in order for the solvent to evaporate. When enough crystals had formed to perform all the required analyses, they were carefully removed from the solution and spread out on laboratory filter paper in order for the residual surface solvent to evaporate. The crystals were subsequently characterised using the analytical methods described in section 3.2 (Guillory, 1999:188).

The solubility of stavudine in most organic solvents was comparable to its solubility in water, except for chloroform, benzene and diethyl ether which required between 2 - 10 times the amount of solvent when compared to other solvents in order to prepare a saturated solution. This may be due to the polarity of stavudine which would make it dissolve more easily in polar solvents and reduce its solubility in non-polar solvents (like benzene, diethyl ether and chloroform). Acetic acid, propionic acid and formic acid did not yield any stavudine polymorphs since stavudine is degraded in acidic solutions (Shi *et al.*, 2004:2159). Solutions of stavudine in dimethylsulfoxide (DMSO) did not yield stavudine crystals after a period of 6 months, thus DMSO was considered to be an unsuitable solvent for recrystallisation. All the solvents used were purchased from Merck Chemicals (Pty) Ltd. (South Africa), except *N*-methyl-2-pyrrolidone which was obtained from Sigma-Aldrich (St. Louis MO, USA), and water which was Milli-Q water prepared in the laboratory using a Millipore water purification system (Millipore, USA). The different solvents that were used for the recrystallisations are shown in table 3.1.

Table 3.1 The various solvents and their boiling points that were used during the recrystallisation of stavudine raw material (Merck & Co., Inc., 2001:1818)

Solvent	Boiling point (°C)
Acetone	56.50°C
Methanol	64.70°C
Ethanol	78.50°C
n-Propanol	97.20°C
Iso-propanol	82.50°C
n-Butanol	118.00°C
Water	100.00°C
Tetrahydrofuran (THF)	66.00°C
Dimethylformamide (DMF)	153.00°C
Ethyl acetate	77.00°C
Chloroform	62.00°C
Acetonitrile (ACN)	81.60°C
Diethyl ether	34.60°C
Benzene	81.10°C
Dioxane	101.10°C
2-Butanol	99.50°C
Dichlorormethane	39.75°C
N-methyl-2-pyrrolidone (NMP)	202.00°C

3.1.2 Stavudine raw material

The stavudine raw material that was used throughout this study was purchased from Xiamen Mchem Laboratories Ltd. (6 Yangtai Road, Xinyang Industrial Area, Haicang, Xiamen, China). Batch number of the raw material: 0601002, manufacturing date: January 2006, expiry date: January 2009. The chemical properties of this batch are summarised in the certificate of analyses given in table 3.2.

Table 3.2 The certificate of analysis of the stavudine raw material used in this study

Tests	Specifications (USP28[1] and In-House)	Results
Description	White to off-white crystalline powder	Complies
Identification	1. IR[2] 2. HPLC[3]	Complies
Specific optical rotation	-40° ~ -45°	-45°
Heavy metals	≤ 20 ppm[4]	< 5 ppm[4]
Melting range	160 ~ 166°C	163 ~ 164.5°C
Residue on ignition	≤ 0.20%	0.04%
Water	≤ 0.5%	0.32%
Related substances	Other individual impurity ≤ 0.1% Thymine ≤ 0.5% Total impurity ≤ 1.0%	N.D.[5] 0.04% 0.04%
Residual solvents	Acetone ≤ 0.5% Ethyl acetate ≤ 0.5% Iso propyl ≤ 0.5% Acetic acid ≤ 0.5% Methanol ≤ 0.3% Toluene ≤ 0.089% DMF[6] ≤ 0.088% NMP[7] ≤ 0.053%	N.D.[5] N.D.[5] N.D.[5] N.D.[5] N.D.[5] N.D.[5] N.D.[5] N.D.[5]
Assay (by HPLC[3])	98.0% ~ 102% ($C_{10}H_{12}N_2O_4$)	99.6%
Conclusion: The product complies with USP28[1] and In-House standard		

[1] United States Pharmacopeia 28 – National Formulary 23
[2] Infrared spectroscopy
[3] High Performance Liquid Chromatography
[4] Parts per million
[5] None detected
[6] Dimethylformamide
[7] *N*-methyl-2-pyrrolidone

3.2 Polymorphic characterisation techniques

This section provides an overview of the techniques and apparatus that were used to study the physicochemical properties of the polymorphic forms of stavudine. These characterisation techniques were used throughout this study, unless stated otherwise. The techniques and apparatus that were used to determine and compare the solubility of the polymorphic forms of stavudine will be presented in chapter 5.

3.2.1 X-ray crystallography

3.2.1.1 X-ray powder diffraction (XRPD)

All X-ray diffraction techniques are based on Bragg's law (equation 3.1) which states that parallel incident X-rays striking a crystal plane at an angle of θ are diffracted at the same angle. For these X-rays to reinforce each other, their path lengths has to differ by one wavelength (λ) and must be relatable to the distance between the molecular planes in the crystal (*d*) (see figure 3.1) (Brittain, 1999:229-238; Yu *et al.*, 1998:120).

$$n\lambda = 2d \sin\theta \qquad (3.1)$$

Where: n = order of the diffraction pattern

λ = wavelength of the incident beam

d = distance between the planes in the crystal

θ = angle of beam diffraction.

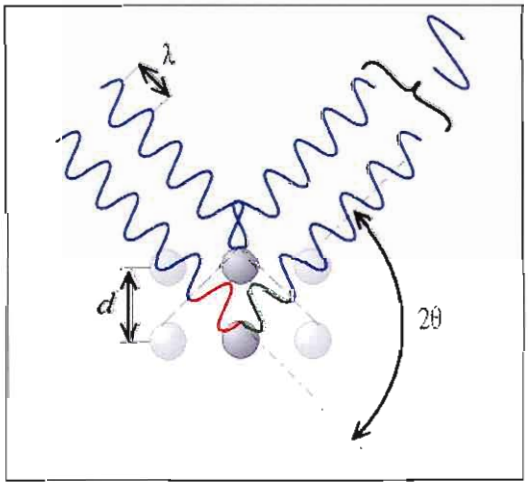

Figure 3.1 An illustration demonstrating Bragg's law (Anon, 2007).

Polymorphism in crystal structures imply various arrangements of the molecules (and atoms) in space, and will result in different diffraction angles and peak intensities for each form, i.e. the X-ray diffractogram of a polymorph is similar to a fingerprint (unique to each crystal form).

The field of X-ray crystallography can be subdivided into two main disciplines namely, single crystal X-ray diffraction and X-ray powder diffraction. The former is used primarily to determine the unit cell parameters, density, crystal disorder, molecular conformation, molecular packing and hydrogen-bonding patterns of polymorphs, whilst the latter is used to establish the polymorphic identity of a sample by comparing the powder pattern with that of a reference material, and for quantitative determination of polymorphic mixtures. It is also possible to determine the unit cell dimensions using the XRPD pattern, and only X-ray powder diffraction was used during this study (Brittain, 1999:229-238; Yu *et al.*, 1998:120).

The XRPD and VT-XRPD patterns were recorded using a Bruker D8 Advanced diffractometer (Bruker, Germany). The measurement conditions were: target, Cu; voltage, 40 kV; current, 30 mA; divergence slit, 2 mm; anti-scatter slit, 0.6 mm; detector slit, 0.2 mm; monochromator; scanning speed, 2°/min with a step size of 0.025° and a step time of 1.0 seconds. Samples were packed in an aluminium sample holder after being ground in a pestle and mortar, and the XRPD sample accessory was rotated at 15 revolutions per minute in order to reduce the potential influence of preferred orientation, which is defined as a non-random orientation of plate- or needle-like crystals due to the interaction with each other in the powder bed resulting in a variation in diffraction intensity. The peak positions and intensities were generated from the diffractograms using the Eva© software (version 10.0 revision 1) which is part of the Diffrac^{plus} 2004 software package (Bruker, Germany) (Byrn *et al.*, 1999).

3.2.1.2 Variable temperature X-ray powder diffraction (VT-XRPD)

This is a useful method for studying the effects of temperature on the different crystal forms, especially interconversion and desolvation reactions (Byrn *et al.*, 1999:64). The samples were prepared and analysed using the VT-XRPD sample holder and the diffractometer setup as stated in section 3.2.1.1 (except for the rotation of the sample accessory which is not possible with VT-XRPD). Samples were heated up to different temperatures (to a maximum of 164°C) using an Anton Paar TTK 450 low temperature camera (Anton Paar, Austria) with a heating rate of 1°C/sec, and were maintained at predetermined temperatures for the duration of each diffraction analysis (form 3 – 40°2θ).

3.2.2 Diffuse reflectance infrared Fourier transform spectroscopy (DRIFTS)

Different polymorphic forms of the same drug have different arrangements of the molecules in the solid states, which may result in a variation in the intermolecular interactions between the functional groups in the various crystal forms. This could lead to a variation in the vibrational energies of the molecules in the different solid states, and might yield different (unique) infrared (IR) spectra for each polymorphic form. Infrared spectroscopy can be used for both qualitative (identification) and quantitative purposes during polymorphic studies (Brittain, 1999:256-262).

In diffuse reflectance infrared Fourier transform spectroscopy (DRIFTS) a beam of infrared light is focused on the sample (which is ground and mixed with a halide salt, KBr), where it is reflected, scattered and transmitted through the sample. The reflected IR light is collected by detector optics and are used to construct the IR spectrum of the sample. Since DRIFTS requires minimal sample preparation, it is less likely to lead to polymorphic transformations, making it a preferred method in polymorphic studies (Bernstein, 2002:129).

The infrared spectra of the samples were recorded on a Nicolet Nexus™ 470 spectrometer (Nicolet Instrument Corporation, Madison WI, USA) over a range of 4000 – 400 cm^{-1} with the samples placed in an Avatar Diffuse Reflectance smart accessory after being mixed and ground with dried KBr (Merck, Darmstadt, Germany). The peak positions and intensities of the spectra recorded were determined using version 7.3 of the OMNIC© software package (Thermo Electron Corporation, USA).

3.2.3 Thermal methods of analysis

3.2.3.1 Differential scanning calorimetry (DSC)

Differential scanning calorimetry is a method of measuring the amount of energy absorbed or released by a sample as it is heated, cooled or held at a constant temperature. This energy is measured as the difference in heat flow (ΔT) between the sample (T_s) and a reference standard (T_r) (which is usually an empty aluminium pan similar to the sample pan). A plot of the difference in the heat flow (ΔT) versus the temperature yields the DSC thermogram, and integration of the area under the heat flow peaks in the thermogram quantifies the enthalpy change of the thermal events. DSC is mostly used for determining the melting point, heat capacity and heat of fusion of samples, as well as determining polymorphic transitions, stability and compatibility of excipients during preformulation studies (Rodrígues-Spong *et al.*, 2004:267-268).

For the purpose of this study between two and five milligrams of each sample were placed in a 40 µl aluminium sample pan (Mettler Toledo, Switzerland), crimp sealed with a pierced aluminium lid (the lid was pierced to relieve possible pressure build up which could cause a variation in results), and analysed using a Mettler Toledo DSC823^e (Greifensee, Switzerland) that was calibrated using an indium standard. Samples were analysed at temperatures from 25 - 210°C with a heating rate of 10°C/min and a nitrogen gas flow rate of 50 ml/min. The melting points were calculated from the thermograms using the STAR^e software programme (version 9.0*x*) (Mettler Toledo, Switzerland).

3.2.3.2 Thermogravimetric analysis (TGA)

Thermogravimetric analysis measures the change in mass of a sample as a function of temperature. The sample is heated in a furnace whilst a microbalance records the change in mass of the sample. TGA has a wide variety of applications in pharmaceutical research, including measuring the temperature of desolvation, determining the stoichiometry of a solvate, quantification of the amount of a solvent in a solid phase, constructing a stability diagram of the solvate and determining the desolvation (or degradation) kinetics. Equation 3.2 illustrates the equation that was used to determine the theoretical weight loss and the stoichiometry of the solvates obtained in this study (Sichina, 2001:23).

$$\%\,Weight\ loss = \frac{Mw_{solvent}}{(Mw_{solvent} \times n_{solvent\ in\ unit\ cell}) + (Mw_{stavudine} \times n_{stavudine\ in\ unit\ cell})} \times 100\% \quad (3.2)$$

Where: M_w = the molecular weight

n = the number of solvent or stavudine molecules.

For the purpose of this study, between six and ten milligrams of each sample were placed in a 100 µl aluminium pan and covered with a pierced lid (not crimped sealed). Samples were analysed using a calibrated Mettler Toledo TGA/SDTA851^e (Greifensee, Switzerland), with the samples analysed from 25 - 140°C at a heating rate of 10°C/min and a nitrogen gas flow rate of 50 ml/min. The weight loss of the samples was calculated using the STAR^e software programme (version 9.0*x*) (Mettler Toledo, Switzerland).

3.2.4 Microscopy

3.2.4.1 Polarising optical and hot-stage microscopy (HSM)

Polarizing microscopy is a fast method for distinguishing between crystalline (anisotropic) and amorphous (isotropic) polymorphs. Crystalline materials will change from bright to dark, or change colour, because the polarised light beams are refracted unequally by the unit cells in the different faces of the crystal, thus changing the velocity (the wavelength and colour) of the polarised light (this phenomenon in known as birefringence). Amorphous materials, which have no long range order (i.e. no continuous unit cells), and crystals having unit cells of cubic symmetry will not refract the light and will thus not change colour (Byrn *et al.*, 1999:70-75).

Hot-stage microscopy (thermal microscopy) involves heating a small amount of sample on a microscopic slide and observing the sample at the same time. This is often done to confirm the results that were generated using DSC, but it is also used to detect desolvation reactions (darkening or cracking of the crystal, or bubble formation in silicon oil), changes in crystal structure (a change in the birefringence of the crystal), solid-state transformations (changes in transparency or appearance of the crystal) and to confirm the melting points of polymorphs (Byrn *et al.*, 1999:73).

During this study a small amount of sample was placed on a microscope slide and either covered with silicon oil (Fluka Chemika, Switzerland) and a cover slide (in the case of solvates), or only a cover slide. A Nikon Eclipse E400 thermo-microscope (Tokyo, Japan) with a Leitz 350 heating unit (Leitz – now known as Leica Microsystems – Wetzlar, Germany) and a Metratherm 1200d thermostat was used for the hot-stage microscopy, and a Nikon Simple Polarizing Attachment (Tokyo, Japan) was used on the same microscope for the polarising optical microscopy. Photographs were taken using a Nikon Coolpix 5400 digital camera (Tokyo, Japan) which was attached to the microscope.

3.2.4.2 Scanning electron microscopy (SEM)

Scanning electron microscopy uses electron beams instead of light beams, permitting a greater resolution and thus a greater magnification of samples. It has the disadvantage of subjecting samples to a vacuum and bombarding them with electrons, and this may change the properties of some samples. It is however a powerful method for studying the morphology and surface characteristics of the particles, and can also be used for distinguishing between different crystal habits (Yu *et al.*, 1998:121; Bernstein, 2002:144).

Samples were analysed by covering the carbon tape on the SEM pin with sample, and it was then covered with a gold-palladium film (Eiko engineering ion coater IB-2, Japan) in a vacuum. The samples were placed in the microscope sample holder and analysed using a FEI Quanta 200 ESEM & Oxford INCA 400 EDS microscope system (FEI Corporation, Hillsboro OR, USA).

3.2.5 Karl Fischer analysis

Karl Fischer titration is a method used for quantifying the water content of samples, and it is based on the Bunsen Reaction between iodine and sulphur dioxide in a water medium:

$$\underset{\text{[alcohol]}}{ROH} + SO_2 + \underset{\text{[base]}}{R'N} \longrightarrow \underset{\text{[alkylsulfite salt]}}{[R'NH]SO_3R} + \underset{\text{[water]}}{H_2O} + \underset{\text{[iodine]}}{I_2} + 2R'N \longrightarrow \underset{\text{[hydroiodic acid salt]}}{2[R'NH]I} + \underset{\text{[alkylsulfate salt]}}{[R'NH]SO_4R}$$

The reactive alcohol (ROH) is usually methanol or 2-(2-ethoxyethoxy)ethanol, whilst the Karl Fischer reagent (base) is either pyridine, imidazole or a primary amine. Water and iodine are consumed in a 1:1 ratio in the Bunsen Reaction, and once all the water is consumed, the excess iodine is detected by an indicator electrode. The amount of water present in the sample is calculated based on the concentration of the excess iodine and the amount of Karl Fischer reagent used in the titration (EMD Chemicals Inc., 2007). A Metrohm 701 KF Titrino (Herisau, Switzerland) calibrated with purified water and sodium tartrate dihydrate (Riedel-de Haën, Germany) was used in the moisture determinations during this study.

3.3 The solid state forms of stavudine

The objective of this part of this study was to prepare the known polymorphic and pseudopolymorphic forms of stavudine that are described in the literature, and to investigate the possibility of preparing a novel solid state form of stavudine.

3.3.1 Polymorphs obtained from different solvents

As stated in section 3.1.1, various solvents were used during the recrystallisation process in order to prepare the polymorphic forms of stavudine. Figure 3.2 illustrates the different polymorphs of stavudine that were obtained from the various solvents. The form I/II mixture appears to be a mixture between polymorphic form I and form II of stavudine, but this will be explained in the following section.

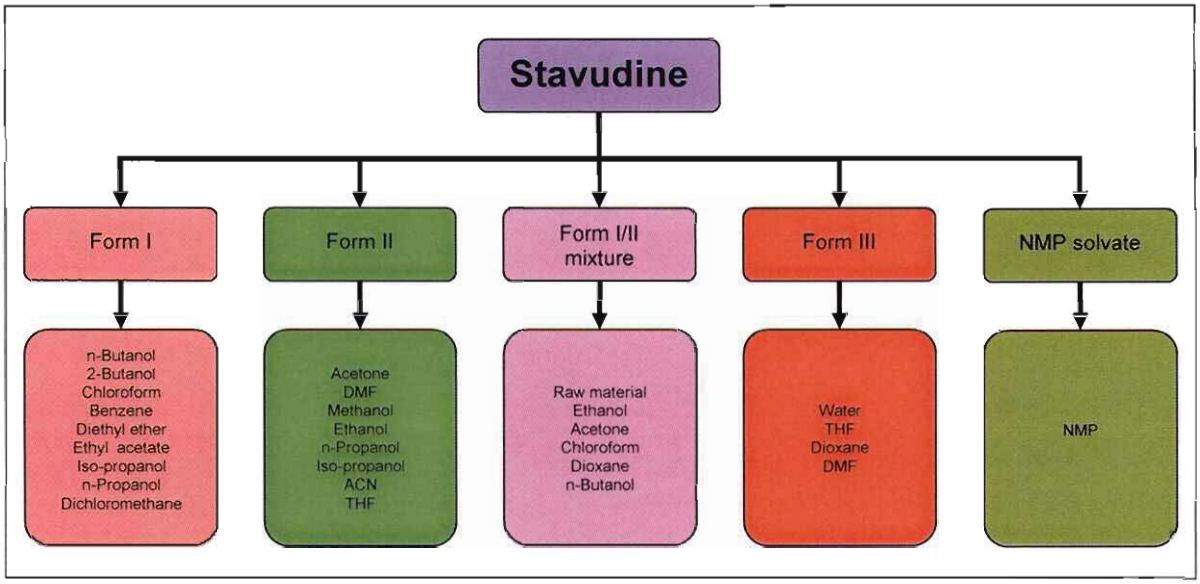

Figure 3.2 An illustration of the different polymorphic forms of stavudine and the corresponding solvents from which they were obtained by recrystallisation.

3.3.2 Stavudine form I, form II and form I/II mixture

Stavudine has two known polymorphic forms, i.e. form I and form II, and a mixture of these two polymorphs is also obtainable (Gandhi *et al.*, 2000:221). The X-ray powder diffractograms of form I, form II and the form I/II mixture is shown in figure 3.3, and the diffraction angles and corresponding relative intensities of the peaks in the diffractograms are shown in table 3.3. The unique peaks of each polymorphic form are highlighted in table 3.3, and the presence of these peaks in the diffraction pattern of the form I/II mixture is also highlighted.

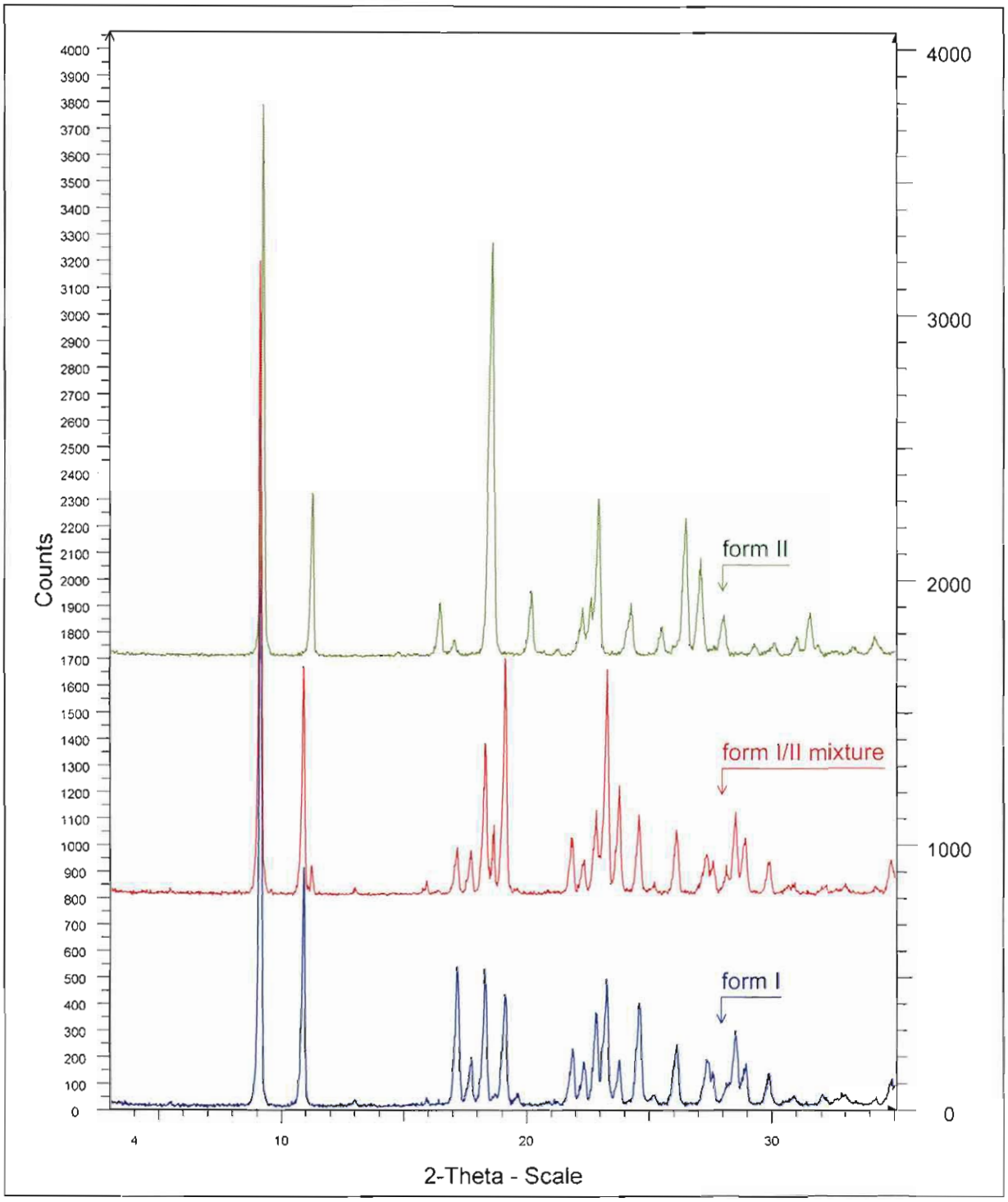

Figure 3.3 The XRPD patterns of form I, form II and the form I/II mixture.

Form I and form II have unique X-ray powder diffractograms, and according to Gandhi *et al.* (2000:224), form I has a characteristic diffraction peak at 19.1°2θ whilst the unique peaks of form II are at 11.2 and 18.6°2θ. Figure 3.3 and table 3.3 confirm the presence of these peaks in the diffractograms of the form I and form II that were prepared.

The form I/II mixture contains all three of these characteristic peaks, and its diffractogram appears to be a combination of the form I and form II XRPD patterns. It is suspected of being an amalgamation of the diffraction patterns of these two polymorphic forms, and the stavudine raw material (which is included in this group) has a similar diffractogram and will not be referred to separately during the remainder of this discussion. It must be emphasised that the form I/II mixture is not classified here as a separate polymorph, but it is considered to be a mixture of the two different polymorphic forms, i.e. form I and form II. This form I/II mixture is an example of the concomitant polymorphic character of form I and II of stavudine, denoting the simultaneous appearance of form I and II of stavudine under identical recrystallisation conditions (Bernstein, 2002:75).

The infrared absorption spectra (see figure 3.4) of these two polymorphs and the form I/II mixture show a similar trend, with polymorphic form I and form II having corresponding but unique absorption spectra, and unique absorption peaks (see table 3.4), and the form I/II mixture appearing to be a combination of these two spectra.

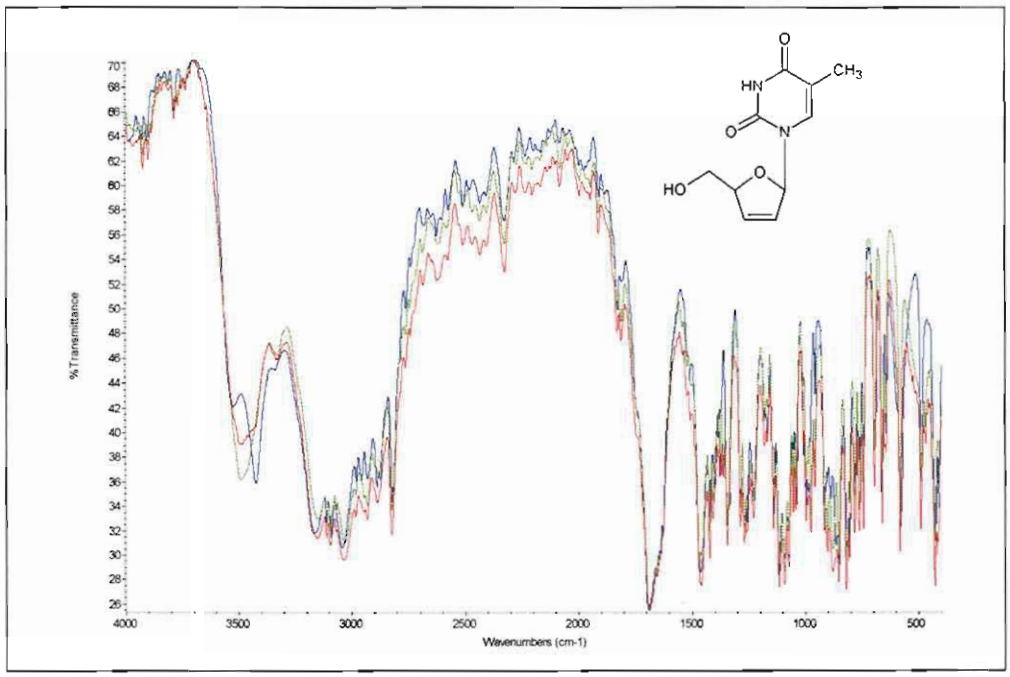

Figure 3.4 The infrared absorption spectra of form I, form II and the form I/II mixture.

According to Gandhi *et al.* (2000:225) form I has unique infrared absorption peaks at 3528, 3425 and 865 cm^{-1}, whilst form II has characteristic absorption peaks at 3485 and 975 cm^{-1}, and these peaks are highlighted in table 3.4. It is however more difficult to distinguish between form I and form II using the infrared absorption spectra than by using the XRPD patterns, since the infrared spectra of form I and II demonstrate some similarities whilst the XRPD patterns demonstrate clear discernable differences.

Table 3.3 The diffraction angles and relative intensities of the peaks in the XRPD patterns of form I, form II and the form I/II mixture

Form I		Form II		Form I/II mixture	
Position (°2θ)	**Intensity (I/I_o)**	**Position (°2θ)**	**Intensity (I/I_o)**	**Position (°2θ)**	**Intensity (I/I_o)**
5.385	1.0	-	-	5.401	1.4
9.112	100.0	9.245	100.0	9.118	100.0
10.852	34.7	-	-	10.874	36.2
-	-	11.243	29.8	11.225	4.9
-	-	-	-	12.156	0.5
12.980	1.3	-	-	12.984	1.5
-	-	14.769	1.2	-	-
15.922	1.7	-	-	15.925	2.6
-	-	16.455	10.2	16.391	1.0
17.159	20.4	17.035	3.3	17.142	7.8
17.722	7.4	-	-	17.709	7.3
18.302	20.1	-	-	18.319	24.2
-	-	18.620	75.1	18.637	9.8
19.117	16.4	-	-	19.127	37.6
19.620	2.3	-	-	19.569	1.3
-	-	20.184	12.3	-	-
21.183	1.1	21.271	1.8	-	-
21.867	8.7	-	-	21.859	9.4
22.334	6.8	22.298	9.2	22.325	5.9
-	-	22.640	11.2	-	-
22.849	13.8	22.948	28.9	22.845	13.6
23.258	18.6	-	-	23.294	35.8
23.777	7.0	-	-	23.793	17.5
-	-	24.257	10.1	-	-
24.604	15.1	-	-	24.594	13.0
25.214	2.0	-	-	25.197	2.5
-	-	25.526	5.9	-	-
26.146	9.2	-	-	26.134	10.5
-	-	26.507	25.4	-	-
-	-	27.106	18.2	-	-
27.387	7.1	-	-	27.366	6.8
27.611	5.4	-	-	27.621	5.8
-	-	28.053	8.0	-	-
28.225	3.4	-	-	28.193	5.1
28.540	11.2	-	-	28.545	13.4
28.939	6.5	-	-	28.926	9.3
-	-	29.331	2.8	-	-
29.921	5.1	-	-	29.909	9.3
-	-	30.113	3.0	-	-
30.955	1.9	-	-	30.925	1.9
-	-	31.068	4.2	-	-
-	-	31.583	8.4	-	-
-	-	31.897	2.7	-	-
32.124	2.0	-	-	32.224	1.7
32.957	2.1	-	-	-	-
-	-	-	-	33.059	2.2
-	-	33.421	1.9	-	-
34.289	1.6	34.260	4.1	34.312	1.6
34.922	3.9	-	-	34.936	5.8

Table 3.4 The main absorption peaks in the infrared spectra of form I, form II and the form I/II mixture

Form I	Form II	Form I/II mixture
Wavenumber (cm^{-1})	Wavenumber (cm^{-1})	Wavenumber (cm^{-1})
410.3	407.7	418.3
427.0	429.5	428.9
-	471.2	469.1
488.3	488.9	488.8
577.2	582.1	581.7
642.0	648.6	644.2
660.9	661.0	661.1
689.0	695.3	695.6
742.5	743.1	742.8
755.7	-	-
764.3	760.5	760.2
784.2	782.2	783.3
802.7	805.1	804.3
818.9	819.5	818.9
850.8	852.5	851.6
865.4	-	-
-	879.3	877.9
889.2	-	-
-	902.7	902.2
915.7	-	-
956.8	957.5	957.6
-	975.2	975.3
998.0	996.7	997.2
1008.4	-	-
1037.5	1040.8	1039.9
-	1053.3	1053.3
1072.0	1072.9	1072.4
1090.3	1092.1	1092.0
1114.3	1115.4	1115.2
1141.3	1141.6	1141.6
1164.8	-	-
-	1180.7	1180.3
1228.4	1227.1	1227.8
1258.4	1252.6	-
-	1268.7	1269.1
1286.0	1285.8	1286.0
1343.2	1343.8	1344.0
-	1361.9	1362.0
1371.5	1376.6	1375.8
1383.9	-	-
1400.4	1407.8	1407.7
1420.1	1422.7	1421.9
1460.6	1466.2	1457.9
1689.8	1686.0	1685.5
-	1811.1	1811.1
1828.7	-	1830.3
1909.5	1911.3	1911.2
-	1946.7	1946.5
1976.4	-	-
-	2081.6	2082.1
-	2202.8	2202.7
2234.7	-	-
2327.3	2326.4	2327.0
2433.6	2434.1	2433.4
2507.8	-	2509.0
2574.4	-	-

Table 3.4 (continued)

2625.6	2620.3	2624.8
2821.3	2824.3	2823.2
2890.4	2884.5	2885.9
2932.7	2932.9	2933.0
2958.1	-	-
3043.1	3033.1	3034.1
3091.5	3096.9	3096.3
3114.3	-	-
3166.9	3152.7	3155.2
3425.4	-	-
-	3491.7	3488.8
3523.7	-	-
3786.5	3785.6	3785.6
3905.3	3899.7	3900.3
3928.6	3923.6	3924.2

From the infrared data in table 3.4 it appears as though the form I/II mixture is in fact polymorphic form II, since it only has the unique absorption peaks of form II and none of the peaks of form I. This is explained by the appearance of the spectra of form II which has two broad characteristic peaks in the range of 3600 – 3400 cm^{-1} and 985 – 960 cm^{-1}, whilst the spectra of form I has two narrower unique peaks in the same regions (see figure 3.4). As the concentration of form II in the mixture increases, these narrow peaks in each region merge yielding only one broad peak corresponding to the unique form II peak, and in the form I/II mixture the form I peaks are thus not visible.

Figure 3.5 shows the DSC thermograms of (a) form I, (b) form II, (c) the form I/II mixture at a heating rate of 10°C/min and (d) the form I/II mixture at a heating rate of 1°C/min. A clear melting endotherm followed by the decomposition of the two polymorphic forms and the form I/II mixture can be seen. At a heating rate of 10°C/min, form I has a melting point ranging from 163.45 – 174.26°C, whilst form II has a melting point from 161.44 – 170.73°C, and the form I/II mixture has a melting point from 167.23 – 172.96°C. The onset of melting and the melting points of form I and form II are overlapping and could not be used with certainty to distinguish between these two polymorphs. The DSC thermograms showed no desolvation endotherms or recrystallisation exotherms thus form I, form II and the form I/II mixture are not solvates, and TGA and Karl Fischer analyses showed negligible weight loss (form I, 0.35%; form II, 0.33%; the form I/II mixture, 0.20%) and demonstrated insignificant water content (form I, 0.33%; form II, 0.30%; the form I/II mixture, 0.28%). The thermogram of the form I/II mixture shows only one sharp melting endotherm at a heating rate of 10°C/min, and it is expected that there would be two sharp melting endotherms corresponding to each of the polymorphs in the mixture when the heating rate is decreased to 1°C/min (see figure 3.5 (d)). This was not observed, thus it is possible that the exposure of the higher melting polymorph

to high temperatures (close to the melting point) results in it degrading without a measurable melting point, and no second melting endotherm is thus observed.

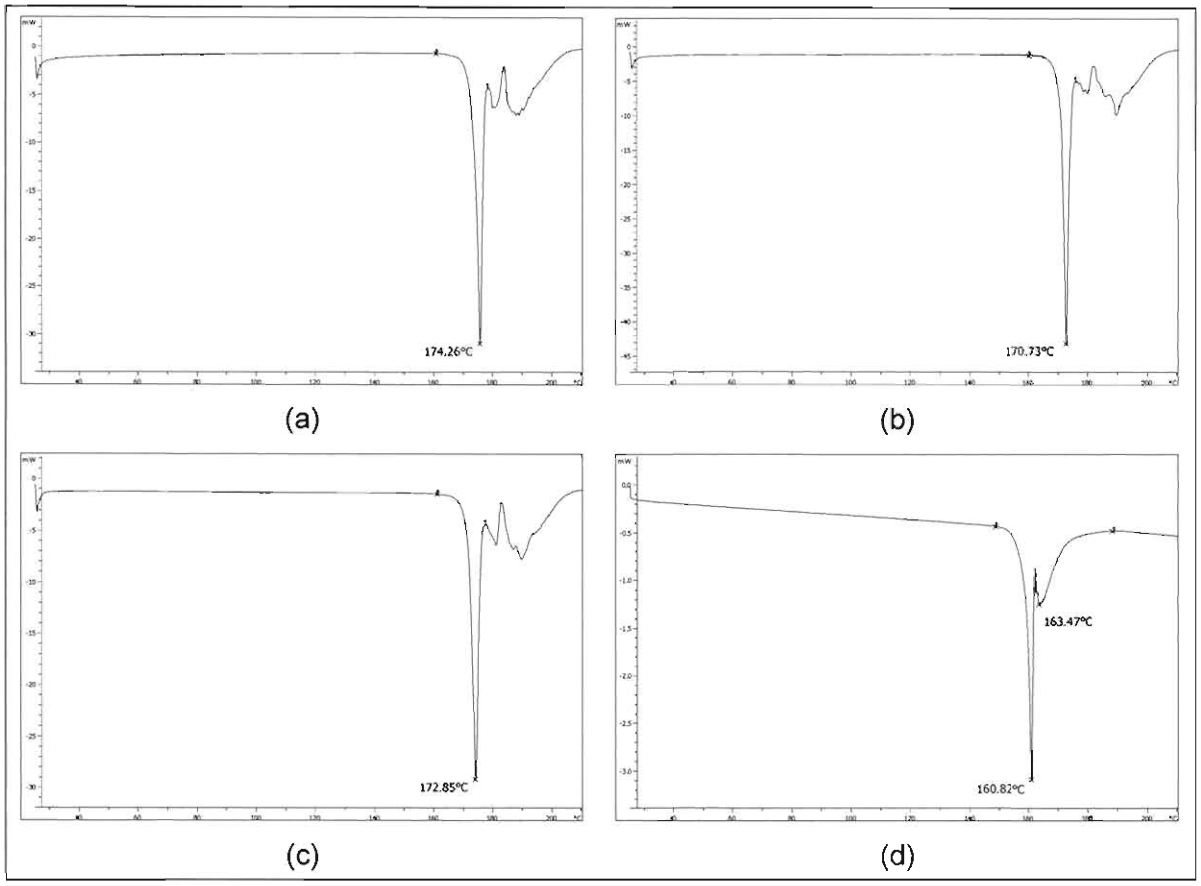

Figure 3.5 The DSC thermograms and corresponding melting points of (a) form I, (b) form II, (c) the form I/II mixture (10°C/min) and (d) the form I/II mixture (1°C/min).

Thermal microscopy studies performed on these three solid states confirmed the DSC results, and are shown in table 3.5. Polarising optical microscopy confirmed the crystallinity of these solids as a result of the birefringence of the polarised light, and the high intensity diffraction peaks in the XRPD patterns of these solid states (see figure 3.3) also demonstrated their crystalline nature.

Scanning electron microscopy (SEM) photomicrographs are shown in table 3.6 and demonstrate the morphological character of form I, form II and the form I/II mixture. Since the crystals of form I and form II are needle-shaped (with some dispersed irregular shaped crystals), scanning electron microscopy or optical microscopy could not be used with confidence to distinguish between these two polymorphs or to identify the form I/II mixture. Thus the most reliable methods to differentiate between these solid states are X-ray powder diffraction or single crystal X-ray diffraction analysis.

Table 3.5 Photomicrographs obtained with polarising optical and hot stage microscopy

Form I		
Photomicrograph	**Technique and temperature**	**Observation**
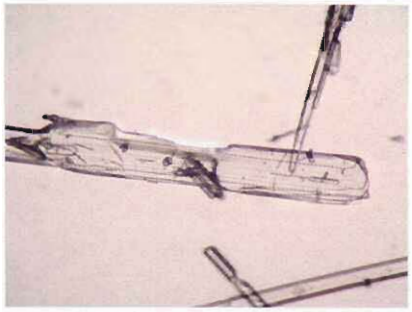	Optical microscopy (23°C)	Needle-shaped, clear crystals
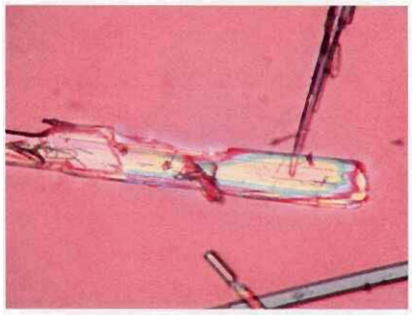	Polarising optical microscopy (23°C)	Birefringence of the polarised light by the crystals (indicative of crystalline materials)
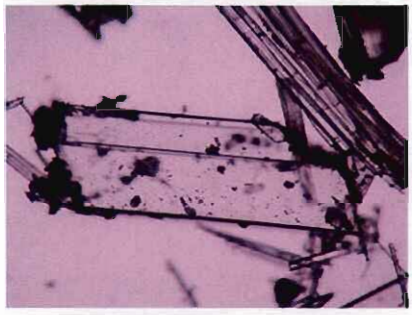	Hot stage microscopy (23°C)	Needle-shaped, clear crystals
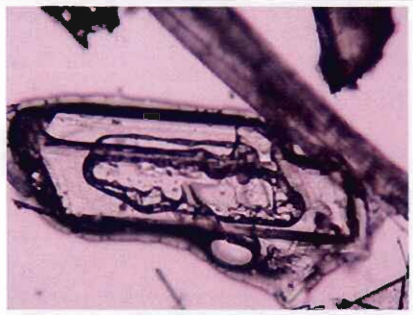	Hot stage microscopy (161°C)	Onset of melting of form I
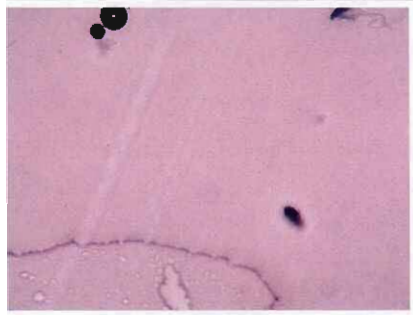	Hot stage microscopy (172°C)	Form I completely melted

Table 3.5 (continued)

Form II		
Photomicrograph	**Technique and temperature**	**Observation**
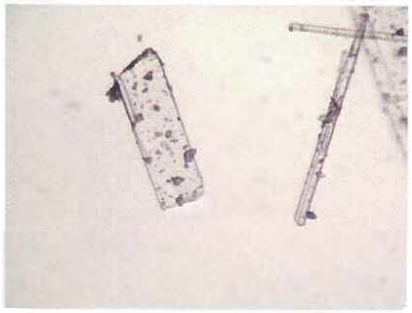	Optical microscopy (23°C)	Needle-shaped, clear crystals
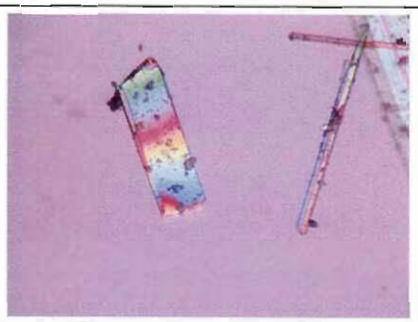	Polarising optical microscopy (23°C)	Birefringence of the polarised light by the crystals (indicative of crystalline materials)
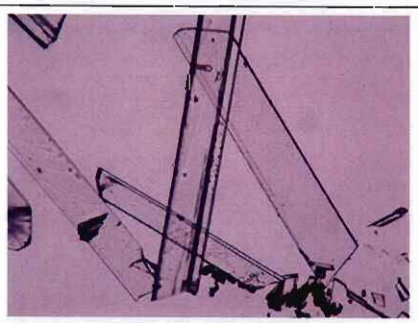	Hot stage microscopy (32°C)	Needle-shaped, clear crystals
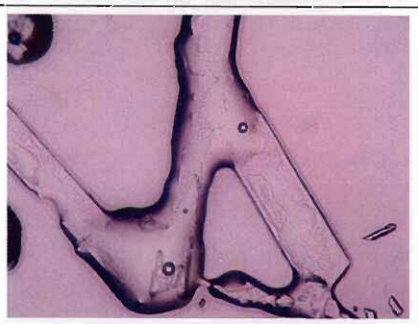	Hot stage microscopy (168°C)	Onset of melting of form II
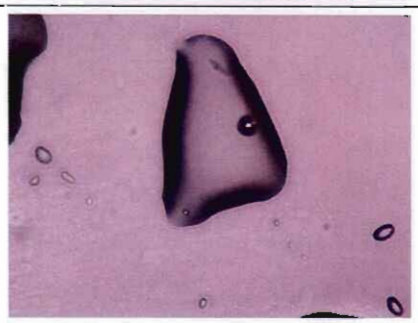	Hot stage microscopy (170°C)	Form II completely melted

Table 3.5 (continued)

The form I/II mixture		
Photomicrograph	**Technique and temperature**	**Observation**
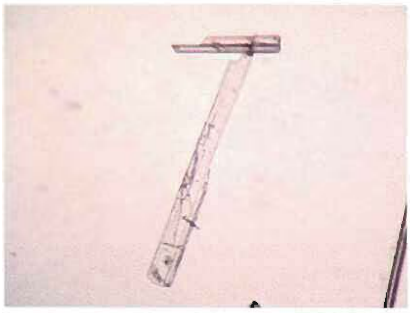	Optical microscopy (23°C)	Needle-shaped, clear crystals
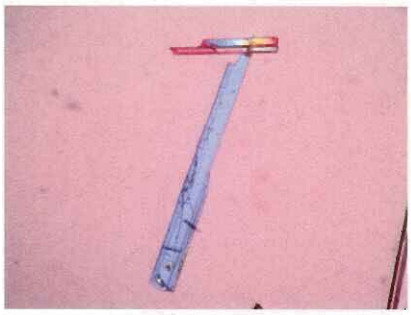	Polarising optical microscopy (23°C)	Birefringence of the polarised light by the crystals (indicative of crystalline materials)
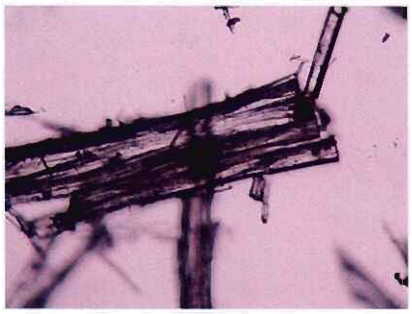	Hot stage microscopy (27°C)	Needle-shaped, clear crystals
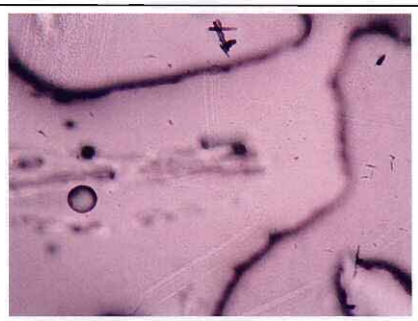	Hot stage microscopy (171°C)	Onset of melting of the form I/II mixture
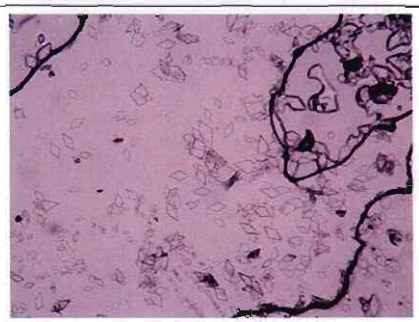	Hot stage microscopy (174°C)	The form I/II mixture completely melted with recrystallised products, assumed to be degradation products

Table 3.6 SEM photomicrographs of form I, form II and the form I/II mixture

Photomicrograph	Description
Form I 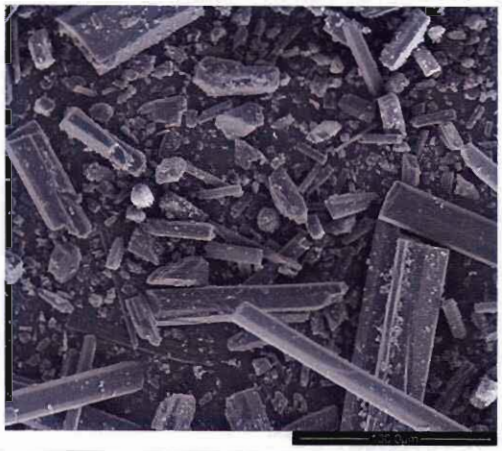	Needle-shaped crystals with dispersed irregular shaped crystals
Form II 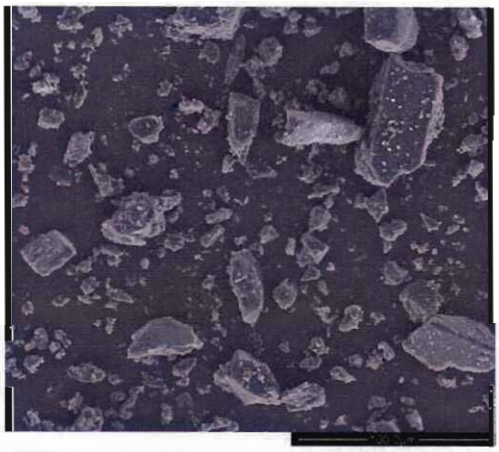	Irregular shaped crystals with dispersed needle-shaped crystals
Form I/II mixture 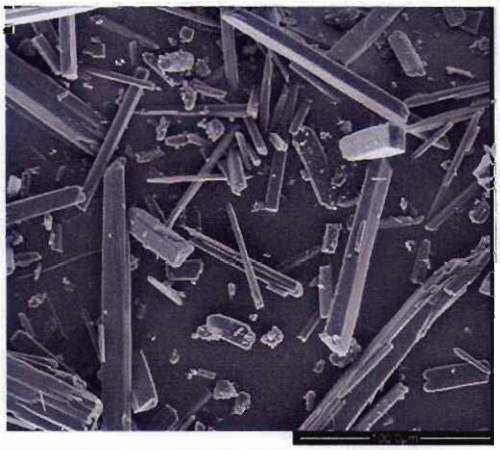	Needle-shaped crystals with dispersed irregular shaped crystals

Polymorphs are said to be enantiotropic when there is a reversible transition at a definite transition temperature below the melting point, whilst monotropic solids show no reversible transition below the melting point on a DSC thermogram (see section 1.2.3.1). A method used to determine the relationship between solid states of a drug is to apply the heat of fusion rule. This rule states that if the higher melting polymorph has the lower heat of fusion (calculated as the integrated area under the melting endotherm in the DSC thermogram) the system is enantiotropic, and if the higher melting polymorph has the higher heat of fusion, the system is monotropic (Grant, 1999:18). The heat of fusion rule could not be applied to determine the relationship between form I and II since the melting of stavudine is immediately followed by degradation. This results in difficulty calculating the heat of fusion (the area under the endotherm), and the melting points of form I and II are also overlapping.

VT-XRPD analysis were used to determine the presence and type of possible transformations that might occur between form I and form II and the form I/II mixture when exposed to increasing temperatures. Figure 3.6 illustrates the VT-XRPD diffractograms of (a) form I, (b) form II and (c) the form I/II mixture, and the XRPD pattern of (d) 99% thymine (Sigma-Aldrich, Steinheim, Germany) which is the main degradation product of stavudine.

It is clear form figure 3.6 (a), (b) and (c) that a gradual increase in the temperature from 25 to 160°C does not change the appearance of the diffractograms of form I, form II and the form I/II mixture, and the unique form I diffraction peak (at 19.1°2θ) and form II diffraction peaks (at 11.2 and 18.6°2θ) remain visible in each diffractogram throughout the analysis. At 160°C the intensities of the diffraction peaks in all three diffractograms decrease since the crystals start to melt, leading to a loss in the crystalline structure of each sample. By comparing figure 3.6 (c) and (d) it can be seen that increasing the temperature beyond 160°C results in the stavudine degrading and recrystallising as the degradation product thymine. It is evident from the VT-XRPD data that no interconversion between form I and form II occurred with an increase in temperature, suggesting that form I and form II are monotropically related. This supports the findings of Mirmehrabi *et al.* (2006:141), but differs from the results of Gandhi *et al.* (2000:235) which stated that form I and II are enatiotropically related.

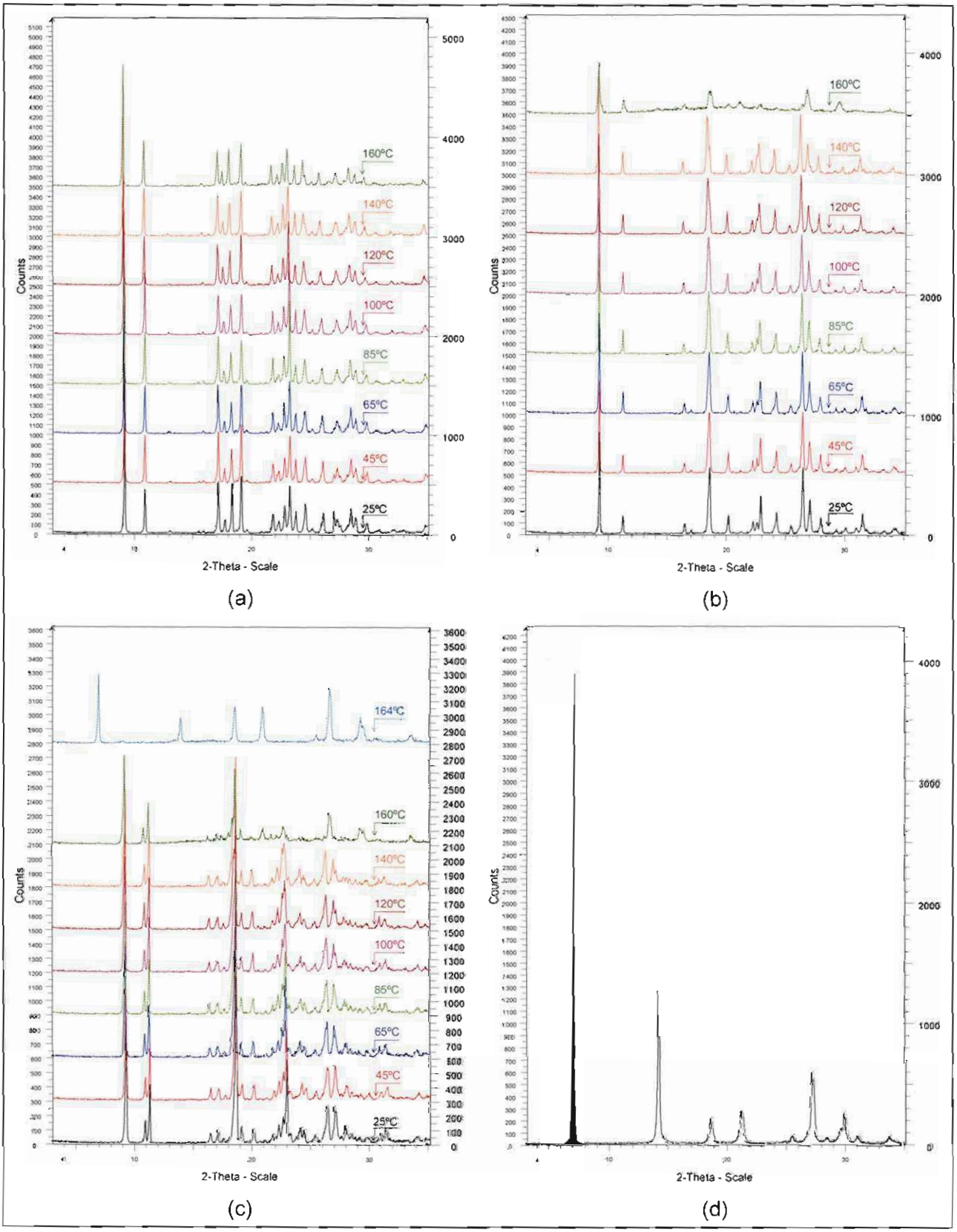

Figure 3.6 The VT-XRPD diffractograms of (a) form I, (b) form II and (c) the form I/II mixture and (d) the XRPD pattern of thymine.

3.3.3 Stavudine solvates (form III (hydrate) and NMP solvate)

There are five known pseudopolymorphs (solvates) of stavudine, form III (a hydrate), the *N*-methyl-2-pyrrolidone (NMP) solvate, the *N,N*-dimethylacetamide (DMA) solvate, the *N,N*-dimethylacrylamide (DMAC) solvate and the *N,N*-dimethylpropionamide (DMP) solvate. Form III is a non-stoichiometric solvate since its unit cell consists of one water molecule and three stavudine molecules, whilst the NMP solvate is a stoichiometric solvate with one stavudine and NMP molecule forming its unit cell. The NMP, DMA, DMAC and DMP solvates are used in various synthetic processes to obtain pure stavudine without any toxic residual solvents, by heating it in order to accelerate desolvation, resulting in the formation of a pure solvent-free anhydrous stavudine powder (Radatus & Murthy, 2003:1; Gandhi *et* al., 2000:221; Viterbo *et al.*, 2000:580).

During this study only form III and the NMP solvate were prepared and their physicochemical properties determined. Figure 3.7 illustrates the X-ray powder diffractograms obtained for form III and the NMP solvate, and the diffraction angles and corresponding relative intensities of the peaks are shown in table 3.7 with the unique peaks of form III and the NMP solvate highlighted.

Form III and the NMP solvate have characteristic diffractograms that make it possible to distinguish these solid states from each other and from the other polymorphs of stavudine. Form III has unique diffraction peaks at 6.5, 7.3 and 15.5°2θ and these peaks are visible in the diffractogram obtained from form III (see figure 3.7). The diffractogram of the NMP solvate is not described in the literature (only unit cell dimensions are described) and no known unique diffraction peaks have been assigned to this pseudopolymorph, however it is clear from figure 3.7 that the peaks at 8.4 and 14.5°2θ are unique to this solvate since these two peaks are not present in the diffractograms of either form I, form II, the form I/II mixture or form III (Gandhi *et al.*, 1996:4).

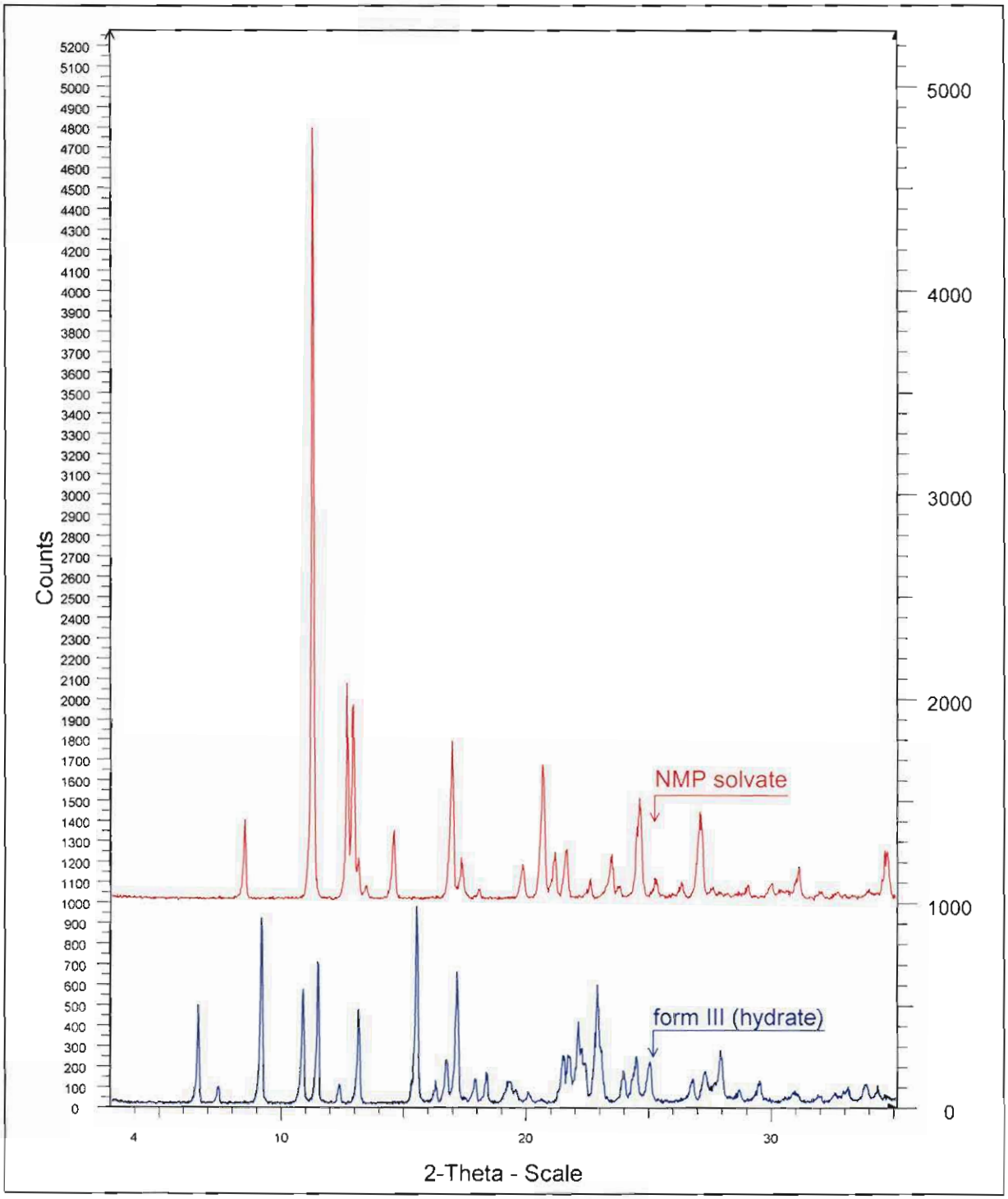

Figure 3.7 The X-ray powder diffractograms of form III and the NMP solvate of stavudine.

Table 3.7 The diffraction angles and relative intensities of the peaks in the XRPD patterns of form III and the NMP solvate

Form III	
Position (°2θ)	**Intensity (I/I_o)**
6.527	50.5
7.364	9.7
9.147	94.2
10.840	58.5
11.440	72.2
12.306	10.9
13.108	48.4
15.507	100.0
16.273	12.8
16.724	23.3
17.151	67.1
17.889	13.7
18.371	17.0
19.309	12.1
19.558	8.3
20.085	7.2
20.595	3.8
21.499	25.4
21.720	25.7
22.122	42.4
22.375	21.5
22.900	60.9
23.979	17.7
24.495	24.9
25.041	22.3
26.781	13.7
27.317	17.6
27.964	27.8
28.715	8.3
29.541	12.6
30.957	7.2
31.986	5.6
32.629	6.9
33.142	9.7
33.900	11.0
34.381	10.5
34.694	5.8

NMP solvate	
Position (°2θ)	**Intensity (I/I_o)**
8.437	10.5
11.238	100.0
12.655	28.3
12.892	25.4
13.422	2.0
14.555	9.1
16.941	20.7
17.339	5.7
18.060	1.6
19.840	4.8
20.667	17.7
21.151	6.3
21.615	6.7
22.610	3.0
23.475	6.1
23.789	2.1
24.633	13.4
25.286	3.1
26.354	2.5
27.121	11.6
27.622	2.0
28.210	1.1
29.065	2.2
30.013	2.3
31.132	4.1
32.035	1.2
32.738	1.3
33.994	1.7
34.743	6.4

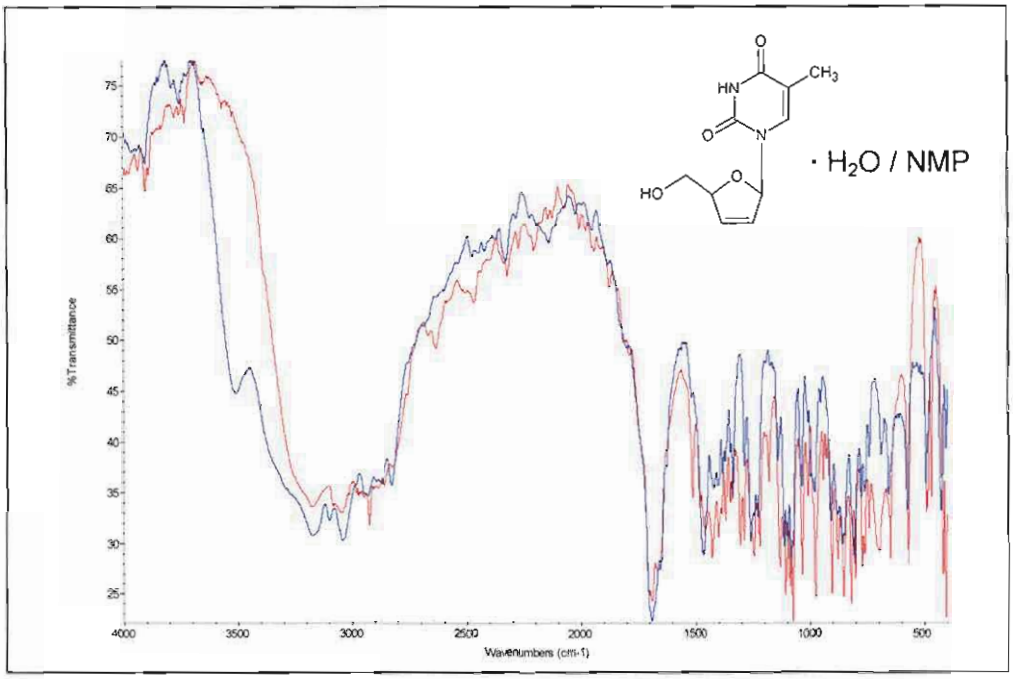

Figure 3.8 The infrared spectra of form III and the NMP solvate.

Figure 3.8 illustrates the infrared absorption spectra that were obtained for form III and the NMP solvate. These spectra are dissimilar and can be used to differentiate between the different solvates, and between the pseudopolymorphs (solvates) and the polymorphs (unsolvated forms) of stavudine. Form III has a unique absorption peak at 3510 cm^{-1} (which is also indicative of the presence of crystalline water in a hydrate), and the infrared spectrum of the NMP solvate is not described in the literature, however the NMP spectrum has no absorption peaks in the 3600 – 3200 cm^{-1} region (the other infrared spectra of stavudine have either one or two peaks in this region) and it has a unique absorption peak at 1305 cm^{-1} which is not present in the other spectra of stavudine (figures 3.8 and 3.4). The infrared absorption peaks in the spectra of form III and the NMP solvate are displayed in table 3.8 and the characteristic peaks of each pseudopolymorph are also highlighted (Gandhi *et al.*, 2000:225; Brittain, 1997:407).

Table 3.8 The main absorption peaks in the infrared spectra of form III and the NMP solvate

Form III
Wavenumber (cm^{-1})
404.4
428.8
493.2
575.0
656.1
690.1
741.3
761.5
776.6
805.9
857.1
909.3
978.1
1035.0
1081.5
1099.2
1112.1
1140.2
1227.4
1258.8
1285.9
1335.2
1381.1
1419.7
1466.9
1690.0
1948.5
2140.9
2327.5
2475.9
2827.6
2931.5
3041.7
3173.4
3512.2
3753.5
3906.4

NMP solvate
Wavenumber (cm^{-1})
406.0
420.0
469.4
491.2
571.0
649.9
697.5
742.4
773.0
801.7
820.8
852.6
878.7
904.4
940.4
975.5
1009.6
1034.0
1075.1
1087.9
1105.5
1131.1
1178.8
1219.9
1244.0
1286.3
1305.1
1348.6
1367.3
1400.1
1427.4
1457.6
1511.3
1689.3
2072.6
2202.7
2318.7
2465.8
2633.2
2925.3
3047.1
3173.0
3733.0
3905.9

Figure 3.9 illustrates the DSC thermograms and the results of the TGA analysis of (a) form III and (b) the NMP solvate at a heating rate of 10°C/min. The DSC thermogram of form III demonstrates a broad endotherm at 125.65°C which is attributed to the dehydration of the hydrate, since this temperature is higher than the boiling point of water (100°C) it indicates that the water molecules are tightly bound within the crystal lattice. TGA analysis of form III showed an average weight loss of 2.53%, and since the DSC analysis highlighted the dehydration step, this weight loss is due to the dehydration of the hydrate. This was confirmed by Karl Fischer analysis which showed an average moisture content of 2.44%. The TGA and Karl Fischer results correspond to the theoretical percentage weight loss (2.60%) calculated from equation 3.2, keeping in mind that the unit cell of form III consists of three molecules of stavudine and one molecule of water. The TGA and Karl Fischer results of form III and the NMP solvate are summarised in table 3.9 (Gandhi *et al.*, 2000:221).

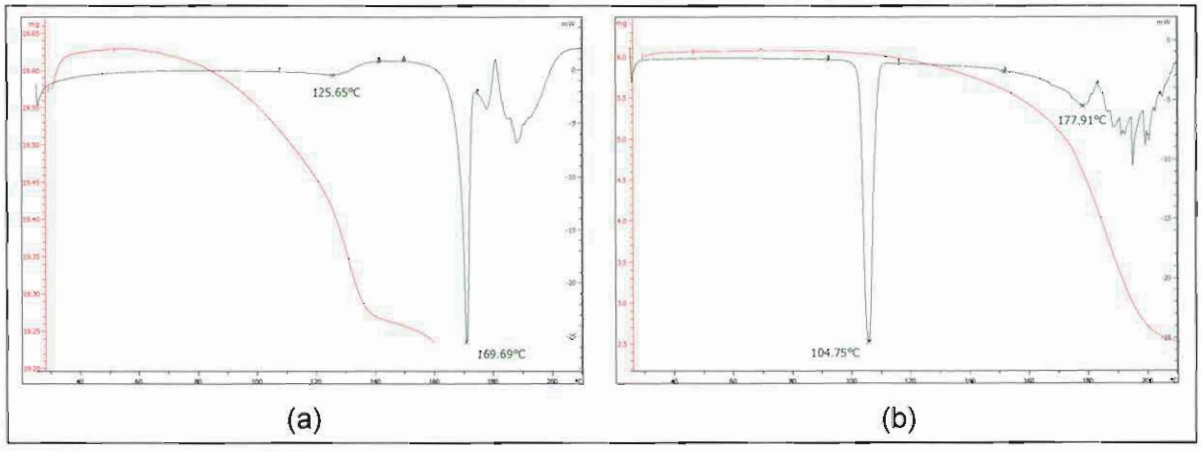

Figure 3.9 The DSC thermogram and TGA curve of (a) form III and (b) the NMP solvate.

The DSC thermogram of the NMP solvate shows a sharp endotherm at 104.75°C, and a smaller endotherm at 177.91°C, followed by degradation of the sample. Table 3.9 illustrates that the NMP solvate has an insignificant moisture content determined from Karl Fischer analysis, and that that the percentage weight loss determined from TGA analysis does not correspond to the theoretical percent weight loss calculated using equation 3.2, keeping in mind that the unit cell of the NMP solvate contains one molecule of stavudine and one molecule of NMP (Viterbo *et al.*, 2000:580). However, figure 3.9 (b) shows that the weight loss of the NMP solvate is due to the degradation of the sample, since the weight loss occurs over the temperature region at which stavudine melts and decomposes (160 – 210°C). Thermal microscopy (see table 3.10) provided greater clarity of the thermal behaviour of the NMP solvate, and it showed melting (not observed with VT-XRPD analysis) of the NMP solvate at 105°C immediately followed by recrystallisation, after which a second melting process occurs. It is thus assumed that the NMP solvate melts at 104.75°C, but that the NMP

solvent does not evaporate due to its high boiling point (202°C). After melting of the NMP solvate, stavudine recrystallise followed by a second melting endotherm and degradation of stavudine. The boiling point of the NMP solvent is thus theoretically unattainable because in order for the NMP to evaporate, the crystals have to be heated beyond the degradation temperature of stavudine. This explains the use of the NMP solvate, which is essentially used during the last step in the large scale manufacturing of stavudine, during which it is dissolved and heated in iso-propanol resulting in the extraction of the NMP solvent and the precipitation of pure stavudine (Skonezny *et al.*, 1994:4).

Table 3.9 A summary of the TGA and Karl Fischer analysis of form III and NMP solvate

	The stavudine:solvent ratio in the unit cell	**Experimental % weight loss (determined from TGA data)**	**Theoretical % weight loss (determined from equation 3.2)**	**% Moisture content (determined from Karl Fischer analysis)**
Form III	3:1	2.53	2.60	2.44
NMP solvate	1:1	59.93	30.65	0.41

The results from the thermal microscopy and polarising optical microscopy studies of form III and the NMP solvate are shown in table 3.10 and table 3.11. The thermal microscopy results confirmed the results obtained from DSC, and the polarising optical microscopy results illustrate that form III and the NMP solvate are crystalline.

Scanning electron microscopy (SEM) was used to study the morphology of the crystals of form III and the NMP solvate and the results are shown in table 3.12. The crystals of form III has a dominant needle-shape, whilst the small crystals of the NMP solvate are irregularly shaped with no specific morphology. However the larger NMP solvate crystals have a prismatic appearance.

Table 3.10 Photomicrographs obtained with polarising optical and hot stage microscopy

Form III		
Photomicrograph	**Technique and temperature**	**Observation**
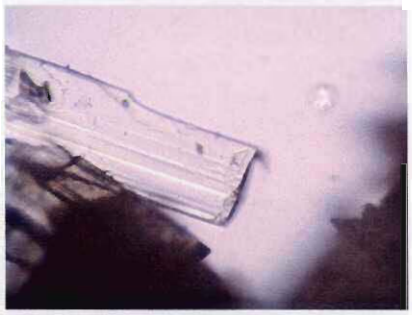	Optical microscopy (23°C)	Needle-shaped, clear crystals
	Polarising optical microscopy (23°C)	Birefringence of the polarised light by the crystals (indicative of crystalline materials)
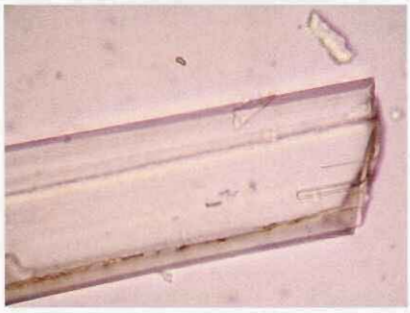	Hot stage microscopy (27°C)	Needle-shaped, clear crystals
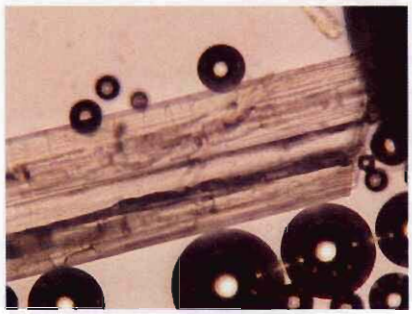	Hot stage microscopy (128°C) (sample covered with silicon oil)	Desolvation of the hydrate, observed as bubble formation when the sample is submerged in silicon oil
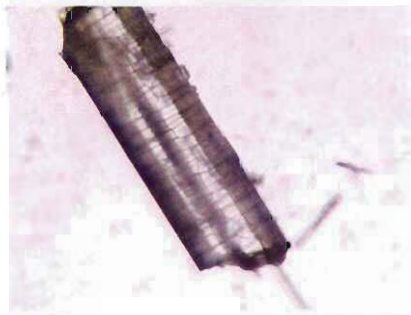	Hot stage microscopy (sample not covered with silicon oil) (125°C)	Desolvation of the hydrate, observed as cracking of the crystal

Table 3.10 (continued)

Form III		
Photomicrograph	**Technique and temperature**	**Observation**
	Hot stage microscopy (152°C)	Onset of melting of form III
	Hot stage microscopy (165°C)	Form III completely melted

Table 3.11 Photomicrographs obtained with polarising optical and hot stage microscopy

NMP solvate		
Photomicrograph	**Technique and temperature**	**Observation**
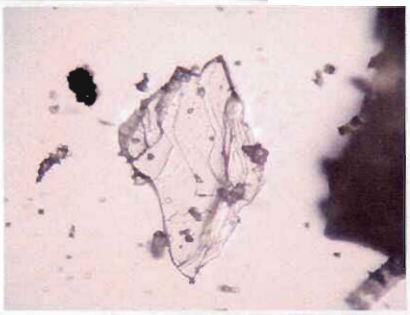	Optical microscopy (23°C)	Irregular-shaped, clear crystals
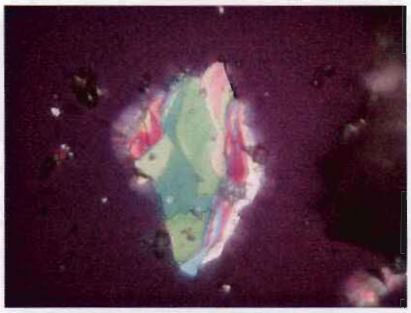	Polarising optical microscopy (23°C)	Birefringence of the polarised light by the crystals (indicative of crystalline materials)
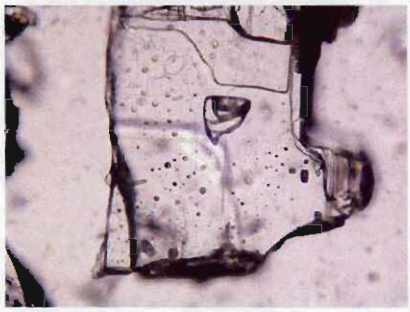	Hot stage microscopy (29°C)	Irregular-shaped, clear crystals
	Hot stage microscopy (104°C) (sample covered with silicon oil)	No bubble formation, only darkening of the clear crystals with apparent crystal growth on the crystal surface, without NMP evaporation
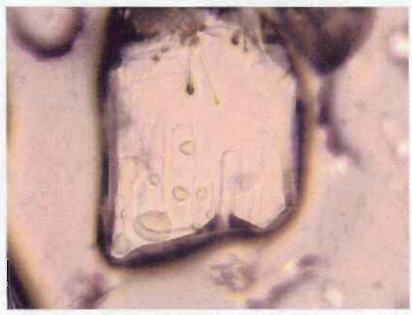	Hot stage microscopy (sample not covered with silicon oil) (106°C)	Melting of the NMP solvate

Table 3.11 (continued)

NMP solvate		
Photomicrograph	**Technique and temperature**	**Observation**
	Hot stage microscopy (108°C)	NMP solvate melted with recrystallised product dispersed throughout
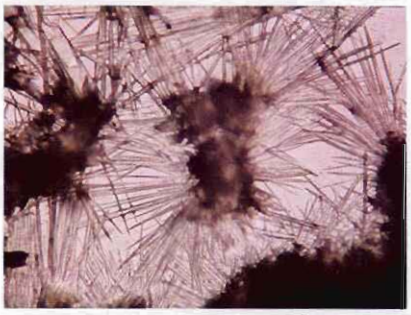	Hot stage microscopy (110°C)	Recrystallisation of stavudine from the melt
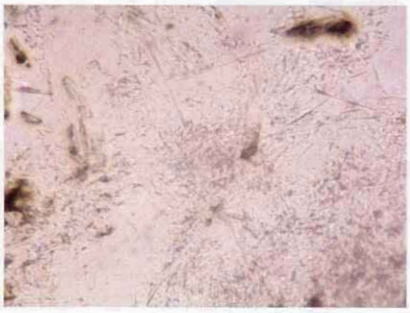	Hot stage microscopy (170°C)	Melting and degradation of the recrystallised product

Table 3.12 SEM photomicrographs of form III and the NMP solvate

Photomicrograph	Description
Form III 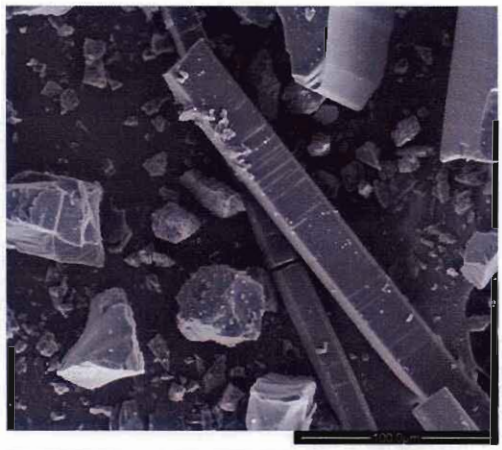	Needle-shaped crystals
NMP solvate 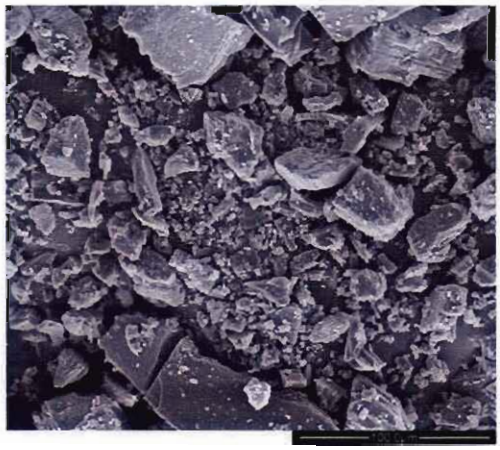	Irregular shaped crystals

In order to further understand the thermal behaviour of form III and the NMP solvate, and to determine the polymorphic form that these pseudopolymorphs interconvert to after dehydration (or melting and recrystallisation in the case of the NMP solvate), VT-XRPD analysis were performed on these two solid states (see figure 3.10).

Figure 3.10 illustrates that the diffractograms of form III start to show a significant change in appearance when the temperature increases from 120 to 140°C, and this corresponds to the temperature range in which dehydration of form III occurs (see figure 3.9 (a)). The VT-XRPD patterns of the NMP solvate illustrates that a significant change in the appearance of the diffractograms take place between 100 and 120°C, and this corresponds to the temperature range where melting of the solvate and recrystallisation of stavudine occurs (see figure 3.9 (b) and table 3.11).

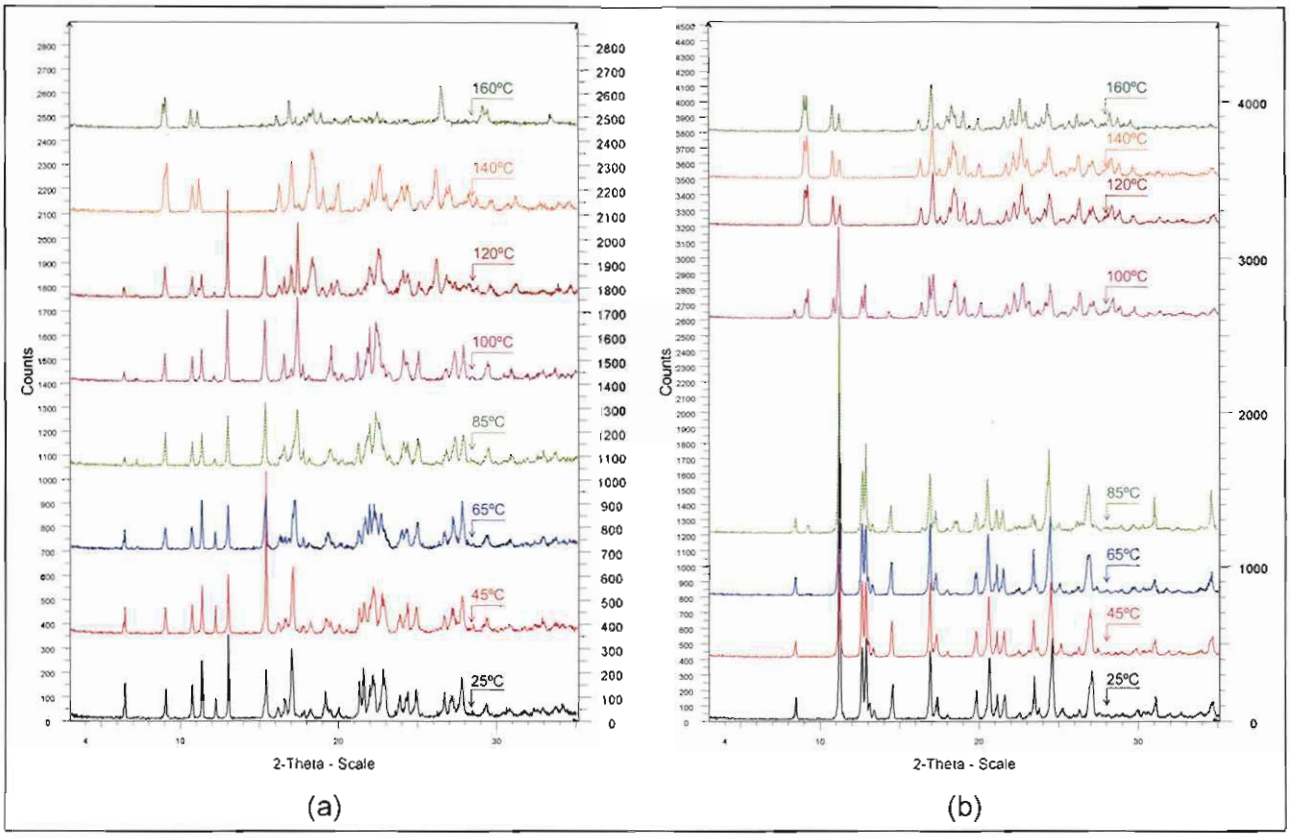

Figure 3.10 The VT-XRPD patterns obtained for (a) form III and (b) the NMP solvate.

As can be seen in figure 3.10 the VT-XRPD pattern of form III at 140 and 160°C, and the VT-XRPD pattern of the NMP solvate at 120, 140 and 160°C have a similar appearance, and it also corresponds to the diffractogram of the form I/II mixture illustrated in figure 3.3. Table 3.13 represents a comparison between the unique diffraction peaks that is found in the diffractograms of form III and the NMP solvate at 120, 140 and 160°C, and the unique peaks of polymorphic form I and form II.

Table 3.13 A comparison between the diffraction peaks of form III and the NMP solvate at 120, 140 and 160°C, and the unique diffraction peaks of form I and form II

	Form I	Form II	The form I/II mixture	Form III		NMP solvate		
				140°C	160°C	120°C	140°C	160°C
Position (°2θ)	-	11.243	11.225	11.226	11.206	11.238	11.225	11.211
	-	18.620	18.637	18.566	18.597	18.601	18.600	18.527
	19.117	-	19.137	19.110	19.132	19.107	19.113	19.052

The intensities of the peaks in the diffractograms of form III and the NMP solvate at 160°C decrease, and the peaks show a change in position compared to the peaks of the diffractograms at 120 and 140°C. The decrease in intensity is due to the onset of melting of stavudine, leading to a loss in the unit cells of the crystals and thus a decrease in the crystallinity of the samples. This also disrupts the powder bed surface in the sample holder resulting in a change in the diffraction angles of the peaks.

It is clear from table 3.13 that after dehydration of form III, and after melting and recrystallisation of the NMP solvate, the crystal structure of the pseudopolymorphs transform to polymorphic form I and form II to create a form I/II mixture. This is contradictory to the results of Gandhi *et al.* (2000:228), which suggested that form III transforms to polymorphic form I.

3.3.4 Amorphous (glassy) stavudine

A new glassy form of stavudine that is not described in the literature was prepared during this study, and a description of the preparation technique and the physicochemical properties of this new solid state will be discussed in chapter 4.

Conclusion

The two polymorphic forms of stavudine were successfully prepared, although the solvent and recrystallisation conditions had to be carefully controlled in order to avoid the formation of the form I/II mixture (the recrystallisation experiments were performed at 21°C). The physicochemical analysis performed in this study on these polymorphs confirmed those results described in the literature, whilst it was shown that form I and II are not enantiotropically related. Two known pseudopolymorphic forms of stavudine, the hydrate and the NMP solvate, were prepared and the study of these solid states confirmed previously published data. It was however shown that the hydrate and the NMP solvate transform to a mixture of form I and II, and not to pure form I, when desolvation (or melting and recrystallisation in the case of the NMP solvate) occurs.

CHAPTER 4

The glassy solid state of stavudine

Introduction

An increase in the solubility of the solid state of a drug offers the advantage of providing a greater systemic absorption of the drug, and results in a reduced amount of the drug being required in the dosage form in order to achieve the same therapeutic effect as the original product. The solid state that generally meets this requirement is the amorphous or glassy state, but it has the disadvantage of being thermodynamically unstable when compared to the original solid state. There are however methods that can be used to increase the stability of the glassy state, of which nano-coating is the most recently discovered that offers the most promising applications for the future (Wu *et al.*, 2006:1).

4.1 The glassy solid state of stavudine

During this study a glassy solid state of stavudine was prepared and characterised using the analytical techniques described in chapter 3, and the results will be presented in this section. The dissolution behaviour of this glassy solid state was also determined and compared to the dissolution behaviour of form I and form II of stavudine, and the technique and method used as well as the results obtained are described in the following chapter.

4.2 Preparation of glassy stavudine

The glassy stavudine was prepared by heating a small amount of the stavudine raw material on a microscope slide using a Velp® Scientifica (Italy) heating magnetic stirrer, and allowing the melt to cool to ambient temperature. Since stavudine decomposes after melting (Gandhi *et al.*, 2000:224), extreme caution had to be exercised to ensure that the stavudine did not decompose during this melting process. Hence, only small quantities (approximately 30 – 50 mg) of the raw material were spread out on the microscope slide, and as soon as melting commenced, the microscope slide was removed from the heat source and placed on a cold granite surface. The residual heat of the melt caused the whole sample to melt.

4.3 Characterisation of the glassy stavudine

4.3.1 Thin-layer chromatography (TLC)

Thin-layer chromatography (TLC) was used in order to confirm that the stavudine did not decompose during this melting procedure of preparing the glassy stavudine. The TLC method for stavudine capsules, as described in the United States Pharmacopeia 2007 (USP30:NF25) was used as a guide, and will be briefly described (United States Pharmacopeial Convention, 2007).

The stavudine raw material (Xiamen Mchem Laboratories Ltd., Xiamen, China) was used as the stavudine reference, and thymine (Sigma-Aldrich, Steinheim, Germany) was used as the degradation product reference. One milligram each (weighed using a Mettler Toledo microbalance that was calibrated using a 1 mg calibration standard (grade E2), Greifensee, Switzerland) of the glassy stavudine, the stavudine raw material and the thymine were dissolved in five millilitres of Milli-Q water, using sonication (Metason 120, Struers, Copenhagen, Denmark) to yield three separate solutions with concentrations of 0.2 mg/ml each. Ten micro litres of each solution (applied in two 5 µl portions) were spotted on an Alugram® Sil G/UV_{254} TLC plate (Macherey-Nagel GmbH & Co. KG, Düren, Germany), using micropipettes (BRAND GMBH, Wertheim, Germany) and allowed to dry. The chromatogram was developed in a chamber, saturated with the mobile phase (chloroform:ethanol (Merck Chemicals (Pty) Ltd., South Africa):water (100:50:2)). The TLC plate was allowed to develop until the solvent front had moved 10 cm from the origin. The TLC plate was removed from the chamber, the solvent front was marked and the plate allowed to dry for 5 – 10 minutes at ambient conditions. The spots were visualised using an ultraviolet lamp at a wavelength of 254 nm (Camag Reprostar, Switzerland) (United States Pharmacopeial Convention, 2007).

The R_f values (calculated using equation 4.1 and figure 4.1) of the stavudine raw material and the glassy stavudine were 0.700 and corresponded with each other, whist the R_f value of thymine (0.650) differed from this value. This indicated that the stavudine did not decompose during the melting process and that the glassy stavudine did not contain detectable traces of degradation products.

$$R_f = \frac{R_1}{R_2} \qquad (4.1)$$

Where: R_1 = the distance travelled by each spot from the origin

R_2 = the distance travelled by the mobile phase from the origin.

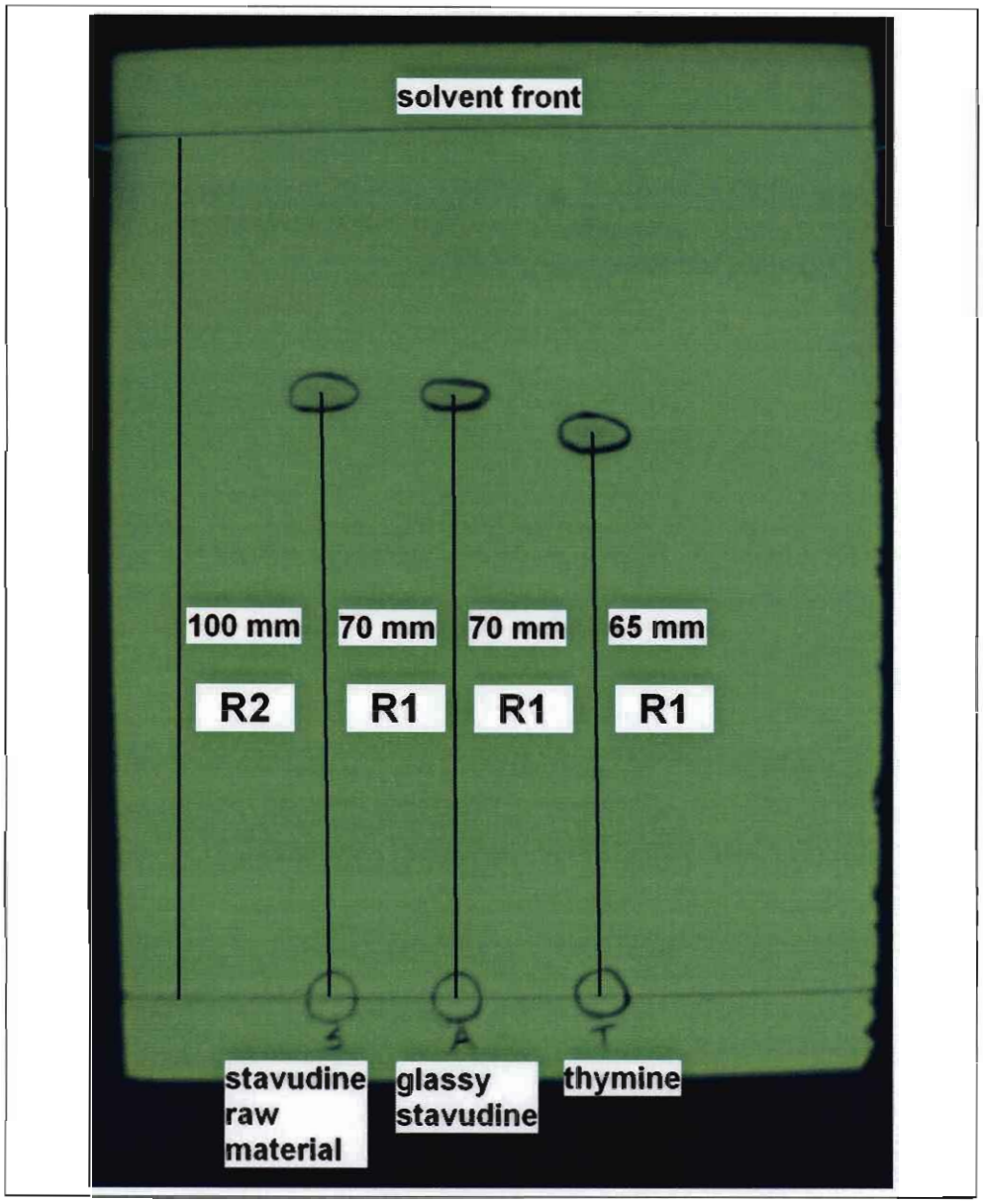

Figure 4.1 A photograph of the TLC plate obtained from the TLC analysis.

4.3.2 X-ray powder diffraction (XRPD)

In order to confirm the glassy (amorphous) behaviour, XRPD analysis was performed on the glassy stavudine, using the equipment and technique mentioned in section 3.2.1.1. The diffractogram in figure 4.2 shows a broad hump which is also called the amorphous halo, and this is indicative of amorphous solid states. No clearly defined peaks were detected for the glassy stavudine.

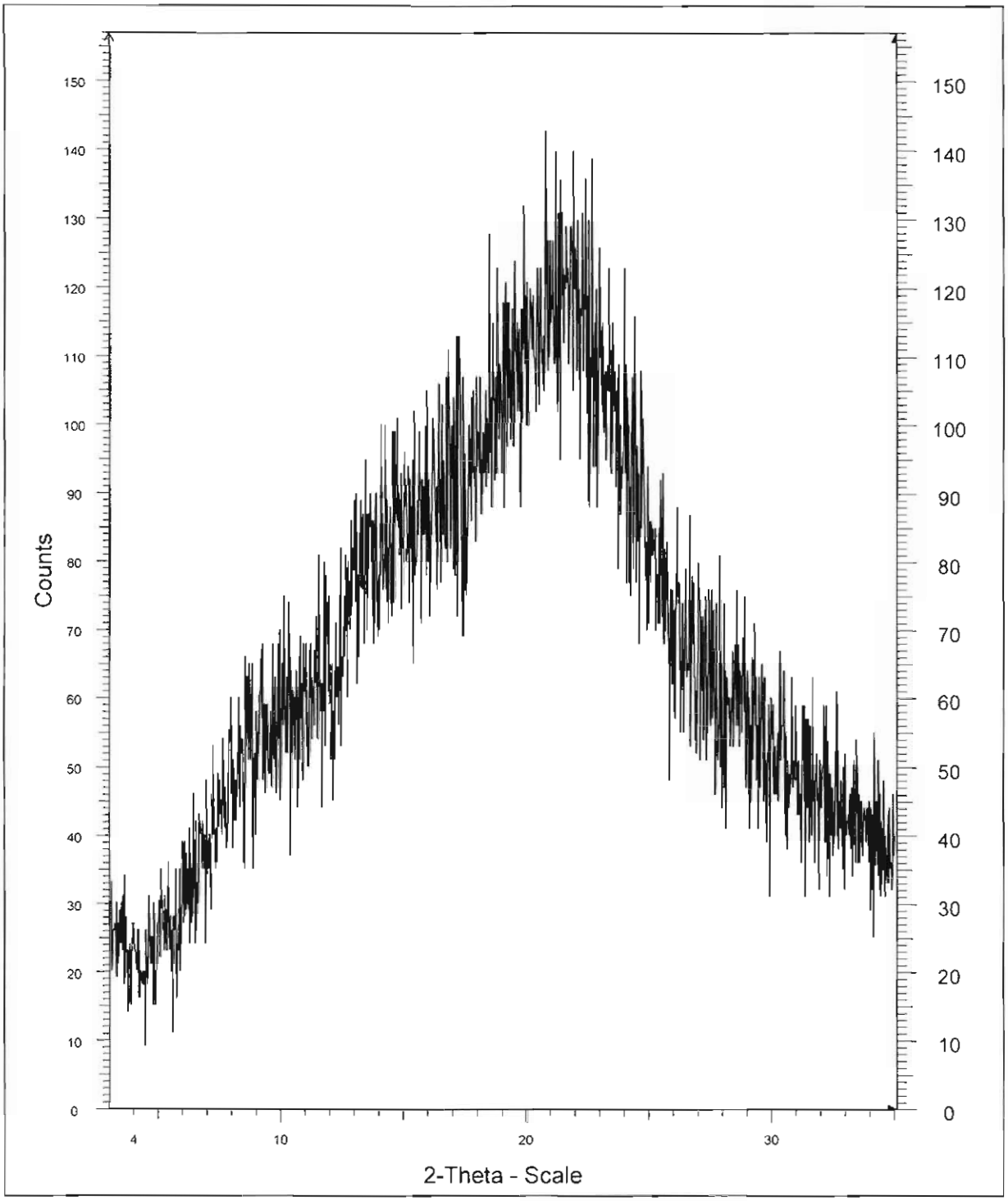

Figure 4.2 The X-ray powder diffractogram of the glassy stavudine.

4.3.3 Diffuse reflectance infrared Fourier transform spectroscopy (DRIFTS)

The infrared (IR) spectrum of the glassy stavudine is shown in figure 4.3 (a). This spectrum differed from that of the crystalline forms of stavudine as is seen in figure 4.3 (b). The IR spectrum of the glassy stavudine has an unique absorption band at 551 cm^{-1}, and no absorption bands in the 3600 – 3200 cm^{-1} region. Although the IR spectrum of the NMP solvate also has no absorption bands in this region, the IR spectrum of the glassy stavudine has a broader peak in this region compared to the NMP solvate.

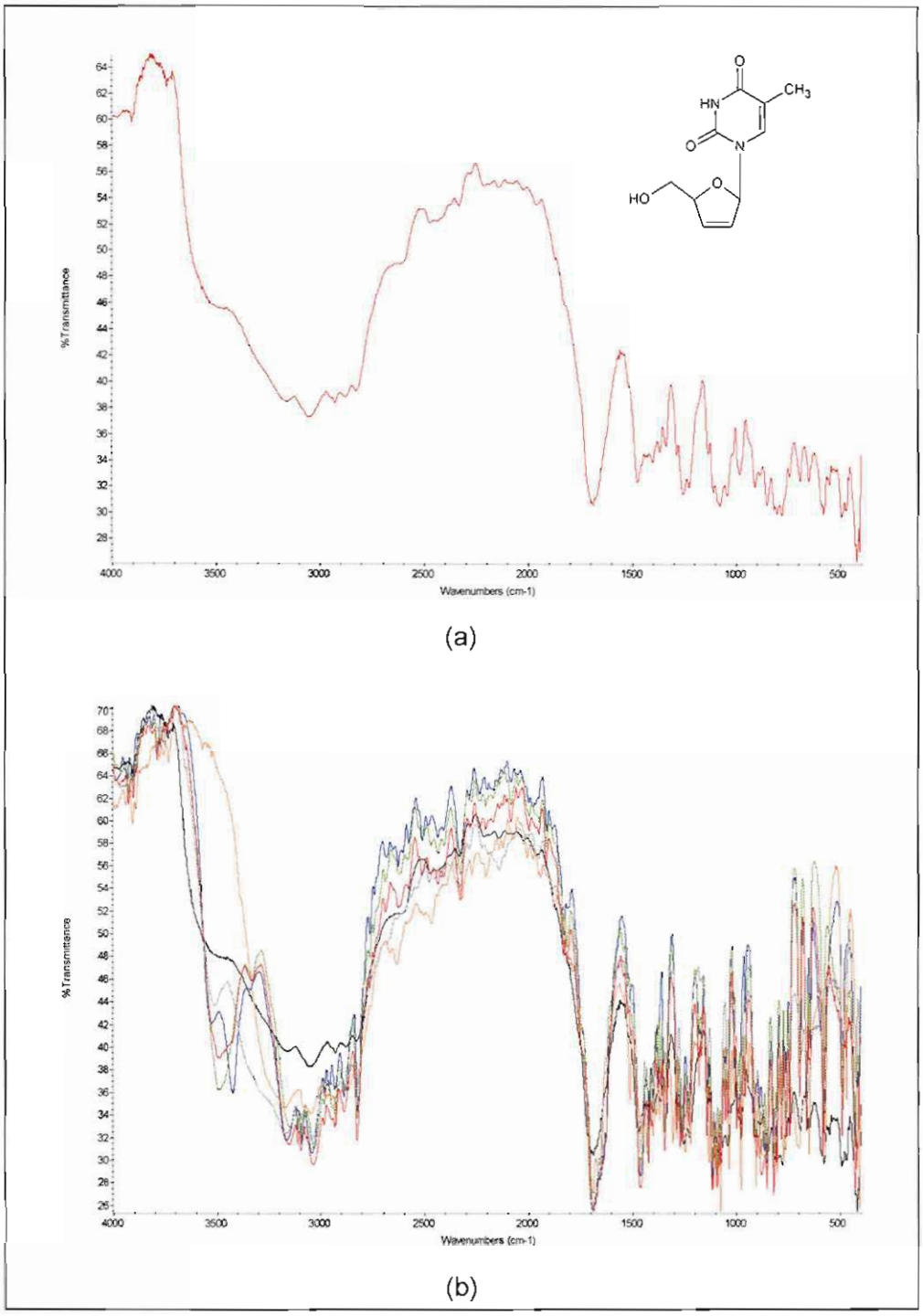

Figure 4.3 (a) The IR spectrum of the glassy solid state of stavudine. (b) An overlay of the IR spectra of the solid states of stavudine studied (form I, form II, the form I/II mixture, form III, NMP solvate and glassy stavudine).

The main absorption peaks in the infrared spectrum of the glassy stavudine is presented in table 4.1, and the unique absorption peak is highlighted.

Table 4.1 The main absorption peaks in the infrared spectra of the glassy stavudine

Glassy stavudine
Wavenumber (cm^{-1})
405.6
419.1
467.2
492.5
551.1
577.6
650.8
691.3
743.1
777.5
801.5
849.2
907.6
979.1
1041.1
1075.1
1107.4
1133.3
1223.8
1250.3
1283.2
1333.8
1364.5
1399.9
1473.2
1560.6
1685.8
1959.8
2139.1
2211.5
2332.2
2468.7
2826.9
2874.8
2928.4
3056.6
3165.1
3480.3
3735.9
3771.1
3801.9
3816.4
3854.8
3905.4

4.3.4 Differential scanning calorimetry (DSC)

The DSC thermogram of the glassy stavudine is shown in figure 4.4, and it clearly demonstrated the presence of a glass transition temperature (T_g) at 46.11°C (a baseline-shift). The T_g is the temperature below which the molecules are configurationally frozen in the glassy state, and thus lack the motion of molecules in the liquid phase (Byrn *et al.*, 1999:249).

The T_g is characteristic of each amorphous solid state and varies according to the rate at which the melt is cooled during the preparation of the glassy solid (the slower the rate of cooling of the melt, the lower the T_g will be). Above the T_g the amorphous solid is said to be in a rubbery state and will flow, and the molecules thus have more configurational motion compared to the glassy state, but it is still not comparable to the liquid state. Figure 4.4 illustrates that above the T_g the stavudine glass recrystallises at a temperature of 110.15°C (the exotherm), after which it melts at 157.84°C (the sharp endotherm), followed by the decomposition of the stavudine.

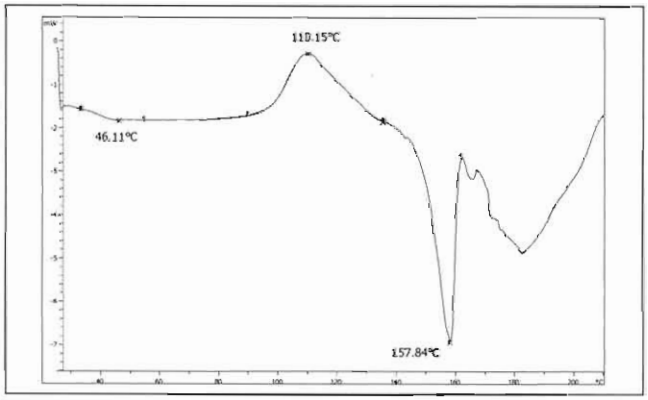

Figure 4.4 The DSC thermogram of the glassy stavudine.

The TGA and Karl Fischer analysis of the glassy stavudine showed an insignificant amount of weight loss (0.02%) and negligible moisture content (0.17%) of the glassy solid.

The fragility of the stavudine glass was calculated using the following equation:

$$\frac{T_m}{T_g} \qquad (4.2)$$

Where: T_m and T_g are the melting and glass transition temperatures respectively.

The stavudine glass had a ratio of 3.42, indicating that it is a strong glass (glasses with a ratio above 1.5 are classified as strong whilst a ratio below 1.5 is indicative of a fragile glass), and the stavudine glass thus exhibits minimal molecular mobility changes at the T_g, hence the small change in heat capacity at the T_g as seen in figure 4.4 (Craig *et al.*, 1999:184).

4.3.5 Polarising optical and hot-stage microscopy (HSM)

Polarising optical microscopy confirmed the amorphous nature of the glassy stavudine since no birefringence of the polarised light was observed (see table 4.2). Hot-stage microscopy (HSM) confirmed the results obtained from DSC, and are presented in table 4.2.

Table 4.2 Photomicrographs obtained with polarising optical and hot stage microscopy

Glassy stavudine		
Photomicrograph	**Technique and temperature**	**Observation**
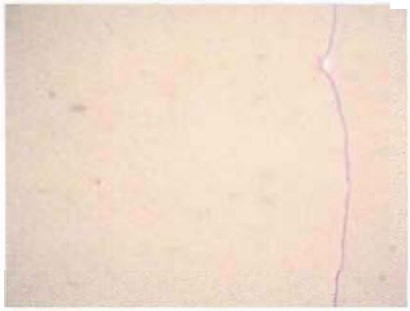	Optical microscopy (25°C)	Clear, irregular shaped solid
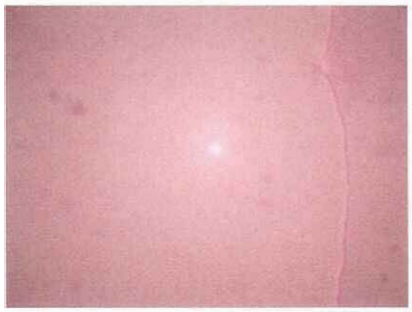	Polarising optical microscopy (25°C)	Clear, irregular shaped solid (no birefringence of polarised light)
	Hot stage microscopy (25°C)	Clear, irregular shaped solid
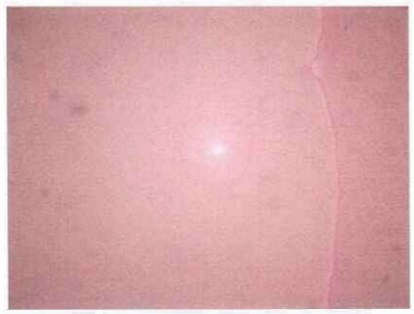	Hot stage microscopy (45°C) combined with polarising optical microscopy	Clear, irregular shaped solid (no visible change in appearance at T_g)
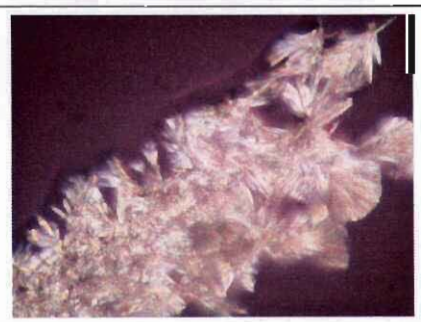	Hot stage microscopy (100°C) combined with polarising optical microscopy	Onset of recrystallisation of stavudine from the glass (visible due to birefringence of polarised light)

Table 4.2 (continued)

Glassy stavudine		
Photomicrograph	**Technique and temperature**	**Observation**
	Hot stage microscopy (116°C) combined with polarising optical microscopy	Further recrystallisation of stavudine (visible due to birefringence of polarised light)
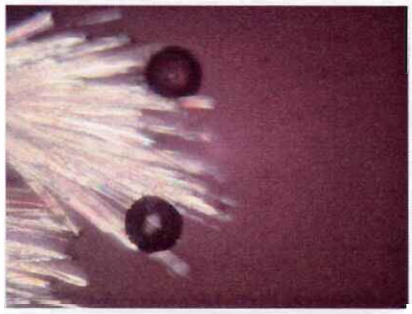	Hot stage microscopy (125°C) combined with polarising optical microscopy	The end of the recrystallisation process
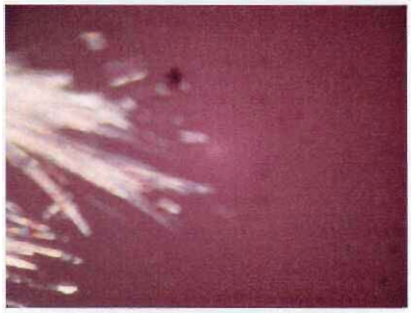	Hot stage microscopy (141°C) combined with polarising optical microscopy	Onset of melting of the recrystallised stavudine
	Hot stage microscopy (159°C)	Stavudine completely melted

4.3.6 Scanning electron microscopy (SEM)

Scanning electron microscopy was used to study the morphology of the glassy stavudine. The glassy stavudine did not have a particular morphological shape, however it had a liquid-like appearance (figure 4.5).

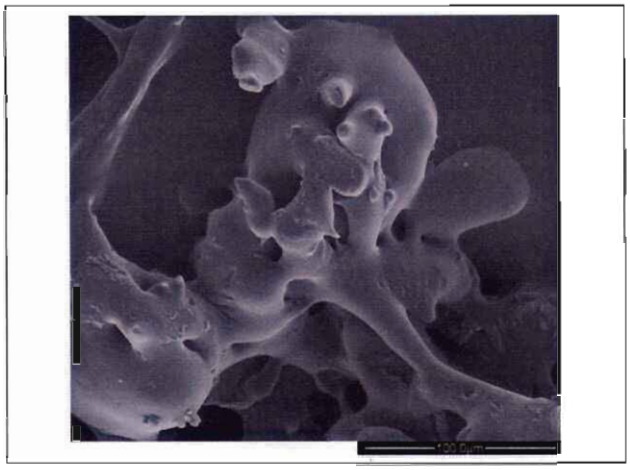

Figure 4.5 The SEM photomicrograph of the glassy stavudine.

4.3.7 Variable temperature X-ray powder diffraction (VT-XRPD)

VT-XRPD analysis was performed on the glassy stavudine in order to determine which polymorphic form recrystallised beyond the glass transition temperature. The results from this analysis are shown in figure 4.6 (a).

As can be seen in figure 4.6 (a) the diffractograms of the glassy stavudine between 85 and 120°C resemble the diffractogram of the form I/II mixture of stavudine (see figure 3.3 in the previous chapter). The glassy stavudine thus recrystallises as a mixture of form I and form II, comparable to the form I/II mixture described throughout this dissertation. Table 4.3 demonstrates the diffraction angles of form I, form II and the form I/II mixture, as well as the diffraction angles in the diffractogram of the glassy stavudine which are detected at 120°C, and this indicates that this diffractogram is similar to the diffractogram of the form I/II mixture.

Table 4.3 A comparison of the diffraction peaks of the glassy stavudine at 120°C and the diffraction peaks of form I, form II and the form I/II mixture

	Form I	Form II	The form I/II mixture	Glassy stavudine 120°C
Position (°2θ)	-	11.243	11.225	11.225
	-	18.620	18.637	18.633
	19.117	-	19.137	19.160

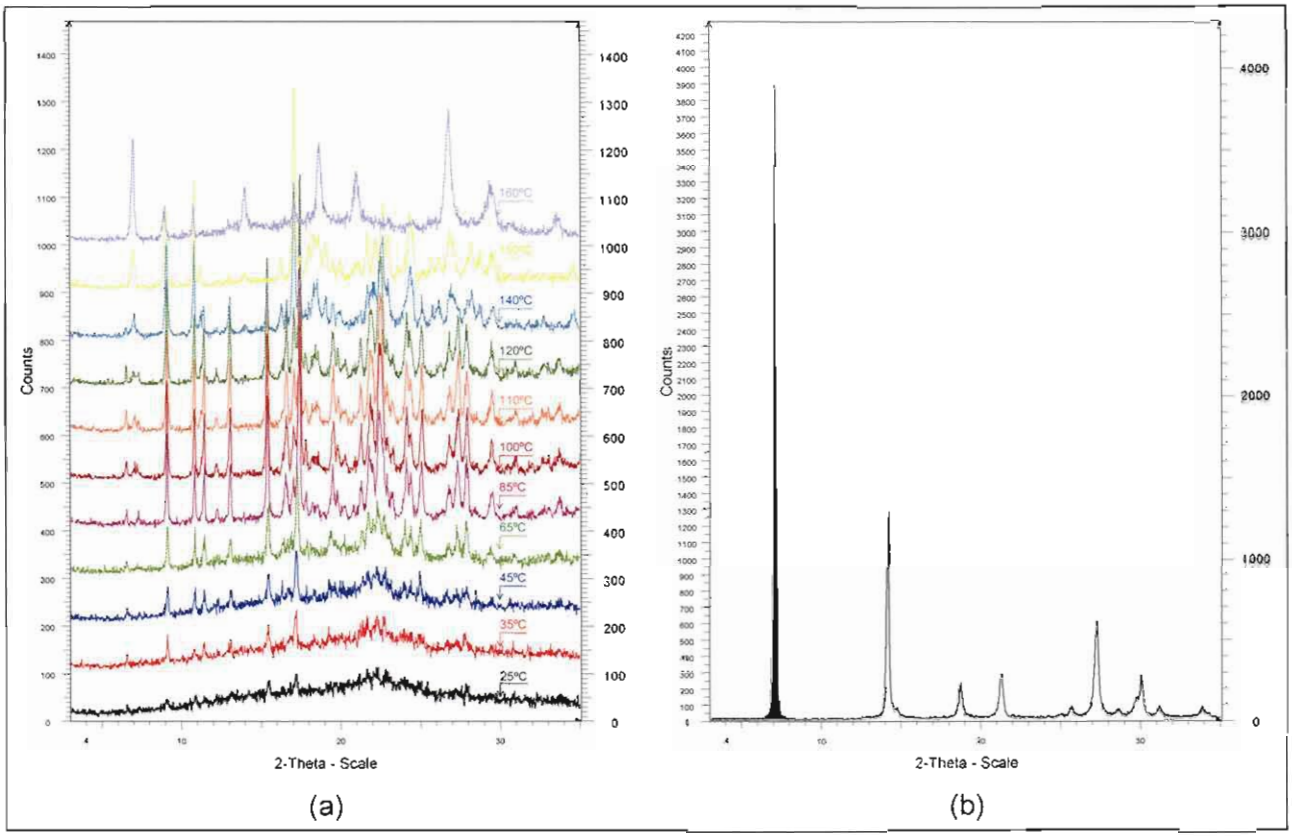

Figure 4.6 The VT-XRPD diffractograms of (a) glassy stavudine and (b) the XRPD pattern of thymine.

Above 120°C the product that recrystallised from the glassy stavudine starts to decompose and form the degradation product, thymine, as the temperature reaches the melting point. This is evident from the appearance of the diffraction peaks at 7.11 and 14.27°2θ, which are the characteristic peaks of the XRPD pattern of thymine (see figure 4.6 (b)).

Conclusion

A glassy solid state of stavudine was successfully prepared and characterised, and the amorphous nature of this solid state was demonstrated. During the next chapter the dissolution behaviour of this glassy stavudine will be compared to that of form I and form II of stavudine.

CHAPTER 5

Dissolution behaviour of the polymorphic forms of stavudine

Introduction

In order for a drug to exert a systemic pharmacological effect after being administered orally, it has to be absorbed from the gastrointestinal tract into the systemic circulation. This is achieved once the drug is in solution. The rate of systemic absorption is often limited by the rate of dissolution of the drug. The dissolution rate might thus be the rate-limiting step during the absorption process of drugs, and it is vital that the dissolution rate be determined in order to predict the absorption and pharmacokinetic behaviour of drugs (Aulton, 2002:16).

5.1 The theory and mechanism of dissolution

The term dissolution refers to the transfer of molecules or ions from a solid state into a solvent, resulting in the formation of a solution containing these molecules or ions. The extent of the dissolution process under a set of experimental conditions is referred to as the solubility of the solute in that particular solvent (Aulton, 2002:16).

The dissolution process, illustrated in figure 5.1, is comprised of two consecutive steps. Firstly, an interfacial reaction occurs between the solute and the solvent resulting in the release of molecules from the solid phase. The resulting solution that is in direct contact with the solid phase is thus saturated with solute molecules, and the concentration of this boundary layer solution is denoted C_s. During the second stage of the dissolution process the solute molecules in the boundary layer solution are transported from the solid-liquid interface into the bulk solution by way of diffusion, and the concentration of the molecules in the bulk solution is denoted C (Aulton, 2002:18).

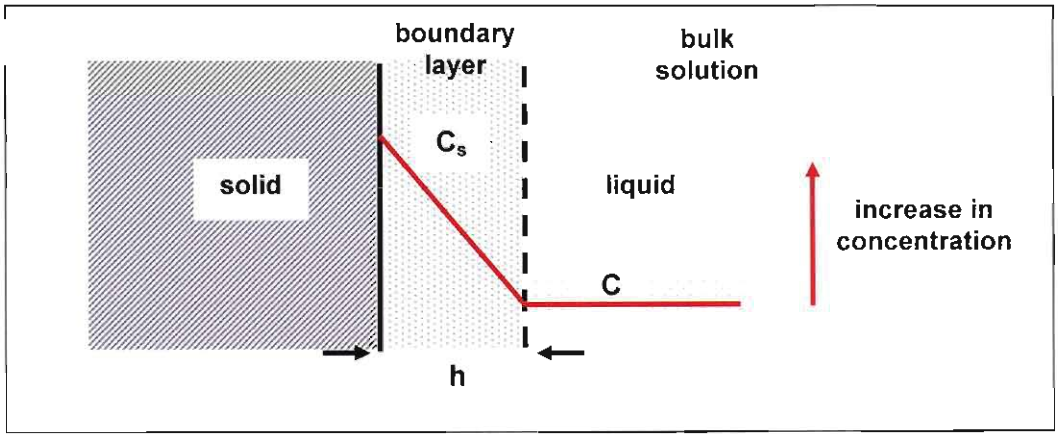

Figure 5.1 An illustration of the dissolution process from a solid particle (Aulton, 2002:19).

Equation 5.1 illustrates the Noyes-Whitney equation that is used to determine the dissolution rate of a drug from a single spherical particle:

$$\frac{dm}{dt} = \frac{kA(C_s - C)}{h} \qquad (5.1)$$

Where: $\frac{dm}{dt}$ = the rate of mass transfer of solute molecules through the boundary layer

k = the diffusion coefficient

A = the area of the particle

C_s = the boundary layer concentration

C = the bulk solution concentration

h = the thickness of the boundary layer.

There are a variety of factors that influence the dissolution rate of solid particles in liquids, and these factors may either accelerate or hinder the dissolution process. Table 5.1 provides a summary of some of these factors (Aulton, 2002:19-20).

Table 5.1 A summary of factors that influence the dissolution rate of solids (Aulton, 2002:20)

Factors affecting the dissolution rate	The influence of these factors on the dissolution rate
Particle size	The smaller the particles, the greater the rate of dissolution (A α 1/particle size)
Dispersibility of the particles	If the particles are poorly dispersed, the surface area decrease resulting in a decrease in the dissolution rate
Porosity of the particles	Highly porous particles have a greater surface area and thus a greater dissolution rate
Temperature	Dissolution is either exothermic or endothermic, and temperature may thus accelerate or hinder dissolution
Nature of the dissolution medium	Changing the pH or addition of co-solvents may increase or decrease the dissolution rate depending on the polarity of the solute
Molecular structure of the solute	Ionic substances tend to dissolve at a greater rate in polar solvents compared to organic molecules
Crystalline form of the solute	Different polymorphs demonstrate differences in solubility (see section 1.2.3.2)
Presence of other compounds	The presence of common ions or the formation of molecular complexes may decrease the dissolution rate

Table 5.1 (continued)

Volume of the dissolution medium	The larger the volume of the medium, the smaller the concentration in the bulk (C), thus the faster the rate of diffusion and dissolution
Removal of dissolved solute	Adsorption of the solute onto an adsorbent material lowers the bulk concentration (C), thus increasing the dissolution rate due to faster diffusion
Thickness of the boundary layer	The slimmer the boundary layer the faster dissolution will occur since the molecules diffuse into the bulk at a faster rate
Diffusion coefficient	The diffusion coefficient is influenced by the size of the solute and the viscosity of the medium, larger molecules has a lower rate of diffusion (and dissolution), and highly viscous fluids decrease the rate of diffusion (and dissolution)

5.2 Method

Dissolution testing was performed on three of the polymorphic forms of stavudine described throughout this study i.e.: form I, form II and the glassy stavudine, as well as on the form I/II mixture. For the purpose of this study, the dissolution method for stavudine capsules that is described in the United States Pharmacopeia 2007 (USP30:NF25) was used as a guide to determine the dissolution behaviour of the various stavudine polymorphic forms, with the exception that instead of using stavudine capsules during the dissolution testing, 40 mg of the various polymorphic powders (which were weighed using a calibrated Sartorius analytical balance – Goettingen, Germany) were added to each dissolution vessel. It must be emphasised that the polymorphic powders that were used during the dissolution testing were manually sieved using a 45 µm Madison test sieve (Madison Filter Solutions, Madison Filter SA Pty (Ltd.), Johannesburg, South Africa), thus ensuring uniform particle size distribution of the polymorphic powders. This was done in order to eliminate the possible influence of particle size variations of the various polymorphic powders on the results of the dissolution testing (United States Pharmacopeial Convention, 2007).

5.3 Apparatus

The dissolution tests were performed using a Vankel VK7000 dissolution tester (Varian Inc., Palo Alto CA, USA). The dissolution samples were analysed spectrophotometrically using a Varian Cary 50 UV-Visible Spectrophotometer (Varian Inc., Palo Alto CA, USA).

5.4 Technique

As directed by the United States Pharmacopeia 2007 (USP30:NF25), the dissolution medium that was used was 900 mL of degassed purified water maintained at a temperature of 37±0.5°C, the dissolution apparatus 2 (paddles) was used with a rotational speed of 75 revolutions per minute, and the dissolution tests were performed for a period of 30 minutes. Since stavudine is soluble in water (i.e. between 10 and 30 parts of solvent are required to dissolve 1 part solute according to the USP30:NF25), it is expected that the added stavudine powder will completely dissolve within five minutes, and it was decided to withdraw samples of five millilitres of the dissolution medium from each of the six dissolution vessels at intervals of 1, 5, 10, 15 and 30 minutes from the time that the dissolution testing commenced. As stated in the United States Pharmacopeia 2007 (USP30:NF25), a dissolution test commences at the moment that the paddles start to rotate, and this is done as soon as the dosage form (or powder in this case) reaches the bottom of the dissolution vessel (United States Pharmacopeial Convention, 2007).

The amount of dissolved stavudine was calculated using the ultraviolet (UV) spectrophotometry method described by Gandhi *et al.* (2000:224). The principle of UV spectrophotometry is described by the Beer-Lambert law, which states that the absorbance (A) of light at a certain wavelength by a sample is directly proportional to the concentration (c) of the sample, the molar absorbtivity (ε) of the sample and the path length over which the incident light travels (*l*) (see in equation 5.2 and figure 5.2) (Sheffield Hallam University, 2007).

$$A = \varepsilon \, l \, c \qquad (5.2)$$

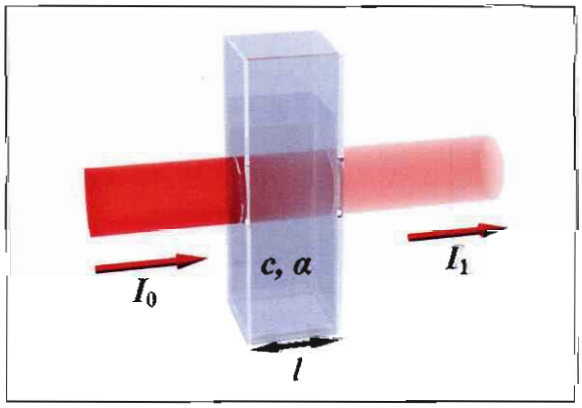

Figure 5.2 An illustration of the Beer-Lambert law (I_0, the intensity of the incident light; I_1, the intensity of the light passing through the sample; α, absorption coefficient; c, the concentration of the sample; *l*, the path length over which the incident light travels) (Anon, 2007).

Prior to determining the amount of dissolved stavudine by UV spectrophotometry, a calibration curve of absorbance (A) versus concentration (c, measured in µg/ml) was plotted in order to determine if there is a linear relationship between the absorbance and the concentration of stavudine solutions, and this plot was also used to determine the concentration of stavudine in the various dissolution samples. This calibration curve was produced by preparing a series of seven stavudine solutions with concentrations of 1, 5, 10, 15, 20, 25 and 50 µg/ml, which were respectively analysed using the spectrophotometer (solutions analysed by spectrophotometry need to be diluted since the Beer-Lambert law is not obeyed by highly concentrated solutions). Figure 5.3 shows the resulting calibration curve which was obtained, and it is clear from this graph that there is a linear relationship between the absorbance and the concentration of the various stavudine solutions within the range of 0 – 50 µg/ml. The equation that is displayed on the graph was used in order to determine the concentration of stavudine in the dissolution samples, and the potency of the stavudine standard was also compensated for during the calculations.

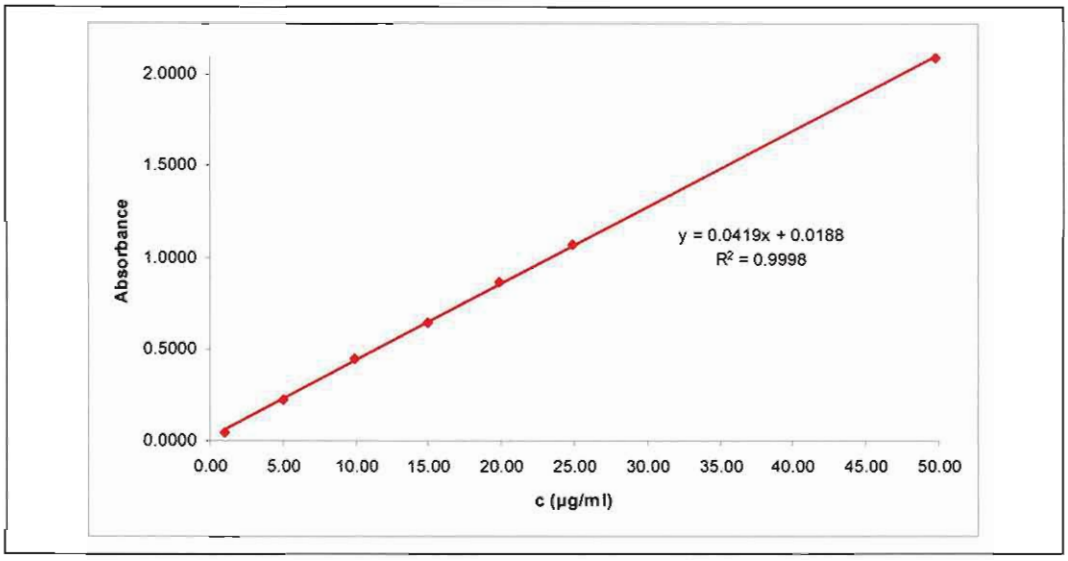

Figure 5.3 The calibration curve plotted for a series of standard stavudine solution.

In order to determine the amount of dissolved stavudine in the dissolution samples using the UV spectrophotometric method, two millilitres of the withdrawn dissolution medium was diluted to 10 ml with purified water in a volumetric flask, and the absorbance of the resulting solutions were determined at a wavelength of 265 nm. The withdrawn dissolution samples were diluted, since it was previously determined that this dilution would yield a solution with a stavudine concentration of approximately 10 µg/ml, and this concentration of stavudine solutions would be in the range of the concentrations used for constructing the calibration curve.

5.5 Results

The results of the dissolution tests are presented in table 5.2 and figure 5.4, and it is clear from these results that during the first minutes of the dissolution tests, a greater amount (between 5 and 16%) of the glassy stavudine had dissolved compared to the other polymorphic forms and the powder mixture tested. This was expected, since the glassy solid state (amorphous form) of a drug is generally more soluble than the polymorphic and pseudopolymorphic forms of the same drug (section 1.3.6). The amount of stavudine that had dissolved after one minute slightly differed between form I and form II, and after a period of five minutes the stavudine from all four samples had completely dissolved. The dissolution results of the polymorphic forms and the powder mixture of stavudine that were tested thus conformed to our in-house requirements that not less than 80% of the stavudine should dissolve within 30 minutes.

Table 5.2 A summary of the dissolution test results

Time (minutes)	Amount of stavudine dissolved (%)			
	Form I	Form II	Glass	Form I/II mixture
0	0	0	0	0
1	83.72	79.59	89.30	73.48
5	102.01	105.34	104.43	105.90
10	101.89	106.13	103.45	105.57
15	101.05	105.14	102.87	104.85
30	100.58	103.02	102.24	104.28

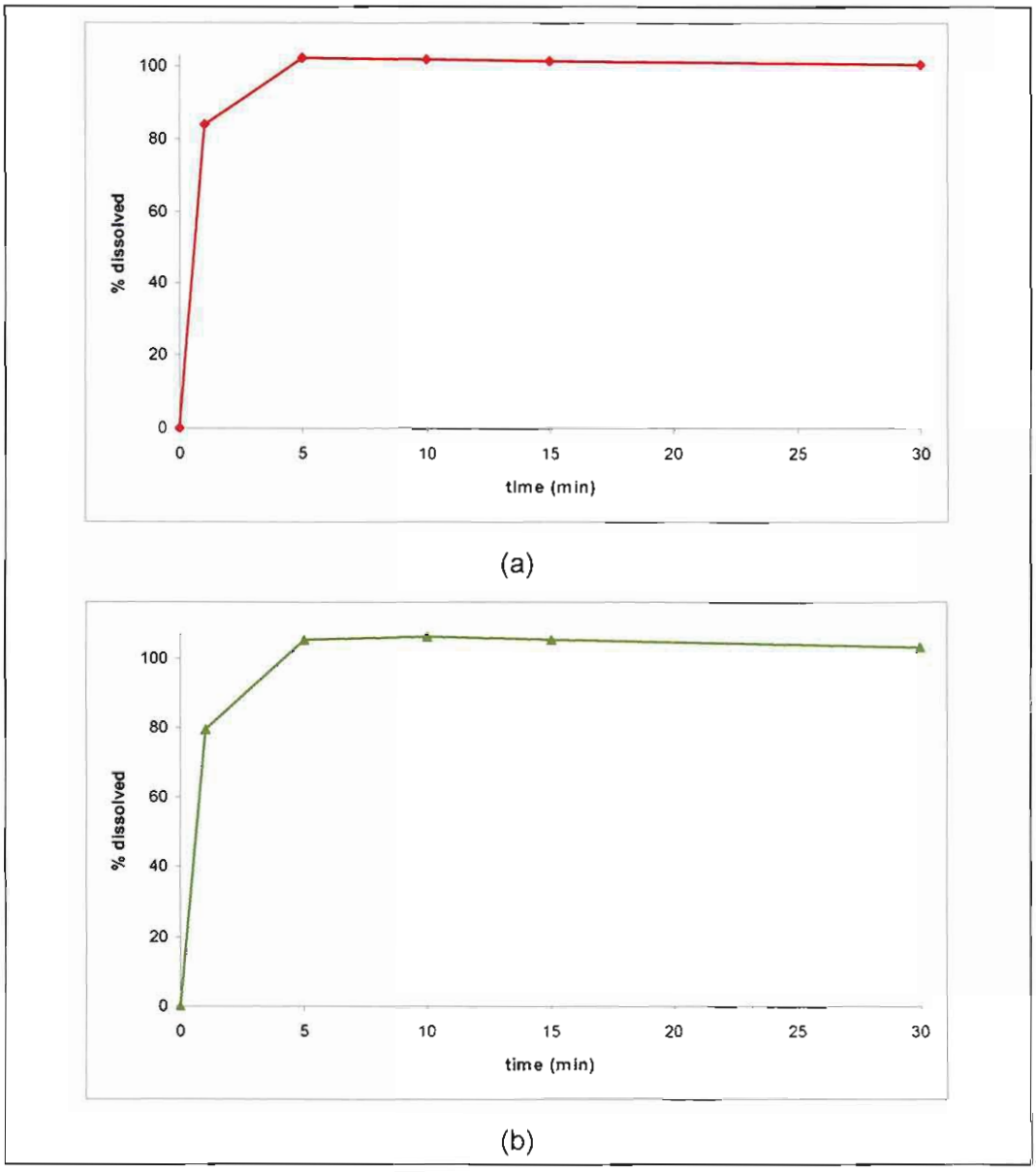

Figure 5.4 The dissolution profiles of (a) form I, (b) form II, (c) the glassy stavudine, (d) the form I/II mixture and (e) a summary of the dissolution profiles obtained.

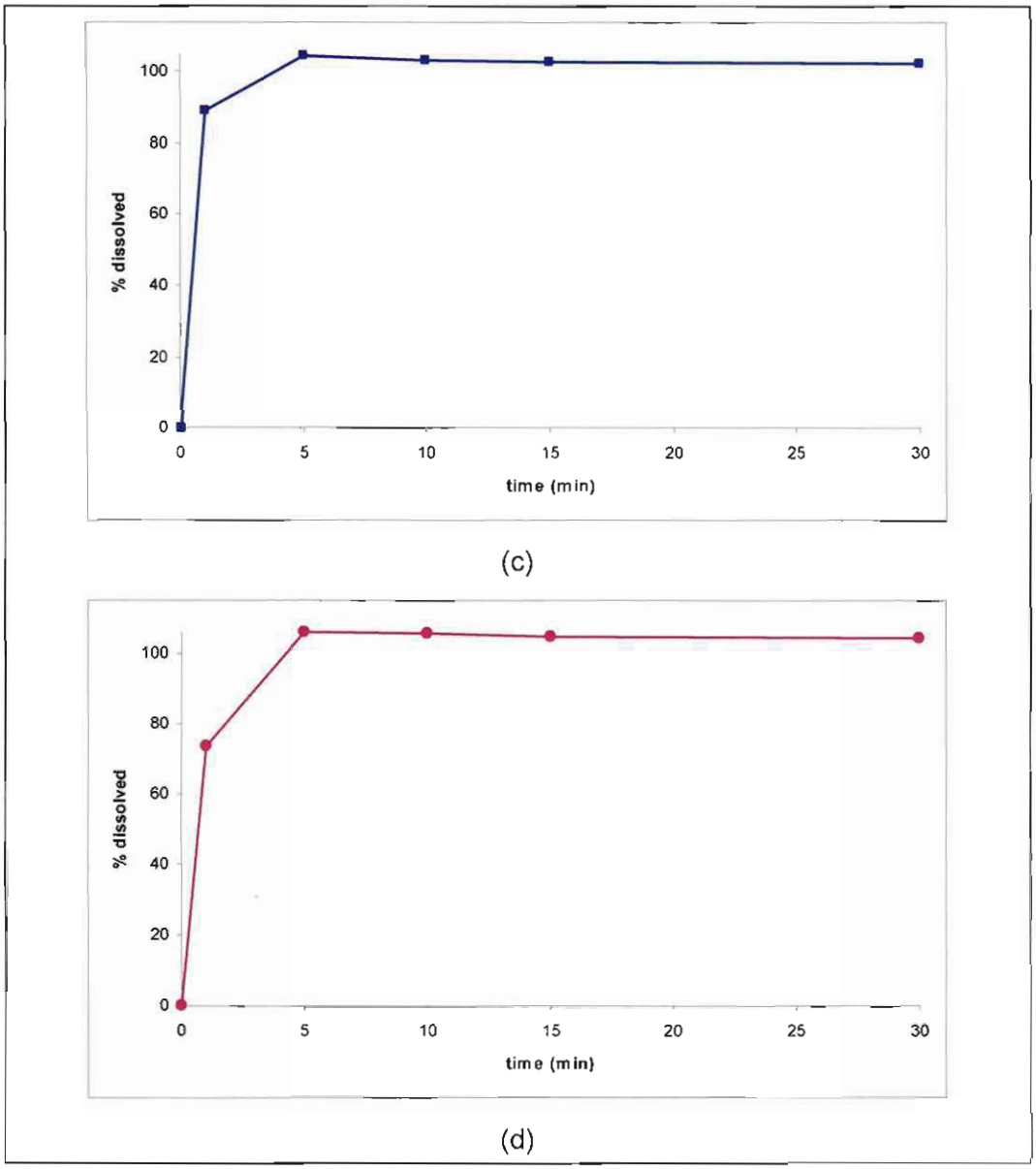

Figure 5.4 (continued)

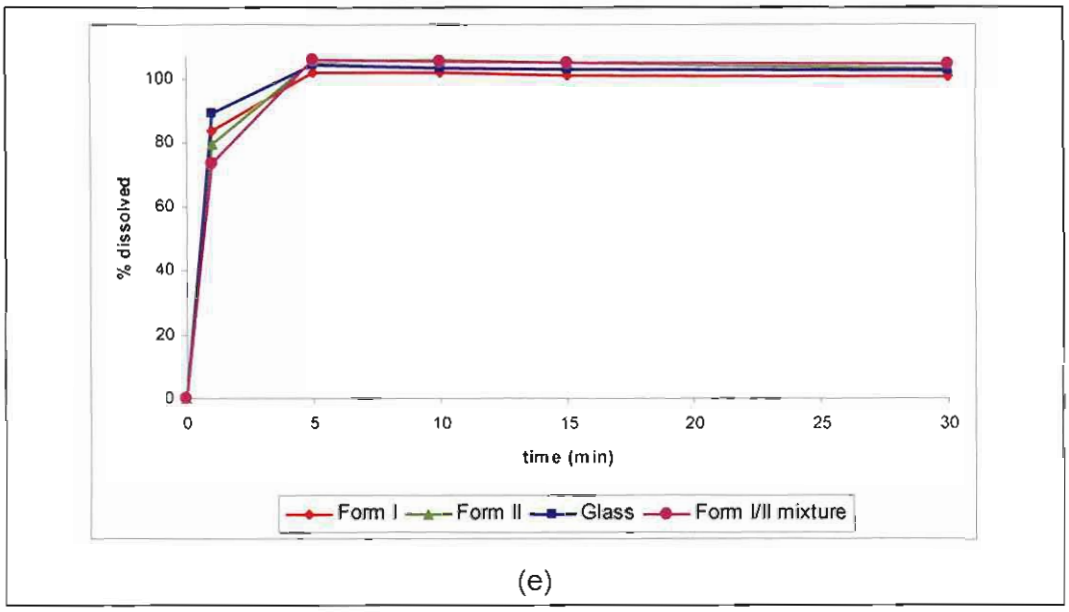

(e)

Figure 5.4 (continued)

The similarity factor (f_2), derived by Moore & Flanner (1996:66) (see equation 5.3), is used to compare the dissolution profiles of multipoint dissolutions:

$$f_2 = 50 \log \left\{ \left[1 + \frac{1}{n} \sum_{t=1}^{n} (R_t - T_t)^2 \right]^{-0.5} \times 100 \right\} \qquad (5.3)$$

Where: R_t = the percentage of the reference sample that dissolved

T_t = the percentage of the test sample that dissolved

n = the amount of withdrawals made during the dissolution testing.

The requirements for the comparison of dissolution profiles stipulated by the Medicines Control Council of South Africa were used during the comparison of the dissolution profiles of the stavudine samples. The dissolution profile of polymorphic form I was chosen as the reference profile (R_t), and the other dissolution profiles were thus compared with the profile of form I. According to these requirements, the profiles of form I and form II, form I and the glassy stavudine, and form I and the form I/II mixture are similar, since both the reference and the test sample show more than 85% dissolution within 15 minutes (see table 5.2), i.e. it is not necessary to calculate a similarity factor for these profiles (Medicines Control Council, 2006:5-6).

Conclusion

The available literature state that stavudine is highly soluble in water and this fact was undoubtedly proven during the dissolution tests performed during this study. A greater amount of the glassy stavudine had dissolved after one minute compared to the other polymorphic forms and the form I/II mixture tested, and the dissolution profiles of form I, form II, the glassy stavudine and the form I/II mixture are similar. It is possible that there might be a difference in the dissolution behaviour of the polymorphic forms of stavudine, and this difference could be detected using the intrinsic dissolution method, since a constant surface area of the powder is exposed to the dissolution medium during intrinsic dissolution testing.

CHAPTER 6

Quantification of mixtures of stavudine polymorphic forms

Introduction

This chapter describes the quantification of two polymorphic forms (form I and form II) of stavudine in a mixture, using either diffuse reflectance infrared Fourier transform spectroscopy (DRIFTS), or X-ray powder diffraction (XRPD). This was considered necessary since the stavudine raw material purchased for use in the pharmaceutical industry in South Africa is often found to be such a mixture, and these methods may thus be used to establish the composition of such stavudine raw material for quality control purposes.

6.1 Quantitative diffuse reflectance infrared Fourier transform spectroscopy

6.1.1 Background and introduction

Diffuse reflectance infrared Fourier transform spectroscopy (DRIFTS) is a powerful method for performing qualitative and quantitative analysis. The Kubelka-Munk equation (equation 6.1) is an accepted function that is used for quantitatively describing diffuse reflected radiation:

$$F(R_\infty) = \frac{(1 - R_\infty)^2}{2R_\infty} + \frac{2.303ac}{s} \qquad (6.1)$$

Where: $F(R_\infty)$ = the Kubelka-Munk reflectance

R_∞ = the reflectance of the sample relative to that of a non-absorbing standard

a = the molar absorption coefficient

c = the molar concentration of the analyte

s = the scattering coefficient.

In order to have a linear relationship between intensity and concentration, the scattering coefficient must be constant, and this is best achieved by controlling the sample homogeneity, bulk density (or packing density), particle size and shape, and specular reflectance. Once these requirements have been adhered to, a plot of the Kubelka-Munk intensity of a peak at a certain wavenumber, against the concentration of the specific analyte (calculated as a percentage of the inert matrix-sample mixture), should yield a straight line. This method has been successfully used by Hartauer *et al.* (1992:172-173) to quantify the

two polymorphic forms of sulfamethoxazole in a mixture of the two forms (Stephenson *et al.*, 2001:73).

There are also two other methods that can be used for the quantification of polymorphic mixtures using DRIFTS. In one method the absorbance - or intensity ratio of a characteristic peak to an inert peak is plotted against the percentage concentration of one of the polymorphic forms in the mixture, to obtain a linear correlation that can be used for quantitative analysis of samples with unknown concentrations. This method was used to quantify the amounts of two polymorphic forms of paroxetine hydrochloride, ranitidine hydrochloride, as well as stavudine (Buxton *et al.*, 1988:140; Mirmehrabi *et al.*, 2004:79; Mirmehrabi *et al.*, 2006:143). This then formed the basis for the quantitative DRIFTS method that was developed and used during this study.

The other method is slightly different from the first two in that peak intensities are not calculated to establish a relationship. Instead, the area of a unique peak in the absorption spectrum is determined and plotted against the percent content of one of the polymorphic forms in the mixture. This approach should yield a linear relationship, and it has been used successfully in the quantitative analysis of two polymorphic forms of the drug SC-41930 (a LTB_4 (leukotriene B_4 receptor) antagonist) (Roston *et al.*, 1993:299; Sharma & Mohammed, 2006:14). This method was applied during this study as well.

6.1.2 Sample preparation

For the purpose of this study pure batches of polymorphic form I and form II of stavudine were prepared by recrystallisation of stavudine raw material from single solvents. Methanol and n-propanol (Merck Chemicals, South Africa) were used as solvents to obtain polymorphic form I and form II respectively.

According to Mirmehrabi *et al.* (2004:77), the size distribution of the particles used in quantitative DRIFTS analysis, cause the intensity of the absorption bands (peaks) in the infrared spectrum to fluctuate, and can thus influence the results obtained from the analysis. In order to eliminate this problem they proposed using a narrow size distribution of particles by grinding and sieving the polymorphic powders. The grinding process may, however, cause interconversion of the different polymorphs and might not always be a feasible practice. This is critical to keep in mind during sample preparation. During this study, each batch of polymorphic stavudine was ground in a mortar and pestle and analysed by X-ray powder diffraction (XRPD), and diffuse reflectance infrared Fourier transforms spectroscopy (DRIFTS), both prior to and after the grinding process, to ensure that no interconversion

occurred, and to ensure that the correct polymorphic form had been obtained from the recrystallisation process. The two batches were separately sieved, using a 45 µm Madison test sieve (Madison Filter Solutions, Madison Filter SA Pty (Ltd.), Johannesburg, South Africa), and particles smaller than 45 µm were used for the subsequent quantitative DRIFTS analyses (particle size analyses, calculated using a volume density graph, showed a mean particle size of 23.48 and 24.96 µm for form I and II respectively, with a similar particle size distribution). The samples were sieved to ensure a narrow particle size distribution and to reduce the possibility of intensity fluctuations during the quantitative DRIFTS analyses, and were stored in a desiccator to prevent any moisture sorption.

Eleven binary mixtures of approximately 10 mg each, containing varying amounts of polymorphic form I and form II, were prepared by weighing pre-determined amounts of each polymorphic form (see table 6.1), using a calibrated Mettler Toledo microbalance (Greifensee, Switzerland). A constant mass of finely ground potassium bromide (KBr) (Merck, Darmstadt, Germany) was added to each polymorphic mixture to serve as diluent and background. Preliminary studies indicated that 275 mg of KBr should be added to each binary mixture, in order to ensure that the packing density of the samples in the Avatar Diffuse Reflectance smart accessory would be the same for each standard sample. This way the Avatar Diffuse Reflectance smart accessory would be completely filled with the samples during the analysis. Each binary mixture and the added 275 mg KBr were mixed together in a politop at 35 revolutions per minute for 10 minutes, and then at 21 revolutions per minute for another 10 minutes, on an Edmund Bühler Tübingen rotary mixer (Labotec, South Africa). This was done to ensure that the standard samples were subjected to exactly the same mixing conditions, as well as to obtain a homogeneous mixture of the polymorphic mixture and the added KBr. The exact amount of each polymorphic form and KBr weighed for each standard sample is summarised in table 6.1.

Table 6.1 The weighed amount of the stavudine polymorphs and KBr in each standard DRIFTS sample

Form I		Form II		Form I + II	KBr		Standard sample
Theoretical mass (mg)	Experimental mass (mg)	Theoretical mass (mg)	Experimental mass (mg)	Total mass (mg)	Theoretical mass (mg)	Experimental mass (mg)	Total mass (mg)
10.000	10.172	0.000	0.000	10.172	275.000	275.092	285.264
9.000	9.056	1.000	1.090	10.146	275.000	275.051	285.197
8.000	8.074	2.000	2.050	10.124	275.000	275.063	285.187
7.000	7.079	3.000	3.067	10.146	275.000	275.064	285.210
6.000	6.055	4.000	4.077	10.132	275.000	275.083	285.215
5.000	5.058	5.000	5.063	10.121	275.000	275.041	285.162
4.000	4.078	6.000	6.070	10.148	275.000	275.011	285.159
3.000	3.065	7.000	7.059	10.124	275.000	275.034	285.158
2.000	2.090	8.000	8.054	10.144	275.000	275.070	285.214
1.000	1.068	9.000	9.045	10.113	275.000	275.057	285.170
0.000	0.000	10.000	10.157	10.157	275.000	275.090	285.247

6.1.3 Apparatus

The infrared spectra of the all samples were recorded on a Nicolet Nexus™ 470 spectrometer (Nicolet Instrument Corporation, Madison WI, USA) over a range of 4000 – 400 cm^{-1}, with the samples placed in an Avatar Diffuse Reflectance smart accessory.

6.1.4 Technique

Each standard sample was quantitatively transferred to the Avatar Diffuse Reflectance smart accessory and analysed three successive times using the infrared spectrometer. The average of the three spectra obtained for each standard sample was determined using version 7.3 of the OMNIC© software package (Thermo Electron Corporation, USA), and subsequently used during the standard curve construction and further data analysis.

6.1.5 Results

A variety of absorption bands (peaks) were tested for their suitability in the quantitative DRIFTS analysis of the two polymorphic forms of stavudine, and the peak heights as well as the peak areas were determined to serve as a comparison between these two methods of determining the peak intensity. The intensity (peak height and peak area) of these absorption bands were determined using version 7.3 of the OMNIC© software package (Thermo Electron Corporation, USA). Figure 6.1 (a) illustrates how the peak areas were determined by integration, whilst figure 6.1 (b) demonstrates how the peak heights were determined. Absorption bands (peaks) of only three of the standard samples are shown, with the sample

containing 100% of form II at the top, the sample containing 50% of form I and 50% of form II in the middle, and the sample containing 100% form I at the bottom in both illustrations.

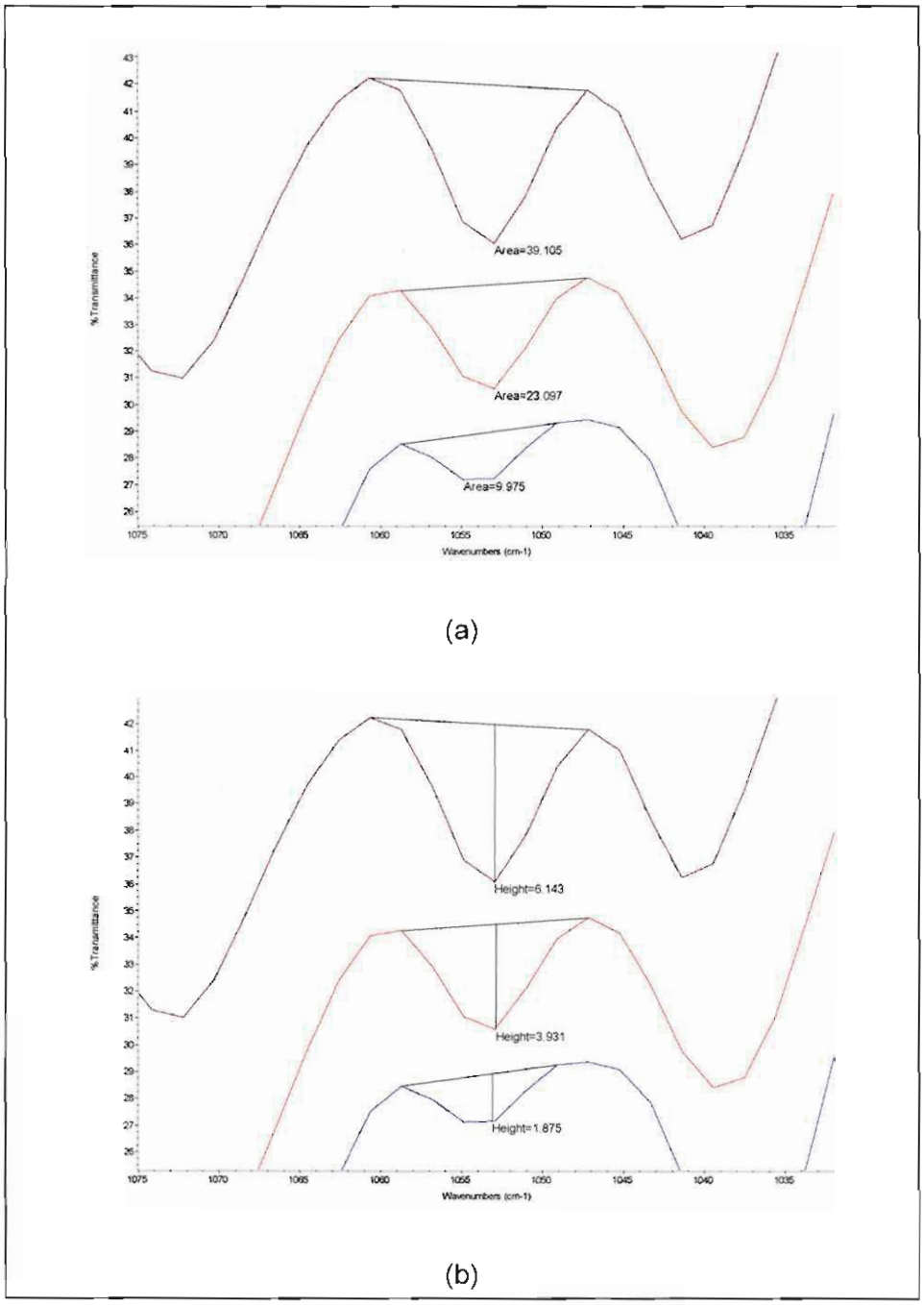

Figure 6.1 Illustrations of how (a) the peak areas and (b) the peak heights of the selected absorption bands of the standard samples were determined (sample containing 100% of form II at the top, the sample containing 50% of form I and 50% of form II in the middle, and the sample containing 100% of form I at the bottom).

A summary of the results obtained from these analyses is given in table 6.2. Table 6.2 illustrates that the two peaks, at 1166 cm^{-1} and 2507 cm^{-1}, generated the best linear

correlation coefficients (r^2), when graphs of the peak heights (h_I) to weight fraction of form I (w_I) of each peak is constructed (r^2 = 0.9573 and 0.9698 respectively). The r^2-values of the graphs of the peak areas (AUC_I) to weight fraction of form I (w_I) of the mentioned two peaks are 0.9678 and 0.9336 respectively, with the peak at 1166 cm^{-1} having the best linear correlation coefficient, and the peak at 2507 cm^{-1} having the 6th best r^2-value. The absorption band (peak) at 1166 cm^{-1} was thus chosen as the characteristic form I peak for the construction of the standard curve of form I, and for further data analysis, since both of its linear correlation coefficients in respect of the peak height - and peak area graphs are greater compared to that of the other absorption bands of form I.

Table 6.2 also shows that the peak at 1054 cm^{-1} has the best linear correlation coefficients when graphs of the peak heights (h_{II}) and the peak areas (AUC_{II}) to weight fraction of form II (w_{II}) are constructed, and this peak was subsequently chosen as the characteristic form II peak for the construction of the standard curve of form II and for further data analysis.

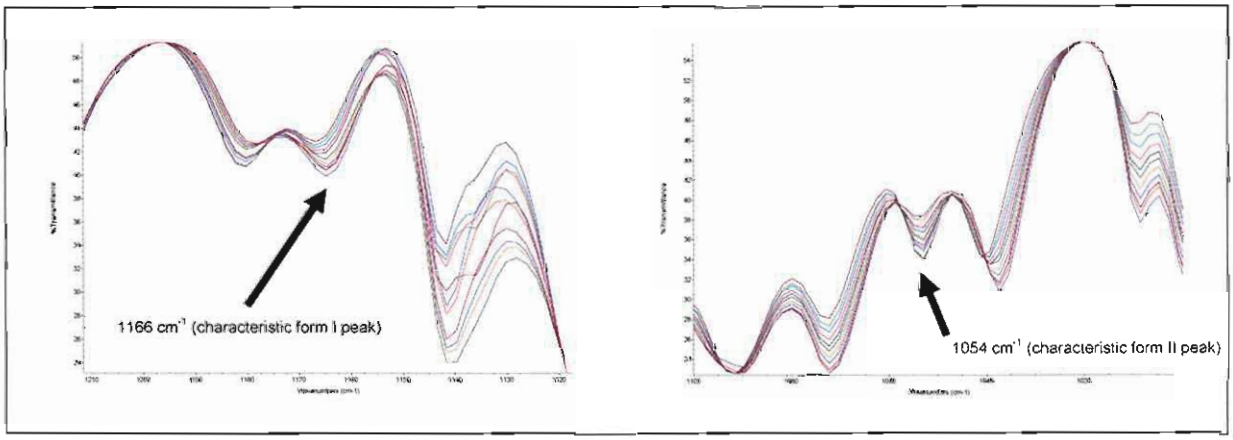

Figure 6.2 The characteristic absorption bands (peaks) in the infrared spectra of the polymorphic forms of stavudine used in further data analysis.

Table 6.2 The results obtained from the analyses of the peak intensities (heights and areas) of possible peaks in the infrared spectrum of polymorphic form I and form II of stavudine, when plotted against the weight fraction of either form I or form II

Polymorphic weight fraction used to construct the graph	Peak position (cm^{-1})	Linear correlation coefficient (r^2) of the graph of peak height vs. weight fraction	Linear correlation coefficient (r^2) of the graph of peak area vs. weight fraction
Form I	488	0.9471	0.9645
	661	0.8791	0.9083
	742	0.7727	0.6419
	1037	0.9020	0.9568
	1072	0.9268	0.9606
	1092	0.5348	0.0895
	1166	0.9573	0.9678
	1180	0.8980	0.9135
	1830	0.9488	0.9478
	2507	0.9698	0.9336
	2649	0.9452	0.9213
	3114	0.7224	0.8471
	3786	0.9513	0.8966
Form II	471	0.9566	0.9607
	852	0.6942	0.9515
	1054	0.9823	0.9792
	1269	0.9409	0.6992
	2081	0.8529	0.8844
	3071	0.9796	0.9668

Mirmehrabi *et al.* (2004:77) proposed a method to determine the ratio of two absorption bands (peaks) in the infrared spectrum (IR) of a binary mixture during the data analysis, and plotting this ratio against the weight fraction of the constituents of the mixture. This peak ratio consists of the intensity of a unique, or characteristic peak, of the specific polymorphic form, to an inert peak in the spectrum whose intensity remains constant. This method ensures a greater linear correlation, since it reduces the potential problems associated with varying size distribution of the active pharmaceutical ingredient (API) in the KBr matrix.

Inspection of the IR-spectra of stavudine revealed that the absorption band at 2823 cm^{-1} was a communal absorption band to both form I and II, and it did not reveal any significant changes in intensity over the entire range of polymorphic mixtures, and it can thus be considered an inert peak.

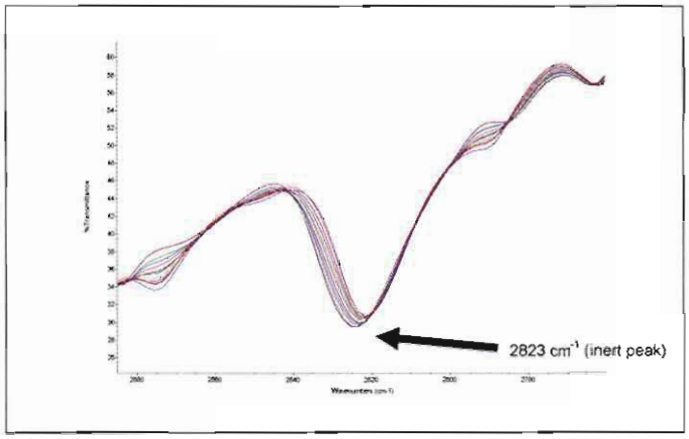

Figure 6.3 The inert absorption band (peak) in the infrared spectra of stavudine used in the data analysis.

In figure 6.4, the graphs of the peak heights of the inert peak at 2823 cm^{-1} *versus* the weight fraction of (a) form I and (b) form II, in the binary mixtures of the two polymorphs, revealed that the gradients of these two graphs approached zero, indicating that the peak heights of the inert peak did not reveal significant fluctuations between the various polymorphic mixtures.

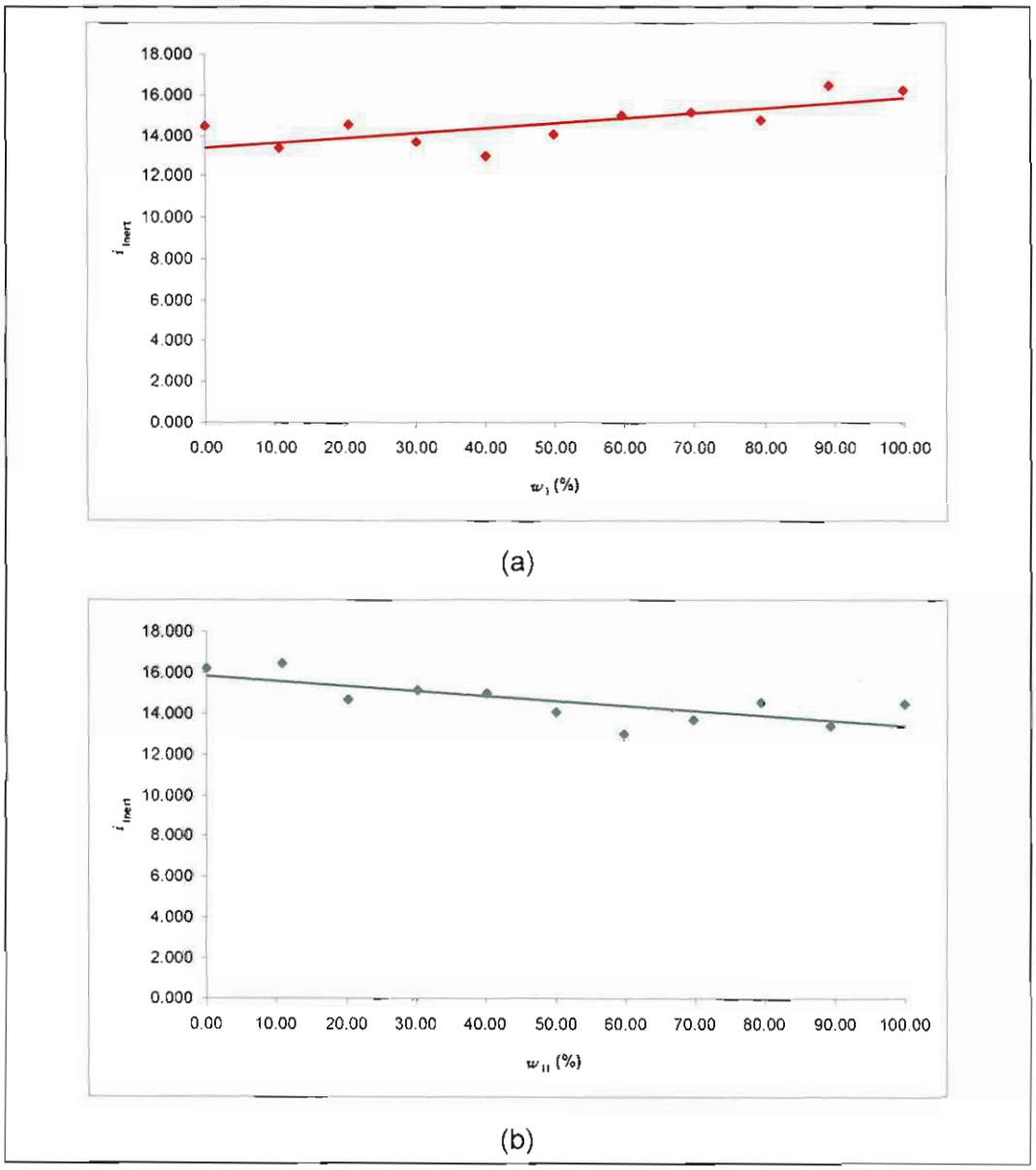

Figure 6.4 Graphs of the peak heights of the inert peak at 2823 cm^{-1} *versus* the weight fraction of (a) form I – w_I and (b) form II – w_{II} in the binary mixture of the two polymorphs.

Plotting the ratio of the characteristic peak height of form I and the height of the inert peak, and the ratio of the characteristic peak height of form II and the height of the inert peak, against the weight fraction of form I and form II respectively, yielded a greater linear correlation, when compared to the graphs in which only the characteristic peak heights were plotted against the relevant weight fractions of the polymorphic forms (see table 6.3).

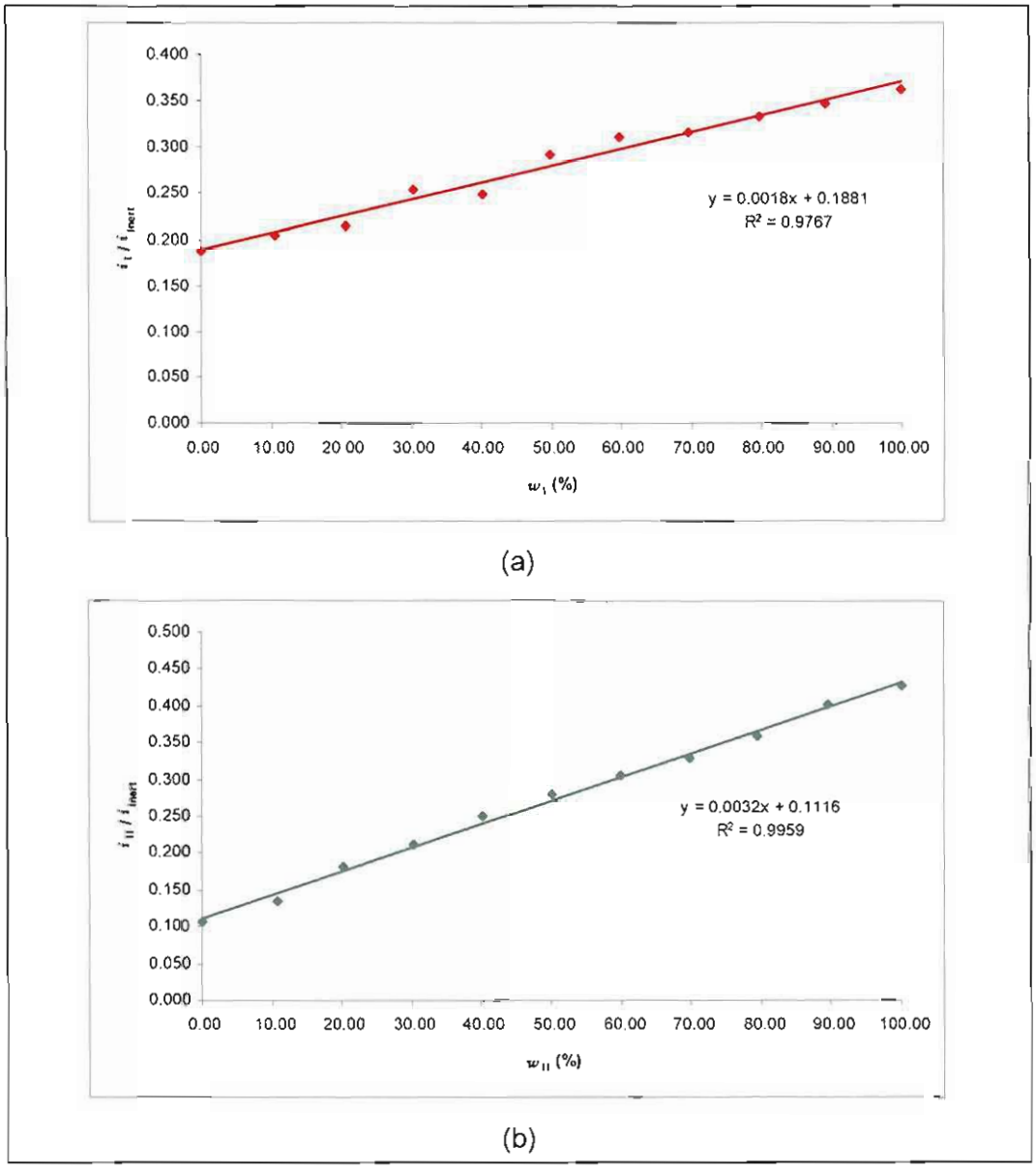

Figure 6.5 (a) Graph of the ratio of the characteristic peak height of form I at 1166 cm^{-1} and the height of the inert peak at 2823 cm^{-1} (i_I / i_{inert}) *versus* the weight fraction of form I (w_I). (b) Graph of the ratio of the characteristic peak height of form II at 1054 cm^{-1} and the height of the inert peak at 2823 cm^{-1} (i_{II} / i_{inert}) *versus* the weight fraction of form II (w_{II}).

It is evident from the illustrations in figure 6.2 and from the plots in figure 6.5, that the selected characteristic peaks of form I and form II do not have an absolute zero peak height and peak area value (i.e. the y-intercept is not zero in the absence of the polymorphic form as theoretically predicted), this was also reported in the quantitative IR analysis of stavudine polymorphs by Mirmehrabi *et al.* (2006:143).

Table 6.3 A comparison of the linear correlation coefficients obtained from the plots of the characteristic peak height/inert peak height – ratios *versus* the weight fractions, and of the characteristic peak height *versus* weight fractions

Graph	Linear correlation coefficient (r^2)	Graph	Linear correlation coefficient (r^2)
i_I vs. w_I	0.9573	i_I / i_{inert} vs. w_I	0.9767
i_{II} vs. w_{II}	0.9823	i_{II} / i_{inert} vs. w_{II}	0.9959

Graphs of the area under the inert peak *versus* the weight fraction of (a) form I and (b) form II, are shown in figure 6.6, and the gradients of these graphs also approach zero, indicating that the areas under the inert peak did not reveal significant fluctuations between the binary polymorphic mixtures.

The same principal of plotting the ratio of the characteristic peak and the inert peak height has also been applied, but instead of using the peak heights, the areas under the various characteristic and inert peaks (AUC) were used. This also resulted in better linear correlation compared to the plots of the AUC *versus* the corresponding weight fractions (see table 6.4).

Table 6.4 A comparison of the linear correlation coefficients obtained from the plots of the area under the characteristic peak/the area under the inert peak – ratios *versus* the weight fractions, and of the area under the characteristic peak *versus* weight fractions

Graph	Linear correlation coefficient (r^2)	Graph	Linear correlation coefficient (r^2)
AUC_I vs. w_I	0.9678	AUC_I / AUC_{inert} vs. w_I	0.9921
AUC_{II} vs. w_{II}	0.9792	AUC_{II} / AUC_{inert} vs. w_{II}	0.9958

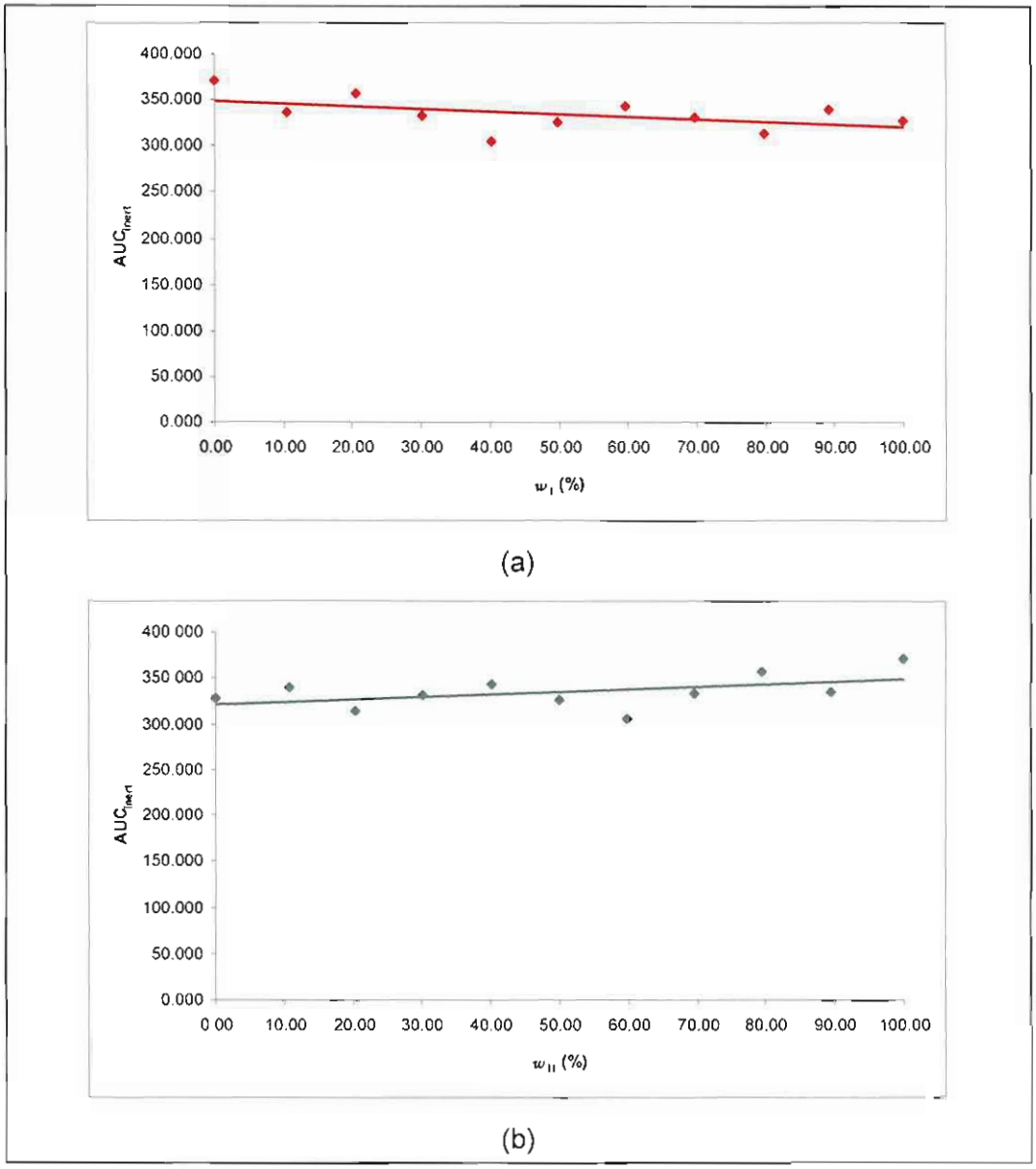

Figure 6.6 Graphs of the areas under the inert peak at 2823 cm^{-1} *versus* the weight fraction of (a) form I – w_I and (b) form II – w_{II} in the mixture of the two polymorphs.

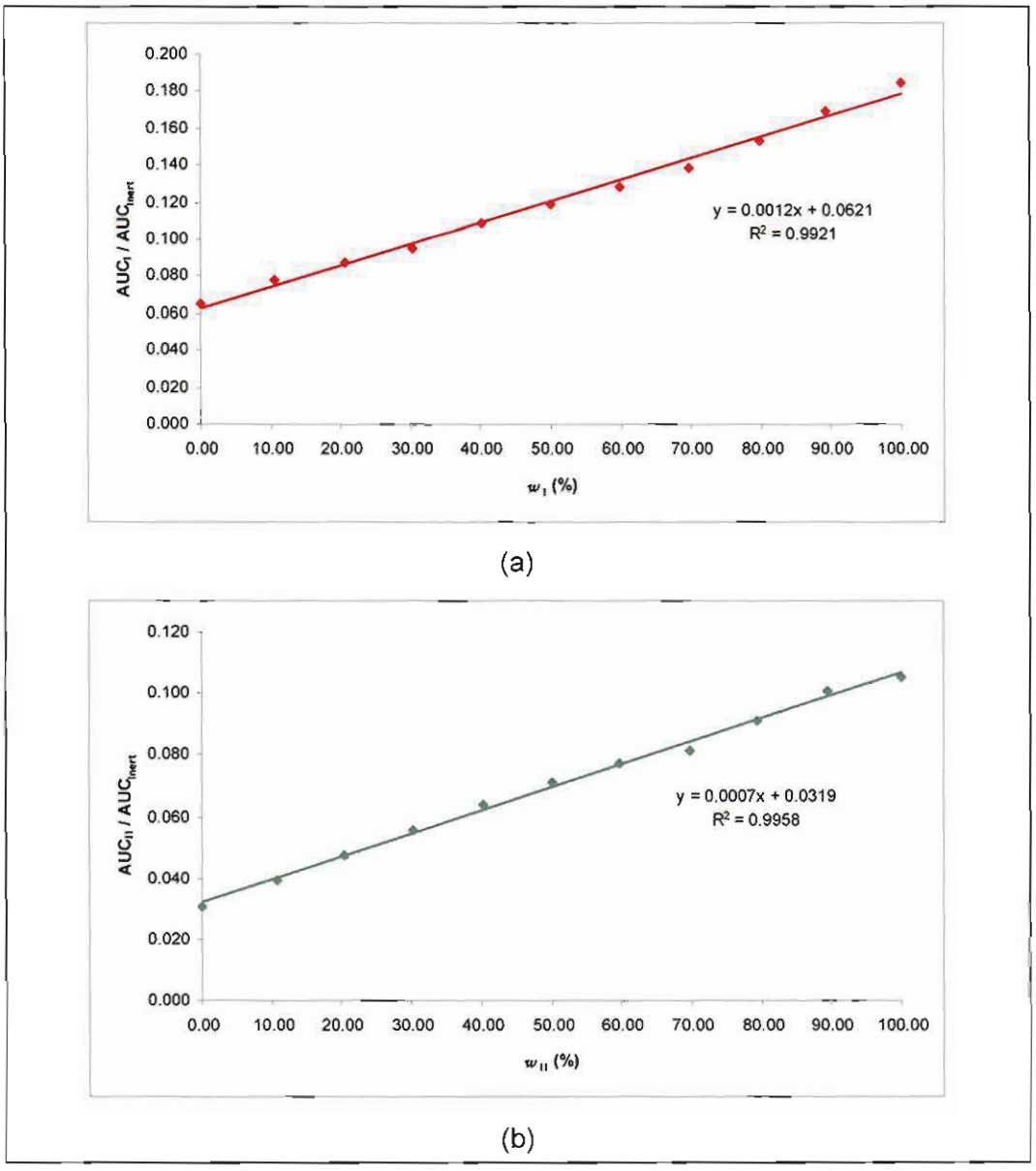

Figure 6.7 (a) Graph of the ratio of the area under the characteristic peak of form I at 1166 cm^{-1} and the area under the inert peak at 2823 cm^{-1} (AUC_I / AUC_{inert}) *versus* the weight fraction of form I (w_I). (b) Graph of the ratio of the area under the characteristic peak of form II at 1054 cm^{-1} and the area under the inert peak at 2823 cm^{-1} (AUC_{II} / AUC_{inert}) *versus* the weight fraction of form II (w_{II}).

In order to establish the relationship between the height and area ratios of the form I peak (i_I / i_{inert} and AUC_I / AUC_{inert}), and the height and area ratios of the form II peak (i_{II} / i_{inert} and AUC_{II} / AUC_{inert}), the graphs in figure 6.8 were constructed.

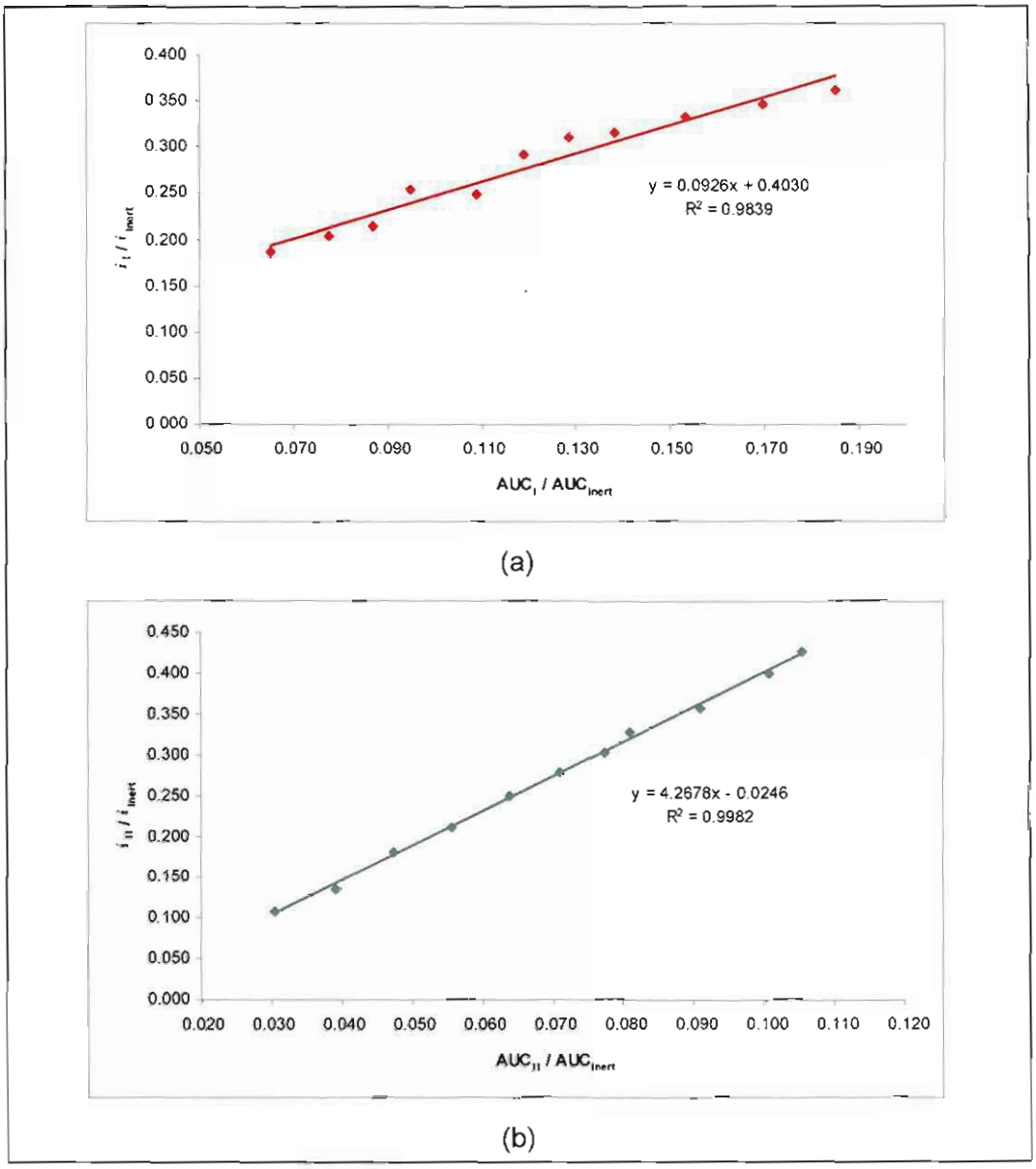

Figure 6.8 (a) Graph of the ratio of the characteristic peak height and the inert peak height (i_I / i_{inert}) *versus* the ratio of the area under the characteristic peak and the area under the inert peak (AUC_I / AUC_{inert}) of form I. (b) Graph of the ratio of the characteristic peak height and the inert peak height (i_{II} / i_{inert}) *versus* the ratio of the area under the characteristic peak and the area under the inert peak (AUC_{II} / AUC_{inert}) of form II.

Both plots in figure 6.8 revealed a linear relationship between the height ratio and the area ratio of form I and form II. In figure 6.8 (b) the plot of the ratios of the form II peak has a greater linear correlation coefficient (r^2) compared with (a) the plot of the ratios of the form I peak (0.9982 for form II *versus* 0.9839 for form I). This indicates that the height ratio (i_{II} / i_{inert}) and the area ratio (AUC_{II} / AUC_{inert}) of the form II peak could be considered equally good indicators for calculating the amount of a polymorphic constituent in a binary mixture. For the

characteristic form I peak though, one of these ratios (either i_I / i_{inert} or AUC_I / AUC_{inert}) is the better indicator, compared to the other.

In order to determine which of the ratios of the form I peak is best used to calculate the composition of a binary mixture, the graphs in figure 6.9 were constructed. The (a) height ratios (i_I / i_{inert} and i_{II} / i_{inert}) and (b) the area ratios (AUC_I / AUC_{inert} and AUC_{II} / AUC_{inert}) of both of the characteristic peaks were plotted against the weight fraction of form I (w_I) to determine the point of intersection. The graphs in figure 6.9 could also have been constructed using the weight fraction of form II (w_{II}) since this will not affect the point of intersection because it would only result in a 180° rotation of both graphs around the y-axis.

Theoretically, both graphs in figure 6.9 should intersect at a point that has an x-coordinate of 50%. The reason is that the height (or the area) ratio of the form I peak will increase with increasing amounts of form I in the mixture, and the height (or the area) ratio of the form II peak will decrease proportionately as the amount of form II in the mixture decreases. Thus to increase or decrease the height (or the area) ratio to 50% of the maximum value, the weight fraction must increase or decrease to 50% correspondingly.

Figure 6.9 illustrates that (a) the graphs of the height ratios intersect at an x-coordinate of 48.60% (close to 50%), while (b) the graphs of the area ratios intersect at an x-coordinate of 23.47% (far from 50%).

This suggests that the height ratios of both of the form I and form II peaks (i_I / i_{inert} and i_{II} / i_{inert}) are good indicators for determining the amount of a polymorphic form in the binary mixture, and that one of the area ratios (either the form I or the form II peak (AUC_I / AUC_{inert} or AUC_{II} / AUC_{inert}) ratio) is a better indicator compared to the other area ratio. It has been determined in the above paragraphs that the area ratio (AUC_{II} / AUC_{inert}) of the form II peak is a good indicator since it has a linear correlation coefficient of 0.9958, which suggests that the area ratio (AUC_I / AUC_{inert}) of the form I peak has to be an inferior indicator for determining the composition of the polymorphic mixture.

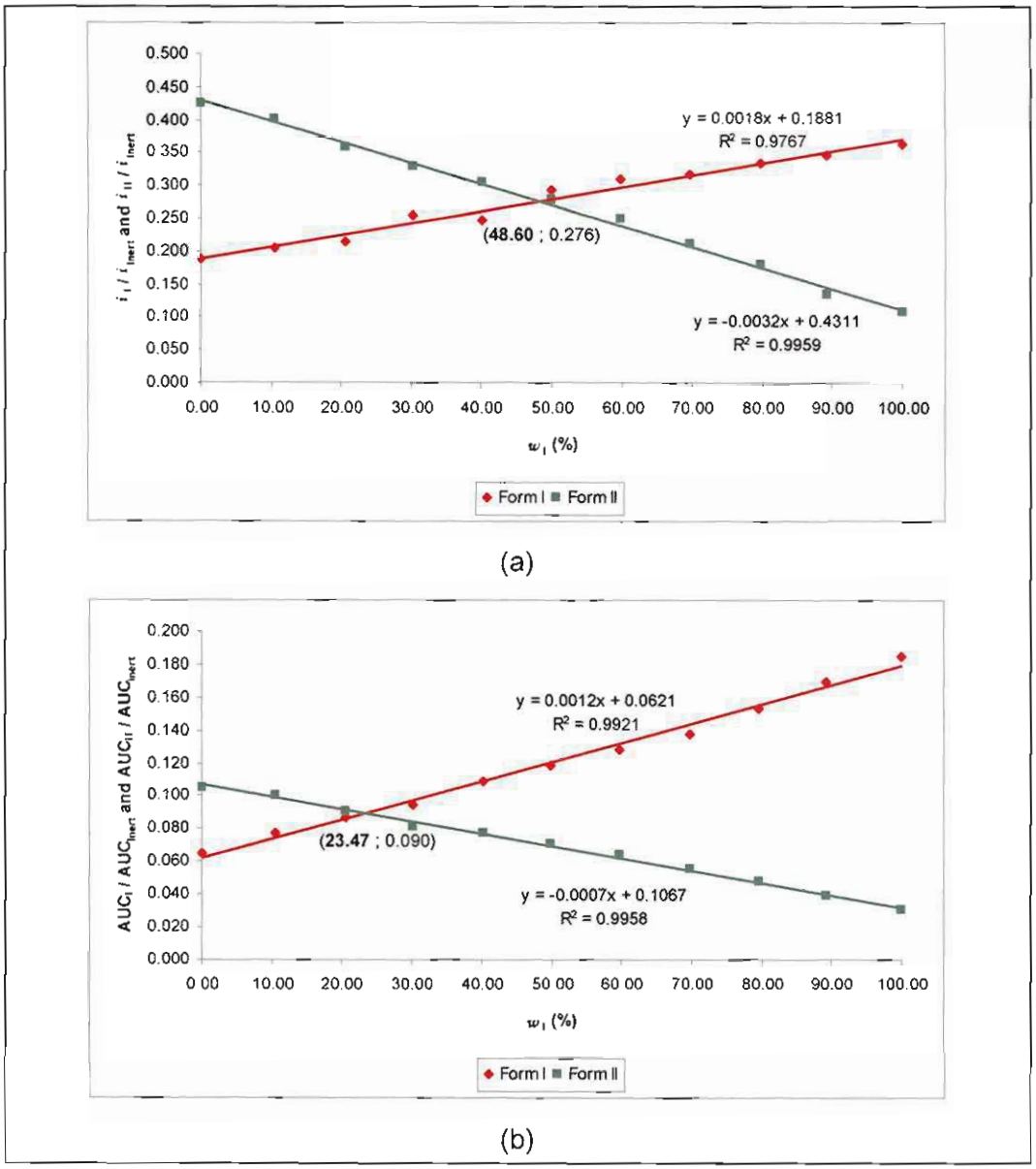

Figure 6.9 (a) Graph of the peak height ratios (i_I / i_{inert} and i_{II} / i_{inert}) of both characteristic peaks *versus* the weight fraction of form I (w_I). (b) Graph of the area under the peak ratios (AUC_I / AUC_{inert} and AUC_{II} / AUC_{inert}) of both of the characteristic peaks *versus* the weight fraction of form I (w_I).

It is thus established that the height ratio (i_I / i_{inert}) of the form I peak is superior to the area ratio (AUC_I / AUC_{inert}) when calculating the amount of a polymorphic form in a binary mixture. This might be because the form I peak is not as symmetrical as the form II peak (see figure 6.2), which will influence the calculation of the area under the peak more than the calculation of the peak height. For the form II peak the height and area ratios are equally applicable for calculating the content of a polymorphic mixture, but since only the height ratio of the form I peak will be used, it was decided to also use only the height ratio of the form II peak for

further calculations in order to be able to compare the results obtained from each peak. The quantitative DRIFTS method that was developed, thus made use of the peak height ratios.

In order to validate the quantitative DRIFTS method utilising the peak height ratios of form I and form II, five polymorphic mixtures with known concentrations were prepared and analysed in duplicate, using the preparation technique, apparatus, and analytical technique described in sections 6.1.2 – 6.1.4. In order to compare the results generated by the quantitative DRIFTS method, utilising the form I and form II height ratios, a sample of unknown polymorphic composition were analysed in duplicate, using the apparatus and analytical technique described in sections 6.1.3 – 6.1.4. The percentage form I and form II in each sample (average experimental content) was calculated, using the equations in figure 6.5 (a) and (b) respectively. Table 6.5 provides a summary of the results obtained, with the content of each sample expressed with reference to the percentage of form I in each sample.

Table 6.5 Validation results (expressed as % form I) from the quantitative DRIFTS method

		Form I peak height ratio method			**Form II peak height ratio method**		
	Sample number	**Theoretical content = a (%)**	**Average experimental content = b (%)**	**a – b**	**Theoretical content = c (%)**	**Average experimental content = d (%)**	**c – d**
Validation samples	1	100.00	97.45	2.55	100.00	97.36	2.64
	2	75.01	72.96	2.05	75.01	73.33	1.68
	3	49.97	49.09	0.88	49.97	49.34	0.63
	4	25.02	25.08	-0.06	25.02	25.30	-0.28
	5	0.00	2.46	-2.46	0.00	2.33	-2.33
Standard deviation	-	-	-	1.99 (≈2)	-	-	1.91 (≈2)
Test sample	1	-	25.36 ± 2	-	-	24.61 ± 2	-

Table 6.5 demonstrates that the quantitative DRIFTS methods were comparable when using the peak height ratios of form I and II, since the amount of form I, as determined in each of the validation samples and the test sample, are comparable. The standard deviation for the difference between the theoretical and average experimental content for the validation samples is approximately 2. It is also clear from table 6.5 that these quantitative DRIFTS methods could be considered suitable for determining the content of a polymorphic mixture of stavudine, since the average experimental content of the test sample is similar.

6.2 Quantitative X-ray powder diffraction

6.2.1 Background and introduction

There are primarily two methods used for the quantitative analysis of powder mixtures using X-ray diffraction techniques. The one method utilises the entire diffraction pattern to determine integrated intensity parameters, unit-cell parameters and peak profile parameters in order to establish a relationship between the constituents of the mixture (this is also known as the whole powder-pattern decomposition method – WPPD). The other method uses only single peaks in the X-ray diffractogram to establish a relationship between the constituents of the powder mixture. This method is comprised of two variants, of which the first expresses the intensity of a single peak relative to the intensity of the pure phase, and the second expresses the intensity of a single peak relative to the intensity of an internal standard (Stephenson *et al.*, 2001:70-71).

Leroy Alexander and Harold P. Klug were the first to describe the mathematical relationship underlying the quantitative X-ray diffraction analysis of powder mixtures (Alexander & Klug, 1948:887-888), based on the second method of using individual peaks:

$$I_{i1} = \frac{Kx_1}{\rho_1[x_1(\mu_1^* - \mu_M^*) + \mu_M^*]} \qquad (6.2)$$

Where: I_{i1} = the intensity of a specific peak of component 1 at i

K = a constant

x_1 = the weight fraction of component 1

ρ_1 = the density of component 1

μ_1^* = the mass absorption coefficient of component 1

μ_M^* = the mass absorption coefficient of the powder matrix.

They further proposed three possible scenarios where this equation could be applied, which includes a mixture of n components with $\mu_1^* = \mu_M^*$, or a mixture with $\mu_1^* \neq \mu_M^*$, and a mixture of two components with $\mu_1^* \neq \mu_M^*$. During this study, the principles of quantitative X-ray diffraction analysis was applied to mixtures of different ratios of two polymorphic forms of the same compound, thus the mass absorption coefficients of the two components could be considered similar. Therefore equation 6.2 can be simplified to equation 6.3:

$$I_{i1} = \frac{Kx_1}{\rho_1 \mu_1^*} \qquad (6.3)$$

A corresponding equation can also be written for the second component in the polymorphic mixture.

$$I_{i2} = \frac{Kx_2}{\rho_2 \mu_2^*} \qquad (6.4)$$

For a matrix consisting of 100% of component 1, then x_1 = 1 and equation 6.3 may also be re-written as:

$$(I_{i1})_{100\%} = \frac{K}{\rho_1 \mu_1^*} \qquad (6.5)$$

In order to calculate the relative intensity of the peak of component 1 at *i*, equation 6.3 is divided by equation 6.5 to give equation 6.6:

$$\frac{I_{i1}}{(I_{i1})_{100\%}} = x_1 \qquad (6.6)$$

A plot of the relative intensity ($(I_{i1}/(I_{i1})_{100\%})$) of the specific peak of component 1 at *i*, calculated using the peak height, *versus* the weight fraction of component 1 should give a straight line through zero with a slope of one. The same reasoning and equations, as described above, can also be applied when working with a specific peak that is unique to the second component of the polymorphic mixture (Alexander & Klug, 1948:887-888; Campbell Roberts *et al.*, 2002:1151).

The abovementioned equations and principles have been successfully applied in the analysis of various polymorphic mixtures, including the determination of the relative amounts of α-carbamazepine and β-carbamazepine in a mixture of the two, and the determination of the relative amounts of anhydrous carbamazepine and carbamazepine dihydrate in a mixture of the two. Quantitative X-ray diffraction analysis has also been used to determine the amount of crystalline and amorphous content of α-lactose-monohydrate in powder mixtures of these two products, and to determine the percentage crystallinity of samples consisting of mixtures between indomethacin and silica gel (Suryanarayanan, 1989:1017; Suryanarayanan, 1990:155; Pan *et al.*, 2006:E1; Fix & Steffens, 2004:513).

Determining the amount of a certain substance in a powder mixture by quantitative X-ray diffraction analysis may be influenced by various factors. These factors influence the results of the measurement of the peak intensity, and can thus have a significant impact on the accuracy of the results obtained, and must be born in mind and/or eliminated during the development of the experimental procedure. Some of these factors are summarized in table 6.6 (Hurst *et al.*, 1997:234).

The most important factors to consider when performing quantitative X-ray diffraction analysis, that pertain to samples consisting of a mixture of two polymorphic forms, is particle size and morphology, preferred orientation, sample mixing, sample packing, microabsorption and primary extinction. It is preferable to have a homogeneous sample consisting of particles of similar size, or a very small size, not demonstrating preferred orientation, microabsorption and primary extinction. This is best achieved by grinding the sample in a mortar and pestle or an analytical mill, but it should be remembered that this may lead to phase transformation and can thus influence the analysis. The sample should also be packed into the sample holder ensuring the smoothest surface possible (Suryanarayanan, 1989:1021; Stephenson *et al.*, 2001:68-69).

Table 6.6 A summary of the factors that influence quantitative X-ray diffraction analysis of powder samples (Hurst *et al.*, 1997:234)

Instrumental or systematic factors	**Factors relating to the inherent properties of the phase/compound**	**Factors relating to the preparation of the sample**
X-ray source intensity, kV and mA settings of the generator	Structure factor, F	Size distribution of coherent diffraction domains
Scan rate	Multiplicity	Preferred orientation
Chopper increment	Long-range order, crystallinity	Sample homogeneity
Divergence slit width	Absorption factor, μ, and transparency	Average mass attenuation coefficient, $\bar{\mu}$
Receiving slit width	Primary extinction	Microabsorption
Detector deadtime	Secondary extinction	Size of exposed sample surface
Lorentz-polarization factor	Temperature factor	Thickness of the powder
Counting statistics		Sample surface characteristics
Total sample irradiated		Powder packing and transparency
Sample displacement		Method for making powder mounts
$K_{\alpha 2}$ stripping or not		Choice of internal standards
Degree of data smoothing		
Method of peak area measurement		
Background and choice of subtraction method		
Parameters of special software routines		

6.2.2 Sample preparation

Particle size, morphology, sample homogeneity, sample packing and preferred orientation are some of the most critical factors pertaining specifically to the sample during quantitative XRPD analysis. These factors can result in a variation in the intensity of the peaks in the XRPD pattern thus influencing the accuracy and repeatability of the results obtained. In order to minimise the influence of these factors on the results, the ground and sieved batches of polymorphic form I and form II of stavudine (with a narrow particle size distribution determined by particle size analysis), used during the quantitative DRIFTS analysis, were also used to prepare the standard samples in the quantitative XRPD analysis.

Eleven binary mixtures with different content-ratios of the two polymorphic forms were prepared by weighing varying amounts of each polymorphic form, using a calibrated Sartorius analytical balance (Goettingen, Germany). Pilot studies indicated that 140 mg of the powdered sample was required to fill the aluminium sample holder, ensuring good sample packing of the sample holder. Each binary mixture was mixed in a politop at 35 revolutions per minute for 10 minutes, and then at 21 revolutions per minute for another 10 minutes, on an Edmund Bühler Tübingen rotary mixer (Labotec, South Africa). This was done to ensure that the standard samples are uniformly mixed to promote reproducibility of the method. The standard samples were stored in a desiccator containing dried silica to prevent any moisture sorption. The amount of each polymorphic form weighed for each standard sample is summarised in table 6.7.

6.2.3 Apparatus

The XRPD patterns were recorded using a Bruker D8 Advanced diffractometer (Bruker, Germany). The measurement conditions were: target, Cu; voltage, 40kV; current, 30mA; divergence slit, 2 mm; anti-scatter slit, 0.6 mm; detector slit, 0.2 mm; monochromator; scanning speed, 2°/min with a step size of 0.025° and a step time of 1.0 seconds. Campbell Roberts *et al.* (2002:1149) indicated that rotation of the sample accessory reduces the influence of preferred orientation effects. During this study all the XRPD samples were rotated at 15 revolutions per minute to reduce the potential interference of preferred orientation.

Table 6.7 The amount of each polymorphic form in the standard samples prepared for quantitative XRPD analysis

Form I		Form II		Form I + II
Theoretical mass (mg)	Experimental mass (mg)	Theoretical mass (mg)	Experimental mass (mg)	Total mass (mg)
140.00	140.14	0.00	0.00	140.14
126.00	126.14	14.00	14.00	140.14
112.00	112.08	28.00	28.15	140.23
98.00	98.30	42.00	42.16	140.46
84.00	84.28	56.00	56.10	140.38
70.00	70.15	70.00	70.01	140.16
56.00	56.20	84.00	84.00	140.20
42.00	42.05	98.00	98.01	140.06
28.00	28.16	112.00	112.02	140.18
14.00	14.05	126.00	126.20	140.25
0.00	0.00	140.00	140.23	140.23

6.2.4 Technique

Each mixed standard sample was quantitatively transferred to the aluminium sample holder, and the powder surface was levelled and smoothed, using a glass slide, in order to achieve optimum sample packing. The samples were subsequently analysed, using the X-ray diffractometer, and the peak intensity (height) values that were used for constructing the graphs, were generated from the diffractograms using the Eva© software (version 10.0 revision 1) which is part of the Diffrac^{plus} 2004 software package (Bruker, Germany).

6.2.5 Results

According to Gandhi *et al.* (2000:224), polymorphic form I of stavudine has a unique X-ray diffraction peak at 19.1°2θ, whilst form II has unique diffraction peaks at 11.2 and 18.6°2θ. For the construction of the calibration curves of the quantitative XRPD analysis, it was decided to use this unique diffraction peak of form I and the diffraction peak of form II at 11.2°2θ. These two peaks are clearly discernable and do not reveal significant peak-overlapping with adjacent peaks in the diffractogram that may adversely influence the calculation of the peak intensity (see figure 6.10).

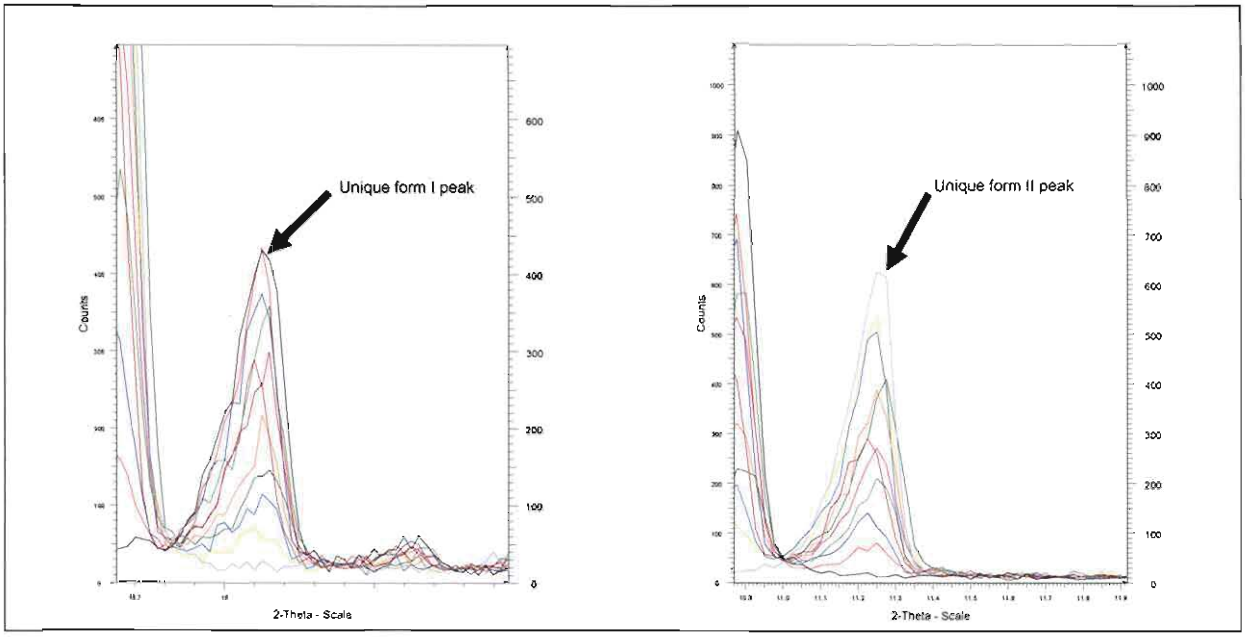

Figure 6.10 The two unique diffraction peaks used during the quantitative XRPD analyses.

The peak intensities (heights) of the two selected peaks for each standard sample were calculated using the Eva© software (version 10.0 revision 1). Calculation of the peak intensities were done without any modification of the raw data (such as background subtraction, $K_{\alpha 2}$ stripping or smoothing of the diffractograms).

Equation 6.6 derived from the Alexander and Klug expression (equation 6.2) could not be applied in the construction of the standard curve for these quantitative XRPD analyses, since a sample with an unknown polymorphic composition has only one unique form I and form II diffraction peaks at 19.1 and 11.2°2θ respectively. Thus such samples do not have a second maximum diffraction peak at these positions, which are required in order to apply equation 6.6 in calculating a relative peak intensity ratio. Instead plots of a peak intensity ratio and corresponding weight fractions of (a) form I and (b) form II (figure 6.11) were constructed, with this ratio being calculated by dividing the peak intensity of the characteristic form I and form II peaks (I_I for form I, or I_{II} for form II) by the sum of the intensity of the unique form I and form II peaks (i.e. $I_I + I_{II}$). Theoretically, these plots should have a gradient of one and a y-intercept of zero (as does equation 6.6), since a sample containing 100 % form I (0% form II) has a ratio ($I_I / I_I + I_{II}$) of 1. As can be seen in figure 6.11, both plots do not intersect the y-axis at zero. The reason for this could be attributed to the fact that no background subtraction was performed on the raw data, which could increase the effect of preferred orientation, resulting in a peak intensity being measured when the weight fraction is 0%, due to the presence of minor background noise. Both plots show good linear correlation coefficients (r^2) and slopes that approach one, indicating that this method may be suitable for quantifying the amount of polymorphic form I or form II in a binary mixture.

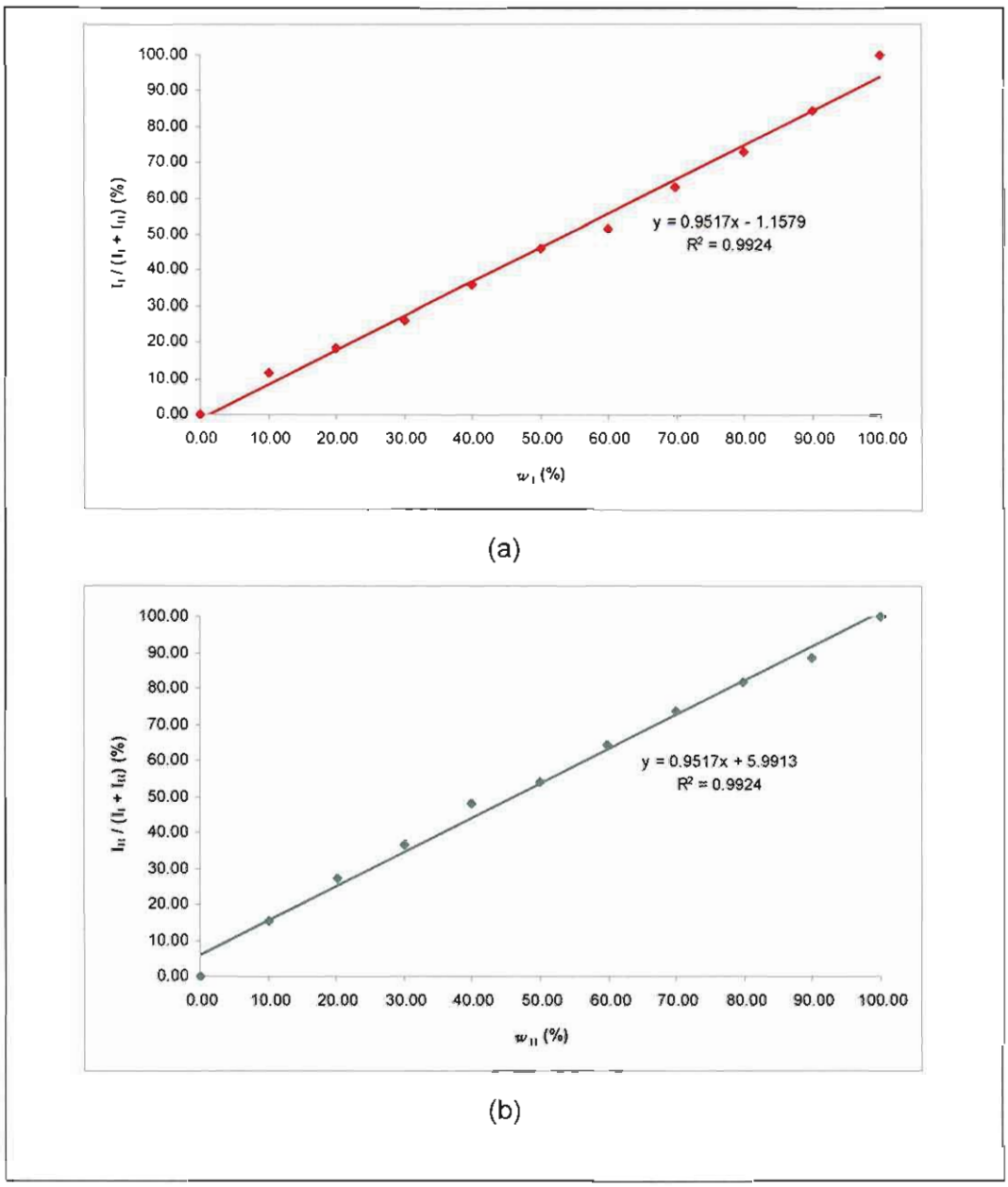

Figure 6.11 (a) Graph of the peak intensity ratio of the unique form I peak (I_I / I_I + I_{II}) *versus* the weight fraction of form I (w_I) in the binary polymorphic mixtures, and (b) graph of the peak intensity ratio of the unique form II peak (I_{II} / I_I + I_{II}) *versus* the weight fraction of form II (w_{II}) in the binary polymorphic mixture.

In order to validate the quantitative XRPD method, five polymorphic mixtures with known form I and form II concentrations were prepared and analysed in duplicate, using the preparation technique, apparatus and analytical technique, described in sections 6.2.2 – 6.2.4. In order to test the applicability of the quantitative XRPD method, a sample of unknown polymorphic composition was also analysed in duplicate, using the apparatus and analytical technique, described in sections 6.2.3 – 6.2.4, and the results of this sample was also compared with the results of the same sample generated using the quantitative DRIFTS

method. The percentage of form I in each sample (average experimental content) was calculated using the equation in figure 6.11 (a). Table 6.8 provides a summary of the results obtained, with the content of each sample expressed with reference to the percentage of form I in each sample. It should be emphasised that the amount of polymorphic form I of stavudine could be calculated using either the equation in figure 6.11 (a), or (b) (the answer generated from the equation in figure 6.11 (b) should merely be subtracted from 100), since a common denominator ($I_I + I_{II}$) is used in calculating the intensity ratios.

Table 6.8 A summary of the results obtained (expressed as % form I) from the validation of the quantitative XRPD method

	Sample number	Theoretical content = e (%)	Average experimental content = f (%)	e – f
Validation samples	1	100.00	106.30	-6.30
	2	75.01	73.83	1.18
	3	49.97	49.58	0.39
	4	25.02	24.87	0.15
	5	0.00	1.22	-1.22
Standard deviation	-	-	-	3
Test sample	1	-	32.10 ± 3	-

From table 6.8 it can be concluded that the quantitative XRPD method may be deemed suitable for determining the content of a polymorphic mixture of form I and II of stavudine, since the amount of form I determined in each of the validation samples, are comparable. The standard deviation for the difference between the theoretical and average experimental content for the validation samples is 3.

It is noticed that the standard deviation (SD) of the difference between the theoretical form I content and the experimental form I content, determined by quantitative XRPD analysis ((e – f) in table 6.8), is greater than the SD of the difference between the theoretical form I content and the experimental form I content, determined by quantitative DRIFTS analysis ((a – b) and (c – d) in table 6.5). This phenomenon could be attributed to the preferred orientation of stavudine, since the particles are needle-shaped (see table 3.6 in section 3.3.2), resulting in the measured XRPD peak intensities (i.e. polymorphic content) possibly being greater than the true XRPD peak intensities (i.e. polymorphic content). It should be emphasised that the

occurrence of preferred orientation influences XRPD analysis and not DRIFTS analysis, and although measures were implemented in order to minimise the influence of preferred orientation (reduction in the particle size, sieving of the samples to ensure a uniform particle size, and rotation of the sample accessory), it presumably was not eliminated completely.

Table 6.9 provides a comparison of the results of the validation and testing of both the quantitative XRPD and DRIFTS methods, and it is evident that increasing the form I content of the samples result in an increase in the difference ((g – h) in table 6.9) between the percentages of form I, calculated using the quantitative XRPD method and the DRIFTS method. It is assumed that this could be attributed to an over-estimation of the amount of form I in samples consisting primarily of polymorphic form I during the application of the quantitative XRPD method. The reason for this may be that the form I particles demonstrate a greater tendency for preferred orientation than the form II particles, since form I appears to be more needle-shaped compared to form II (see table 3.6 in section 3.3.2), resulting in a greater XRPD peak intensity (i.e. form I content) being measured for samples consisting primarily of form I.

Table 6.9 A comparison of the validation results generated (expressed as % form I) during the quantitative XRPD and DRIFTS analyses

	Sample number	Experimental XRPD content = g (%)	Average Experimental DRIFTS content = h (%)	g – h
Validation samples	1	106.30	97.41	8.89
	2	73.83	73.15	0.68
	3	49.58	49.22	0.36
	4	24.87	25.19	-0.32
	5	1.22	2.40	-1.18
Standard deviation	-	-	-	4.09 (≈4)
Test sample	1	32.10 ± 3	24.49 ± 2	-

Conclusion

During this chapter two methods for quantifying the amount of both polymorphic form I and form II of stavudine in mixtures, were developed, using diffuse reflectance infrared Fourier transform spectroscopy and X-ray powder diffraction analysis. Both methods yielded promising results and were shown to be suitable for the quantification of such binary mixtures. The DRIFTS method appears to be more accurate, when compared to the XRPD method, when quantifying the polymorphic content of a mixture between form I and II, since it presumably is unaffected by preferred orientation, and the standard deviation of the difference between the theoretical and average experimental content for the DRIFTS method is less compared to the XRPD method. However, the DRIFTS method requires additional sample preparation, such as thorough mixing between the sample and the potassium bromide in order to ensure a homogeneous mixture, and the XRPD method appears to be more convenient, since it requires minimal sample preparation, and yields results reasonably fast. The accuracy of the quantitative XRPD method may be improved by performing background subtraction, $K_{\alpha 2}$ stripping and smoothing of the peaks in the X-ray diffractograms, in order to further reduce the influence of preferred orientation on the results.

CHAPTER 7

Summary and conclusion

Solid state studies of active pharmaceutical ingredients are vital during the research and development of a suitable large scale preparative technique and dosage form for a drug, since polymorphism impacts three key areas during drug development and dosage form selection. These three areas include (1) the stability of the drug (both the physical and the chemical stability of the drug) in the dosage form, (2) the solubility of the drug (which includes the bioavailability of the drug from the site of absorption), and (3) the application and selection of a specific manufacturing process for a drug and its corresponding dosage form. The impact of these factors on a drug substance were highlighted in chapter one and the different kinds of polymorphism that is obtainable, including true polymorphs, polychromism, pseudopolymorphism, desolvated solvates, co-crystals and amorphous solids, were also described. It is apparent from chapter one that the phenomenon of polymorphism may be utilised by drug companies during the life-cycle management of a drug substance in order to extend the period of maximum profitability and market exclusivity of a blockbuster drug.

Stavudine is a nucleoside reverse transcriptase inhibitor (NRTI) that is used in the treatment of human immunodeficiency virus (HIV) infections in patients, and was the fourth anti-retroviral drug available on the market in the United States of America after receiving FDA (Food and Drug Administration) approval. Some of the physicochemical properties of stavudine including its appearance, colour, storage instructions and method of preparation were described. The pharmacological properties, pharmacokinetic properties, side-effects, interactions and contraindications of stavudine described in chapter two, illustrated the effectiveness of stavudine during the treatment of HIV infections and highlighted the precautions that must be considered before initiating treatment with this drug.

It was apparent from the literature and from the recrystallisation study performed that stavudine exhibits polymorphism. There are two known polymorphic forms of stavudine, including form I and form II, which are obtainable from a variety of solvents as well as a mixture consisting of these two polymorphs, and five known pseudopolymorphic forms including form III (a hydrate), an NMP (*N*-methyl-2-pyrrolidone) solvate, a DMA (*N,N*-dimethylacetamide) solvate, a DMAC (*N,N*-dimethylacrylamide) solvate and a DMP (*N,N*-dimethylpropionamide) solvate.

Various characterisation techniques were used to determine the physicochemical properties of the two polymorphic forms and the hydrate and NMP solvate of stavudine. It was determined that X-ray powder diffraction (XRPD) is a definitive method to distinguish between form I, form II and the solvates of stavudine, and variable temperature X-ray powder diffraction (VT-XRPD) analysis revealed that form I and form II are monotropically related and that no interconversion between these two polymorphs occur with an increase in temperature. However, VT-XRPD analysis illustrated that the hydrate and NMP solvate of stavudine transform to a mixture consisting of form I and form II with an increase in temperature, whilst differential scanning calorimetry (DSC) and thermogravimetric analysis (TGA) showed that the NMP solvate might not desolvate upon heating, and it was suggested that the NMP solvate melts with an increase in temperature resulting in destruction of the crystal lattice, release of the NMP and simultaneous recrystallisation of a mixture of form I and II (see figure 7.1).

A novel solid state of stavudine that was previously not described in the literature was prepared and characterised, and it was shown to be an amorphous (glassy) form. This glassy stavudine had an observable glass transition temperature (T_g) and the fragility ratio calculated for this glass proved that it is a strong glass, indicating minimal molecular mobility changes at the T_g and thus a small change in heat capacity at T_g (which was observed in the DSC thermogram). It was shown (using VT-XRPD analysis) that this glass is unstable and that it transforms to a mixture of form I and form II of stavudine during increasing temperatures.

The dissolution profiles of form I, form II, the glassy stavudine and the form I/II mixture were determined, and it was shown that a greater amount of the glassy stavudine dissolved in one minute when compared to the other dissolution profiles. A comparison of the dissolution profiles, based on the requirements of the Medicines Control Council of South Africa, indicated that the profiles of form I and form II, form I and the glassy stavudine, and form I and the form I/II mixture are similar.

Finally, two methods were developed (based on the analytical techniques of DRIFTS and XRPD) in order to quantify the amount of form I and form II of stavudine in a mixture consisting of these two polymorphs. The motivation behind this initiative was the phenomenon that the stavudine raw material purchased from manufacturing companies abroad for use in South Africa appears to be a mixture consisting of form I and form II of stavudine, and this created the need to be able to quantify the constituents of such a mixture for quality control purposes. Both methods were validated and tested and it was illustrated

that the method based on the XRPD technique could be implemented with less effort, whilst the method based on the DRIFTS technique is more accurate.

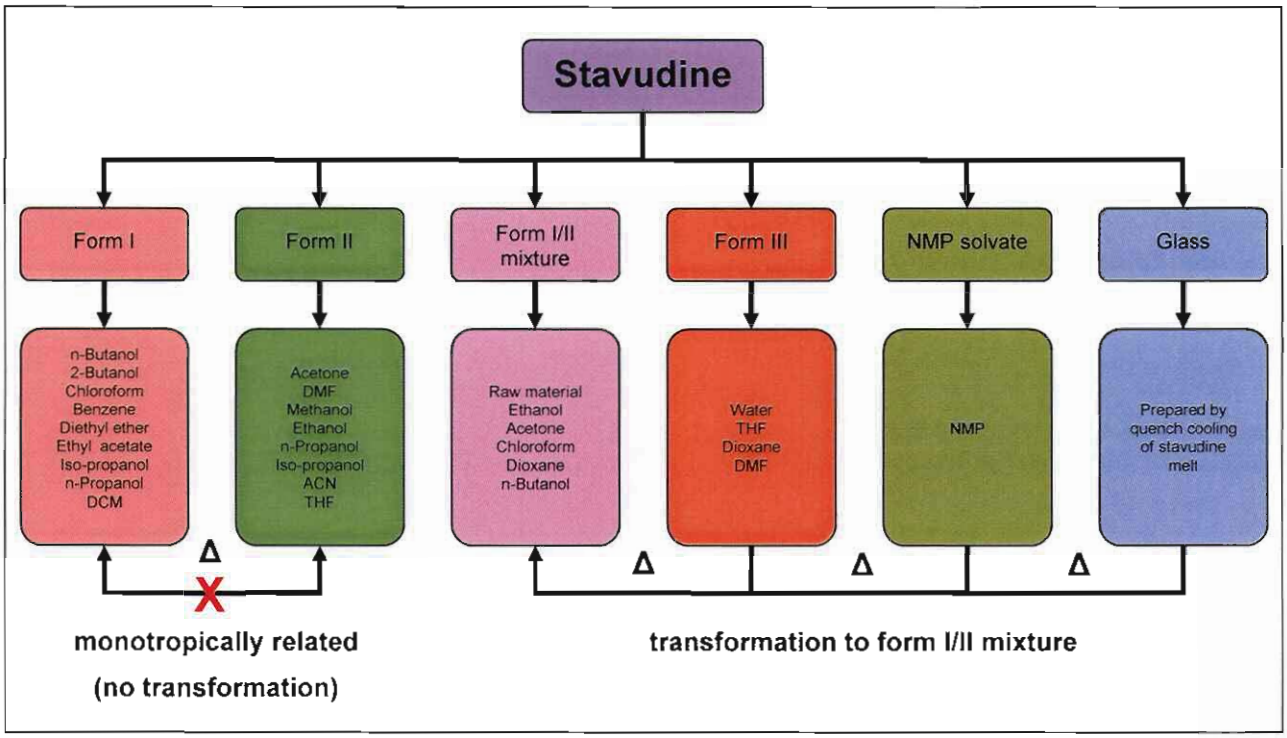

Figure 7.1 A summary of the polymorphic forms of stavudine, the various solvents (or preparative techniques) from which they were obtained and transformations that occur with increasing temperatures (DCM, dichloromethane).

During the course of this study the importance of polymorphism in the fields of pharmaceutical research and industrial pharmacy was highlighted, and I have gained valuable knowledge, experience and skills about this subject matter and its relation to the anti-retroviral drug stavudine during this project. I have also come to the conclusion that the different fields of the sciences are intertwined and that the amount of information in each field is so vast that it is impossible for mere mortals to gain an in-depth understanding of each subject area, unless it is reduced to its simplest forms and extensively researched. Each scientist thus has a duty to expand the knowledge base of his/her chosen subject area until all the possibilities and questions pertaining to this area are exhausted, and no further contributions can be made by him/her in this field. Only then will the researcher's career be complete.

BIBLIOGRAPHY

AGUIAR, A.J., KRC, J., KINKEL, A.W. & SAMYN, J.C. 1967. Effect of polymorphism on the absorption of chloramphenicol from chloramphenicol palmitate. *Journal of Pharmaceutical Sciences*, 56(7):847-853, Jul.

AIRAKSINEN, S., LUUKKONEN, P., JØRGENSEN, A., KARJALAINEN, M., RANTANEN, J. & YLIRUUSI, J. 2003. Effects of excipients on hydrate formation in wet masses containing theophylline. *Journal of Pharmaceutical Sciences*, 92(3):516-528, Mar. Available: Wiley-InterScience.

ALEXANDER, L. & KLUG, H.P. 1948. Basic aspects of X-ray absorption. *Analytical Chemistry*, 20(10):886-889. Available: American Chemical Society.

ANDERSON, P.A., KAKUDA, T.N. & LICHTENSTEIN, K.A. 2004. The cellular pharmacology of nucleoside- and nucleotide-analogue reverse-transcriptase inhibitors and its relationship to clinical toxicities. *Clinical Infectious Diseases*, 38:743-753. http://www.journals.uchicago.edu/CID/journals/issues/v38n5/31998/31998.text.html Date of access: 14 Feb. 2006.

ANON. 2007. Bragg's law. http://en.wikipedia.org/wiki/Bragg%27s_law Date of access: 16 Jan. 2007.

ANON. 2007. Beer-Lambert law. http://en.wikipedia.org/wiki/Beer-Lambert_law Date of access: 21 Mar. 2007.

AULTON, M. 2002. Dissolution and solubility. (*In* Aulton, M.E. *ed.* Pharmaceutics: the science of dosage form design. New York : Churchill Livingstone. p. 15-32.)

BAUER-BRANDL, A. 1996. Polymorphic transitions of cimetidine during manufacture of solid dosage forms. *International Journal of Pharmaceutics*, 140:195-206. Available: ScienceDirect.

BERNSTEIN, J. 2002. Polymorphism in molecular crystals. Oxford : Oxford University Press. 410 p.

BERNSTEIN, J. 2006. Polymorphism and patents from a chemist's point of view. (*In* Hilfiker, R. *ed.* Polymorphism in the pharmaceutical industry. Weinheim : Wiley-VCH. p. 365-384.)

BLOMSMA, E. 2006. Drug life-cycle management through solid form discovery – the new game in the industry. *Drug Development*, 2006. http://www.touchbriefings.com/pdf/1842/Blomsma.pdf Date of access: 4 Feb. 2007

BRISTOL-MYERS SQUIBB. 2000. Zerit® (stavudine), package insert. http://www.fda.gov/cder/foi/label/2001/zeritwng.pdf Date of access: 10 Feb. 2006.

BRITTAIN, H.G. 1997. Spectral methods for the characterisation of polymorphs and solvates. *Journal of Pharmaceutical Sciences*, 86(4):405-412, Apr.

BRITTAIN, H.G. 1999. Methods for the characterisation of polymorphs and solvates. (*In* Brittain, H.G. *ed.* Polymorphism in pharmaceutical solids. New York : Marcel Dekker, Inc. p. 227-278.)

BRITTAIN, H.G. & BYRN, S.R. 1999. Structural aspects of polymorphism. (*In* Brittain, H.G. *ed.* Polymorphism in pharmaceutical solids. New York : Marcel Dekker, Inc. p. 73-124.)

BRITTAIN, H.G. & GRANT, D.J.W. 1999. Effects of polymorphism and solid-state salvation on solubility and dissolution rate. (*In* Brittain, H.G. *ed.* Polymorphism in pharmaceutical solids. New York : Marcel Dekker, Inc. p. 279-330.)

BUXTON, P.C., LYNCH, I.R. & ROE, J.M. 1988. Solid-state forms of paroxetine hydrochloride. *International Journal of Pharmaceutics*, 42:135-143, Sep.

BYRN, S.R., PFEIFFER, R.R. & STOWELL, J.G. 1999. Solid-state chemistry of drugs. 2nd ed. West Lafayette : SSCI Inc. 574 p.

CAMPBELL ROBERTS, S.N., WILLIAMS, A.C., GRIMSEY, I.M. & BOOTH, S.W. 2002. Quantitative analysis of mannitol polymorphs. X-ray powder diffractometry – exploring preferred orientation effects. *Journal of Pharmaceutical and Biomedical Analysis*, 28:1149-1159. Available: ScienceDirect.

CARLESS, J.E., MOUSTAFA, M.A. & RAPSON, H.D.C. 1966. Cortisone acetate crystal forms. *Journal of Pharmacy and Pharmacology*, 18:190S-197S.

CHEMBURKAR, S.R., BAUER, J., DEMING, K., SPIWEK, H., PATEL, K., MORRIS, J., HENRY, R., SPANTON, S., DZIKI, W., PORTER, W., QUICK, J., BAUER, P., DONAUBAUER, J., NARAYANAN, B.A., SOLDANI, M., RILEY, D. & McFARLAND, K. 2000. Dealing with the impact of ritonavir polymorphs on the late stages of bulk drug process development. *Organic Process Research & Development*, 4(5):413-417.

COX, J.S.G., WOODARD, G.D. & McCRONE, W.C. 1971. Solid-state chemistry of cromolyn sodium (disodium cromoglycate). *Journal of Pharmaceutical Sciences*, 60(10):1458-1465, Oct.

CRAIG, D.Q.M., ROYALL, P.G., KETT, V.L. & HOPTON, M.L. 1999. The relevance of the amorphous state to pharmaceutical dosage forms: glassy drugs and freeze dried systems. *International Journal of Pharmaceutics*, 179:179-207. Available: ScienceDirect.

CRETTON, E.M., ZHOU, Z., KIDD, L.B., McCLURE, H.M., KAUL, S., HITCHCOCK, M.J. & SOMMADOSSI, J.P. 1993. *In vitro* and *in vivo* disposition and metabolism of 3'-deoxy-2',3'-didehydrothymidine [abstract]. *Antimicrobial Agents and Chemotherapy*, 37(9):1816-1825. Available: American Society for Microbiology.

DE VILLIERS, M.M., VAN DER WATT, J.G. & LÖTTER, A.P. 1991. The interconversion of the polymorphic forms of chloramphenicol palmitate (CAP) as a function of environmental temperature. *Drug Development and Industrial Pharmacy*, 17(10):1295-1303.

DUNGE, A., SHARDA, N., SINGH, B. & SINGH, S. 2005. Establishment of inherent stability of stavudine and development of a validated stability-indicating HPLC assay method. *Journal of Pharmaceutical and Biomedical Analysis*, 37:1115-1119. Available: ScienceDirect.

EMD CHEMICALS INC. 2007. Karl Fischer titration basics. http://www.emdchemicals.com/analytics/literature/KF_Titration_Basics.pdf Date of access: 16 Jan. 2007.

ERIK, P., HENGELSBERG, H., HADDOW, M.F. & VAN GELDER, R. 2004. The innovative momentum of crystal engineering. *CrystEngComm*, 6(78):474-483. Available: Royal Society of Chemistry

FIX, I. & STEFFENS, K.J. 2004. Quantifying low amorphous or crystalline amounts of alpha-lactose-monohydrate using X-ray powder diffraction, near-infrared spectroscopy, and differential scanning calorimetry. *Drug Development and Industrial Pharmacy*, 30(5):513-523. Available: EBSCOhost.

FLOREY, K. 1976. Cephradine. (*In* Florey, K. *ed.* Analytical profiles of drug substances. Volume 5. New York : Academic Press. p. 22-60.)

FUKUOKA, E., MAKITA, M. & YAMAMURA, S. 1986. Some physicochemical properties of glassy indomethacin. *Chemical Pharmaceutical Bulletin*, 34(10):4314-4321.

FUKUOKA, E., MAKITA, M. & YAMAMURA, S. 1989. Glassy state of pharmaceuticals III: thermal properties and stability of glassy pharmaceuticals and their binary glass systems. *Chemical Pharmaceutical Bulletin*, 37(4):1047-1050, Apr.

GANDHI, R., BARTLETT, J.G. & LINKINHOKER, M. 1999. Life cycle of HIV infection. http://www.hopkins-aids.edu/hiv_lifecycle/hivcycle_txt_html Date of access: 18 Apr. 2006.

GANDHI, R.B., BOGARDUS, J.B., BUGAY, D.E., PERRONE, R.K. & KAPLAN, M.A. 2000. Pharmaceutical relationships of three solid state forms of stavudine. *International Journal of Pharmaceutics*, 201:221-237. Available: ScienceDirect.

GANDHI, R.B., BOGARDUS, J.B., GAROFALO, P.M., MARR, T.R., PERRONE, R.K., KAPLAN, M.A. 1996. d4T polymorphic form I process. Patent: EP 0 749 969 A2. 12 p.

GARDNER, C.R., WALSH, C.T. & ALMARSSON, Ö. 2004. Drugs as materials: valuing physical form in drug discovery. *Drug Discovery*, 3:926-934, Nov. Available: nature.com.

GRANT, D.J.W. 1999. Theory and origin of polymorphism. (*In* Brittain, H.G. *ed.* Polymorphism in pharmaceutical solids. New York : Marcel Dekker, Inc. p. 1-33.)

GRIESSER, U.J. 2006. The importance of solvates. (*In* Hilfiker, R. *ed.* Polymorphism in the pharmaceutical industry. Weinheim : Wiley-VCH. p. 211-234.)

GU, Z., GAO, Q., FANG, H., PARNIAK, M.A., BRENNER, B.G. & WAINBERG, M.A. 1994. Identification of novel mutations that confer drug resistance in the human immunodeficiency virus polymerase gene [abstract]. *Leukemia*, 8(suppl. 1):S166-S169. Available: Pubmed (NCBI: National Centre for Biotechnology Information).

GUILLORY, J.K. 1999. Generation of polymorphs, hydrates, solvates, and amorphous solids. (*In* Brittain, H.G. *ed.* Polymorphism in pharmaceutical solids. New York : Marcel Dekker, Inc. p. 183-226.)

HALEBLIAN, J. & McCRONE, W. 1969. Pharmaceutical applications of polymorphism. *Journal of Pharmaceutical Sciences*, 58(8):911-929, Aug.

HANCOCK, B.C. & ZOGRAFI, G. 1997. Characteristics and significance of the amorphous state in pharmaceutical systems. *Journal of Pharmaceutical Sciences*, 86(1):1-12, Jan. Available: Wiley-InterScience.

HARTAUER, K.J., MILLER, E.S. & GUILLORY, J.K. 1992. Diffuse reflectance infrared Fourier transform spectroscopy for the quantitative analysis of mixtures of polymorphs. *International Journal of Pharmaceutics*, 85:163-174, Mar.

HERPER, M. & KANG, P. 2006. The world's ten best-selling drugs. http://www.forbes.com/2006/03/21/pfizer-merck-amgen-cx_mh_pk_0321topdrugs.html Date of access: 4 Feb. 2007.

HILFIKER, R., BLATTER, F. & VON RAUMER, M. 2006. Relevance of solid-state properties for pharmaceutical products. (*In* Hilfiker, R. *ed.* Polymorphism in the pharmaceutical industry. Weinheim : Wiley-VCH. p. 1-20.)

HO, H.T. & HITCHCOCK, M.J.M. 1989. Cellular pharmacology of 2',3'-dideoxy-2',3'-didehydrothymidine, a nucleoside analog active against human immunodeficiency virus. *Antimicrobial Agents and Chemotherapy*, 33(6):844-849. Available: American Society for Microbiology.

HORWITZ, J.P., CHUA, J., DA ROOGE, M.A., NOEL, M. & KLUNDT, I.L. 1966. Nucleosides IX. The formation of 2',3'-unsaturated pyrimidine nucleosides *via* a novel β-elimination reaction. *Journal of Organic Chemistry*, 31:205-211, Jan.

HURST, V.J., SCHROEDER, P.A. & STYRON, R.W. 1997. Accurate quantification of quartz and other phases by powder X-ray diffractometry. *Analytica Chimica Acta*, 337:233-252. Available: ScienceDirect.

IVASHKIV, E. 1973. Ampicillin. (*In* Florey, K. *ed.* Analytical profiles of drug substances. Volume 2. New York : Academic Press. p. 1-62.)

JOHNNIC COMMUNICATIONS. 2006. MIMS: monthly index of medical specialities. 46(8):471, Aug. Johannesburg : Johnnic Communications. 476 p.

JOSHI, B.V., RAO, S.T. & REESE, C.B. 1992. Conversion of some pyrimidine 2'-deoxyribonucleosides into the corresponding 2',3'-didehydro-2',3'-dideoxynucleosides. *Journal of the Chemical Society Perkin Transactions I*, 19:2537-2544.

KAISER, G.E. 2005. Animal virus life cycles: the life cycle of HIV. http://student.ccbcmd.edu/course/bio141/lecguide/unit2/viruses/hivlc.html Date of access: 18 Apr. 2006.

KIVELSON, D. & TARJUS, G. 2002. Apparent polyamorphism and frustration. *Journal of Non-Crystalline Solids*, 307-310:630-363. Available: ScienceDirect.

LACEY, S.F. & LARDER, B.A. 1994. Novel mutation (V75T) in human immunodeficiency virus type 1 reverse transcriptase confers resistance to 2',3'-didehydro-2',3'-deoxythymidine in cell culture. *Antimicrobial Agents and Chemotherapy*, 38(6):1428-1432. Available: American Society for Microbiology.

LIN, T.S. & PRUSOFF, W.H. 1990. Use of 3'-deoxythymidin-2'-ene (3'deoxy-2',3'-didehydrothymidine) in treating patients infected with retroviruses. Patent: US 4,978,655. 9 p.

LOHANI, S. & GRANT, D.J.W. 2006. Thermodynamics of polymorphs. (*In* Hilfiker, R. *ed.* Polymorphism in the pharmaceutical industry. Weinheim : Wiley-VCH. p. 21-42.)

LUND, W. *ed.* 1994. The pharmaceutical codex. 12th ed. London : The Pharmaceutical Press. 1117 p.

MARTIN, A. 1993. Physical pharmacy: physical chemical principles in the pharmaceutical sciences. 4th ed. Baltimore : Lippincott Williams & Wilkins. 622 p.

MEDICINES CONTROL COUNCIL. 2006. Dissolution, 1-10, July. Available: www.mccza.com

MEI, X, & WOLF, C. 2006. Conformational polymorphism of 1,8-dipyridylnaphthalene and encapsulation of chains of fused cyclic water pentamers in a hydrophobic crystal environment. *CrystEngComm*, 8:377-380. Available: Royal Society of Chemistry

MERCK & CO., INC. 2001. The Merck Index: an encyclopedia of chemicals, drugs and biologicals. 13th ed. Whitehouse Station, NJ. 1818 p.

MICROSOFT ENCARTA PREMIUM SUITE 2005. 2005. Crystals. [CD].

MIRMEHRABI, M., ROHANI, S., MURTHY, K.S.K. & RADATUS, B. 2004. Solubility, dissolution rate and phase transition studies of ranitidine hydrochloride tautomeric forms. *International Journal of Pharmaceutics*, 282:73-85. Available: ScienceDirect.

MIRMEHRABI, M., ROHANI, S., MURTHY, K.S.K. & RADATUS, B. 2006. Polymorphic behavior and crystal habit of an anti-viral/HIV drug: stavudine. *Crystal growth and design*, 6(1):141-149. Available: American Chemical Society.

MOORE, J.W. & FLANNER, H.H. 1996. Mathematical comparison of dissolution profiles. *Pharmaceutical Technology*, 64-74, Jun.

MORRIS, K.R. 1999. Structural aspects of hydrates and solvates. (*In* Brittain, H.G. *ed.* Polymorphism in pharmaceutical solids. New York : Marcel Dekker, Inc. p. 125-181.)

MORRIS, K.R., GRIESSER, U.J., ECKHARDT, C.J. & STOWELL, J.G. 2001. Theoretical approaches to physical transformations of active pharmaceutical ingredients during manufacturing processes. *Advanced Drug Delivery Reviews*, 48:91-114. Available: ScienceDirect.

MULLINS, J.D. & MACEK, T.J. 1960. Some pharmaceutical properties of novobiocin. *Journal of the American Pharmaceutical Association*, 49(4):245-248, Apr.

NEWMAN, A.W. & BYRN, S.R. 2003. Solid-state analysis of the active pharmaceutical ingredient in drug products. *Drug Discovery Today*, 8(19):898-905, Oct. Available: ScienceDirect.

NICHOLS, G. 2006. Light microscopy. (*In* Hilfiker, R. *ed.* Polymorphism in the pharmaceutical industry. Weinheim: Wiley-VCH. p. 167-210.)

NICHOLS, G. & FRAMPTON, C.S. 1998. Physicochemical characterization of the orthorhombic polymorph of paracetamol crystallised from solution. *Journal of Pharmaceutical Sciences*, 87(6):684-693, Jun.

OCHSENBEIN, P. & SCHENK, K.J. 2006. Crystallography for polymorphs. (*In* Hilfiker, R. *ed.* Polymorphism in the pharmaceutical industry. Weinheim : Wiley-VCH. p. 139-166.)

PAN, X., JULIAN, T. & AUGSBURGER, L. 2006. Quantitative measurement of indomethacin crystallinity in indomethacin-silica gel binary system using differential scanning calorimetry and X-ray powder diffractometry. *AAPS PharmSciTech*, 7(1):E1-E9, article 11. Available: AAPSPharmSciTech.org.

PEROLD, Z. 2006. The polymorphic and pseudopolymorphic behaviour of gatifloxacin crystal modifications. Potchefstroom : NWU. (Thesis – M.Sc.) 244 p.

PFEIFFER, R.R., ENGEL, G.L. & COLEMAN, D. 1976. Stable antibiotic sensitivity disks. *Antimicrobial Agents and Chemotherapy*, 9(5):848-851, May.

PHADNIS, N.V. & SURYANARAYANAN, R. 1997. Polymorphism in anhydrous theophylline: implications on the dissolution rate of theophylline tablets. *Journal of Pharmaceutical Sciences*, 86(11):1256-1263, Nov.

PHARMACEUTICAL PRESS. 2006. Martindale – The complete drug reference. Available: Thomson MICROMEDEX.

PIENAAR, E.W. 1994. Characterisation of anhydrous and monohydrate crystal forms of nitrofurantoin. Potchefstroom : PU for CHE. (Thesis – Ph.D.) 196 p.

PIKAL, M.J., LUKES, A.L. & LANG, J.E. 1977. Thermal decomposition of amorphous β-lactam antibacterials. *Journal of Pharmaceutical Sciences*, 66(9):1312-1316, Sep.

RADATUS, B.K. & MURTHY, K.S.K. 2003. Process for the preparation of substantially pure stavudine and related intermediates useful in the preparation thereof. Patent: US 6,635,753. 6 p.

RAFFANTI, S. & HAAS, D.W. 2001. Antimicrobial agents (continued): Antiretroviral agents. (*In* Hardman, J.G. & Limbird, L.E. *ed.* Goodman and Gilman's The pharmacological basis of therapeutics. 10th ed. New York : McGraw-Hill. p. 1349-1380.)

RIDDLER, S.A., ANDERSON, R.E. & MELLORS, J.W. 1995. Antiretroviral activity of stavudine (2',3'-didehydro-3'-deoxythymidine, D4T). *Antiviral Research*, 27:189-203. Available: ScienceDirect.

RODRÍGUES-SPONG, B., PRICE, C.P., JAYASANKAR, A., MATZGER, A.J. & RODRÍGUES-HORNEDO, N. 2004. General principles of pharmaceutical solid polymorphism: a supramolecular perspective. *Advanced Drug Delivery Reviews*, 56:241-274. Available: ScienceDirect

ROSTON, D.A., WALTERS, M.C., RHINEBARGER, R.R. & FERRO, L.J. 1993. Characterization of polymorphs of a new anti-inflammatory drug. *Journal of Pharmaceutical and Biomedical Analysis*, 11(4/5):293-300.

SHARMA, J.N. & MOHAMMED, L.A. 2006. The role of leukotrienes in the pathophysiology of inflammatory disorders: is there a case for revisiting leukotrienes as therapeutic targets? *Inflammopharmacology*, 14:10-16. Available: Springerlink.

SHEFFIELD HALLAM UNIVERSITY. 2007. Beer's law. http://teaching.shu.ac.uk/hwb/chemistry/tutorials/molspec/beers1.html Date of access: 21 Mar. 2007.

SHI, J., RAY, A.S., MATHEW, J.S., ANDERSON, K.S., CHU, C.K. & SCHINAZI, R.F. 2004. 2',3'-Didehydro-2',3'-dideoxynucleosides are degraded to furfuryl alcohol under acidic conditions. *Bioorganic & Medicinal Chemistry Letters*, 14:2159-2162. Available: ScienceDirect.

SICHINA, W.J. Characterization of pharmaceuticals using thermal analysis. *American Laboratory*, 2001:16-25, Jan. http://www.iscpubs.com/articles/index.php?3-all-al/a0101sic.pdf Date of access: 22 Feb. 2006.

SINGHAL, D. & CURATOLO, W. 2004. Drug polymorphism and dosage form design: a practical perspective. *Advanced Drug Delivery Reviews*, 56:335-347. Available: ScienceDirect.

SKONEZNY, P.M., EISENREICH, E., STARK, D.R., BOYHAN, B.T. & BAKER, S.R. 1994. Process for large scape preparation of 2',3'-didehydro-2',3'-dideonucleosides. Patent: EP 0 653 435 A1. 11 p.

SMITH, A. 2006. Zocor and Zoloft face patent expiration: Merck and Pfizer both stand to lose billions of dollars in sales. http://money.cnn.com/2006/06/15/news/companies/zoloft_zocor/index.htm?postversion=2006061514 Date of access: 4 Feb. 2007.

SMITH, J., MACNAMARA, E., REFTERY, D., BORCHARDT, T. & BYRN, S. 1998. Application of two-dimensional ^{13}C solid-state NMR to the study of conformational polymorphism. *Journal of the American Chemical Society*, 120:11710-11713, Aug. Available: American Chemical Society.

STARRETT, J.E., MANSURI, M.M., MARTIN, J.C., FULLER, C.E. & HOWELL, H.G. 1990. Production of 2',3'-dideoxy-2',3'-didehydronucleosides. Patent: US 4,904,770. 12 p.

STEPHENSON, G.A. 2005. Applications of X-ray powder diffraction in the pharmaceutical industry. *The Rigaku Journal*, 22(1):2-15. Available: http://www.rigaku.com/downloads/journal/Vol22.1.2005/22_2.pdf

STEPHENSON, G.A., FORBES, R.A. & REUTZEL-EDENS, S.M. 2001. Characterization of the solid state: quantitative issues. *Advanced Drug Delivery Reviews*, 48:67-90. Available: ScienceDirect.

STEPHENSON, G.A., STOWELL, J.G., TOMA, P.H., DORMAN, D.E., GREENE, J.R. & BYRN, S.R. 1994. Solid-state analysis of polymorphic, isomorphic and solvated forms of dirithromycin. *Journal of the American Chemical Society*, 116(13):5766-5773. Available: American Chemical Society.

STEZOWSKI, J.J. 1977. Chemical-structural properties of tetracycline antibiotics. 4. Ring A tautomerism involving the protonated amide substituent as observed in the crystal structure of α-6-Deoxyoxytetracycline hydrohalides. *Journal of the American Chemical Society*, 99(4):1122-1129, Feb. Available: American Chemical Society.

SURYANARAYANAN, R. 1989. Determination of the relative amounts of anhydrous carbamazepine ($C_{15}H_{12}N_2O$) and carbamazepine dihydrate ($C_{15}H_{12}N_2O \cdot 2H_2O$) in a mixture by powder X-ray diffractometry. *Pharmaceutical research,* 6(12):1017-1024, Jun.

SURYANARAYANAN, R. 1990. Determination of the relative amounts of α-carbamazepine and β-carbamazepine in a mixture by powder X-ray diffractometry. *Powder Diffraction*, 5(3):155-159, Sep.

TAKENAKA, H., KAWASHIMA, Y. & LIN, S.Y. 1981. Polymorphism of spray-dried microencapsulated sulfamethoxazole with cellulose acetate phthalate and colloidal silica, montmorillonite, or talc. *Journal of Pharmaceutical Sciences*, 70(11):1256-1260, Nov.

THE DANISH UNIVERITY OF PHARMACEUTICAL SCIENCES. 2006. HydrateControl – role of anhydrate/hydrate equilibrium in the performance of solid dosage form. http://www.dfuni.dk/fileadmin/DRA/dra_opslag_october2006_project2.pdf Date of access: 7 Feb. 2007

UNITED STATES PHARMACOPEIAL CONVENTION. 2007. USP30:NF25 Online. Available: www.uspnf.com

VAN TONDER, E.C., MAHLATJI, M.D., MALAN, S.F., LIEBENBERG, W., CAIRA, M.R., SONG, M. & DE VILLIERS, M.M. 2004. Preparation and physicochemical characterisation of 5 niclosamide solvates and 1 hemisolvate. *AAPS PharmSciTech*, 5(1):1-10, article 12. Available: AAPSPharmSciTech.org.

VIPPAGUNTA, S.R., BRITTAIN, H.G. & GRANT, D.J.W. 2001. Crystalline solids. *Advanced Drug Delivery Reviews*, 48:3-26.

VITERBO, D., MILANESIO, M., HERNÁNDEZ, R.P., TANTY, C.R., GONZÁLES, I.C., CARRAZANA, M.S. & RODRÍGUES, J.D. 2000. 2',3'-Didehydro-3'-deoxythymidine *N*-methyl-2-pyrrolidone solvate (D4T·NMPO). *Acta Crystallographica Section C*, C56:580-581.

VOET, M.A. 2005. The generic challenge: understanding patents, FDA & pharmaceutical life cycle management. Boca Raton, FL, USA : BrownWalker Press. 116 p.

WU, T., LI, N., DE VILLIERS, M.M. & YU, L. 2006. Nano-coating for inhibiting surface crystallization and improving physical properties of amorphous indomethacin. 1-15 p. Personal communication with the author: lyu@pharmacy.wisc.edu.

YORK, P. 1999. Strategies for particle design using supercritical fluid technologies. *Pharmaceutical Science & Technology Today*, 2(11):430-440, Nov. Available: ScienceDirect.

YU, L. 2001. Amorphous pharmaceutical solids: preparation, characterisation and stabilisation. *Advanced Drug Delivery Reviews*, 48:27-42. Available: ScienceDirect

YU, L., REUTZEL, M.R. & STEPHENSON, G.A. 1998. Physical characterisation of polymorphic drugs: an integrated characterization strategy. *Pharmaceutical Science & Technology Today*, 1(3):118-127, Jun. Available: ScienceDirect.

YU, L., STEPHENSON, G.A., MITCHELL, C.A., BUNNELL, C.A., SNOREK, S.V., BOWYER, J.J., BORCHARDT, T.B., STOWELL, J.G. & BYRN, S.R. 2000. Thermochemistry and conformational polymorphism of a hexamorphic crystal system. *Journal of the American Chemical Society*, 122:585-591. Available: American Chemical Society.

ACKNOWLEDGEMENTS

I would just like to take this opportunity to express the following words of appreciation:

To God, thank You for Your generosity in awarding me the strength, wisdom, courage and willpower that enables me to continue achieving my dreams

- To my parents, Willie and Corrie, my brother Alwyn and my sister Carla, thank you for all your support and encouragement throughout the years.
- To my grandparents, my aunts and uncles, my cousins and the rest of my family, thank you for your continued support and interest.
- To Prof. Wilna Liebenberg and Mr. Marius Brits, thank you for your excellent guidance and support throughout this study.
- To my fellow students and friends, in particular Yasmin Bawa, Carin Jansen van Vuuren, Raadhiya Cassim, Nicóle Stieger, Mari-Alet de Jager, Marique Aucamp and Danie Otto, thank you for your friendship and your words of encouragement.
- To the Research Institute for Industrial Pharmacy (RIIP), thank your for allowing me to utilise your outstanding facilities and equipment.
- To all the personnel at the RIIP, especially Dr. Erna Swanepoel, Elmarie du Preez, Stefan Nieman, Chris Liebenberg, Dr. Elsa van Tonder, Anita Wessels and Lizelle Fourie, thank you for all your assistance and support.
- To Prof. Melgardt de Villiers, thank you for the inspiration and for your interest.
- To Dr. Louwerns Tiedt, thank you for your assistance with the SEM microscopy.
- To Madelein Geldenhuys, thank you for your assistance during the dissolution testing.
- To Julia Handford, thank you for your assistance.
- Thank you to the staff of the NWU Library, especially Anriette Pretorius.
- Thank you to the National Research Foundation (NRF) for the financial support.
- And thank you to the personnel at Midvaal Pharmacy for your assistance during my practical pharmacy training.

ANNEXURE 1

Poster presented at the 4th International Conference on Pharmaceutical and Pharmacological Sciences

NORTH-WEST UNIVERSITY
YUNIBESITI YA BOKONE-BOPHIRIMA
NOORDWES-UNIVERSITEIT

Preparation and thermal stability of polymorphic forms of stavudine

Schalk Strydom[1], Marius Brits[1], Wilna Liebenberg[1]
[1]Research Institute for Industrial Pharmacy, School of Pharmacy, North-West University, Potchefstroom Campus, Potchefstroom 2520, South Africa

PURPOSE

The goal of this study is to prepare the two polymorphic forms and one pseudopolymorphic form of stavudine (d4T), and to confirm the thermal stability of these solid states.

BACKGROUND

Stavudine is a synthetic thymidine analog and a nucleoside reverse transcriptase inhibitor (NRTI) that is active against HIV. Stavudine rapidly enter cells by passive diffusion after which it is phosphorylated to stavudine triphosphate by thymidine kinase. Stavudine triphosphate inhibits the reverse transcriptase enzyme of HIV by competing with the nucleoside, 2-deoxythymidine-5-triphosphate, resulting in DNA chain termination.[1]

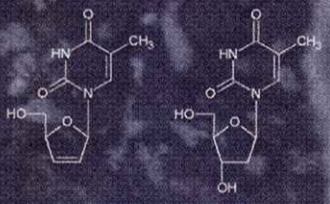

Fig 1. The chemical structure of stavudine (left) and thymidine (right).

There are two known polymorphic forms, one hydrate, and a few solvates of stavudine. Form I is considered to be the stable polymorph, with form II being metastable and form III is the hydrate of stavudine.[2],[3]

METHODS

The polymorphic crystal forms of stavudine were prepared by recrystallization of the same stavudine raw material in a series of analytical grade solvents. An array of physico-chemical analyses, specifically differential scanning calorimetry (DSC), thermogravimetric analysis (TGA), thermal microscopy (TM), infrared spectroscopy (IR), Karl Fischer (KF) water determination and X-ray powder diffractometry (XRPD) were performed on the crystals obtained in order to characterize the polymorphic forms. The thermal stability of two of the prepared polymorphs (form II and form III) and of the raw material (which appears to be a mixture of form I and form II) were determined by means of variable temperature X-ray powder diffractometry (VTXRPD).

RESULTS

Polymorphic form I and II, as well as the hydrate (form III), were successfully prepared by the recrystallization of stavudine raw material. Form I was prepared using short chain alcohols, ACN, and acetone as solvents. Form II was prepared using medium chain alcohols, chloroform, benzene and ethyl acetate as solvents, whereas the hydrate was prepared using THF and water as solvents.

The DSC thermograms of all three crystal forms show a sharp endotherm with a peak maximum at 167°C – 174°C indicating the melting of stavudine, followed by decomposition. Form III has a small additional exotherm/endotherm at 132°C – 140°C indicating dehydration of the hydrate. TM analysis illustrates the dehydration taking place at 130°C – 140°C.

The theoretical weight loss of form III [(d4T)$_2$.H$_2$O] after dehydration is 2.61%. The KF and TG analysis of the hydrate prepared from THF shows a moisture content of 2.42% and a weight loss of 1.89%, and the hydrate prepared from water shows a moisture content of 2.91% and a weight loss of 3.05%.

Three slightly different IR spectra were obtained for form I, II and III. These spectra are very similar and have to be used with other analyses in order to make an accurate distinction between the different polymorphs.

According to XRPD analyses, each polymorphic form has unique diffraction angles: form I – 19.1°, form II – 11.2° and 18.6°, and form III – 6.5°, 7.3° and 15.4°. The raw material, as well as a few polymorphs recrystallized, have diffraction angles corresponding to both form I and II and are assumed to be a mixture of these two polymorphs. Form II, the mixture of form I and II, and form III (obtained from THF) were subjected to increasing temperatures, with increments of 10°C between each diffractogram, from 25°C – 160°C during VTXRPD analysis. The diffractograms of form II and the mixture show no significant change in peak intensities or diffraction angles, whereas form III converts to form I as it dehydrates with an increase in temperature.

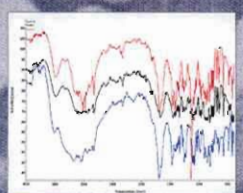

Fig 2. An overlay of the IR spectra of form I (black), form II (red) and form III (blue).

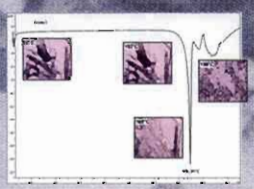

Fig 3. The DSC thermogram and thermal microscopy pictures of form I of stavudine.

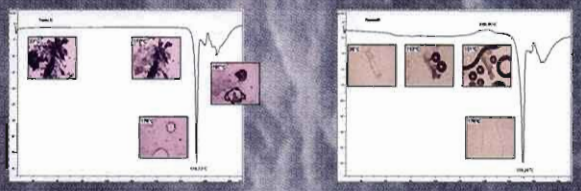

Fig 4. The DSC thermograms and thermal microscopy pictures of form II (left) and form III (right) of stavudine.

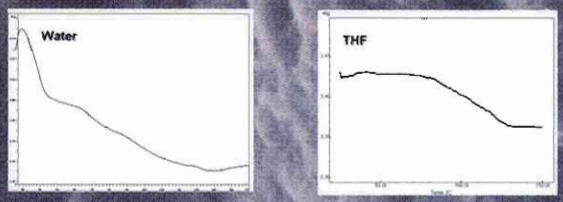

Fig 5. The TGA thermograms of the hydrate of stavudine obtained from water (left) and from THF (right).

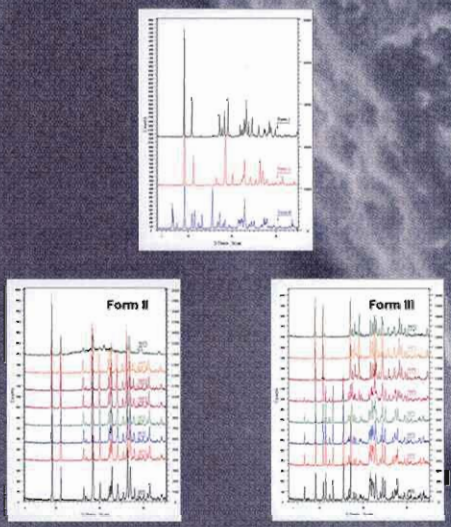

Fig 6. An overlay of the XRPD diffractograms of all three solid states of stavudine (top), and the VTXRPD diffractograms of form II (left) and form III (right).

CONCLUSION

The different polymorphic forms of stavudine can be prepared in a pure form, and XRPD is the most accurate method to use for distinguishing between the different forms. Form III undergoes dehydration and converts to form I, but form II, and mixtures of form I and II, remain stable with an increase in temperature. Form II does not convert to form I according to VTXRPD analysis, and they appear to be monotropically related.

REFERENCES

(1) S.A. Rekker, R.E. Anderson and J.W. Mellors, Antiretroviral activity of stavudine (2',3'-didehydro-3'-deoxythymidine, D4T). Antivir. Res. 27, 189-203 (1995).

(2) R.B. Gandhi, J.B. Bogardus, D.E. Bugay, R.K. Perrone and M.A. Kaplan, Pharmaceutical relationships of three solid state forms of stavudine. Int. J. Pharm. 201, 221-237 (2001).

(3) M. Mirmehrabi, S. Rohani, K.S.K. Murthy and B. Radatus, Polymorphic behavior and crystal habit of an anti-viral/HIV drug: stavudine. Crystal Growth & Design, 6(1), 141-149.

Article in process of submission

The glassy solid state of stavudine

Schalk Strydom[1], Wilna Liebenberg[1], Marius Brits[1]

[1]Research Institute for Industrial Pharmacy, North-West University, Potchefstroom Campus, Potchefstroom, 2520

Abstract

A glassy (amorphous) solid state of stavudine was prepared and characterised, and the fragility ratio of this glass demonstrated that it is a strong glass. Variable temperature X-ray powder diffraction analysis of this glassy solid illustrated that it reverts to a crystalline state with an increase in temperature and that it transforms to a mixture of form I and form II of stavudine at 120°C. A comparison of the dissolution profiles of form I and form II of stavudine, the glassy stavudine and the form I/II mixture of stavudine revealed that a greater amount of the glassy stavudine dissolves in one minute.

Keywords: Stavudine; Glassy; Amorphous; Polymorphism

1. Introduction

Stavudine is a nucleoside reverse transcriptase inhibitor (NRTI) that is used in the treatment of human immunodeficiency virus (HIV) infections [1].

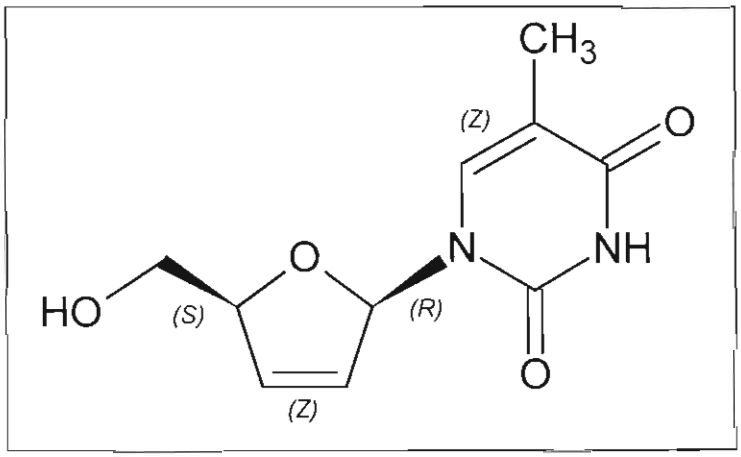

Figure 1 The structural formula of stavudine [2].

Stavudine exhibits polymorphism and the two polymorphic forms (form I and form II) and five pseudopolymorphic forms (form III (a hydrate), an NMP (*N*-methyl-2-pyrrolidone) solvate, a DMA (*N,N*-dimethylacetamide) solvate, a DMAC (*N,N*-dimethylacrylamide) solvate and a

DMP (*N,N*-dimethylpropionamide) solvate) are described in the literature [3],[4],[5]. An increase in the solubility of the solid state of a drug offers the advantage of providing a greater systemic absorption of the drug, and results in a reduced amount of the drug being required in the dosage form in order to achieve the same therapeutic effect as the original product. The solid state that generally meets this requirement is the amorphous or glassy state, but it has the disadvantage of being thermodynamically unstable when compared to the original solid state. There are however methods that can be used to increase the stability of the glassy state, of which nano-coating is the most recently discovery and offers the most promising applications for the future [6],[7].

2. Materials and methods

2.1 Materials

Stavudine raw material (batch number 0601002) was purchased from Xiamen Mchem Laboratories Ltd. (6 Yangtai Road, Xinyang Industrial Area, Haicang, Xiamen, China). The various polymorphic forms of stavudine were prepared by recrystallisation of the raw material in various solvents (which were obtained from Merck Chemicals (Pty) Ltd., South Africa) as illustrated in figure 2.

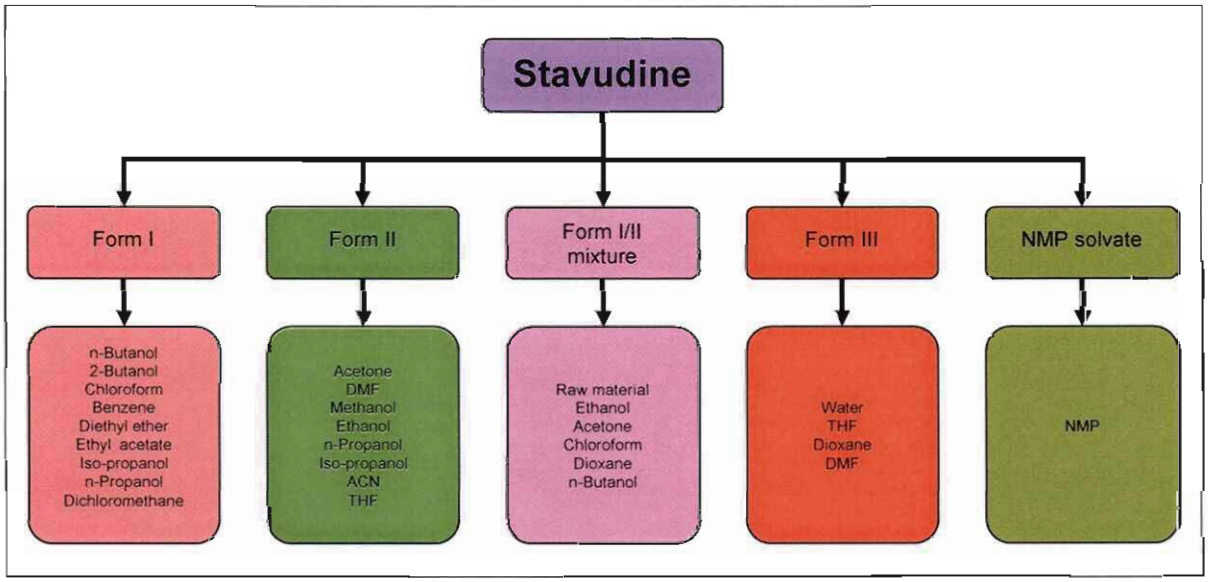

Figure 2 The various polymorphic forms of stavudine and the solvents from which they were obtained.

2.2 *Preparation of the glassy stavudine*

The glassy stavudine was prepared by heating a small amount of the stavudine raw material on a microscope slide using a Velp® Scientifica (Italy) heating magnetic stirrer, and allowing the melt to cool. Since stavudine decomposes after melting, extreme caution had to be exercised in order to ensure that the stavudine does not decompose during this melting process. Hence only small quantities (approximately 30 – 50 mg) of the raw material were spread out on the microscope slide and melted, and as soon as melting commenced the microscope slide was removed from the heat source and placed on a cool piece of granite. The residual heat of the melt caused the whole sample to melt.

2.3 *Characterisation techniques*

2.3.1 *Thin-layer chromatography (TLC)*

Thin-layer chromatography (TLC) was used in order to confirm that the stavudine did not decompose during this melting procedure when preparing the glassy stavudine. The TLC method for stavudine capsules described in the United States Pharmacopeia 2007 (USP30:NF25) was used as a guide and will be briefly described. The stavudine raw material (Xiamen Mchem Laboratories Ltd., Xiamen, China) was used as the stavudine reference, and thymine (Sigma-Aldrich, Steinheim, Germany) was used as the degradation product reference. One milligram (weighed using a Mettler Toledo microbalance that was calibrated using a one milligram calibration standard (grade E2), Greifensee, Switzerland) of the glassy stavudine, the stavudine raw material and the thymine were dissolved in five millilitres of Milli-Q water using sonication to yield solutions with concentrations of 0.2 mg/ml each. Ten micro litres of each solution (applied in two 5 µl portions) were spotted on an Alugram® Sil G/UV_{254} TLC plate (Macherey-Nagel GmbH & Co. KG, Düren, Germany) using micropipettes (BRAND GMBH, Wertheim, Germany) and allowed to dry. The chromatogram was developed in a chamber saturated with the mobile phase (consisting of chloroform and ethanol (obtained from Merck Chemicals (Pty) Ltd., South Africa) and water with a ratio of 100:50:2 respectively). The TLC-plate was allowed to develop until the solvent front had moved 10 cm from the origin. The TLC plate was removed from the chamber, the solvent front was marked and the plate allowed to dry for 5 – 10 minutes at ambient conditions. The spots were visualised using an ultraviolet lamp at a wavelength of 254 nm (Camag Reprostar, Switzerland) [8].

2.3.2 *X-ray powder diffraction (XRPD)*

The XRPD patterns were recorded using a Bruker D8 Advanced diffractometer (Bruker, Germany). The measurement conditions were: target, Cu; voltage, 40 kV; current, 30 mA; divergence slit, 2 mm; anti-scatter slit, 0.6 mm; detector slit, 0.2 mm; monochromator; scanning speed, 2°/min with a step size of 0.025° and a step time of 1.0 seconds. Samples were packed in an aluminium sample holder after being ground in a pestle and mortar, and the XRPD sample accessory was rotated at 15 revolutions per minute in order to reduce the potential influence of preferred orientation, which is defined as a non-random orientation of plate- or needle-like crystals due to the interaction with each other in the powder bed resulting in a variation in diffraction intensity. The peak positions and intensities were generated from the diffractograms using the Eva© software (version 10.0 revision 1) which is part of the Diffrac^{plus} 2004 software package (Bruker, Germany).

2.3.3 *Variable temperature X-ray powder diffraction (VT-XRPD)*

VT-XRPD analyses were performed using the diffractometer with the VT-XRPD sample holder and diffractometer setup stated in 2.2.1 (except for the rotation of the sample accessory which is not possible with VT-XRPD). Samples were heated up to different temperatures (to a maximum of 164°C) using an Anton Paar TTK 450 low temperature camera (Anton Paar, Austria) with a heating rate of 1°C/sec, and were maintained at those temperatures for the duration of each diffraction analysis (form 3 – 40°2θ).

2.3.4 *Diffuse reflectance infrared Fourier transform spectroscopy (DRIFTS)*

The infrared spectra were recorded on a Nicolet Nexus™ 470 spectrometer (Nicolet Instrument Corporation, Madison WI, USA) over a range of 4000 – 400 cm^{-1} with the samples placed in an Avatar Diffuse Reflectance smart accessory after being mixed and ground with dried KBr (Merck, Darmstadt, Germany). The peak positions and intensities of the spectra recorded were determined using version 7.3 of the OMNIC© software package (Thermo Electron Corporation, USA).

2.3.5 *Differential scanning calorimetry (DSC)*

Between two and five milligrams of sample was placed in a 40 µl aluminium sample pan (Mettler Toledo, Switzerland), crimp sealed with a pierced aluminium lid (the lid was pierced to relieve possible pressure build up which could cause a variation in results), and analysed using a Mettler Toledo DSC823^e (Greifensee, Switzerland) that was calibrated using an indium standard. Samples were analysed at temperatures from 25 - 210°C with a heating

rate of 10°C/min and a nitrogen gas flow rate of 50 ml/min. The melting points (and other data) were calculated from the thermograms using the STAR^e software programme (version 9.0*x*) (Mettler Toledo, Switzerland).

2.3.6 Thermogravimetric analysis (TGA)

Between six and ten milligrams of sample was placed in a 100 µl aluminium pan and covered with a pierced lid (not crimped sealed). Samples were analysed using a calibrated Mettler Toledo TGA/SDTA851^e (Greifensee, Switzerland), with the samples analysed from 25 - 140°C at a heating rate of 10°C/min and a nitrogen gas flow rate of 50 ml/min. The weight loss of the samples was calculated using the STAR^e software programme (version 9.0*x*) (Mettler Toledo, Switzerland).

2.3.7 Karl Fischer (KF) analyses

A Metrohm 701 KF Titrino (Herisau, Switzerland) calibrated with purified water and sodium tartrate dihydrate (Riedel-de Haën, Germany) was used in the Karl Fischer determinations.

2.3.8 Polarising optical and hot-stage microscopy (HSM)

A small amount of sample was placed on a microscope slide and either covered with silicon oil (Fluka Chemika, Switzerland) and a cover slide (in the case of solvates), or only a cover slide. A Nikon Eclipse E400 thermo-microscope (Tokyo, Japan) with a Leitz 350 heating unit (Leitz – now known as Leica Microsystems – Wetzlar, Germany) and a Metratherm 1200d thermostat was used for the hot-stage microscopy, and a Nikon Simple Polarizing Attachment (Tokyo, Japan) was used on the same microscope for the polarising optical microscopy. Photographs were taken using a Nikon Coolpix 5400 digital camera (Tokyo, Japan) which was attached to the microscope.

2.3.9 Scanning electron microscopy (SEM)

Samples were analysed by covering the carbon tape on the SEM pin with sample, and it was then covered with a gold-palladium film (Eiko engineering ion coater IB-2, Japan) in a vacuum. The samples were placed in the microscope sample holder and analysed using a FEI Quanta 200 ESEM & Oxford INCA 400 EDS microscope system (FEI Corporation, Hillsboro OR, USA).

2.3.10 Dissolution

The dissolution method for stavudine capsules that is described in the United States Pharmacopeia 2007 (USP30:NF25) was used as a guide to determine the dissolution behaviour of the various stavudine polymorphic forms, with the exception that instead of using stavudine capsules during the dissolution testing, 40 mg of the various polymorphic powders (which were weighed using a calibrated Sartorius analytical balance – Goettingen, Germany) were added to each dissolution vessel. The polymorphic powders that were used during the dissolution testing were manually sieved using a 45 µm Madison test sieve (Madison Filter Solutions, Madison Filter SA Pty (Ltd.), Johannesburg, South Africa), thus ensuring uniform particle size distribution of the polymorphic powders. This was done in order to eliminate the possible influence of particle size variations of the various polymorphic powders on the results of the dissolution testing [8]. The dissolution tests were performed using a Vankel VK7000 dissolution tester (Varian Inc., Palo Alto CA, USA). The dissolution samples were analysed using a Varian Cary 50 UV-Visible Spectrophotometer (Varian Inc., Palo Alto CA, USA) at a wavelength of 265 nm. As directed by the United States Pharmacopeia 2007 (USP30:NF25), the dissolution medium that was used was 900 mL of degassed purified water maintained at a temperature of 37±0.5°C, the dissolution apparatus 2 (paddles) was used with a rotational speed of 75 revolutions per minute, and the dissolution tests were performed for a period of 30 minutes. Since stavudine is highly soluble in water [8], and it is expected that the added stavudine powder will completely dissolve within five minutes, it was decided to withdraw samples of five millilitres of the dissolution medium from each of the six dissolution vessels at intervals of 1, 5, 10, 15 and 30 minutes from the time that the dissolution testing commenced [8]. Prior to determining the amount of dissolved stavudine by UV spectrophotometry, a calibration curve of absorbance (A) versus concentration (c, measured in µg/ml) was plotted in order to determine if there is a linear relationship between the absorbance and the concentration of stavudine solutions, and this plot was also used to determine the concentration of stavudine in the various dissolution samples. This calibration curve was produced by preparing a series of seven stavudine solutions with concentrations of 1, 5, 10, 15, 20, 25 and 50 µg/ml, which were respectively analysed using the spectrophotometer (solutions analysed by spectrophotometry need to be diluted since the Beer-Lambert law is not obeyed by highly concentrated solutions). Figure 5.3 shows the resulting calibration curve which was obtained, and it is clear from this graph that there is a linear relationship between the absorbance and the concentration of the various stavudine solutions within the range of 0 – 50 µg/ml. The equation that is displayed on the graph was used in order to determine the concentration of stavudine in the dissolution

samples, and the potency of the stavudine standard was also compensated for during the calculations.

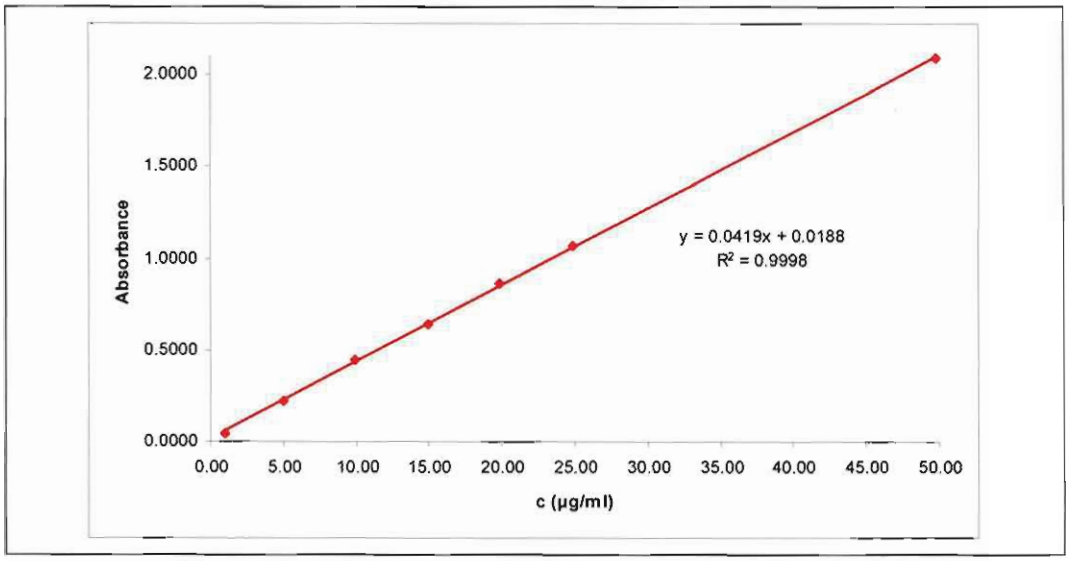

Figure 3 The calibration curve plotted for a series of standard stavudine solution.

In order to determine the amount of dissolved stavudine in the dissolution samples using the UV spectrophotometric method, two millilitres of the withdrawn dissolution medium was diluted to 10 ml with purified water in a volumetric flask, and the absorbance of the resulting solutions were determined at a wavelength of 265 nm. The withdrawn dissolution samples were diluted, since it was previously determined that this dilution would yield a solution with a stavudine concentration of approximately 10 µg/ml, and this concentration of stavudine solutions would be in the range of the concentrations used for constructing the calibration curve.

3. Results and discussion

The Rf values (calculated using equation 1 and figure 4) of the stavudine raw material and the glassy stavudine were 0.700 and corresponded with each other, whist the Rf value of thymine (0.650) differed from this value. This indicates that the stavudine did not decompose during the melting process and that the glassy stavudine does not contain degradation products.

$$R_f = \frac{R_1}{R_2} \qquad (1)$$

Where: R_1 = the distance travelled by each spot

R_2 = the distance travelled by the mobile phase.

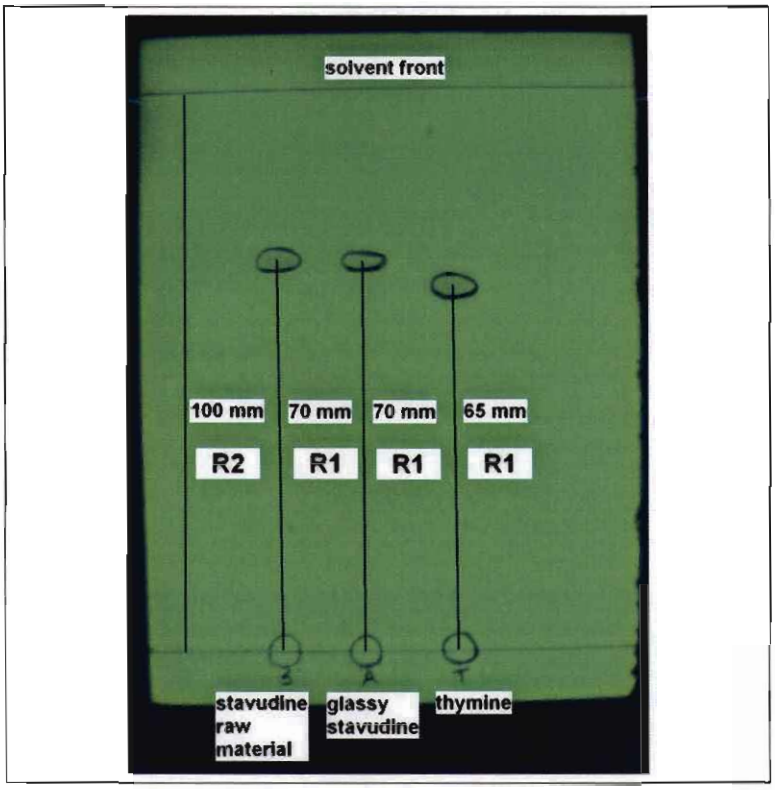

Figure 4 A photograph of the chromatographic plate obtained from the TLC analysis.

The diffractogram in figure 5 shows a broad hump which is also called the amorphous halo, and this is indicative of amorphous solid states. No clearly defined peaks were denoted for the glassy stavudine.

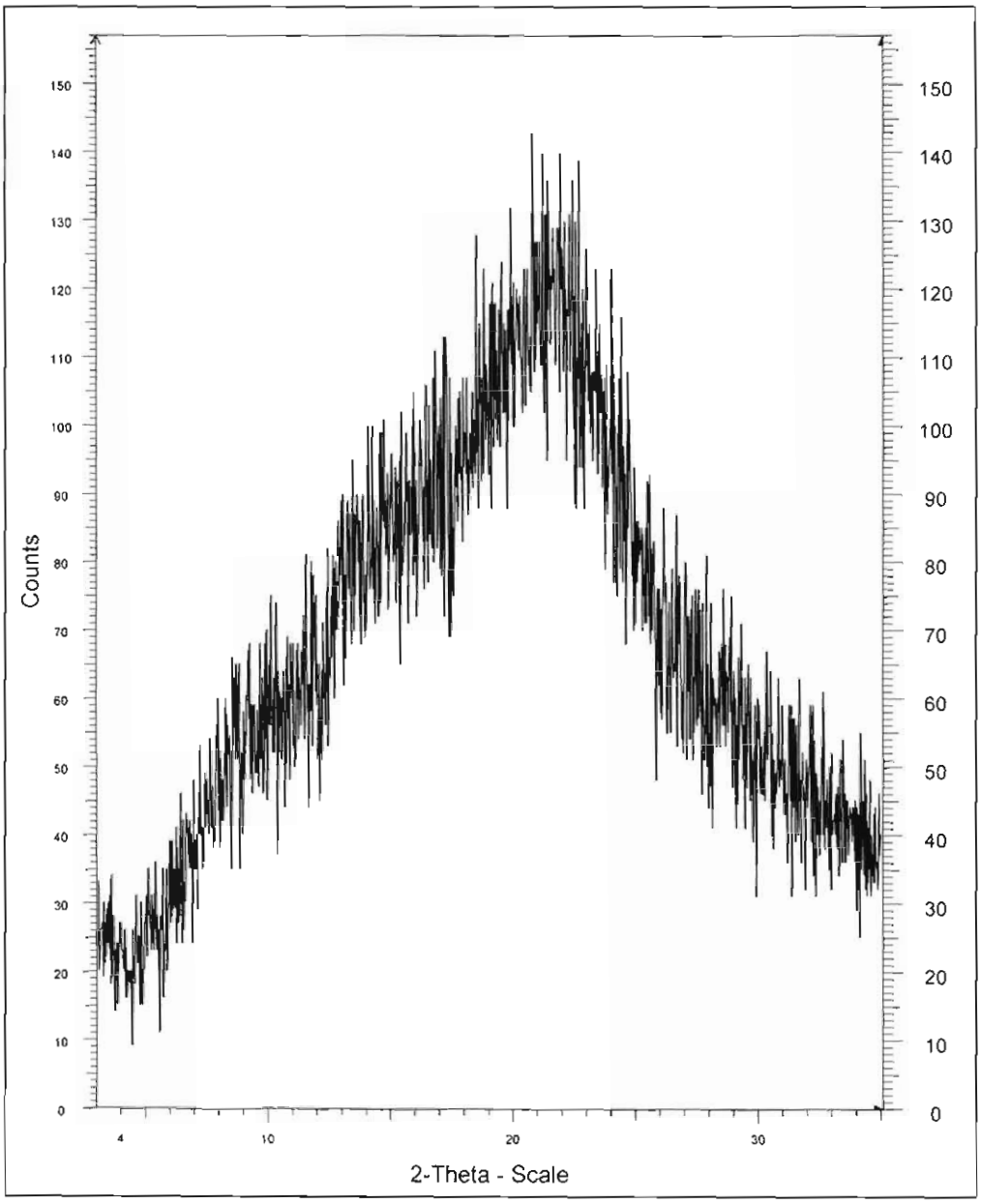

Figure 5 The X-ray powder diffractogram of the glassy stavudine.

The infrared (IR) spectrum of the glassy stavudine is shown in figure 6 (a). This spectrum differed from that of the crystalline forms of stavudine as seen in figure 6 (b). The IR spectrum of the glassy stavudine has a unique absorption band at 551 cm^{-1}, and no absorption bands in the 3600 – 3200 cm^{-1} region, and although the IR spectrum of the NMP solvate also has no absorption bands in this region, the IR spectrum of the glassy stavudine has a broader peak in this region compared to the NMP solvate.

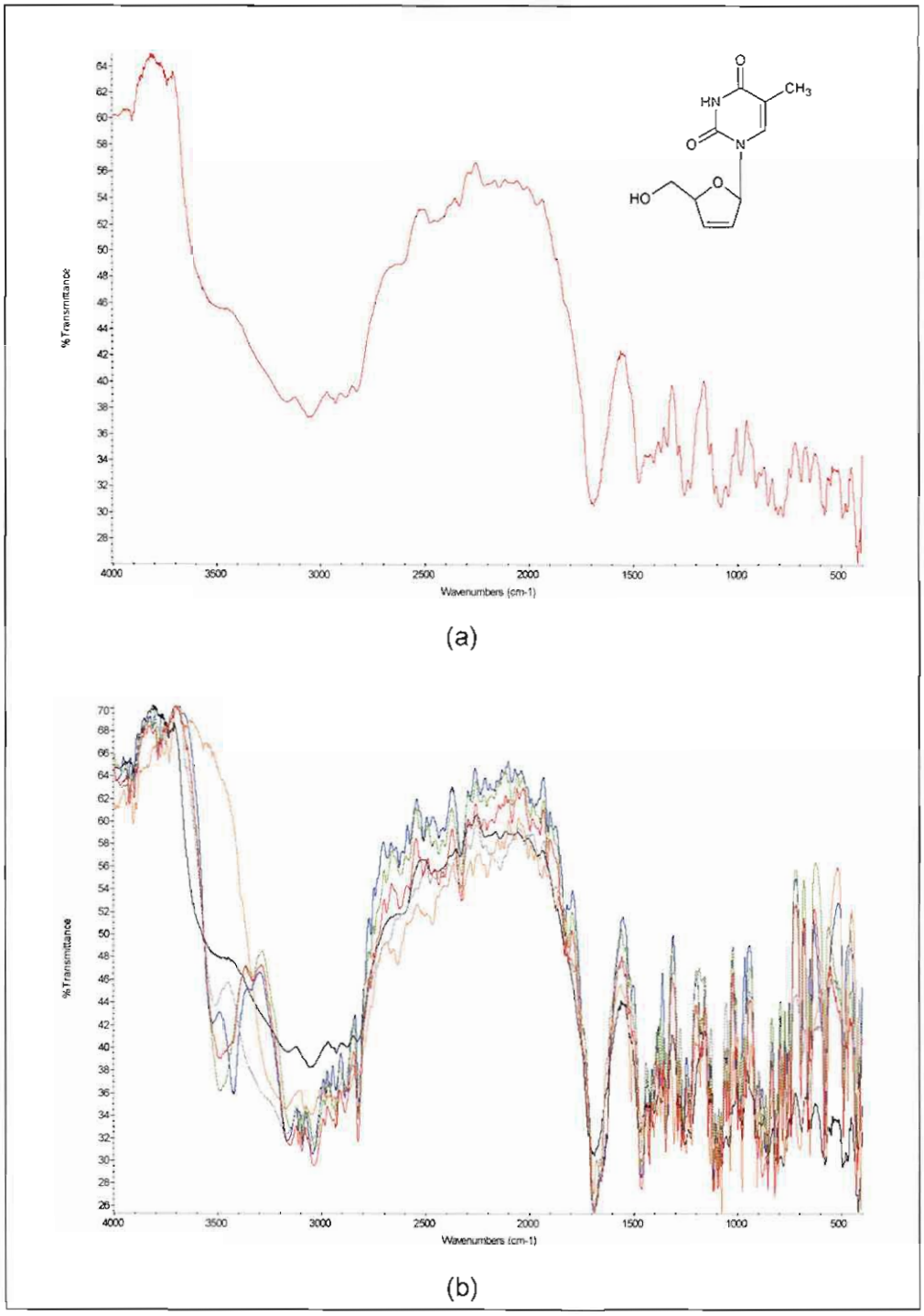

Figure 6 (a) The infrared spectrum of the glassy solid state of stavudine. (b) An overlay of the infrared spectra of the solid states of stavudine studied (form I, form II, the form I/II mixture, form III, NMP solvate and glassy stavudine).

The DSC thermogram of the glassy stavudine is shown in figure 7, and it clearly demonstrated the presence of a glass transition temperature (T_g) at 46.11°C (a baseline-shift). The T_g is the temperature below which the molecules are configurationally frozen in the glassy state, and thus lack the motion of molecules in the liquid phase [6].

The T_g is characteristic of each amorphous solid state and varies according to the rate at which the melt is cooled during the preparation of the glassy solid (the slower the rate of cooling of the melt, the lower the T_g will be). Above the T_g the amorphous solid is said to be in a rubbery state and will flow, and the molecules thus have more configurational motion compared to the glassy state, but it is still not comparable to the liquid state. Figure 7 illustrates that above the T_g the stavudine glass recrystallises at a temperature of 110.15°C (the exotherm), after which it melts at 157.84°C (the sharp endotherm) followed by the decomposition of the stavudine.

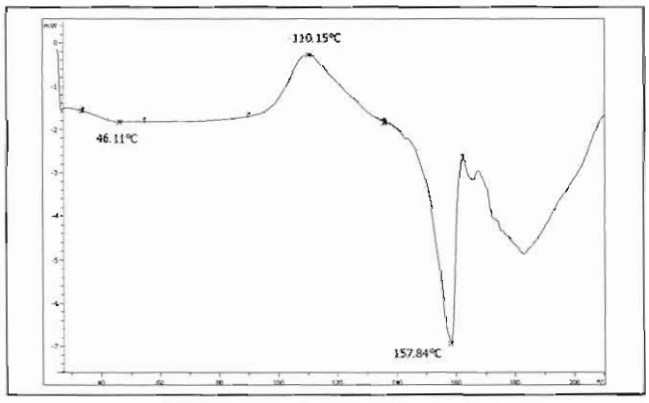

Figure 7 The DSC thermogram of the glassy stavudine.

The TGA and Karl Fischer analysis of the glassy stavudine revealed an insignificant amount of weight loss (0.02%) and negligible moisture content (0.17%) of the glassy solid.

The fragility of the stavudine glass was calculated using the following equation:

$$\frac{T_m}{T_g} \qquad (2)$$

Where: T_m and T_g are the melting and glass transition temperatures respectively.

The stavudine glass had a ratio of 3.42 indicating that it is a strong glass (glasses with a ratio above 1.5 are classified as strong whilst a ratio below 1.5 is indicative of a fragile glass), and the stavudine glass thus exhibits minimal molecular mobility changes at the T_g, hence the small change in heat capacity at the T_g as seen in figure 7 [9].

Polarising optical microscopy confirmed the amorphous nature of the glassy stavudine since no birefringence of the polarised light was observed (see table 1). Hot-stage microscopy (HSM) confirmed the results obtained from DSC, and is presented in table 1.

Table 1 Photomicrographs obtained with polarising optical and hot stage microscopy

Glassy stavudine		
Photomicrograph	**Technique and temperature**	**Observation**
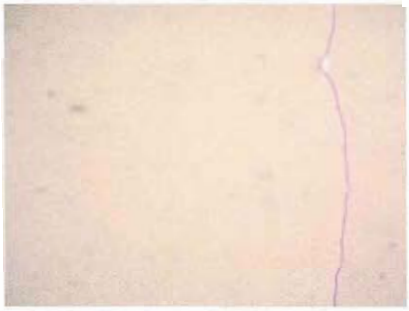	Optical microscopy (25°C)	Clear, irregular shaped solid
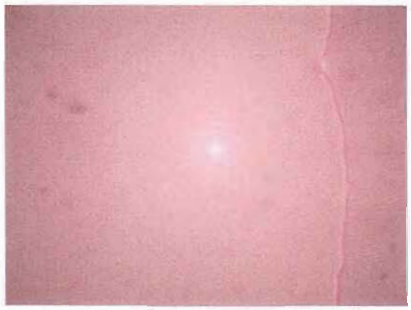	Polarising optical microscopy (25°C)	Clear, irregular shaped solid (no birefringence of polarised light)
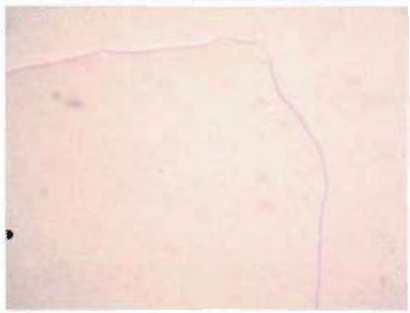	Hot stage microscopy (25°C)	Clear, irregular shaped solid
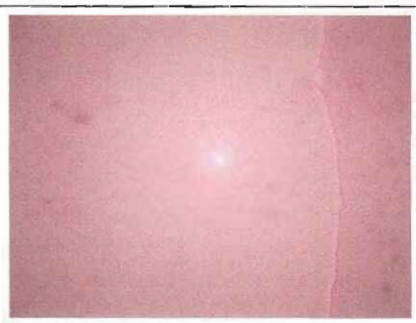	Hot stage microscopy (45°C) combined with polarising optical microscopy	Clear, irregular shaped solid (no visible change in appearance at T_g)

Table 1 (continued)

Glassy stavudine		
Photomicrograph	**Technique and temperature**	**Observation**
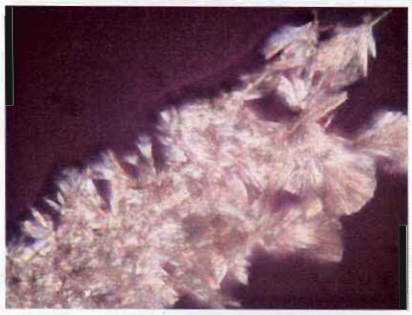	Hot stage microscopy (100°C) combined with polarising optical microscopy	Onset of recrystallisation of stavudine from the glass (visible due to birefringence of polarised light)
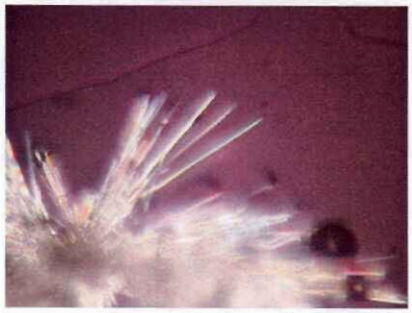	Hot stage microscopy (116°C) combined with polarising optical microscopy	Further recrystallisation of stavudine (visible due to birefringence of polarised light)
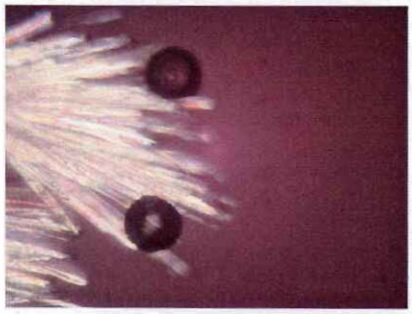	Hot stage microscopy (125°C) combined with polarising optical microscopy	The end of the recrystallisation process
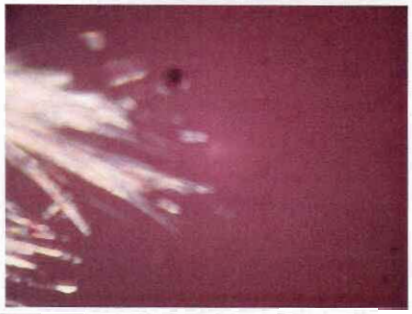	Hot stage microscopy (141°C) combined with polarising optical microscopy	Onset of melting of the recrystallised stavudine
	Hot stage microscopy (159°C)	Stavudine completely melted

Scanning electron microscopy was used to study the morphology of the glassy stavudine. The glassy stavudine did not have a particular morphological shape, however it had a liquid-like appearance (figure 8).

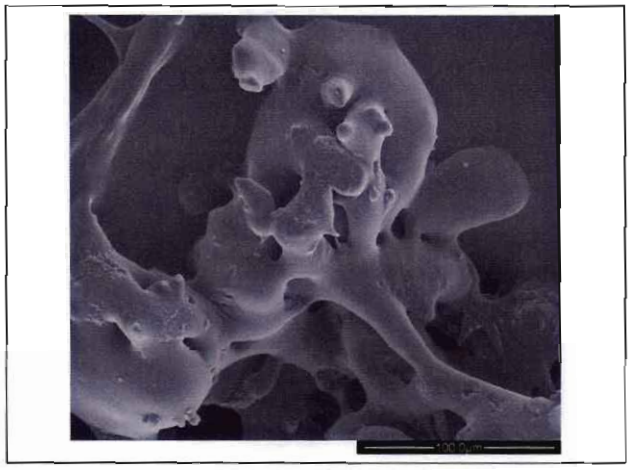

Figure 8 The SEM photomicrograph of the glassy stavudine.

The result from the VT-XRPD analysis of the glassy stavudine is shown in figure 9 (a). As can be seen in figure 9 (a) the diffractograms of the glassy stavudine between 85 and 120°C resemble the diffractogram of the form I/II mixture of stavudine (see figure 9 (c)), the glassy stavudine thus recrystallises as a mixture of form I and form II. Table 2 demonstrates the diffraction angles of form I, form II and the form I/II mixture, as well as the diffraction angles in the diffractogram of the glassy stavudine which are detected at 120°C, and this indicates that this diffractogram is similar to the diffractogram of the form I/II mixture.

Table 2 A comparison between the diffraction peaks of the glassy stavudine at 120°C and the diffraction peaks of form I, form II and the form I/II mixture

	Form I	Form II	The form I/II mixture	Glassy stavudine 120°C
Position (°2θ)	-	11.243	11.225	11.225
	-	18.620	18.637	18.633
	19.117	-	19.137	19.160

Above 120°C the product that recrystallised from the glassy stavudine starts to decompose and form the degradation product, thymine, as the temperature reaches the melting point, and this is evident by the appearance of the diffraction peaks at 7.11 and 14.27°2θ, which are the characteristic peaks of the XRPD pattern of thymine (see figure 9 (b)).

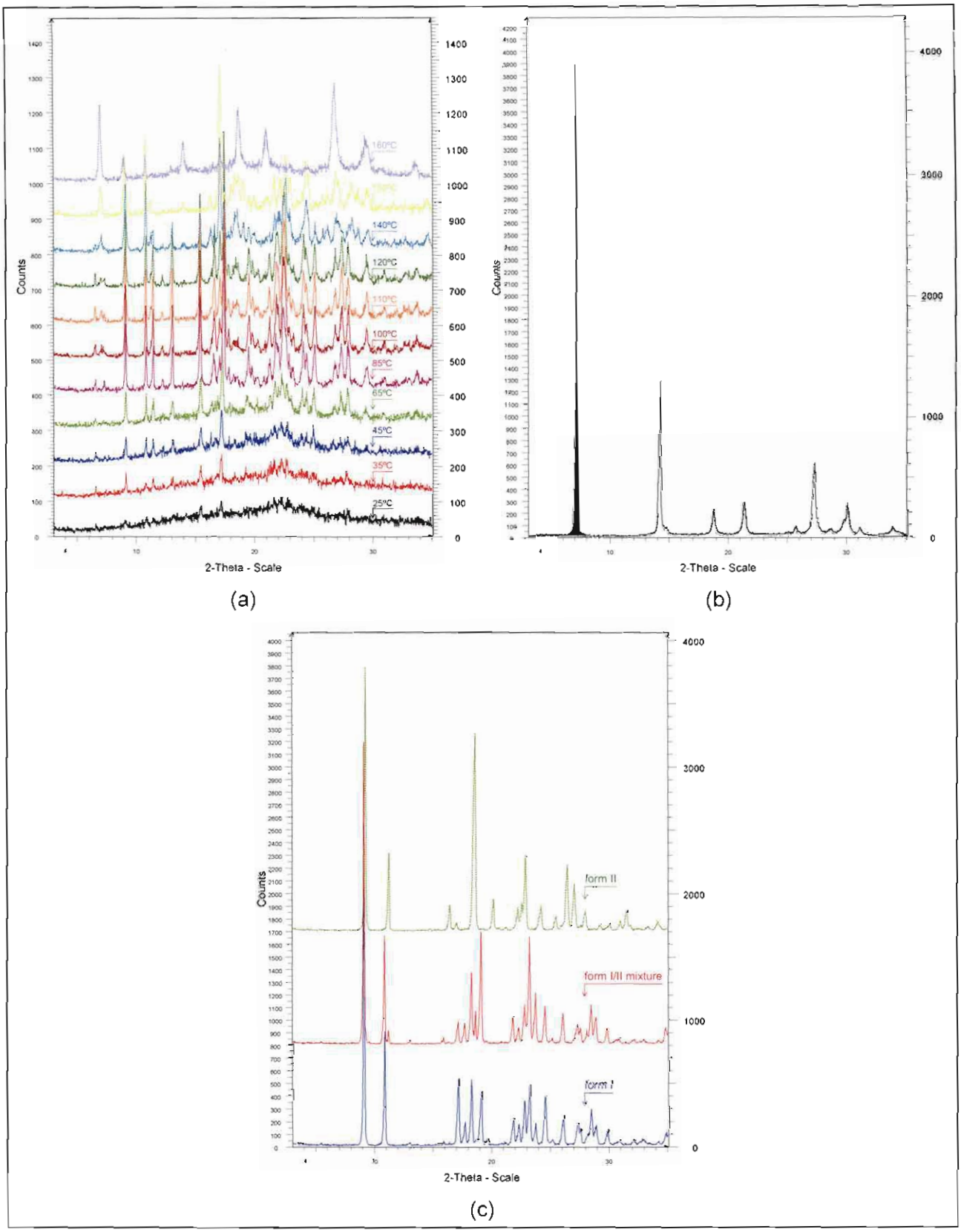

Figure 9 The VT-XRPD diffractograms of (a) glassy stavudine and (b) the XRPD pattern of thymine and (c) the XRPD patterns of form I, form II and the form I/II mixture.

The results of the dissolution tests are presented in table 3 and figure 10, and it is clear from these results that during the first minute of the dissolution tests, a greater amount (between 5 and 16%) of the glassy stavudine had dissolved compared to the other polymorphic forms

and the powder mixture tested. This was expected, since the glassy solid state (amorphous form) of a drug is generally more soluble than the polymorphic and pseudopolymorphic forms of the same drug. The amount of stavudine that had dissolved after one minute slightly differed between form I and form II, and after a period of five minutes the stavudine from all four samples had completely dissolved. The dissolution results of the polymorphic forms and the powder mixture of stavudine that were tested thus conformed to our in-house requirements that not less than 80% of the stavudine should dissolve within 30 minutes.

Table 3 A summary of the dissolution test results

Time (minutes)	Amount of stavudine dissolved (%)			
	Form I	Form II	Glass	Form I/II mixture
0	0	0	0	0
1	83.72	79.59	89.30	73.48
5	102.01	105.34	104.43	105.90
10	101.89	106.13	103.45	105.57
15	101.05	105.14	102.87	104.85
30	100.58	103.02	102.24	104.28

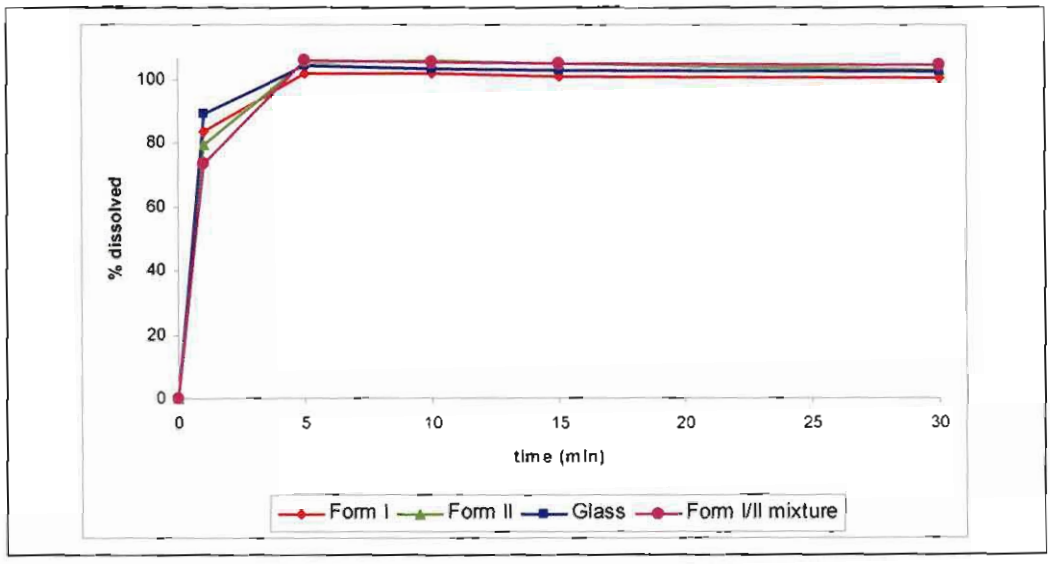

Figure 10 A summary of the dissolution profiles obtained.

The similarity factor (f_2), derived by Moore & Flanner (1996:66) (see equation 5.3), is used to compare the dissolution profiles of multipoint dissolutions [10]:

$$f_2 = 50 \log \left\{ \left[1 + \frac{1}{n} \sum_{t=1}^{n} (R_t - T_t)^2 \right]^{-0.5} \times 100 \right\} \qquad (3)$$

Where: R_t = the percentage of the reference sample that dissolved

T_t = the percentage of the test sample that dissolved

n = the amount of withdrawals made during the dissolution testing.

The requirements for the comparison of dissolution profiles stipulated by the Medicines Control Council of South Africa were used during the comparison of the dissolution profiles of the stavudine samples. The dissolution profile of polymorphic form I was chosen as the reference profile (R_t), and the other dissolution profiles were thus compared with the profile of form I. According to these requirements, the profiles of form I and form II, form I and the glassy stavudine, and form I and the form I/II mixture are similar, since both the reference and the test sample show more than 85% dissolution within 15 minutes (see table 3), i.e. it is not necessary to calculate a similarity factor for these profiles [11].

4. Conclusion

A glassy solid state of stavudine, which has not been described before, was successfully prepared and characterised, and the amorphous nature of this solid state was demonstrated.

References

1. **RAFFANTI, S. & HAAS, D.W.** 2001. Antimicrobial agents (continued): Antiretroviral agents. (*In* Hardman, J.G. & Limbird, L.E. *ed.* Goodman and Gilman's The pharmacological basis of therapeutics. 10th ed. New York: McGraw-Hill. p. 1349-1380.)

2. **MIRMEHRABI, M., ROHANI, S., MURTHY, K.S.K. & RADATUS, B.** 2006. Polymorphic behavior and crystal habit of an anti-viral/HIV drug: stavudine. *Crystal growth and design*, 6(1):141-149. Available: American Chemical Society.

3. **RADATUS, B.K. & MURTHY, K.S.K.** 2003. Process for the preparation of substantially pure stavudine and related intermediates useful in the preparation thereof. Patent: US 6,635,753. 6 p.

4. **VITERBO, D., MILANESIO, M., HERNÁNDEZ, R.P., TANTY, C.R., GONZÁLES, I.C., CARRAZANA, M.S. & RODRÍGUES, J.D.** 2000. 2',3'-Didehydro-3'-deoxythymidine *N*-methyl-2-pyrrolidone solvate (D4T·NMPO). *Acta Crystallographica Section C*, C56:580-581.

5. **GANDHI, R.B., BOGARDUS, J.B., BUGAY, D.E., PERRONE, R.K. & KAPLAN, M.A.** 2000. Pharmaceutical relationships of three solid state forms of stavudine. *International Journal of Pharmaceutics*, 201:221-237. Available: ScienceDirect.

6. **BYRN, S.R., PFEIFFER, R.R. & STOWELL, J.G.** 1999. Solid-state chemistry of drugs. 2nd ed. West Lafayette: SSCI Inc. 574 p.

7. **WU, T., LI, N., DE VILLIERS, M.M. & YU, L.** 2006. Nano-coating for inhibiting surface crystallization and improving physical properties of amorphous indomethacin. 1-15 p. Personal communication with the author: lyu@pharmacy.wisc.edu.

8. **UNITED STATES PHARMACOPEIAL CONVENTION.** 2007. USP30:NF25 Online. Available: www.uspnf.com

9. **CRAIG, D.Q.M., ROYALL, P.G., KETT, V.L. & HOPTON, M.L.** 1999. The relevance of the amorphous state to pharmaceutical dosage forms: glassy drugs and freeze dried systems. *International Journal of Pharmaceutics*, 179:179-207. Available: ScienceDirect.

10. **MOORE, J.W. & FLANNER, H.H.** 1996. Mathematical comparison of dissolution profiles. *Pharmaceutical Technology*, June:64-74.

11. **MEDICINES CONTROL COUNCIL.** 2006. Dissolution, 1-10, July. Available: www.mccza.com